Ilya Viktorovich Gorelkin

Concepts and models of the catalytic dehydrogenation of propane

Thesis for the degree of Philosophiae Doctor

Trondheim, March 2013

Norwegian University of Science and Technology
Faculty of Natural Sciences and Technology
Department of Chemical Engineering

NTNU – Trondheim
Norwegian University of
Science and Technology

NTNU
Norwegian University of Science and Technology

Thesis for the degree of Philosophiae Doctor

Faculty of Natural Sciences and Technology
Department of Chemical Engineering

ISBN 978-82-471-4250-9 (printed version)
ISBN 978-82-471-4251-6 (electronic version)
ISSN 1503-8181

Doctoral theses at NTNU, 2013:76

Printed by Skipnes Kommunikasjon as

Dedicated to Valentina Mikhailovna Gorshkova and Viktor Aleksandrovich Gorelkin

PREFACE

The work for this thesis was carried out at the Norwegian University of Science and Technology in Trondheim, Norway between July 2008 and July 2012.

The thesis is written as a monograph divided into sections, chapters and parts. A literature study on the catalytic propane dehydrogenation as well as catalytic hydrogen combustion is included in the Theory section. The model of reaction is described in the Microkinetic model section. The experimental set-up together with experimental conditions used in experimental part of the work are described in the Experimental work section. The Results and discussion section is divided into four chapters, devoted to experiments with Pt-Sn catalyst, Pt catalyst, experiments with empty reactor and model simulations. The most important discoveries are summarized in the Conclusions section. Some ideas on possible improvements for the experimental technique as well as for the model construction are listed in the Further work section. The reference data, calculation procedures, programme code (Matlab) used in the work are given in the Appendices.

ABSTRACT

Propene is an important feedstock for the chemical industry. It is produced mainly as a sideproduct of ethylene production by steam cracking or in refinery processes (primarily catalytic cracking). Due to an increase in the consumption of chemicals and materials produced from propene, the demand for processes for direct propene production (e.g. by catalytic dehydrogenation of propane) is growing.

For the reaction of propane dehydrogenation the equilibrium conversion increases with temperature. Acceptable conversion at atmospheric pressure is reachable at temperatures which are higher then 500 ℃, the proper catalytic system is needed in order to get high reaction rate, high selectivity and highest reachable conversion. Different approaches for technological implementation of the process are under development (dehydrogenation, oxidative dehydrogenation, dehydrogenation + selective hydrogen combustion; catalytic processes, gas-phase processes, catalytic ignition of gas-phase processes). There are commercialised technologies for the dehydrogenation of hydrocarbons with use of Pt, Cr or chromium oxide catalysts. These catalytic systems still give side reactions and need periodical regeneration of the catalyst, thus further research on the optimal conditions and catalysts for propane dehydrogenation is necessary.

In this work emphasis is put on both modelling and experimental work. The work on modelling includes preparing the set of elementary equations; describing the route of main products formation; making the microkinetic model based on standard calculation techniques; computer simulation of the model and comparison of its result with the experimental results. The experimental work is focused on detection of influence of the feed components concentration ratios (air, hydrogen, propane) on the results of dehydrogenation process.

Ternary composition-property diagrams were used to study the influence of the ratio between components of a fed gas mixture (propane, oxygen, hydrogen) on the results of the reaction. The reaction was carried out over Pt-Sn and Pt catalysts, as well as

with empty reactor at different temperatures in the range 350~650 ℃. Product yields and reactant conversions were plotted against the concentrations of the reactants with the aim of determining the optimal conditions for the process and check the viability of the DH+SHC approach.

Some interesting process features for the reaction H_2+O_2+C_3H_8 over PtSn/HT, Pt/HT catalysts and in gas phase were found. Hydrogen amounts below the stoichiometric concentration (for the reaction of water production) can be selectively combusted. There is a difference between hydrogen premixed in the feed and hydrogen formed in the reaction. Premixed (feed) hydrogen reacts rapidly with oxygen, either upstream of the catalyst bed (in gas-phase) or in the initial part of the bed. The hydrogen formed in the reaction does not see any oxygen (the oxygen is consumed since oxidation reactions are fast).

For Pt water selectivity is lower than for PtSn catalyst. There is more than one route to the production of products such as H_2O and CO_2. One route to CO_2 production is formation from propene, another - production from coke precursors. One route of production of H_2O is the direct hydrogen oxidation, another route incorporates CO as an intermediate compound; the formation of water from coke precursors was also observed. CO_2 production is not obviously correlated with CO production, whereas the correlation between CO production and H_2O production was observable.

The PtSn catalyst is less active than Pt catalyst for some of the unwanted reactions. Pt is more active for production of CO_2, CO, C_2H_6, CH_4, especially at temperatures up to 600 ℃ (in comparison with PtSn whose activity for these products is very low). At higher temperatures the results for both catalysts are similar to gas phase reactions (increase in the byproducts CO, C_2H_4, CH_4, C_2H_6), whereas the Pt is still more active for reactions producing CH_4, C_2H_6 and for oxidation reactions producing CO, CO_2.

The formation of CO, CO_2 promotes the stability of the catalyst at a certain range and coincides with the maximum in propene production over PtSn catalyst. For the Pt catalyst oxidation reactions are so fast that the positive effect of stabilisation of the catalyst is overlapped by the negative effect of propene oxidation.

The ratio between H_2 and O_2 fed to the reactor plays a significant role in the reaction mechanism. For different compounds we can see some features in their selectivity connected with the water production stoichiometric line (border between conditions where either hydrogen or oxygen is in excess). Whereas the oxygen specific concentration 20% (presumably important for autothermal regime, when half of hydrogen in the system is completely combusted) almost is not playing important role. The only obvious influence of it is observed for propene yield over PtSn catalyst (the yield maximum lays near this concentration).

The optimal feed composition for the highest yield of propylene at relevant industrial temperatures (550~625 ℃) and atmospheric pressure over PtSn was found to be: O_2 – 17%, C_3H_8 – 57~50%, H_2 – 26~33%. It was found that the autothermal regime takes place over PtSn catalyst and with hydrogen for combustion added to the feed. No signs of the autothermal regime over Pt catalyst were found.

A model describing the behaviour of the Pt catalyst was developed. This is the microkinetic model, it includes surface reactions where species containing C, H and O elements participate. The UBI-QEP method was used for calculation of the activation energies and TST for calculation of the preexponentials. The model describes qualitatively well the experimental observations. The simulation showed high influence of the adsorptive properties of compounds and coverage effects on the result of reaction. Using the model it is possible to check the behaviour of the reaction mixture over a range of conditions: with different compositions of the initial mixture ($[O_2]$, $[C_3H_8]$, …); with different monometallic catalysts (Pt, Pd, Au …); with different parameters of the catalyst (mass of the sample), flow rate (residence time in reactor).

ACKNOWLEDGEMENTS

First of all I would like to thank my supervisor prof. Edd A. Blekkan for guidance during my Ph.D studies and research, for his patience and energy he put in the corrections (both scientific and language) while reading the manuscripts.

I would also like to thank people that helped me to do the research. I am grateful to master student Virginie Herauville for work in laboratory on Pt catalyst preparation and running experiments with Pt catalysts; to PhD student Andrey Volynkin for the help with some of characterisation techniques; to Liudmila Ilyukhina for her help with the calculation of symmetry numbers.

The atmosphere of friendship in the Catalysis group and good working environment in the university are greatly acknowledged. Special thanks to professors provided courses and help: Anders Holmen, Hilde J. Venvik, De Chen, Magnus Rønning, Reidar Tunold.

I thank the technical and administrative personnel of the Chemical Engineering Department that helped me to solve different practical challenges. Here I would like to especially mention higher executive officer Lisbeth H. Blekkan Roel, engineers Hurry T. Brun, Jan-Morten Roel and Arne Fossum.

The funding of the research project by the Research council of Norway through the GASSMAKS programme and financial support from the Norwegian university of science and technology are greatly acknowledged.

I would like to especially thank my family. I thank my parents for their constant moral support and belief in me. I thank my wife Liudmila Ilukhina for her support and help throughout the time of my PhD research. And finally I would like to thank little Vasilisa, my daughter, who adorned the last year of my work.

LIST OF PUBLICATIONS AND PRESENTATIONS

Oral and poster presentations:

1. "New concepts in the catalytic dehydrogenation of propane" Poster presentation at inGAP-NANOCAT Summer School, 21-26.06.2009, Trondheim.

2. "Possible reaction mechanisms of the catalytic dehydrogenation of propane" Poster presentation at Norwegian Symposium on Catalysis, 30.11-1.12.2009, Trondheim.

3. "Concepts and models of the catalytic dehydrogenation of propane" Oral presentation at Norwegian Catalysis symposium, 29-30.11.2010, Bergen, Norway

4. "Concepts and Models of the Catalytic Dehydrogenation of Propane" Oral presentation at 22nd North American Catalysis Society Meeting, 1-6.06.2011, Detroit, USA

5. "Concepts and Models of the Catalytic Dehydrogenation of Propane" Poster presentation at EuropaCat X, 28.08-2.09.2011, Glasgow, UK

Publications:

1. I.V. Gorelkin, E.A. Blekkan. Catalytic dehydrogenation of propane coupled with hydrogen combustion studied over a Pt-Sn catalyst using ternary yield plots. Submitted to Chem. Eng. J. (Article is based on Ch. 5.1.2 of this thesis).

2. I.V. Gorelkin, E.A. Blekkan. Catalytic dehydrogenation of propane coupled with hydrogen combustion studied over a Pt catalyst using ternary yield plots. In preparation. (Article is based on Ch. 5.2.2 of this thesis).

3. I.V. Gorelkin, E.A. Blekkan. Modelling the catalytic dehydrogenation of propane coupled with hydrogen combustion over a Pt catalyst. In preparation. (Article is based on Chs. 3 and 5.4 of this thesis).

LIST OF SYMBOLS AND ABBREVIATIONS

BDE	Bond dissociation energy
CSTR	Continuously-stirred tank reactor
DFT	Density functional
DH	Dehydrogenation
DME	Dimethylether
ER	Eley-Rideal mechanism
FBD	Fluidised bed dehydrogenation
FCC	Fluid-catalytic cracking
GAM	Group additivity method
GAV	Group additivity values
GC	Gas chromatograph
HT	Hydrotalcite
LDH	Layered double hydroxide
LH	Langmuir-Hinshelwood mechanism
LNG	Liquefied natural gas
LPG	Liquefied petroleum gases
MFC	Mass flow control
MTO	Methanol-to-olefin process
MTP	Methanol-to-propylene process
NGL	Natural gas liquids
ODE	Ordinary differential equations
PFR	Plug-flow reactor
SEM	Scanning electron microscope
SHC	Selective hydrogen combustion
TST	Transition state theory
UBI-QEP	Unity bond index - quadratic exponential potential method
VOC	Volatile organic compounds
WGS	Water-gas shift reaction

CONTENTS

1 INTRODUCTION

1.1 NATURAL GAS AS PROPANE SOURCE

Propane comes from both oil refinery production and production of natural gas. In a refinery it comes primarily from two units - the reformer and fluid catalytic cracking unit - which are important units in the production of gasoline.

Crude oil includes Natural gas liquids (NGL) and condensate (light oil that contains a proportion of wet gas) after gas and water have been separated during processing.

Natural gas mainly consists of methane, ethane, propane and butane with 80~100% of methane. Natural gas is separated into two gases: wet gas, containing components such as ethane, propane, butane, naphtha and condensate; and dry gas, containing methane.

Norway is the largest holder of natural gas and oil reserves in Europe. In 2010 Norway was the second largest exporter of natural gas in the world [1]. Its reserves and production of oil and gas look stable at least for a decade (Figs. 1.1.1*a* (from [2]), 1.1.1*b* (from [3])).

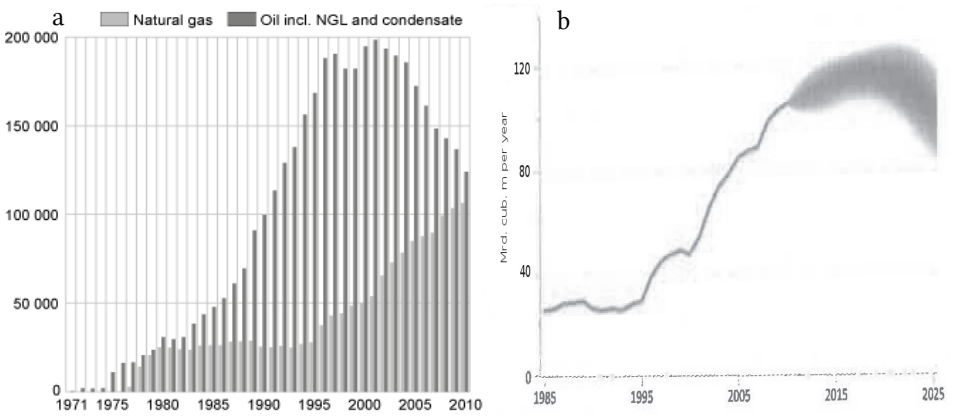

Fig. 1.1.1: The production of natural gas and oil including condensate and NGL in Norway, in 10^6 m^3 per year (a); and prognosis for gas production, in 10^9 m^3 per year (b).

There are plants in Norway aimed for processing of crude oil and gas with different processing depth. Complexes in Kårstø, Tjeldbergodden, Kollsnes, Sture, Mongstad, Snøhvit, Nyhamna, Melkøya, Rafnes are among them [3], [4].

The Tjeldbergodden industrial complex in the Nordmøre region of western Norway has several components – a gas receiving terminal, plants for methanol production, air separation and gas liquefaction plant for the production of liquefied natural gas (LNG). The methanol plant is the biggest in Europe. The facility has an annual capacity of about 900,000 tonnes of methanol. Production capacity for LNG is about 12 000 tonnes per year [3], [4].

The Kårstø processing plant north of Stavanger plays a key role in the transport and treatment of gas and condensate (light oil). The daily capacity at Kårstø is ~$90 \cdot 10^6$ m^3. It has a plant for removing carbon dioxide from gas. The unprocessed condensate is stabilised and fractionated in a dedicated plant. ~$4 \cdot 10^6$ tonnes of stabilised condensate per year are shipped from Kårstø by sea. NGLs are separated from the rich gas, these are fractionated into propane, normal butane, isobutane, naphtha and ethane. The propane is stored in two artificial rock caverns with a total capacity of 90 000 tonnes. Normal butane, isobutane, naphtha and ethane are held in conventional tanks. The Kårstø complex is the third largest export port in the world for liquefied petroleum gases (LPG). The capacity for ethane separation on the plant is ~950 000 tonnes per year. Dry gas is exported from Kårstø by the pipe systems [4].

The processing plant at Kollsnes west of Bergen can treat ~$140 \cdot 10^6$ m^3 of gas per day. NGL is separated from the rich gas, the dry gas is pressurised and is driven by compressors through the gas pipe systems to customers. NGL from the Kollsnes plant goes as well to the Mongstad refinery for fractionation into propane, butanes and naphtha [4].

The Sture terminal near Bergen in western Norway is an export port for crude oil and condensate (light oil), which arrives by pipelines from the North Sea. The Sture facility includes five artificial rock caverns for crude oil with a total capacity of ~10^6 m^3 and a cavern for liquefied petroleum gases (LPG) of ~60 000 m^3. The terminal also has a plant

for recovering volatile organic compounds (VOC), which is environmentally important when loading tankers. Processing facilities at Sture recover the lightest components from the crude, which are extracted as an LPG mix (propane and butane) and as naphtha. Stabilised crude and LPG mix are stored in the relevant rock caverns before being shipped out. LPG mix and naphtha are also transported from the terminal through the pipeline to Mongstad.

The oil refinery at Mongstad in western Norway is a modern plant with a capacity of $10{\cdot}10^6$ tonnes of crude per year. The principal outputs are petrol, diesel oil, jet fuel and other light petroleum products. The heaviest components in the feedstock are used to produce such products as petroleum coke (petcoke), a raw material for the anodes required by aluminium industry [4].

LNG is exported from Snøhvit, Melkøya [3].

Norwegian industry has the necessary materials and competences to develop relevant technologies and introduce new approaches into production cycle to rich the deeper processing of the oil and gas. One of promising processes is propylene production.

1.2 PROPYLENE PRODUCTION

Propene, one of the most important feedstocks for the chemical industry, is produced mainly as a sideproduct of ethylene production by steam cracking or in refinery processes (primarily catalytic cracking). Thus, the availability of propene is determined primarily by the demand for the main products. The increased consumption of propene, especially due to polypropylene production, has led to an increase in the interest in processes for propene production by dedicated processes such as catalytic dehydrogenation of propane. Various processes suitable for this purpose have been developed [5].

1.2.1 PRODUCTION AS BYPRODUCT OF ETHYLENE PRODUCTION

Depending on cracking feedstocks and cracking conditions the cracked gas with different composition can be produced. One of several variants of a process for

propane production is as follows. A C_3 fraction is obtained as overhead product from the depropanizer in the processing of cracked gas. The C_3 fraction contains such hydrocarbons as propane, propene, propadiene and propyne as well as traces of C_2 and C_4 hydrocarbons. Because of this, the C_3 fraction requires further treatment. It is fed to a selective hydrogenation unit to remove propadiene and propyne (palladium catalysts being used). The amount of hydrogen added is calculated so that, complete conversion of C_3H_4 to C_3H_6 is achieved, but the smallest possible amount of propene is hydrogenated to propane. If required, these can be scrubbed out after hydrogenation with a small amount of C_3 in a scrubber. The methane introduced with the hydrogen is then stripped off and recycled to the cracked gas processing unit of the steam cracker to recover entrained propene. The bottom product of the C_3 stripper is the propene of chemical-grade (97 wt% of purity). Chemical-grade propene is purified to polymer-grade propene (99.6 wt% of purity) in a downstream propene – propane separation column. In usual ethylene production the propane separated in the C_3 splitter is recycled as cracking feedstock [5].

1.2.2 PRODUCTION AS BYPRODUCT OF REFINERY PROCESSES

The propene produced in refineries also originates from cracking processes. However, these processes use different feedstocks and have different production objectives. Refinery cracking processes operate either thermally or catalytically. The most important process for propene production is the fluid- catalytic cracking (FCC) process in which the powdery catalyst flows as a fluidized bed through the reaction and regeneration phases. This process converts heavy gas oil or atmospheric residues preferentially into gasoline and light gas oil. Purely thermal cracking processes, which in refineries contribute to propene production, are used in coking and visbreaker units. In coking units, residues from the atmospheric and vacuum distillation of the crude oil undergo relatively severe cracking and are converted into gas oil, coke, gasoline, and smaller amounts of cracked gas (6~12wt% of C_4 and lighter). The cracked gas from the coking unit normally contains 10~15 mol% C_3, mostly propane. In visbreaker units, vacuum residues are subjected to mild thermal cracking, with the object of reducing

the viscosity of the residue oil. Smaller amounts of gas oil, gasoline, and cracked gas (2~3wt% of C_4 and lighter) are formed here. The separation of the C_3 fraction generally occurs as follows: the light components are separated in a deethanizer, the C_5 and heavier hydrocarbons are removed from the bottom product in a debutanizer, the C_3–C_4 fraction obtained as overhead product is desulfurized on molecular sieves, dried and split into individual fractions in a depropanizer [5].

1.2.3 MTP/MTO PROCESSES

Production of propylene from methanol (methanol-to-propylene (MTP) and methanol-to-olefins (MTO) processes) can be an alternative to traditional production of propylene from petroleum by cracking technologies. The processes utilise zeo-type catalysts. The catalyst has high selectivity, thus, the purification stage consists only of a reduced cold box system.

The methanol is converted in adiabatic prereactor to dimethylether (DME) and water. The stream of methanol, water and DME is passed to the MTP reactor, where steam is added. Methanol and DME are mainly converted to propylene. The product mixture is cooled and gas, organic liquid and water are separated. The gas is compressed, traces of water, CO_2 and DME are removed. The cleaned gas is processed yielding chemical-grade or polymer-grade propylene.

The catalyst requires regeneration by annealing in air in a catalyst regeneration system. A fluidised bed reactor and regeneration system are used. The reactor operates in the vapour phase at temperatures 350~550 °C and pressure 1~3 bar.

In MTO process the ethylene-to-propylene products ratio can be varied following the chosen operational conditions [6].

1.2.4 PROPANE DEHYDROGENATION

Propane dehydrogenation is an endothermic equilibrium limited reaction that is generally carried out in the presence of a noble- or heavy-metal catalyst such as platinum or chromium.

$$C_3H_8 \rightarrow C_3H_6 + H_2 \qquad (1.2.4.1)$$

The process is highly selective; overall yields of propene from propane of ~90% are claimed for commercially available processes. Higher temperature and lower pressure increase propene yield. However, increased process temperature also causes pyrolysis (cracking) of propane to coke in addition to its dehydrogenation to propene (i.e., reduced selectivity), whereas lower operating pressure increases selectivity. Coke formation wastes feedstock and deactivates the dehydrogenation catalyst. Consequently, propane dehydrogenation processes are operated near atmospheric pressure at around 500~700 °C. A number of technologies are available commercially for the dehydrogenation of propane to propene: these include Oleflex (developed by UOP, US); Catofin (Air Products and Chemicals, US); STAR (ThyssenKrupp Uhde). These processes differ in their modes of operation, the dehydrogenation catalyst, and the methods of catalyst regeneration.

The chemical properties of propene are characterized by the reactivity of its double bond. Propene undergoes a number of industrially important polymerization, addition, and oxidation reactions. Refinery-grade propene (50~70% pure propene in propane) is obtained from refinery processes. Its main uses are in LPG for thermal use or as an octane-enhancing component in motor gasoline. It can also be used in chemical syntheses (e.g., of cumene or isopropanol). Chemical-grade propene is used for most chemical derivatives (e.g., oxo alcohols, acrylonitrile, or polypropylene). Polymer-grade propene contains minimal levels of impurities such as carbonyl sulphide that can poison catalysts used in polypropylene and propylene oxide manufacture [5].

1.3 SCOPE OF THIS WORK

Selective hydrogen combustion combined with propane dehydrogenation have been studied in the catalysis group at NTNU for some years, resulting in dissertations [7], [8], [9] and other. The focus was oxidative dehydrogenation of propane over VMgO catalysts and selective hydrogen combustion in the presence of hydrocarbons over

SiO_2-supported Pt-based catalysts (Pt, PtSn) and metal-oxide catalysts (In_2O_3, Bi_2O_3, PbO_x, Cr_2O_3); as well as influence of catalyst preparation methods (sol, impregnation, co-impregnation, consecutive impregnation, flame pyrolysis) and different supports on the conversion and selectivities of chemical reactions (catalytic systems such as TiO_2-supported Au, hydrotalcite-supported Pt, PtSn, Pd, PdSn, Rh, RhSn, Ir and IrSn, alumina and silica supported vanadium were studied); dehydrogenation of propane over hydrotalcite-supported Pt, PtSn in steam-hydrogen atmosphere. The work presented here is the continuation of that work.

In this work emphasis is made on both modelling and experimental work. The work on modelling includes preparing the set of elementary equations; describing the route of the main products formation; developing the microkinetic model based on standard calculation techniques; computer simulation of the model and comparison of its result with the experimental results. The experimental work is focused on detection of the influence of the feed components concentration ratios (air, hydrogen, propane) on the results of dehydrogenation process. The comparison of responses for gas-phase reactions, and reactions carried over hydrotalcite-supported PtSn and Pt catalysts as well as with modelled result can give improved understanding of the reaction pathways and the catalyst features influencing/determining the observed results.

2 THEORY

2.1 REACTIONS AND THERMODYNAMICS

Different reactions of several types may occur in the system under consideration (a gas mixture of propane, oxygen and hydrogen). Some of these reactions can be dominant at low temperatures, others at high temperatures, making it difficult to compare the overall reaction results at different temperatures. Reaction thermochemistry data is from [10] and [11].

Dehydrogenation:

$$C_3H_8 \rightarrow C_3H_6 + H_2 \quad , \qquad \Delta H^0_{298} = 123.4 \ \ kJ/mol \qquad (2.1.1)$$

$$C_3H_6 \rightarrow C_3H_4 + H_2 \quad , \qquad \Delta H^0_{298} = 298 \ \ kJ/mol \qquad (2.1.2)$$

Oxidative dehydrogenation:

$$C_3H_8 + 1/2O_2 \rightarrow C_3H_6 + H_2O \quad , \qquad \Delta H^0_{298} = -117 \ \ kJ/mol \qquad (2.1.3)$$

Partial oxidation:

$$C_3H_8 + 3/2O_2 \rightarrow 3CO + 4H_2 \quad , \qquad \Delta H^0_{298} = -227 \ \ kJ/mol \qquad (2.1.4)$$

$$C_3H_8 + 7/2O_2 \rightarrow 3CO + 4H_2O \quad , \qquad \Delta H^0_{298} = -1194 \ \ kJ/mol \qquad (2.1.5)$$

$$C_3H_6 + 3O_2 \rightarrow 3CO + 3H_2O \quad , \qquad \Delta H^0_{298} = -1077 \ \ kJ/mol \qquad (2.1.6)$$

Combustion:

$$C_3H_8 + 5O_2 \rightarrow 3CO_2 + 4H_2O \quad , \qquad \Delta H^0_{298} = -2043 \ \ kJ/mol \qquad (2.1.7)$$

$$C_3H_6 + 9/2O_2 \rightarrow 3CO_2 + 3H_2O \quad , \qquad \Delta H^0_{298} = -1925 \ \ kJ/mol \qquad (2.1.8)$$

$$H_2 + 1/2O_2 \rightarrow H_2O \quad , \qquad \Delta H^0_{298} = -242 \ \ kJ/mol \qquad (2.1.9)$$

$$CO + 1/2\,O_2 \rightarrow CO_2 \quad , \qquad \Delta H^0_{298} = -283 \;\; kJ/mol \qquad (2.1.10)$$

Water-gas shift reaction:

$$CO + H_2O \rightarrow CO_2 + H_2 \quad , \qquad \Delta H^0_{298} = -41 \;\; kJ/mol \qquad (2.1.11)$$

Coke formation and gasification:

$$CH_4 \rightarrow C + 2\,H_2 \quad , \qquad \Delta H^0_{298} = 75 \;\; kJ/mol \qquad (2.1.12)$$

$$2\,CO \rightarrow C + CO_2 \quad , \qquad \Delta H^0_{298} = -172 \;\; kJ/mol \qquad (2.1.13)$$

$$C + 1/2\,O_2 \rightarrow CO \quad , \qquad \Delta H^0_{298} = -111 \;\; kJ/mol \qquad (2.1.14)$$

$$C + H_2O \rightarrow CO + H_2 \quad , \qquad \Delta H^0_{298} = 131 \;\; kJ/mol \qquad (2.1.15)$$

Cracking and hydrogenolysis:

$$C_3H_8 \rightarrow C_2H_4 + CH_4 \quad , \qquad \Delta H^0_{298} = 81 \;\; kJ/mol \qquad (2.1.16)$$

$$C_3H_8 + H_2 \rightarrow C_2H_6 + CH_4 \quad , \qquad \Delta H^0_{298} = 50 \;\; kJ/mol \qquad (2.1.17)$$

$$C_3H_8 + 2\,H_2 \rightarrow 3\,CH_4 \quad , \qquad \Delta H^0_{298} = -139 \;\; kJ/mol \qquad (2.1.18)$$

Steam reforming:

$$C_3H_8 + 3\,H_2O \rightarrow 3\,CO + 7\,H_2 \quad , \qquad \Delta H^0_{298} = 498 \;\; kJ/mol \qquad (2.1.19)$$

The reaction of propane dehydrogenation is endothermic and equilibrium limited, for higher conversions it requires high temperature and low pressure. Equilibrium conversion of propane at different pressures and temperatures is shown on Fig. 2.1.1.

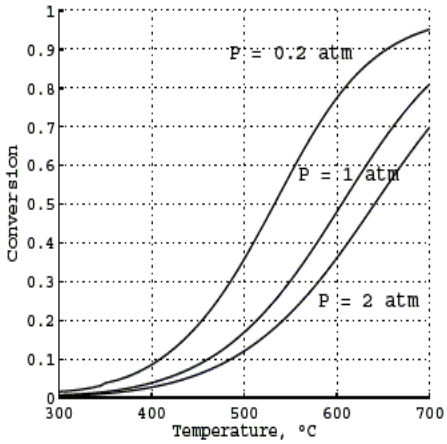

Fig. 2.1.1: Propane dehydrogenation equilibrium conversion at pressures 0.2, 1 and 2 atm.

2.2 HYDROGEN COMBUSTION

The reaction of hydrogen combustion over noble metals was one of the first catalytic processes studied. Despite of its seeming simplicity this process is continuously under research. Hydrogen combustion is an exothermic process and can be used as energy source for different appliances. The hydrogen and oxygen as fuels and water as product of the reaction makes this process very environmentally friendly. Hydrogen combustion plays an important role in fuel cells, electrolytic processes and as part of a complex catalytic processes.

A review of results of many studies on the hydrogen combustion process was made in [12]. The following is a summary of the findings in [12].

It was generally agreed that the Pt is the most active catalyst for the reaction and the reaction proceeds either via Langmuir-Hinshelwood (LH) mechanism or via the Eley-Rideal (ER) mechanism.

The adsorption of H_2 and O_2 influence each other and can be a rate limiting step for the overall reaction.

Hydrogen is dissociatively adsorbed on transition metal surfaces, and a successful adsorption event requires several surface atoms. Hydrogen adsorption is strongly

dependent on the surface coverages of both adsorbed hydrogen and oxygen. It is usually assumed to be adsorbed on a three-fold hollow site.

Oxygen is dissociatively adsorbed on transition metal surfaces. At elevated temperatures the formation of the surface metal oxide is possible. This can influence the further adsorption of H_2 and O_2 and the reaction of H_2 combustion. The kinetics of oxygen adsorption varies from metal to metal and from crystal plane to crystal plane. It can be adsorbed as O_2 molecule as a precursor for further dissociation.

The adsorption of water as a product of the reaction can influence the reaction kinetics. Water is physisorbed on unreactive surfaces such as Au. On metals with large heats of oxygen adsorption (W, Mo, Co etc.) water is dissociatively adsorbed.

Most reactive metals (for hydrogen combustion reaction, such as Pt etc.) bind oxygen weakly and do not dissociate H_2O. H_2O is bonded to surface by the O-atom, the water molecular structure is preserved. Preadsorbed oxygen blocks water adsorption. Water is weakly chemisorbed and desorbs at ~170 K. Whereas preadsorbed oxygen stabilises some oxygen-hydrogen containing surface complex to ~300 K. Preadsorbed hydrogen prevents the water adsorption (at 195 K).

The OH groups on the surface were detected in some studies and they are believed to be intermediates for the reaction.

The hydrogen is mobile on the platinum group metals at ambient temperatures while the oxygen is not. Oxygen on Pt achieves mobility at temperatures of a few hundreds of K.

At $T \gg 200$ K, water desorbs rapidly, the reaction is controlled by adsorption kinetics and surface mechanism in a complex way. At $T \gg 400$ K, at low pressure ($\leq 10^{-3}$ Pa) the major adsorbed component is O; for high pressure less is known about energetics and kinetics of adsorption and oxide overlayers can be considered.

At 298 K, dissociative adsorption of hydrogen can be a rate limiting step. There were signs that oxygen does not block sites for hydrogen chemisorption. Preadsorbed hydrogen blocks sites for oxygen adsorption and reduces reaction rate. Reaction

between preadsorbed H and O starts 170 K and has a maximum rate at ~200 K. The formation of water through direct interaction of $H_{2(gas)}$ and $O_{(ads)}$ as one of the possible reaction routes was reported (Eley-Rideal mechanism).

Increasing sticking coefficients (for H on different crystal planes) lead to increase in reaction rates. The reaction mechanism appears not to change in the range of 10^5~10^6 Pa. For supported catalysts the reaction rate in excess O_2 is independent on Pt particle size, whereas in hydrogen excess the reaction rate is highest for the most dispersed catalysts.

The observation of oscillations in the observed reaction rates on Pt were reported (under conditions of excess oxygen). It correlated to changes in the surface of the catalyst. This is also the case when adsorption energies or activation energies for reactions are dependent on surface coverages [12].

In [13] the detailed model of the catalytic reaction $H_2(g) + O_2(g) \leftrightarrow H_2O\ (g)$ on the Pt catalyst was described. In Fig. 2.2.1 the mechanism used is shown (the figure is from [13]).

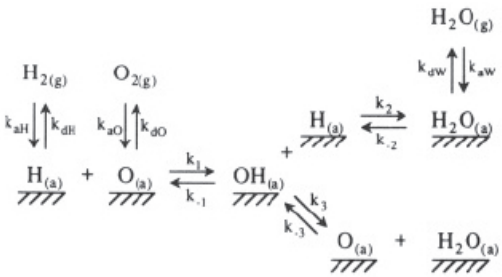

Fig. 2.2.1: Reaction mechanism for a catalytic reaction $H_2(g) + O_2(g) \leftrightarrow H_2O\ (g)$ [13].

The parameters for the kinetic model were fitted with the experimental simulations and the model showed good agreement with experimental results. The OH desorption measurements were used for the determination of the surface rate constants. The surface of the catalyst at high temperatures (1000~1800 K) was mostly uncovered and the limitation for the reaction was the adsorption of reactants. It was concluded that at low temperatures the reaction is limited by the availability of surface sites. The mechanism described here is used in some later models (e.g. [14]).

In [15] the numerical modelling of catalytic ignition was reported. It includes the surface mechanism together with gas phase mechanism. It was shown that there is a dependence of the ignition temperature of hydrogen-oxygen mixtures (and inert N_2) over palladium foil on the gas composition (at atmospheric pressure): the ignition temperature increases with increasing hydrogen concentration (approx. 50 °C at 30% H_2 to 87 °C at 70~80% H_2). The appropriate plot is shown in Fig.2.2.2 (the plot is taken from [15]). The ignition is dependent on coverage and adsorption-desorption reaction steps, it plays an important role in the overall kinetics of the process. A surface initially covered with oxygen gives immediate ignition, but a surface initially covered by hydrogen requires heating of the surface till ignition temperature. There is a transition from a kinetically controlled to a transport-limited regime during ignition.

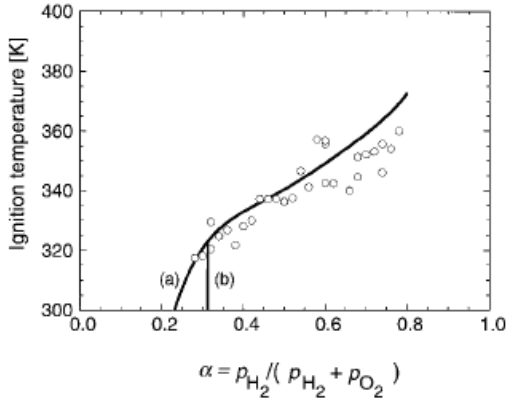

Fig. 2.2.2: Ignition temperature of H_2/O_2 mixtures on a palladium foil as a function of fuel concentration. Experimental (circles) and numerical results (line) [15].

The modelling of H_2/air mixtures ignition was reported in [16]. Fig. 2.2.3 (taken from [16]) shows the ignition temperature as a function of H_2/air composition.

The fuel-lean mixtures can ignite near or below room temperature. Very fuel-lean mixtures ignite upon contact with platinum. Ignition of fuel lean mixtures is caused by competition of surface sites. Reaction exothermicity is significant at high compositions. H_2 self-inhibits its catalytic ignition.

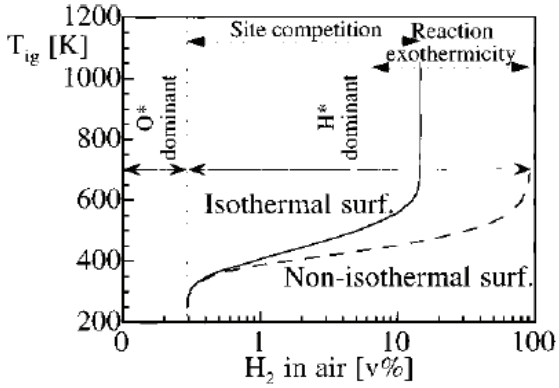

Fig. 2.2.3: Ignition temperature of H_2/air mixture at pressure of 1 atm when the surface temperature is the controlled parameter (an isothermal surface) and when the resistive power input is the controlled parameter (a nonisothermal surface). The dominant mechanism and the dominant surface species prior to ignition are indicated with arrows [16].

It was shown that the effect of preheating of the feed mixture on the T_{ign} is small (T_{in} increases → T_{ign} slightly decreases). Some suggestions were made on the mechanism of combustion. As the ratio H_2/air grows, the catalytic ignition increases due to blocking of Pt sites by H*. Upon ignition a transition occurs from H* blocked sites to O* blocked sites, this causes the transition in the dominant surface reaction of water formation from

$$\frac{1}{2}H_2 \overset{ads}{\leftrightarrow} H^* \overset{+O^*}{\rightarrow} OH^* \overset{+H^*}{\rightarrow} H_2O^* \qquad (2.2.1)$$

to

$$O_2 \overset{ads}{\rightarrow} 2O^* \overset{+2H^*}{\rightarrow} 2OH^* \rightarrow H_2O^* + O^*. \qquad (2.2.2)$$

The system shifts from a kinetics-limited regime at low surface temperatures to a transport limited regime after ignition. The competitive dissociative adsorption of H_2 and O_2, the desorption of H* and diffusion of O_2 and H_2 in a gas phase are the factors that most affect catalytic ignition.

The autothermal behaviour of Pt catalysed hydrogen oxidation was studied in [17]. Experimental and modelling results for both gas-phase and catalytic reactions were compared. The autothermal temperatures as a function of H_2/O_2 ratio (for different dilutions by N_2) were determined, shown in Fig. 2.2.4 (the figure is from [17]).

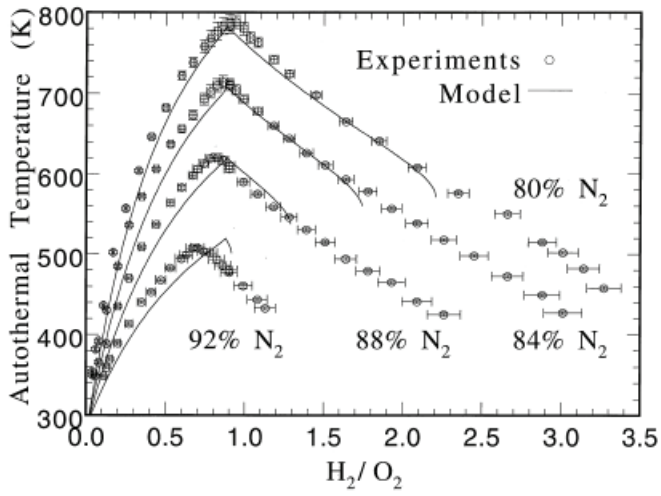

Fig. 2.2.4: Autothermal temperature as a function of H_2/O_2 ratio for atmospheric conditions at four different dilutions. Circles - experimental data with the associated error bars; solid lines - model prediction. As dilution decreases, autothermal temperatures increase, and the upper flammability limit is extended. A sharp maximum in autothermal temperature is seen at $H_2/O_2 < 1$ [17].

The shift of the maximum autothermal temperature from stoichiometric H_2/O_2 ratio 2 to ratio < 1 is explained by transport limitations. H_2/O_2 ratio in the bulk gas ≈ 0.88 corresponds to stoichiometric H_2/O_2 ratio above the catalytic surface. It was concluded that the catalyst-assisted homogeneous combustion behaviour through OH desorption (Pt acts as source of OH radicals) is the case in the H_2 deficient mixture and it is not important for H_2 excess mixtures. Autothermal behaviour that occurs after ignition is transport-controlled.

2.3 PROPANE DEHYDROGENATION

Commercial technologies for dehydrogenation of hydrocarbons have been developed [5], [18]. Among them are CATOFIN, Oleflex, STAR, Linde Process. The endothermic

character of the reaction (2.1.1) leads to some restrictions for the process - high temperatures (500~700 °C), low pressure (typically close to atmospheric pressure or even below). The side reactions (see Ch. 2.1) lead to deactivation of the catalyst by coke formation, this causes the necessity of frequent catalyst reactivation.

The Oleflex process is an adiabatic process in which the heat of the reaction (at 600~630 °C) is supplied by reheating the process stream between the different reaction stages. The process is operated at slight positive pressure (1.5~2 atm) and a proprietary Pt catalyst is used. Fresh propane is mixed with recycled hydrogen and unconverted propane and passed through a row of three radial-flow moving-bed catalytic reaction vessels. The process is continuous, overall selectivity for propene is 89~91%. The catalyst circulates through the reactor before passing to a regeneration vessel for coke removal by combustion in air. The regenerated catalyst passes to the first of dehydrogenation reactors. Propene is recovered by deethanizer-depropanizer splitting.

The CATOFIN process operates under a slight vacuum (~0.3 atm) at 550~750 °C. Adiabatic fixed-bed multiple reactors are used. The catalyst consists of activated alumina pellets impregnated with 18~20 wt% Cr. The process is cyclic, includes periods of reaction, discharge of reactor and in-situ regeneration of the catalyst (20~30 min). Multiple reactors are used in parallel (with asynchronous cycles of regeneration). Combustion of deposited coke during regeneration heats up the catalyst and this heat is used in dehydrogenation stage; additional heat from combusting fuel can also be used. The overall selectivity to propene is 87%. Propene is recovered by propane-propene splitter.

The Linde process operates at low reaction temperature and nearly isothermal conditions (minimization of cracking and coke formation). The chromium oxide catalyst in a fixed-bed tubular reactor is used. The catalyst has a relatively long cycle time before regeneration (9 h). The propane feed is not diluted with hydrogen or steam resulting in high selectivity (91%). Propane separation yields polymer-grade propene.

The STAR process (STeam Active Reforming) differs from other dehydrogenation processes. The steam is used as a diluent reducing partial pressure of propane and

hydrogen in a reactor. The process includes an oxydehydrogenation step [19]. The reactor consists of the section of the conventional steam active reforming process - the steam reformer - combined in series with an additional oxydehydrogenation section using the same catalyst for both sections. The process is performed isothermally in a chain of multiple fixed-bed reactors. The Pt supported by zinc and calcium aluminate is used as catalyst. Each reactor consists of multiple catalyst-packed tubes in a furnace which supplies heat to the catalyst. Reactor operation is cyclic (reactors are sequentially regenerated) and overall dehydrogenation is continuous. The catalyst deactivation is due to coke deposition, the dehydrogenation stage lasts 7 hrs for a reactor, off-line catalyst regeneration by combustion lasts 1 h. The yield of propene for the process is 80%. CO_2 must be removed from product stream before propene separation.

The Snamprogetti/Yarsintez FBD (Fluidised Bed Dehydrogenation) process uses a bubbling fluidized bed reactor-regenerator system [20]. The catalyst used is promoted chromia alumina. The reaction is carried out in a catalytic bubbling fluidized bed at 500~600 °C and 120~150 kPa. Reaction heat is supplied by the heat capacity of the solid catalyst, continuously circulating from the bottom of the reactor to the top of the regenerator and vice versa. The movements of gas and solid in the reactor and in the regenerator are countercurrent. In the regenerator, the initial performance of the catalyst is restored by burning the coke formed on it during the reaction.

Aside the problem of equilibrium limitation the deactivation of the catalyst due to coke formation is an important issue. Different studies on the coke deposition on Pt catalysts have been performed.

In [21], [22] (and others) the coke formation on $PtSn/Al_2O_3$ catalyst in propane dehydrogenation was studied. Two types of coke were identified - one formed on the metal and one formed on the support. Coke formed on the metal contains more hydrogen and the rate of its production depends on the propane pressure. The addition of H_2 to the feed greatly suppresses the coke formation but hydrogen does not remove the formed coke. The ratio H/C in the formed coke is 1.7~2, propylene promotes and hydrogen inhibits the formation of aromatic coke. The graphitization of coke on Pt

surface is low, coke contains mainly aliphatic hydrocarbons. The formation of C_6H_{12}* from two C_3H_6* intermediates was proposed as possible reaction of coke formation on Pt.

2.4 PROPANE DEHYDROGENATION AND SELECTIVE HYDROGEN COMBUSTION

The propane dehydrogenation is a highly endothermic reaction (2.1.1) favoured at high temperature and low pressure. Thus, severe coke deposition on the catalyst causing the necessity for frequent oxidative regeneration is a key feature.

In addition to the commercially available dehydrogenation processes based on Pt and Cr catalysts, oxygen-assisted processes, such as the combination of the exothermic propane oxidation with the endothermic thermal dehydrogenation at high temperatures [23], [24]; oxidative dehydrogenation of propane based on redox-type catalysts (e.g. VO_x - based catalysts) [25]; combination of endothermic propane dehydrogenation (DH - dehydrogenation) with exothermic oxidation of hydrogen (SHC - selective hydrogen combustion) (2.1.9) produced by dehydrogenation [26], [27] were suggested.

The idea of the latter approach is to supply heat for the propane dehydrogenation by in situ combustion of some of the hydrogen formed in the dehydrogenation reaction, and prevent coke formation on the catalyst . The increase of H_2 concentration limits the propene yield by increasing the rate of the reverse reaction. The removal of H_2 produced can shift the equilibrium of the dehydrogenation reaction towards the product side [28]. H_2 can be removed using membranes [29] or selective reactions consuming it. The selective hydrogen combustion can be used for this purpose. The heats of reactions (2.1.1), (2.1.9) can be balanced if approximately half of the hydrogen produced by dehydrogenation is combusted.

In another approach for oxygen-assisted dehydrogenation - oxidative dehydrogenation (2.1.3) the lattice oxygen atoms of the catalyst (usually metal oxides) participate in scission of C-H bonds [25], [30]. Oxidative dehydrogenation is not limited

thermodynamically, but it is limited by competitive oxidation reactions forming CO and CO_2.

Two schemes of a combination of SHC and DH processes were given in [26] and [27] (Fig. 2.4.1, taken from [26] and [27]): DH + SHC redox process mode operation and DH⟶SHC⟶DH co-fed process mode. In a second case the DH and SHC catalysts are physically mixed in one reactor; in a first case the DH and SHC catalysts are arranged in series, the SHC catalyst is kept in a high oxidation state by continuously co-feeding oxygen or air to the SHC reactor. In the stages with non-oxydative propane dehydrogenation zeolite supported Pt-Sn[AL]ZSM5 catalyst was used, for the SHC the In_2O_3/ZrO_2 catalyst was used. Problems arising from the suggested approaches are - necessity for periodic regeneration of reduced SHC catalyst in a redox mode or necessity for separation of O_2 coming from the SHC reactor (2nd stage) to DH reactor (3rd stage).

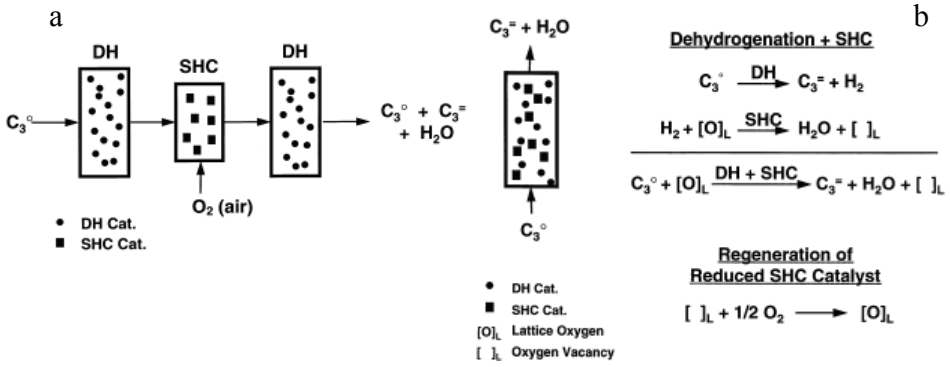

Fig. 2.4.1: Schematics of a) DH + SHC redox process mode operation and b) DH⟶SHC⟶DH co-fed process mode. In (b) the DH and SHC catalysts are physically mixed in one reactor; in (a) the DH and SHC catalysts are arranged in series, the SHC catalyst is kept in a high oxidation state by continuously co-feeding oxygen or air to the SHC reactor [26], [27].

Various catalytic systems were tested for dehydrogenation of propane paralleled with selective hydrogen combustion. Sb_2O_4, In_2O_3, WO_3 and Bi_2O_3 as SHC catalysts on supports SiO_2, Al_2O_3, TiO_2 and ZrO_2 together with PtSnZSM5 as DH catalyst were tested in [26]; Au/TiO_2 as well as Pt, PtSn, Pd, PdSn, Rh, RhSn, Ir, IrSn catalysts on hydrotalcite supports, V_2O_5 on SiO_2, Al_2O_3 supports as SHC+DH catalysts were tested

in [8]; In_2O_3, Bi_2O_3, MgVO, PbO_x, Cr_2O_3, Pt, PtSn on SiO_2 support as SHC+DH or SHC catalysts were tested in [7]; $Ce_{0.95}Cr_{0.05}O_2$ and $Ce_{0.97}Cu_{0.03}O_2$, where cerium oxide was used as oxygen carrying agent in the redox type experiments and Cu and Cr were used as dopants to increase the hydrogen combustion selectivity, were tested as SHC catalyst in [31]. The bimetallic catalysts Pt-M (M = Sn, Cu, Ag, Mg, Ce, La, Ni, Co, Au) were tested as SHC+DH catalysts for ethane, n-butane and iso-butane dehydrogenation in [24]. In [23] the Pt/SiO_2 catalyst was used as igniter for homogeneous gas-phase authothermal oxidative pyrolysis of propane leading to propene and ethene production. The Pt-based catalysts were among most active catalysts.

In [32] zeolite supported Pt/Na-[Fe]ZSM5 was used and the following results were shown. Alkane to alkene selectivities were ~97%, oxygen to water selectivities ~90%. It was easy to restore the initial catalyst activity by oxidative treatment. It was shown that C_2H_4 is formed in the cracking of propane and C_2H_6 is formed in the hydrogenation of C_2H_4, but not by hydrogenolysis of propane. Furthermore, it was suggested that CO_x compounds were formed predominantly in alkenes combustion reactions but not from alkanes. Deactivation of the catalyst was suggested to be due to carbon deposition via CO disproportionation or alkene oligomerization and aromatization reactions caused by high alkene and CO concentrations with the lack of H_2 presence. The staged oxygen introduction led to the combustion of H_2 with ~90% selectivity, alkene yields were higher than equilibrium by a factor of 1.6, whereas cofeed of the propane-oxigen mixtures led to combustion of hydrocarbons and oxygen consumption before the reaction with H_2.

In [28] $PtSn/SiO_2$ was used to combust hydrogen with ~80% selectivity at 550 °C and 90% selectivity at 500 °C as long as the oxygen flow was less than half the flow of hydrogen (stoichiometry to water formation). As soon as the oxygen flow exceeded the stoichiometric amount, the selectivity to CO_x increased. The comparison with Pt/SiO_2 was made here as well as the gas-phase reaction check. For the mixture $[O_2]$:$[C_3H_8]$:$[H_2]$=14:72:14 the oxygen conversion without catalyst achieved 10% at 550 °C, propane conversion was close to 0. For PtSn catalyst the presence of oxygen or

hydrogen was a factor that increased stability of the catalyst due to oxidation of coke or coke precursors and hydrogenation of coke precursors appropriately. The Pt catalyst is more active compared to PtSn but it deactivates faster, oxygen presence has a similar influence on both catalysts. Sn has a stabilising effect on the activity of the catalyst irrespective on the gas composition. H_2 addition enhanced the activity of Pt catalyst avoiding rapid initial coking. The cracking selectivity was lower for PtSn catalyst, but in excess (over stoichiometry with hydrogen) of oxygen it increased. As long as oxygen was fed to reactor at less than stoichiometric amount compared to fed hydrogen, oxygen selectively produced water. With excess of oxygen when the fed hydrogen reacted the rest of oxygen oxidised hydrocarbons (in non-selective manner) producing CO_xs. Pt showed worse selectivity to water even with sub-stoichiometric amounts of oxygen (below stoichiometry with hydrogen). For Pt the selectivity to hydrogen combustion was worse, CO_xs were produced even with amount of oxygen less than stoichiometric. In the CO_xs production the CO_2 was the main product, but with increase of O_2 flow on the Pt the CO selectivity decreased whereas for PtSn it increased. Pt performed higher activity in CO oxidation reaction. Selectivity to CH_4 was lower than expected for cracking to methane and ethylene, oxidation of CH_4 was suggested.

Membrane reactors can be used for the multi-step propane dehydrogenation with selective hydrogen combustion. Dense perovskite ceramic membrane reactor together with PtSn catalyst were described in [33]. With oxygen flow through a membrane the PtSn catalyst showed 74% propane conversion with 45% selectivity to propene at 705 °C. The transient analysis allowed the authors of [33] to make the following conclusions: oxygen species adsorbed on PtSn catalyst oxidises C_3H_8/C_3H_6 to CO, and they also participate in cracking propane to ethylene; H_2 interacts reversibly and probably dissociatively with the catalyst; the presence of gas-phase oxygen does not significantly influence the interaction of hydrogen with the catalyst; PtSn catalyst is not active for H_2 oxidation; PtSn catalyst dehydrogenates propane non-oxidatively.

In [8] it was shown that Pt-Sn catalysts on hydrotalcite supports behave well in processing the propane-hydrogen-oxygen gas mixture indicating good levels (in

comparison with other tested catalytic systems) of propane conversion, oxygen to water selectivity and propene yield.

2.5 HYDROTALCITE BASED CATALYSTS

Hydrotalcite is a natural mineral - layered double hydroxide (LDH) of general formula $Mg_6Al_2(CO_3)(OH)_{16}{\cdot}4(H_2O)$ (aluminum magnesium hydroxy carbonate). Synthetic hydrotalcite and hydrotalcite-like materials (also referred as anionic clays) are used in chemistry, medicine and biochemistry.

Hydrotalcites have a layered structure and consist of brucite-like $[Mg(OH)_2]$ layers with some of the divalent Mg^{2+} ions substituted by a trivalent cations Al^{3+}. The interlayer consist of carbonate CO_3^{2-} anions and water. The positive charge of layers is compensated by anions of interlayer [34].

The general formula of hydrotalcite-like compounds is the following:

$$[M(II)_{1-x}M(III)_x(OH)_2]^{x+}[A_{x/n}{}^{n-}]^{x-}\cdot mH_2O,$$

where M(II) and M(III) are divalent and trivalent cations, and A is the interlayer anion. Usually the cations are Mg^{2+} and Al^{3+}. Varying the divalent and trivalent cations and anions it is possible to synthesise a large class of structured materials with varied properties [34].

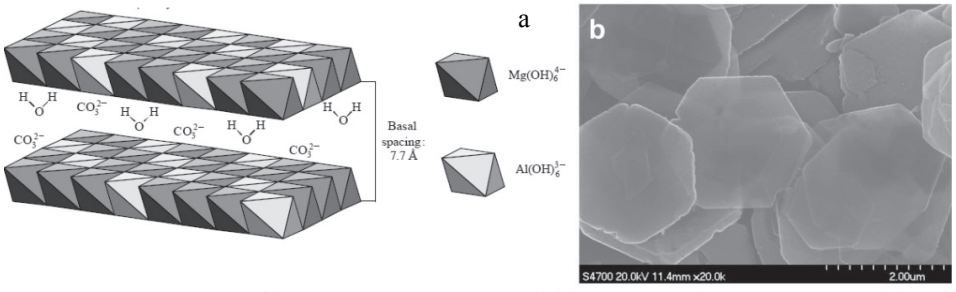

Fig. 2.5.1: The structure of hydrotalcite - like material (a); scanning electron microscope (SEM) image of typical LDH crystals (b).

A schematic representation of hydrotalcite-like materials [35] as well as scanning electron microscope (SEM) image of typical LDH crystals [36] is given on Fig 2.5.1.

If hydrotalcite is used as catalyst support precursor it is often treated by calcination. After calcination the structure of the material changes and has the following properties [34], [37]:

- fine pores and a high surface area
- basic properties
- fine dispersion of active metal ion
- memory effect - possibility to restore the initial structure of hydrotalcite after calcination by water treatment (for calcination below 500 °C when stable spinel $MgAl_2O_4$ start to form)

LDHs are used in commercial products as adsorbents for liquid ions and gas molecules, anion exchangers, acid residue scavengers, flame retardants and polymer stabilizers, in reactive separation applications [36], [38]. It is used in biology and medicine as component of drugs or as carrier for delivery of drug and genes into cells; as hardening and strengthing additives in concrete; in flame retardants; for water treatment (remove oxyanions from waste water); in catalysis as catalyst structured support precursors (with variety of structures: powders, films, with different microstructures) or standalone catalyst [36], [34].

Hydrotalcite-like materials can be treated in diverse ways such as calcination, rehydration, functionalisation; used as support for other catalytic materials. These forms are explored for various catalytic processes such as steam reforming, methanol and higher alcohol synthesis, base-catalyzed organic transformations, selective oxidation, $N_2O/NO_x/SO_x$ decomposition, hydrogenation, Fischer-Tropsch reaction, alkylation of phenol with alcohols and isomerization of allylic compounds, catalytic polymerization and aldol condensation reactions, selective oxidation reactions, synthesis of fine chemicals [34].

2.6 MODELLING

2.6.1 MATHEMATICAL MODELLING

The mathematical modelling is the representation of a real physical-chemical process (chemical technological process) by a set of mathematical relations (functions). The

aim of this procedure is to find a mathematical functional dependency of the rate of the process, or the rate constant, or the yield of the product on the affecting factors (technological, constructional, chemical, ...) [39].

The main factors that determine the process behaviour are concentrations of components, diffusion coefficients, temperatures and pressures in a reactor system, mixing rates, activity of a catalyst, densities of phases, viscosity coefficients, surface forces and geometrical characteristics of a reactor system. The relations between these factors and the process rate can be described with a different level of accuracy or generalisation.

The first step in the modelling is dividing the process into the related parts (levels) and researching all the objective laws (regularities) of these levels. In the mathematical description of every level the main, essential factors influencing the process should be considered. Meanwhile, it is important not to take into account an infinitude of secondary factors, which make the model unresolvable. The computational resources play a big role in the process of making decisions on the level of complexity of the planned modelling.

Studying the process by simple parts but not in the whole complexity is the usual way of model making. For a process description of a laboratory research reactor the following levels can be used:

- kinetic model – the complex of equations, describing dependences of reaction rates and surface coverages on composition, temperatures, pressures
- model of the process in the elementary volume of reactor (on one catalyst grain or particle). The elements of the model are mass transfer and heat transfer in the catalyst grain pores
- model of the process in the reaction volume – catalyst layer – taking into account mass transfer and heat transfer within this layer
- model of the reactor which consists of one or several reaction volumes – catalyst layer arrangements in a reactor

The model of every foregoing level is a constituent part of the next level and does not depend on its scale. Relations between levels are described by heat-balance and mass-balance equations. The analysis of mathematical description of the process includes

determination of concentration and temperature gradients in the system under consideration [39].

The efficiency of the process can be achieved with improvement on every level of the model. In some cases it can be a challenge to make the description of an experiment properly, with adequate description of the roles of every element of the reactor system.

2.6.2 MICROKINETIC ANALYSIS

The mathematical modelling of chemical kinetics consists of solution of the system of nonlinear ordinary differential equations of first order. The reaction rate constants are the coefficients in the system of differential equations.

The system of chemical kinetics equations can be written as follows:

$$\frac{dc_i}{dt} = f_i(c, k) \qquad (i = 1, 2, \ldots, n); \tag{2.6.2.1}$$

with initial conditions $c_i(0) = c_i^0$, where functions $f_i(c, k)$ represent sums of terms:

$k_q[c_i]^p[c_k]^s$,

where c_i - current concentrations; n - number of reactants; p, s - the order of reaction, k_q (q = 1, 2, ..., m) - reaction rate constants k^f_i, k^r_i - rate constants of forward and reverse reactions appropriately.

The solution for the system (2.6.2.1) is a function of time which depends on k_q as on parameters, i.e. $c_i = c_i(t, k)$ [40]. The system of equations (2.6.2.1) can be rewritten, it can be dependent on position in the reactor instead of time (as time of reaction is correlated with a position in reactor through flow rate).

These functions allow the investigation of the effects of reaction rate constants of different elementary reactions on the rate of overall reaction. For surface reactions the concentration term c_i in (2.6.2.1) is replaced by surface fraction θ_i.

There are two main types of mechanisms that describe the kinetics of surface catalytic reactions: Langmuir-Hinshelwood and Eley-Rideal mechanisms. In the Langmuir-

Hinshelwood mechanism it is assumed that all the species participating in a reaction are adsorbed on the surface and react in the chemisorbed state on the surface. In the Eley-Rideal mechanism it is assumed that one of the reactants react directly out of the gas phase without being adsorbed to the surface.

For the Langmuir-Hinshelwood mechanism of a general catalytic reaction:

$$A + B \xrightarrow{catalyst} AB\,, \tag{2.6.2.2}$$

the system of differential equations is derived as follows:

$$\begin{aligned}
&(1) \quad A + * \underset{k_1^r}{\overset{k_1^f}{\rightleftarrows}} \underset{*}{A} \\
&(2) \quad B + * \underset{k_2^r}{\overset{k_2^f}{\rightleftarrows}} \underset{*}{B} \\
&(3) \quad \underset{*}{A} + \underset{*}{B} \underset{k_3^r}{\overset{k_3^f}{\rightleftarrows}} \underset{*}{AB} + * \\
&(4) \quad \underset{*}{AB} \underset{k_4^r}{\overset{k_4^f}{\rightleftarrows}} AB + *
\end{aligned} \tag{2.6.2.3}$$

where (2.6.2.3) represent the elementary steps of a catalytic reaction (2.6.2.2) according to the Langmuir-Hinshelwood mechanism;

$$
\begin{aligned}
r_1 &= k_1^f \cdot p_A \cdot \theta_* - k_1^r \cdot \theta_A \\
r_2 &= k_2^f \cdot p_B \cdot \theta_* - k_2^r \cdot \theta_B \\
r_3 &= k_3^f \cdot \theta_A \cdot \theta_B - k_3^r \cdot \theta_{AB} \cdot \theta_* \\
r_4 &= k_4^f \cdot \theta_{AB} - k_4^r \cdot p_{AB} \cdot \theta_* \\
\theta_* &+ \theta_A + \theta_B + \theta_{AB} = 1
\end{aligned}
\qquad (2.6.2.4)
$$

and (2.6.2.4) are the rates of every elementary reaction (rate per site or a turnover frequency) together with balance of sites;

$$
\begin{aligned}
\frac{d\theta_A}{dt} &= r_1 - r_3 = k_1^f \cdot p_A \cdot \theta_* - k_1^r \cdot \theta_A - k_3^f \cdot \theta_A \cdot \theta_B + k_3^r \cdot \theta_{AB} \cdot \theta_* \\
\frac{d\theta_B}{dt} &= r_2 - r_3 = k_2^f \cdot p_B \cdot \theta_* - k_2^r \cdot \theta_B - k_3^f \cdot \theta_A \cdot \theta_B + k_3^r \cdot \theta_{AB} \cdot \theta_* \\
\frac{d\theta_{AB}}{dt} &= r_3 - r_4 = k_3^f \cdot \theta_A \cdot \theta_B - k_3^r \cdot \theta_{AB} \cdot \theta_* - k_4^f \cdot \theta_{AB} + k_4^r \cdot p_{AB} \cdot \theta_* \\
\frac{d\theta_*}{dt} &= -r_1 - r_2 + r_3 + r_4 = -k_1^f \cdot p_A \cdot \theta_* + k_1^r \cdot \theta_A - k_2^f \cdot p_B \cdot \theta_* + k_2^r \cdot \theta_B \cdot \\
&\quad + k_3^f \cdot \theta_A \cdot \theta_B - k_3^r \cdot \theta_{AB} \cdot \theta_* + r_4 + k_4^f \cdot \theta_{AB} - k_4^r \cdot p_{AB} \cdot \theta_*
\end{aligned}
\qquad (2.6.2.5)
$$

and finally (2.6.2.5) is a set of differential equations describing the coverage of species participating in the reaction [41].

Estimation of the rate constants of the elementary reactions and the surface coverages for a kinetic model can be based on various approaches. The microkinetic modelling combines different types of theoretical calculations and all the range of accessible experimental techniques to estimate the necessary parameters of a reactor system to be able to describe the reaction kinetics and predict the system behaviour [42].

Microkinetic studies incorporate the basic surface chemistry involved in the catalytic reaction. It gives an additional level to process description: model of the surface chemistry. This level serves as the origin for calculation of:

- sticking coefficients
- surface bond energies
- preexponential factors for surface reactions
- activation energies for surface reactions
- surface bonding geometries
- active site densities and ensemble sizes

The rate constant of the elementary reaction is often described by the Arrhenius equation:

$$k = A \cdot \mathrm{e}^{-\frac{E_a}{R \cdot T}} \qquad (2.6.2.6)$$

where A is a preexponential factor, E_a is activation energy, R is the gas constant, T is absolute temperature.

Collision theory and transition-state theory (TST) together with statistical mechanics can be used to estimate the preexponential factors utilising such properties of the reacting species as the translational, rotational and vibrational motions and their relation to the thermodynamic properties of the species.

The activation energies can be determined from experimental data - from the slope of the plot of $\ln(k)$ versus $1/T$. But for complex reaction mechanisms the experimental data describing every elementary reaction is not available, thus several theoretical techniques are used for the activation energy calculation. There are empirical correlations between activation energies and surface thermodynamic quantities (heats of adsorption). One of the semiempirical approaches is Unity bond index - quadratic exponential potential (UBI-QEP) [42], [43]. The UBI-QEP method gives a procedure for calculation of surface bond energies based on heats of formation ΔH_i of the reactants and products of the reaction, and subsequently the activation energies.

Different methods can be used in combination. For calculation of bond energies we can use quantum mechanical electronic structure methods (e.g. Density functional theory (DFT)), UBI-QEP; it can be measured experimentally (e.g. by calorimetry). Based on known surface bond energies the reaction energetics for surface reactions can be found by Monte Carlo statistical techniques, UBI-QEP, molecular dynamics, DFT [44].

Correlations based on chemical similarities between elementary reactions can be used for the estimation of kinetic parameters for cases when the calculations based on theories become too complicated. Thus the activation energies for families of reactions (like C-H bond formation/cleavage reactions, C-C bond formation/cleavage reactions) can be determined by the Evans-Polanyi correlations

$$E_{ai} = E_0 + \alpha \cdot \Delta H_i \quad , \qquad (2.6.2.7)$$

where E_0 and α are constants for the family of reactions [42].

2.6.3 TRANSITION STATE THEORY (TST)

The Transition state theory postulates that the reaction proceeds via an activated complex (transition state) and the energy of the activated complex is a maximum of the energy barrier between reactants an products [41]. Thus the reaction in TST is represented as:

$$R \leftrightarrow R^{\#} \rightarrow P \qquad (2.6.3.1)$$

where R is reactant, $R^{\#}$ is the activated complex and P is a product. The passage over energetic barrier can proceed only in forward direction, R is equilibrated with $R^{\#}$ and equilibrium constant is $K^{\#}$.

The equilibrium constant is expressed through partition functions of the reactants and the transition state, and the reaction rate constant can be expressed as:

$$k = \frac{k_B \cdot T}{h} \cdot K^{\#} = \frac{k_B \cdot T}{h} \cdot \frac{q_0^{\#}}{q} \cdot e^{-\frac{\Delta E}{k_B \cdot T}} \qquad (2.6.3.2)$$

where k_B is the Boltzmann constant, h is the Planck constant, $q^{\#}$ and q are molecular partition functions of the transition state and the reactants ($q = q_A \cdot q_B$ if two reactants are forming the activated complex) appropriately, ΔE is energy barrier.

The rate constant can be written in the thermodynamic form as well:

$$k = \frac{k_B \cdot T}{h} \cdot e^{\frac{-\Delta G_0^{\#}}{R \cdot T}} = \frac{k_B \cdot T}{h} \cdot e^{\frac{\Delta S_0^{\#}}{R}} \cdot e^{-\frac{\Delta H_0^{\#}}{R \cdot T}} , \qquad (2.6.3.3)$$

where $\Delta S_0^{\#}$ and $\Delta H_0^{\#}$ are entropy and enthalpy of reaction of formation of the activation complex.

Comparing this equation with the Arrhenius expression of the rate constant (2.6.2.6), and using the definition E_a [41]:

$$E_a = \Delta H_0^{\#} + R \cdot T \qquad (2.6.3.4)$$

it is possible to express the preexponential factor A as:

$$A_{TST} = \frac{e \cdot k_B \cdot T}{h} \cdot e^{\frac{\Delta S_0^{\#}}{R}} . \qquad (2.6.3.5)$$

where the entropy of the activation complex formation is:

$$\Delta S_0^{\#} = S^0_{AB^{\#}} - (S^0_A + S^0_B) \qquad (2.6.3.6)$$

The entropies of many compounds in a gaseous state are known [10], entropies of some radicals are also known or can be calculated [45]. The assumption about the approximate form (construction) of the transition state complex should be made in order to calculate the entropy of it. The molecular partition functions contribute to the

thermodynamic properties of molecules [46], [45]. The total entropy of gas-state species can be described through translational, rotational and vibrational contributions:

$$S^0_{tot} = S^0_{trans} + S^0_{rot} + S^0_{vib} \qquad (2.6.3.7)$$

Based on the assumed construction of the activated complex the partition functions of the activated complex can be found and the entropy derived [47].

In order to find the preexponential factors for the surface reactions the entropies of adsorbed species are to be known. It is possible to find it using the assumption that the adsorbed species differ from appropriate free species only in suppression of some types of molecular motion, and calculating appropriate changes in the partition functions of translational, vibrational and rotational motions [42].

For an adsorbed species immobile on the surface the translational motion can be neglected. Thus the entropy S_{loc} of adsorbed species can be described through gas-phase species entropies (known from literature) and translational contribution S_{trans} calculated by statistical mechanics:

$$S^0_{loc} = S^0_{rot} + S^0_{vib} = S^0_{tot} - S^0_{trans} \qquad (2.6.3.8)$$

Using the Sackur-Tetrode equation [46] the translational contribution S_{trans} can be found as:

$$S_{trans} = R \cdot \left(\frac{3}{2} \cdot \ln(Mr) + \frac{5}{2} \cdot \ln(T) - \ln(P) - 1.1650 \right) , \qquad (2.6.3.9)$$

where Mr is molar mass, T is absolute temperature [K] and P is a pressure [atm].

2.6.4 UBI-QEP PHENOMENOLOGICAL METHOD

The unity bond index - quadratic exponential potential method is a theoretical technique for determining metal surface reaction energetics. It gives the heats of

adsorption of molecules to a surface and reaction activation energies (barriers). The method is fully described in [43]. Some generalisation and refinements are given in [48], [49].

UBI-QEP needs as input only atomic heats of adsorption and gas-phase molecular bond energies. The UBI-QEP technique is constructed on information deduced from observable phenomena. It postulates that: 1) in a many-body system, all forces are spherical and depend on distance only; 2) each two-body A-B interaction is described by a Morse potential ($E(x(r)) = a(x^2(r) - 2x(r))$), where the variable $x(r)$ is A-B bond order depending on the bond distance r ($x(r) = \exp[-(r - r_0)/b]$), where a is the A-B bond energy at the equilibrium distance r_0, , x_0 is equilibrium bond order, b is distance scaling constant; 3) in a many-body system the total bond order X of all interacting two-center bonds is conserved at unity ($X = \Sigma x_i = 1$).

In these definitions the "body" means an atom or group of atoms that can be treated as a single element. Within the method the heats of chemisorption and reaction activation barriers are independent of the choice of $x(r)$ but depend only on the energy parameters a_i which are thermodynamic observables obtained from atomic chemisorption energies Q_A and gas-phase molecular bond energies D_{AB}.

To use the following formulas for the calculation of adsorption heats it is first necessary to determine the expected form of the adsorbate, the binding site and determine the atom (atoms) that will be the contact atoms interacting with the surface atoms. The contact atoms interact with a certain number n of surface atoms, this number depends on the type of binding site and type of surface (crystal plane). For on-top binding site n=1, for bridging n=2, for fcc(111) hollow n=3, for fcc(100) hollow n=4.

The following formulas are used for surface reaction energetics calculations.

The atomic heat of adsorption ([43], 4.1.2):

$$Q_A = Q_{0A} \cdot \left(2 - \frac{1}{n}\right) \qquad (2.6.4.1)$$

where Q_A is the atomic binding energy, n - the number of metal atoms defining the binding site, Q_{0A} - strength of two-center metal-atom interaction.

Heat of adsorption for mono-coordinated, closed-shell molecules with on-top binding site (n = 1) ([43], 4.2.1.4), weak binding:

$$Q_{AB}=\frac{Q_{0\mathrm{A}}^2}{Q_{0\mathrm{A}}+D_{AB}} \qquad (2.6.4.2)$$

The binding energy for homonuclear diatomics with di-coordination and on-top sites for adatoms ([43], 4.2.1.10):

$$Q_{A2}=\frac{9\cdot Q_{0\mathrm{A}}^2}{6\cdot Q_{0\mathrm{A}}+16\cdot D_{A2}} \qquad (2.6.4.3)$$

Heat of adsorption for high-coordinated sites molecules (n = 2,3..) ([43], 4.2.2.4), strong binding:

$$Q_{AB}=\frac{Q_A^2}{Q_A+D_{AB}} \qquad (2.6.4.4)$$

Heat of molecular chemisorption at medium binding ([43], 4.2.3.1):

$$Q_{AB}=\frac{1}{2}\cdot\left(\frac{Q_{0\mathrm{A}}^2}{\frac{Q_{0\mathrm{A}}}{n}+D_{AB}}+\frac{Q_A^2}{Q_A+D_{AB}}\right) \qquad (2.6.4.5)$$

where D_{AB} - gas-phase bond energies.

The definition of D_{AB} is the enthalpy of the gas-phase reaction that breaks the A-B bonds ([43], 4.3.1.1):

$$B_1-A-B_{2g}\rightarrow B_{1\mathrm{g}}+A_g+B_{2\mathrm{g}} \qquad (2.6.4.6)$$

$$\Delta H^0_{react}=\sum\Delta H^0_f(products)-\sum\Delta H^0_f(reagents) \qquad (2.6.4.7)$$

For asymmetric di-coordination of polyatomic adsorbates A and B represents dissimilar atom groups ([43], 4.2.1.7 - 4.2.1.9):

$$Q_{AB} = \frac{a \cdot b \cdot (a+b) + D_{AB} \cdot (a-b)^2}{a \cdot b + D_{AB} \cdot (a+b)} \qquad (2.6.4.8)$$

$$a = \frac{Q_{0A}^2 \cdot (Q_{0A} + 2 \cdot Q_{0B})}{(Q_{0A} + Q_{0B})^2} \qquad (2.6.4.9)$$

$$b = \frac{Q_{0B}^2 \cdot (Q_{0B} + 2 \cdot Q_{0A})}{(Q_{0A} + Q_{0B})^2} \qquad (2.6.4.10)$$

where Q_{0A} and Q_{0B} are heats of adsorption of pseudo-atom groups A and B in the on-top site ([43], 4.3.2.2.1):

$$Q_{0A} = \frac{Q_{0a}^2}{Q_{0a} + D_i} \qquad (2.6.4.11)$$

where Q_{0a} is the Q_0 value for the contact atom in the A fragment and D_i is the enthalpy required to break the bonds between the contact atom and the rest of the atoms in fragment A.

The intrinsic activation barriers for surface reactions of different types are calculated as follows.

For the dissociation reaction AB ⟶ A + B ([43], 4.6.1.10):

$$\Delta E = \frac{1}{2} \cdot \left(Q_{AB} + D_{AB} - Q_A - Q_B + \frac{Q_A \cdot Q_B}{Q_A + Q_B} \right) \qquad (2.6.4.12)$$

For the recombination reaction A + B ⟶ AB:

$$\Delta E = \frac{1}{2} \cdot \left(Q_A + Q_B - Q_{AB} - D_{AB} + \frac{Q_A \cdot Q_B}{Q_A + Q_B} \right) \qquad (2.6.4.13)$$

For the disproportionation reaction A + BC ⟶ AB + C (where $D_{BC} > D_{AB}$) ([43], 4.6.2.2):

$$\Delta E = \frac{1}{2} \cdot \left(Q_A + Q_{BC} + D_{BC} - D_{AB} - Q_{AB} - Q_C + \frac{Q_{AB} \cdot Q_C}{Q_{AB} + Q_C} \right) \qquad (2.6.4.14)$$

For some of the reactions of type A + B ⟶ AB, where B do not only form a bond with polyatomic A, but also changes bonds in A, (for example CO + O ⟶ CO_2) we use for D_{AB} the following expression ([43], 4.6.3.2):

$$D_{AB} = \sum_b D_b - \sum_f D_f \ , \qquad (2.6.4.15)$$

where D is the gas-phase bond enthalpy for bonds broken D_b and bonds formed D_f.

The UBI-QEP is widely used for the modelling of surface processes in many catalytic applications: modelling the water-gas shift (WGS) reaction on Cu(111) [50]; prediction of catalytic activity of different metal surfaces in a WGS reaction [51]; surface reaction mechanism for CO oxidation on Pt [52]; modelling of the formation of C_1 and C_2 products in the Fischer–Tropsch synthesis over cobalt catalysts [53]; modelling the ethane hydrogenolysis on Pd, Pt, Ni surfaces [54]; and other applications.

2.6.5 THERMODYNAMIC CONSISTENCY

For the catalytic cycle (2.6.2.3) it is necessary to be sure that the reaction steps are thermodynamically and stoichiometrically consistent. The number of sites occupied in the adsorption and dissociation steps must be equal to the number of sites freed in the formation and desorption steps [41].

The values of preexponential factors as well as the values of activation energies used for reaction rate constants determination are to be constrained by two thermodynamic relationships [42], [55]:

$$E_i^r = E_i^f - \Delta H_i^0 \ , \qquad (2.6.5.1)$$

$$A_i^r = A_i^f \cdot e^{\frac{\Delta G_i^0 - \Delta H_i^0}{R \cdot T}} \qquad (2.6.5.2)$$

where E_i^f and E_i^r are forward and reverse activation energies for every *i* elementary reaction, A_i^f and A_i^r are appropriate preexponential factors, ΔH_i^0 and ΔG_i^0 are the standard enthalpy and Gibbs free energy changes in reaction *i*.

In addition there are constraints for the overall mechanism of reaction. The sum of activation energies of elementary reactions composing the route from reactants to products must equal the heat of the net reaction:

$$\sum_{i=1}^{n} \sigma_i \cdot E_i^f - \sum_{i=1}^{n} \sigma_i \cdot E_i^r = \Delta H_{net}^0 \quad , \qquad (2.6.5.3)$$

where σ_i are the stoichiometric Horiuti numbers of elementary steps in a reaction path (coefficients in the linear combination of the elementary steps leading to the overall reaction).

The products of the appropriate preexponential factors of elementary reactions are related to the standard entropy change of the overall reaction:

$$\prod_{i=1}^{n} \left(\frac{A_i^f}{A_i^r} \right)^{\sigma_i} = \mathrm{e}^{\frac{\Delta S_{net}}{R}} \quad , \qquad (2.6.5.4)$$

The problem with the thermodynamic consistency of large mechanisms arises when the parameters for reaction rate constants are determined by methods that do not take into consideration the thermodynamic properties [52]. For example, when preexponential factors are fitted according to experimental data this fitting procedure must include constraints (2.6.5.2) and (2.6.5.4).

The preexponential factors derived by using the TST and activation energies derived by using the UBI-QEP are thermodynamically consistent. This follows from the approaches of these methods (thermodynamic properties such as enthalpies and entropies are important elements of its equations).

The activation energies (2.6.4.12) and (2.6.4.13) are activation energies of the same reaction but for forward and reverse directions appropriately. Rewriting it in a different form gives the constraint (2.6.5.1) [43]:

$$\begin{aligned} E^f &= \frac{1}{2}\cdot\left(\Delta H^0 + \frac{Q_\alpha \cdot Q_\beta}{Q_\alpha + Q_\beta}\right); \\ E^r &= \frac{1}{2}\cdot\left(-\Delta H^0 + \frac{Q_\alpha \cdot Q_\delta}{Q_\alpha + Q_\delta}\right) = E^f - \Delta H^0; \end{aligned} \qquad (2.6.5.5)$$

For the TST preexponential factors the situation is similar.

For a simple reaction

$$A \overset{S_A}{\rightarrow} A^{\#} \overset{S_A^{\#}}{\rightarrow} B \overset{S_B}{} \qquad (2.6.5.6)$$

the entropy change can be expressed in a following way:

$$\begin{aligned} \Delta S &= S_B - S_A; \\ \Delta S_f^{\#} &= S_A^{\#} - S_A; \\ \Delta S_r^{\#} &= S_A^{\#} - S_B; \end{aligned} \qquad (2.6.5.7)$$

Using the relation (2.6.3.5) for a TST preexponential the constraint (2.6.5.2) can be derived:

$$\frac{A^f}{A^r} = \frac{\frac{e\cdot k_B \cdot T}{h}\cdot e^{\frac{\Delta S_f^{\#}}{R}}}{\frac{e\cdot k_B \cdot T}{h}\cdot e^{\frac{\Delta S_r^{\#}}{R}}} = e^{\frac{S_A^{\#} - S_A - (S_A^{\#} - S_B)}{R}} = e^{\frac{\Delta S}{R}} \qquad (2.6.5.8)$$

It is necessary to know the exact mechanism of the reaction under modelling and appropriate Horiuti numbers if the case is solved in the steady-state conditions (the changes of concentrations in a system (2.6.2.5) are equal 0) and the system of equations (2.6.2.5) becomes a system of algebraic equations. If the chemical system is described as

a system of differential equations with a set of initial conditions and the solution depends on time and rate constant, it is possible that some of the concentrations do not change in time and some of reactions do not participate in a mechanism. If the mechanism includes more than one route to products and with changes in rate constants (e.g. with temperature) different routes are active, it becomes difficult to check the constraints (2.6.5.3) and (2.6.5.4).

3 MICROKINETIC MODEL

3.1 REACTION MECHANISM

First we define the reaction mechanism (set of elementary steps) for propane dehydrogenation reaction in the presence of O_2 over a Pt catalyst. According to the experimental observations the reaction mechanism should include routes to formation of H_2O, CO, CO_2, C_3H_6, C_2H_4, C_2H_6, CH_4, H_2 (as main products of the reaction). In addition different types of coke (C_xH_y) can be suggested. It is possible to find different models of similar types of reactions in the literature. Microkinetic models that include surface reactions where species containing C_1, C_2, H and O elements participated can be found e.g. in [56] (methane partial oxidation, reforming, combustion, oxygenate decomposition and oxidation on platinum), [57] (ethylene hydrogenation and ethane hydrogenolysis on Pt), [14] (H_2 oxidation over Pt), [52] (CO oxidation on Pt), [54] (ethane hydrogenolysis on metals), [53] (formation of C_1 and C_2 products in the Fischer–Tropsch synthesis over cobalt), [50] (water–gas shift reaction on Cu).

We use a similar approach as is in the above mentioned literature. For the set of elementary steps the reaction rate constants are calculated (defined in the Arrhenius form). We use the UBI-QEP method for the activation energies calculation and TST for the preexponentials calculation (the theory is in Chapters 2.6.2 - 2.6.4).

The set of proposed elementary reactions is shown in Table 8.2.4.1. Reactions containing C_1, C_2, H and O elements are taken from the above mentioned literature. For C_3 compounds the shortest concurrent routes to products were chosen. The following describes principles that were used for preparation of the set of elementary reactions.

The basic data for UBI-QEP are enthalpies of formation of gas-phase species (Table 3.1.1) participating in a reaction as well as the atomic binding energies (Table 8.1.2.3). In Table 3.1.1 the enthalpies of formation from different sources are combined. Since the enthalpy data is not available for all surface species under

consideration (appropriate gas-phase species) in standard tables, it was necessary to use calculation techniques for the evaluation of the missing data. The calculated values are given in the table in the two last columns (see description below).

For the calculation of the enthalpies the group additivity method (GAM) was used. The group additivity values (GAV) assigned to parts of molecules are summed up to give the enthalpies. The calculation procedure is described in Chapter 3.2.1 . For the first column of calculated values GAVs from [58] were used, for the second column of calculated values (last column in the table) GAVs from [59] were used.

We can see that values calculated by the method described in [58] are close to experimental values in the same source, but both are a bit different from values from other sources. This is because the group additivity values were estimated by use of data they have. By using group additivity values from [59] we get values close to the ones presented in the second column of the table (experimental values in the same source).

Table 3.1.1: Gas phase thermochemistry data. Enthalpy of formation in gas phase at standard conditions (T = 298.15 K; P = 1 atm).

Molecule/Radical	**$\Delta H_{f\ 298,15}^{0}$, [kJ/mol]**					
	From [11]	**From [60]*[a], [59]**	**From [61]*[d]**	**From [58]**	**Calc. (see Ch. 3.2)**	
$CH_3CH_2CH_3$	**−104.680**					
$CH_3CH_2\dot{C}H_2$	**100.500**	100±2		88	85.7	98
$\dot{C}H_2CH_2\dot{C}H_2$				**280.3**	275.2	300.5
$CH_3CH_2C{:}H$					**321**	
CH_3CH_2-C						
$CH_3\dot{C}HCH_3$	**93.300**	88±3		79.9	72.5	87.9
$CH_3\dot{C}H\dot{C}H_2$		20.1**			262.1	**290.4**
$CH_3\dot{C}HC{:}H$					**497.4**	
$CH_3\dot{C}H$-C						
$CH_3C{:}CH_3$					**295.8**	
$CH_3C{:}\dot{C}H_2$					**485.4**	

Molecule/Radical	$\Delta H_{f^0_{298,15}}$, [kJ/mol]					
	From [11]	From [60]*[a], [59]	From [61]*[d]	From [58]	Calc. (see Ch. 3.2)	
$CH_3C{:}C{:}H$					**720.7**	
$CH_3C{:}\text{-}C$						
$CH_3CH{=}CH_2$	**20.000**					
$\dot{C}H_2CH{=}CH_2$	**163.594**	171.0±3.0		164.8	159.3	
$C{:}HCH{=}CH_2$		388.1**			**446.6**	
$CH_3\dot{C}{=}CH_2$		**231.4**		243	161	
$\dot{C}H_2\dot{C}{=}CH_2$		190.7**			**350.5**	
$CH_3CH{=}\dot{C}H$		**267±6**		237.2	243.4	267.4
$CH_3\dot{C}{=}\dot{C}H$		185.0**			**382.6**	
$CH_3CH{=}C{:}$					**381.6***	
$\dot{C}H_2C{\equiv}CH$		**339.0±4.2**		341	337.6	
$C{:}HC{\equiv}CH$				**586**	572.9	
$CH_3C{\equiv}\dot{C}$		**515±13**				524.3
CH_3CH_3	**−83.852**		−84.000			
$CH_3\dot{C}H_2$	**118.658**	118.8±1.3	107.000	113.0	107.5	118.9
$CH_3C{:}H$				**366.1**	342.8	
$CH_3\text{-}C$						
$\dot{C}H_2\dot{C}H_2$		52.3**		300.2	297	**321.4**
$\dot{C}H_2C{:}H$		298.6**			**532.3**	
$\dot{C}H_2\text{-}C$						
$C{:}HC{:}H$					**767.6**	
$CH{\equiv}CH$	**228.2**		227.4			
$CH{\equiv}\dot{C}$	**566.200**	567.4±2.1	569.000	565.0		566.1
$C{\equiv}C$	**830.457**	817±8*[b]	830.457			904
$CH_2{=}CH_2$	**52.500**		52.400			
$CH_2{=}\dot{C}H$	**299.687**	299.6±3.3		284.5	276	309.2
$CH_2{=}C{:}$	**414.788**	419.7±16.7		397.0±14.6	[414]	
$\dot{C}H{=}\dot{C}H$		228.0**			497.6	**546.4**
$\dot{C}H{=}C{:}$		567.0**			**635.8***	
CH_4	**−74.600**		-74.600			

Molecule/Radical	$\Delta H_{f^{298,15}}^{0}$, [kJ/mol]					
	From [11]	From [60]*a, [59]	From [61]*d	From [58]	Calc. (see Ch. 3.2)	
$\dot{C}H_3$	**146.658**	146.7±0.3	146.300	146.0		
C:H_2	**390.365**	391.2±1.6^{t}, 428.8±1.6^{s}	390.421	390.4±4.0		
CH	**597.371**	595.8±0.6	597.370			
C	**716.680**	716.68±0.45	716.680			
H_2	**0.000**		0.000			
H	**217.999**	217.998±0.006	217.998			
O_2	**0.000**		0.000			
O	**249.175**	249.229±0.002	249.180			
CO_2	**−393.510**		- 393.510			
CO	**−110.535**		−110.530			
H_2O	**−241.826**		- 241.826			
$\dot{O}H$	**37.278**	37.36±0.13	39.349			
$CH_3\dot{O}$	**13.000**	21.0±2.1	13.000	14.6		21
HC(O)$\dot{O}$		**−129.7±12.6**^{*b}		−157.7		−71.5
H$\dot{C}$(O)	**42.398**	42.5±0.5	42.000	41.8		41.8
HC:OH						
HC:$\dot{O}$						
:C=O		**−112.3****				
$\dot{C}H_2\dot{O}$		- 108.7		**188.7**	186.1	
CH_2=O	**−108.6**	- 108.6				
$\dot{C}H_2$OH		**−17.0±0.7**				
$\dot{C}$(O)OH	**−213.000**	−194.6±2.9^{tr}, −219.7^{cis}	−213.000	−223	−215	−192.5
$\dot{C}$(O)$\dot{O}$		**- 393.7**				
HO$\dot{O}$		**12.30±0.25**	9.689			

*a on pp. 9-69, 9-79, 9-82, 9-83, 9-89; *b [59], on pp. 1460, 1471, 1472; *d on pp. 161, 166, 202, 213; *c ; t triplet; s singlet; tr trans-; cis cis-; ** calculated (based on dissociation bond energies from [59], see Table 3.1.2); * calculation is based on GAV derived from value for similar radical in [] brackets in the same column. Data from [11] and [61] is data approximated by polynomials, data in [60], [59], [58] is compiled from different sources of experimental data. Chosen for further calculations values are bold faced. Some values of enthalpy of formation can be found in [10].

For further calculation we choose values from the first column of the table, because we can get values for appropriate species over a wide range of temperatures. For species where we lack information in this source we use values from the second column (here it is possible to find temperature dependence through C_p [45]). For the rest of the species we use values calculated by GAM using GAVs from [59], and for the rest with GAV from [58]. The values used in the model are bold faced.

The enthalpies from Table 3.1.1 are used for calculation of the bond dissociation energies (BDEs) needed for calculation of the reaction activation energies. Furthermore, the enthalpies are used for calculation of gas-phase bond energies D_{AB} according to (2.6.4.7), which are then used for the calculation of adsorption energies.

The adsorption energies together with appropriate D_{AB}s are shown in Table 8.2.3.1. The complete calculation procedure is also given there.

In Table 3.1.2 we list the BDEs. The values from literature sources are given there as well. Calculated values are similar to values in literature, but unfortunately not all necessary bond energies are available for comparison.

In the model we do not use such adsorbate as propylene adsorbed to the surface by the CH_3- group, whereas there is available data about appropriate radicals (see Table 3.1.2) and they possibly participate in the reaction.

Using BDEs from [59] we can derive enthalpies of formation for some of the radicals (these derived values are denoted by ** in Table 3.1.1). Calculations for Table 3.1.2 are made in two ways - using enthalpy values derived as mentioned above (in the table these are values between () parentheses), and using enthalpy values from other sources and from group additivity calculations. Thus we have two sets of BDEs, the first of which looks more reliable because it is to a larger extent based on experimental reference data. But at closer investigation we can see that enthalpies of some of the species used in this first set have the following dependencies:

ΔH_f^0 ($\dot{C}H_2$-$\dot{C}H_2$) = ΔH_f^0 (CH_2=CH_2) ≈ 52 [kJ/mol],
ΔH_f^0 (:C=O) = ΔH_f^0 (CO) ≈ -110 [kJ/mol],
ΔH_f^0 ($\dot{C}$H=C:) = ΔH_f^0 (CH≡$\dot{C}$) ≈ 566 [kJ/mol], *(3.1.1)*
ΔH_f^0 ($\dot{C}H_2$C:H) = ΔH_f^0 (CH_2=$\dot{C}$H) ≈ 299 [kJ/mol],
and similar link between some other sets.

The question is how correct this can be for surface reactions where we expect the species (like $\dot{C}H_2$-$\dot{C}H_2$ and CH_2=CH_2) to be different. We also have one case where we can compare values from two sets, in the first set it was derived as mentioned above, in the second set it is an experimental value from literature: for $\dot{C}H_2\dot{C}H_2$, ΔH_f^0 (1) = 52.3; ΔH_f^0 (2) = 300.2 (see Table 3.1.1), a substantial difference.
We need to make a decision about which set to use, and we use second set (values without parentheses) for further calculation of reaction energetics (used values in Table 3.1.1 are marked appropriately). We make such decision because we are not satisfied with the fact of equality of the enthalpies for different species in the first set (3.1.1).

Table 3.1.2: Bond dissociation energies for use in reaction activation energy procedure (in Table 8.2.4.1); calculated by (3.2.1.1) from enthalpies of formation (Table 3.1.1), and values based on experimental data ([60], pp. 9-70, 9-67; [59], pp. 134-154, 205-207; [62], pp. 309, 444-470).

Bond	D^0_{298} [kJ/mol] (calc)	D^0_{298} [kJ/mol] [60], [59]	D^0_{298} [kJ/mol] [62]
$CH_3CH_2CH_2$-H	**423.2**	422.2±2.1	422.0
$CH_3CH_2\dot{C}H$-H	**438.5**		
CH_3CH_2C:-H	--		
CH_3CH(-H)CH_3	**416**	410.5±2.9	412.0
$CH_3\dot{C}$(-H)CH_3	**420.5**		
CH_3CH(-H)$\dot{C}H_2$	**407.9** (137.6)	138.1±2.5	138.7
$CH_3\dot{C}H\dot{C}$H-H	**425**		
CH_3CH=CH-H	**465**	464.8	
CH_3C(-H)=CH_2	**429.4**		459.0

Bond	D^0_{298} [kJ/mol] (calc)	D^0_{298} [kJ/mol] [60], [59]	D^0_{298} [kJ/mol] [62]
CH_2(-H)CH=CH_2	**361.6**	369±3	368.0
$CH_3\dot{C}HC$:-H	--		
$CH_3\dot{C}$(-H)C	--		
$CH_3\dot{C}$(-H)$\dot{C}H_2$	**413**		
CH_3C:$\dot{C}$H-H	**453.3**		
CH_3C:C:-H	--		
$CH_3\dot{C}HCH_2$-H	**415.1** (144.8)	150.2±3.3	148.7
CH_3CH(-H)C:H	**394.4**		
$CH_3\dot{C}$(-H)C:H	**441.3**		
CH_3C(-H)=$\dot{C}$H	**333.6** (136)	136.0±6.3	
$CH_3\dot{C}$=CH(-H)	**369.2** (171.6)		142.0
CH_2(-H)$\dot{C}$=CH_2	**337.1** (177.3)	177.0±8.4	
$\dot{C}$H(-H)CH=CH_2	**501** (442.5)	435.1±14.2	
$\dot{C}H_2C$(-H)=CH_2	**404.9** (245.1)	237.7±3.3	
CH_3CH(-H)C	--		
CH_3C:CH_2-H	**407.6**		
$CH_3\dot{C}$H-H	**465.4**		
CH_3C:-H	--		
CH_2(-H)C	--		
$\dot{C}$H(-H)C	--		
CH(-H)=C:	**439.0** (370.2)	365.3±16.7	
CH(-H)=$\dot{C}$H	**464.7** (146.3)	146.4±3.8	145.7
C:(-H)C	--		
C(-H)≡$\dot{C}$	**482.3**	467.6±8.8	
CH_2(-H)C:H	**384.2**		
CH_2(-H)$\dot{C}H_2$	**420.7** (151.6)	151.5±1.3	150.4
$\dot{C}H_2\dot{C}$H-H	**428.9**		
CH_2=CH-H	**465.2**	464.2±2.5	464.0
CH_2=$\dot{C}$-H	**333.1**	338.1±16.7	
$\dot{C}H_2C$:-H	--		
$\dot{C}$H(-H)C:H	**453.3**		

Bond	D^0_{298} [kJ/mol] (calc)	D^0_{298} [kJ/mol] [60], [59]	D^0_{298} [kJ/mol] [62]
C:HC:-H	--		
CH≡C-H	**556**	557.81±0.30	548.0
CH_3CH_2-H	**420.6**	420.5±1.3	422.0
CH_3-H	**439.3**	439.3±0.4	440.0
$\dot{C}H_2$-H	**461.7**	462.5±1.6	
C:H-H	**425**	422.6±1.7	
C-H	**337.3**	338.4±1.2	
CH_3CH_2-CH_3	**370.1**	370.3±2.1	
CH_3CH_2-$\dot{C}H_2$	**408.6**		
CH_3CH_2-C:H	**395.1**		
CH_3CH_2-C	--		
(-CH_3)$CH_2\dot{C}H_2$	**367.6** (98.5)	99.2±4.2	
$CH_3\dot{C}H$-CH_3	**419.5**		
$CH_3\dot{C}H$-$\dot{C}H_2$	**466.1** (736.4)		
$CH_3\dot{C}H$-C:H	**466.1**		
$CH_3\dot{C}H$-C	--		
CH_3C:-CH_3	--		
CH_3C:-$\dot{C}H_2$	--		
CH_3C:-C:H	--		
CH_3C:-C	--		
CH_3CH=CH_2	**736.5**		
CH_3CH=$\dot{C}H$	**696.5**		
$\dot{C}H_2CH$=CH_2	**759.1** (525.4)	518.8±4.6	
(-CH_3)CH=CH_2	**426.4**	426.3±6.3	
(-CH_3)$\dot{C}$=CH_2	**330.5**	335.1±16.7	
(-CH_3)CH=$\dot{C}H$	**426.1** (107.7)	107.9±6.7	
CH_3-CH_3	**377.3**	377.4±0.8	
CH_3-$\dot{C}H_2$	**418.4**	418.4±2.1	
CH_3-C:H	**378.0**		
CH_3-C	--		
$\dot{C}H_2$-$\dot{C}H_2$	**459.4** (728.5)		

Bond	D^0_{298} [kJ/mol] (calc)	D^0_{298} [kJ/mol] [60], [59]	D^0_{298} [kJ/mol] [62]
$\dot{C}H_2$-C:H	**455.5**		
$\dot{C}H_2$-C	--		
C:H-C:H	**427.2**		
C:H-C	--		
CH≡$\dot{C}$	**747.9**	746.8±2.1	
C-C	--		
C≡C	**602.9**	618.3±15.4	
CH_2=CH_2	**728.3**	728.4±6.3	
CH_2=$\dot{C}$H	**688.1**	688.3±4.2	
CH_2=C:	**692.3**	687.4±16.7	
CH≡CH	**966.6**	954.0±4.2	
H-H	**436**	435.7799±0.0001	
O-O	**498.4**	498.36±0.17	
O-H	**429.9**	429.91±0.29	
HO-H	**497.1**	497.10±0.29	498.0
$\dot{O}$-OH	**274.2**		
C≡O	**1076.4**	1076.38±0.67	
CH_3-$\dot{O}$	**382.9**	377.0±3.3	
$\dot{C}H_2$-$\dot{O}$	**450.9** (748.3)		
CH_2=O	**747.6**		
CH_2(-H)$\dot{O}$	**393.7** (96.3)	88.3±4.0	82.2
CH(-H)=O	**369**		
$\dot{C}$H(-H)$\dot{O}$	--		
$\dot{C}$H(-H)OH	--		
$\dot{C}H_2$O-H	**423.7** (126.3)	126.4±0.8	110.2
$\dot{C}H_2$-OH	**444.7**	444.8±4.2	
C:H-$\dot{O}$	--		
$\dot{C}$H=O	**804.2**		
C:H-OH	--		
C:HO-H	--		
OC=O	**804.3 (530.4)**	532.2±0.4	

Bond	D^0_{298} [kJ/mol] (calc)	D^0_{298} [kJ/mol] [60], [59]	D^0_{298} [kJ/mol] [62]
H-Ċ(O)	**(63.2)**	63.18±0.46	
H-C(O)Ȯ	**- 46**	−46.0±12.6	
HC(O)-Ȯ	**421.3**	417.6±12.6	
Ċ(O)-OH	**(138.0)**	121.3±4.2[tr] 146.4[cis]	
Ċ(O)O-H	**37.3**	19.2±2.9	
Ċ(=O)OH	--		

[tr] trans-; [cis] cis-; for OC=O bond dissociation energy 804.3 ([$2\Delta H_f^0$ (O)+ΔH_f^0 (C)-ΔH_f^0 (CO_2)]/2) is used for reactions where both bonds O=C are formed (C... -> O=C=O), i.e. Dab = 2*804.3 = 1608.6, for reaction with formation of one O=C bond (O=C... ->O=C=O) the value 530.4 is used.

Summarising the inconsistencies described above we have a following consequence: we have two variants of energetics for our reaction mechanisms (if we use BDEs of two different sets in UBI-QEP formulas):

1) for molecules such as $\dot{C}H_2$-$\dot{C}H_2$ and CH_2=CH_2 we have different Q_{AB}s and D_{AB}s,

2) for $\dot{C}H_2$-$\dot{C}H_2$ and CH_2=CH_2 we have different Q_{AB}s and similar D_{AB}s.

As we have chosen ΔH_f^0 ($\dot{C}H_2$-$\dot{C}H_2$) ≠ ΔH_f^0 (CH_2=CH_2) then we are in the first situation.

3.1.1 HEATS OF CHEMISORPTION

The step by step calculation procedures for heats of chemisorption together with the results are given in Table 8.2.3.1. The calculations in the table are performed for the Pt fcc(111) surface; they are based on assumptions on the adsorbate form of species and preferable binding sites. Calculations are made in the following form: for example, heat of adsorption of C atom, taking coordination number n = 3 for fcc(111) hollow binding site ([43], p. 28) and atomic binding energy for C on Pt surface Q_{0A} = 90.0 kcal/mol (376.56 kJ/mol) (Table 8.1.2.3) from (2.6.4.1) gives:

$$Q_A = 376.56\left[\frac{kJ}{mol}\right]\cdot\left(2-\frac{1}{3}\right) = 627.6\left[\frac{kJ}{mol}\right] \qquad (3.1.1.1)$$

Assumptions on the adsorbate forms are based on the following recommendations. For mono-valent radicals having tetra-valent contact atoms the medium binding formula

(2.6.4.5) is used, n = 3; closed shell molecules are treated by the weak binding formulas (2.6.4.2), in the ontop (n = 1) site; for the asymmetric di-coordination adsorption formulae (2.6.4.8 - 2.6.4.11) are used, with heat of adsorption of A and B atom groups as in the ontop site ([43], p. 38).

For some of the molecules adsorbed in a bridge site we use a modified approach. In [43] it is recommended to describe pseudo-atom groups of adsorbed molecule as adsorbed in on-top site, whereas we describe this as adsorbed in hollow site for groups with mono, di, tri valent radical groups and keep calculation procedure as for on-top site only for closed-shell groups (here the closed-shell and radical refer to state in the molecule before the procedure of dividing it to A- and B- pseudo-atom groups). So we use for pseudo-atom groups the same procedure as is used for mono-coordinated adsorbed species. In this approach the forms of the binding sites are close to forms used in DFT calculations [63].

Enthalpies of formation for different temperatures are taken from [11]. Enthalpies not available there are taken from other sources (see Table 3.1.1). Some of the radicals in Table 3.1.1 might not exist in the gas phase, but on the surface such species can be stabilised by interactions with surface metal atoms.

References to literature where the same configurations of adsorbates is used are given for some of the molecules in the Table 8.2.3.1 adjacent to the calculated results.

From source to source we can see see some inconsequences in the use of terms. For example the term - "adsorbed in a bridged site" in some literature means that one contact atom is adsorbed with binding to 2 surface atoms (coordination number n=2), whereas in [43] adsorption in a bridged site means adsorption by to contact atoms (A*-B*) as well.

In [64] there is a review of heats of adsorption of some species on platinum surface, comparing many different sources of computational and experimental values.

The calculated heats of adsorption in Table 8.2.3.1 are in good agreement (similar) with some numbers from [64], although some of their assumptions about forms of adsorbates are different from ours. Sometimes it is difficult to compare the values of

heats of adsorption with values from other sources because they do not give precise determination of the species that they use. For example the common formula C_2H_3 can be shown, but exactly which specie it represents ($C^*H{=}CH_2$, $C^*H{-}C^*H_2$ or $CH_3{-}C^*$) is not reported.

It is important to remember that in [43] it is recommended to use pseudo-atom treatment in the calculation of di-coordinated molecules in cases when the bond between the pseudo-atoms is a traditional single bond. We use here this treatment also for cases with double and triple bonds because we do not have another mechanism to describe the adsorption energies of such molecules and try to follow a maximally unified approach in the description of every adsorbate.

3.1.2 ENERGY BARRIERS FOR REACTIONS

In our model we assume the step by step mechanism of reaction. We try to determine every elementary reaction as the change in one relation between components. Thus the adsorption of H_2 goes in two steps - adsorption of H_2 to surface, and dissociation of H_2^* to $2H^*$.

Molecular hydrogen is not observed in the adsorbed state on the surface (see Ch. 2.2) and in some models its adsorption goes in one step (dissociative adsorption) (e.g. in [13], [53]), but in some models it is described in two steps (as we do) (e.g. in [50]). For the last approach the reaction of H_2^* dissociation is supposed to be very fast.

For the energy barriers of dissociation, recombination and disproportionation reactions formulae (2.6.4.12)-(2.6.4.14) are used.

The adsorption (non-dissociative adsorption) of a gas phase species onto the surface does not have an energy barrier, the energy barrier of desorption of gas phase species from the surface is the reverse of adsorption and is equal to heat of adsorption of the appropriate species:

$$\Delta H^f_{ads} = -Q_A; \quad \Delta E^f_{ads} = 0;$$
$$\Delta H^r_{ads} = Q_A; \quad \Delta E^r_{ads} = Q_A; \qquad (3.1.2.1)$$

In our initial mechanism there are steps where adsorbed species change their form of adsorption (e.g. adsorption via one atom to adsorption via two atoms). For such "additional" adsorption the following formulae are used:

$$A^{*}+^{*}\rightarrow A^{**},$$
$$\Delta E^{f}_{adds}=Q_{A^{*}}-Q_{A^{**}}; \qquad (3.1.2.2)$$
$$\Delta E^{r}_{adds}=Q_{A^{**}}-Q_{A^{*}};$$

For reactions where the change in internal bonds occurs:

$$A^{*}-A^{*} \rightarrow A^{*}=A+^{*},$$
$$\Delta E_{f}=Q_{A^{*}-A^{*}}+D_{\dot{A}-\dot{A}}-D_{A=A}-Q_{A^{*}=A}; \qquad (3.1.2.3)$$
$$\Delta E_{r}=Q_{A^{*}=A}+D_{A=A}-D_{\dot{A}-\dot{A}}-Q_{A^{*}-A^{*}};$$

The calculation of activation energies for gas phase reactions of radical thermodissociation ([58], pp. 77-78) follows:

$$D\approx E_{a}-R\cdot T \qquad (a),$$
$$D\approx E_{a}+R\cdot T \qquad (b), \qquad (3.1.2.4)$$

where (*a*) is used for moderate temperatures (<1000 K) and (*b*) for temperatures in the interval 273-300 K ([58], p. 95).

Thus, the activation energy for every gas phase reaction is (3.2.1.2):

$$E_{a}=D(R_{1}-R_{2})+R\cdot T; \qquad (3.1.2.5)$$

where R_1 and R_2 are radicals composing a molecule.

If gas-phase reaction is accompanied by change in more than one bond, expression (2.6.4.15) can be used instead of bond energy $D(R_1\text{-}R_2)$ for calculation of D_{AB}.

3.1.3 ELEMENTARY STEPS

All suggested elementary steps are shown in Table 8.2.4.1 together with calculation formulae for reaction activation energies and calculated activation energies (for 298 K on Pt(111) surface). This chapter contains the considerations used in the process of choosing the elementary steps used in the model.

At the beginning we choose different possible reactions that include species containing combinations of C, O, H (C_xH_y hydrocarbons, some H_xO_y, C_xO_y, $H_xC_yO_z$ species). All species used are listed in Table 8.2.3.1. We suggest different forms of adsorbed initial components ($CH_3CH_2C^*H_3$, $CH_3C^*H_2CH_3$, $CH_3C^*H_2C^*H_3$ for propane) and combinatorially write similar reactions for these different adsorbate forms. The plan is to exclude reactions after comparison of their activation energies (to choose reaction routes with lowest barrier towards products).

While preparing equations we do not take into consideration such possible phenomena as shielding of C atoms by H atoms in saturated hydrocarbons.

The description of active sites is a special problem. Using the UBI-QEP method for the description of adsorption we get for our model at least two different types of active sites: on-top and hollow sites. For the on-top site one surface atom is used and the adsorbed molecule is placed over this atom. In this case we definitely have equality 1 site = 1 surf. atom. For the hollow site three surface atoms are used partially and an adsorbed molecule is placed over the midst of these three. Thus we can say that the hollow site consists of three $\frac{1}{3}^{rds}$ of three different surface atoms. The attention should be paid to reactions where the change of adsorption sites occurs in order to balance the amount of surface atoms participating.

Every atom can participate in the formation of 3 hollow binding sites. Thus a star * in surface reactions involving a 3-fold hollow site represents ⅓ of an atom. Such usage opens the possibility for a situation when we have an atom participating in formation of 2 hollow sites and thus having ⅓ of itself free for formation of another connection. This ⅓ can form one on-top site. The case with participation of the same atom in

formation of one hollow binding site and one on-top site at once is described by DFT calculations in [63].

It was not possible to calculate activation energies for all suggested elementary reactions. As we had no possibility to calculate values such as $\Delta H_f^0(CH_3C)$, $\Delta H_f^0(CH_3CH_2C)$, ..., and consequently the corresponding bond dissociation energies $D(CH_3C\text{:-}CH_3)$, $D(CH_3CH_2\text{-}C)$, .., then we can not find heats of adsorption of appropriate molecules and can not use these in our system of elementary equations.

We also prepare a short list of possible gas phase reactions. There are many mechanisms for free-radical gas-phase reactions [62], from which we have made a selection. From Table 8.2.4.1 we choose reactions where only mono-radicals participate and write appropriate reactions in the gas phase. In addition, some reactions with di-radicals (carbenes) were selected. Gas-phase reactions with activation barriers are presented in Table 8.2.4.2. The selection is based on decision that we take the shortest routes (least amount of elementary reactions) from the reagents to the products, and we try to have at least two compete routes to every product.

By making analysis of the activation energies of proposed reactions we can exclude some of the low-probable reactions and thus decrease the scale of the system.

Based on activation energies for reactions with similar species it is possible to make some conclusions about preferability for some of the forms of species. We can compare such species as C*H≡C*H and C***H-C***H. The relations between activation energies for mutual transformations are as follows:

$$C^{***}H\,C^{***}H \underset{399}{\overset{0}{\rightleftarrows}} C^{*}H\equiv C^{*}H$$

$$C^{***}H\,C^{***}H \underset{216}{\overset{0}{\rightleftarrows}} C^{***}H + C^{***}H \qquad (3.1.3.1)$$

$$C^{***}H + C^{***}H \underset{188}{\overset{16}{\rightleftarrows}} C^{*}H\equiv C^{*}H$$

We can see that the occurrence of $C^*H{\equiv}C^*H$ on the surface is more probable than the occurrence of $C^{***}H\text{-}C^{***}H$. Furthermore the number of surface active sites needed for adsorbate $C^*H{\equiv}C^*H$ formation is less and this also makes its probability higher. The same tendency we see for pairs of adsorbates $C^*H_2{=}C^*H_2$ and $C^{***}H_2\text{-}C^{***}H_2$; $CH_3C^*H{=}C^*H_2$ and $CH_3C^{***}H\text{-}C^{***}H_2$; and some other similar pairs. Thus we decide that species like $CH_3C^*H{=}C^*H_2$ are more preferable compared to $CH_3C^{***}H\text{-}C^{***}H_2$ and we exclude appropriate reactions from the scheme.

We choose the reactions with the lowest activation barriers. Chosen reactions are depicted in the tables with elementary reactions (Tables 8.2.4.1, 8.2.4.2) by the letter R with a number of this reaction in a new set (R1-R95). Here we should mention that the choice of reaction set was based on activation barriers calculated at 298 K, whereas at high temperatures the order of reactions in a row low energy - high energy can be changed. We use temperature dependent enthalpies in the model simulation.

Using Matlab (see Ch. 8.6.2) we build the graph of the chosen reaction mechanism (Fig. 3.1.3.1).

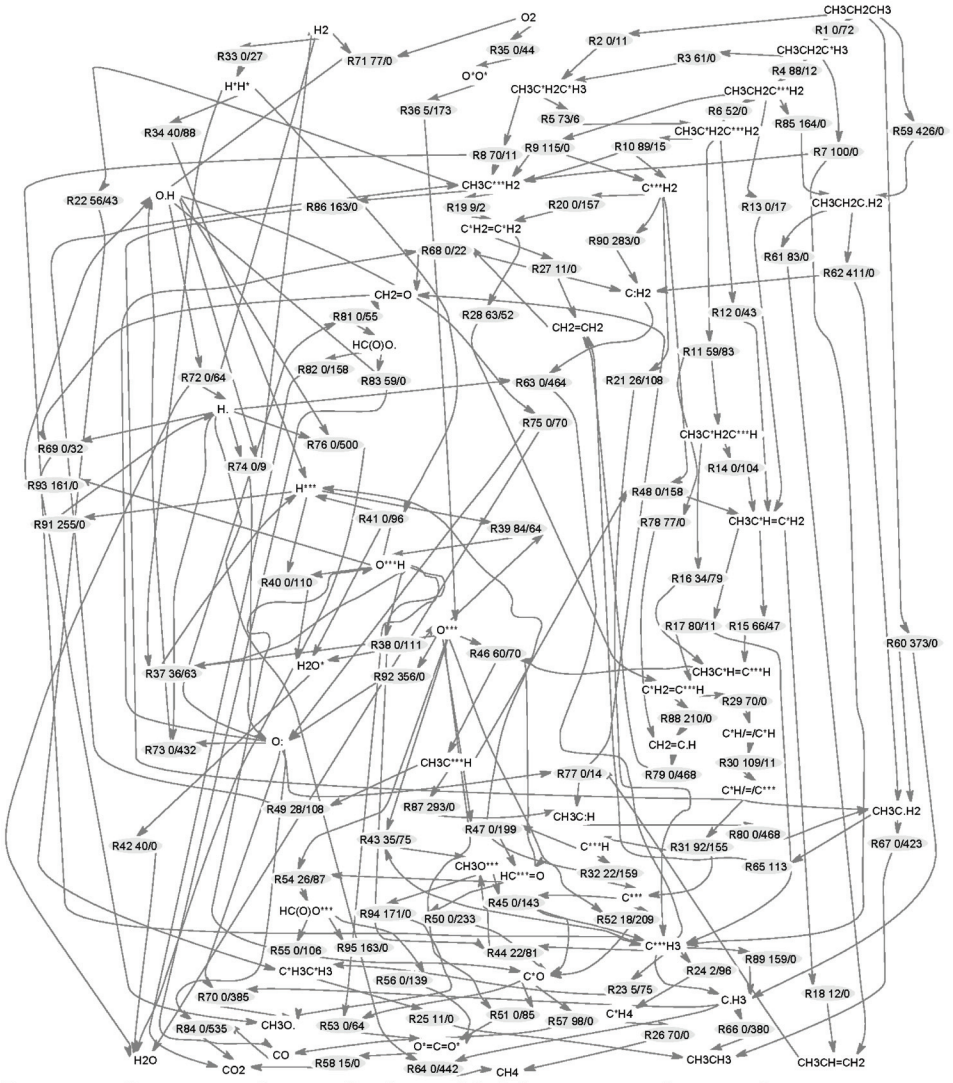

Fig. 3.1.3.1: Reaction mechanism for the model. Substances are shown as flows, reactions are shown as nodes of the graph with reaction number and activation energy for forward/reverse direction.

Concerning the graph as a way to describe the complex reaction mechanism, it must be noted there are different ways to do it and some theory was developed around this. Graphs can help with visualisation, some special mathematical algorithms on graphs can be used for solving tasks of chemical kinetics [65].

We use here an approach where substances are depicted as lines in the graph and reactions as nodes (see description in Ch. 8.6.2). In Fig. 3.1.3.1 we have merged all flows of every individual substance into one appropriate node. This should make the graph more readable.

For the model simulation it is necessary to calculate reaction rate constants. The calculation of preexponentials was made according to procedure described in Chapter 2.6.3 , entropies needed for this were taken from [11]. Some of the entropies lacking there are calculated, the calculation procedure is described in Chapter 3.2.2 .

3.1.4 REACTOR EQUATIONS FOR THE MODEL.

Based on the chosen mechanism the system of differential rate equations was prepared (following the theory from Ch. 2.6.2). It includes equations for the kinetics of change of surface fractions of intermediates as well as equations for a CSTR at non-steady state for the change of moles of terminal (gas-phase) species (3.1.4.1).

As for description of adsorption of species the complex configurations of active sites were used (star * in a reaction is determined as ⅓rd of surface atom ability to form binding connection, 3* define a hollow site, 1* define an on-top site; some of the molecules are adsorbed on two sites of different nature), the ratio between the number of molecules adsorbed and the number of active sites used (number of surface atoms) is different for different compounds. This is taken into consideration while solving the ODE system. A proper transformation of surface fraction from $N^{sites}_{A}/N^{sites}_{Tot}$ to $N^{molec}_{A}/N^{sites}_{Tot}$ was made (see Ch. 8.6.3).

The computer simulation of the initial model with the gas-phase and surface chemistry has encountered some computational problems. Not surprisingly, the system of ODEs becomes very stiff and the Matlab computational functions used to solve ODE did not resolve it (numerical method used for solving the ODEs is numerically unstable as equations include some terms that can lead to rapid variation in the solution - due to big difference in energetic parameters for the gas phase reactions and the surface reactions). If the gas-phase reactions are not taken into consideration, the system of

ODEs is solved successfully, and it gives reasonable results (see Ch. 5.4). The system of differential rate equations (3.1.4.1) is shown without the gas-phase part.

$$\frac{d[CH_3CH_2\underset{*}{C}H_3]}{dt} = +k_1^f \cdot P_{C_3H_8} \cdot [*] - k_1^r \cdot [CH_3CH_2\underset{*}{C}H_3] - k_3^f \cdot [CH_3CH_2\underset{*}{C}H_3] \cdot [*] + \ldots;$$

$$\frac{d[CH_3CH_2\underset{***}{C}H_2]}{dt} = -k_6^f \cdot [CH_3CH_2\underset{***}{C}H_2] \cdot [*] + k_6^r \cdot [CH_3\underset{*}{C}H_2\underset{***}{C}H_2] + \ldots;$$

$$\frac{d[CH_3\underset{*}{C}H=\underset{*}{C}H_2]}{dt} = +k_{13}^f \cdot [CH_3CH_2\underset{***}{C}H_2] \cdot [*]^2 - k_{13}^r \cdot [CH_3\underset{*}{C}H=\underset{*}{C}H_2] \cdot [\underset{***}{H}] + \ldots;$$

$$\frac{d[\underset{*}{H}\,\underset{*}{H}]}{dt} = +k_{33}^f \cdot P_{H_2} \cdot [*]^2 - k_{33}^r \cdot [\underset{*}{H}\,\underset{*}{H}] - k_{37}^f \cdot [\underset{*}{H}\,\underset{*}{H}] \cdot [\underset{***}{O}] \cdot [*] + k_{37}^r \cdot [\underset{***}{O}H] \cdot [\underset{***}{H}] + \ldots;$$

$$\frac{d[\underset{*}{O}\,\underset{*}{O}]}{dt} = +k_{35}^f \cdot P_{O_2} \cdot [*]^2 - k_{35}^r \cdot [\underset{*}{O}\,\underset{*}{O}] - k_{36}^f \cdot [\underset{*}{O}\,\underset{*}{O}] \cdot [*]^4 + k_{36}^r \cdot [\underset{***}{O}]^2;$$

$$\frac{d[\underset{***}{O}]}{dt} = -k_{39}^f \cdot [\underset{***}{H}] \cdot [\underset{***}{O}] + k_{39}^r \cdot [\underset{***}{O}H] \cdot [*]^3 - k_{38}^f \cdot [H_2\underset{*}{O}] \cdot [\underset{***}{O}] \cdot [*]^2 + k_{38}^r \cdot [\underset{***}{O}H]^2 - \ldots;$$

$$\frac{d[H_2\underset{*}{O}]}{dt} = +k_{40}^f \cdot [\underset{***}{H}] \cdot [\underset{***}{O}H] - k_{40}^r \cdot [H_2\underset{*}{O}] \cdot [*]^5 - k_{38}^f \cdot [H_2\underset{*}{O}] \cdot [\underset{***}{O}] \cdot [*]^2 + k_{38}^r \cdot [\underset{***}{O}H]^2 - \ldots; \qquad (3.1.4.1)$$

$$\frac{d[*]}{dt} = -k_1^f \cdot P_{C_3H_8} \cdot [*] - k_1^r \cdot [CH_3CH_2\underset{*}{C}H_3] - 2 \cdot k_2^f \cdot P_{C_3H_8} \cdot [*]^2 + 2 \cdot k_2^r \cdot [CH_3\underset{*}{C}H_2\underset{*}{C}H_2] - \ldots;$$

…

$$\frac{dn_{O_2}}{dt} = \frac{n_{tot}^{in} \cdot R \cdot T}{P} \cdot \frac{\rho_{cat} \cdot C_{t.me} \cdot S_{t.me} \cdot y_{wt}}{10 \cdot N_A} \cdot \frac{1-\epsilon}{\epsilon} \cdot (-k_{35}^f \cdot P_{O_2} \cdot [*]^2 + k_{35}^r \cdot [\underset{*}{O}\,\underset{*}{O}]);$$

$$\frac{dn_{H_2O}}{dt} = \frac{n_{tot}^{in} \cdot R \cdot T}{P} \cdot \frac{\rho_{cat} \cdot C_{t.me} \cdot S_{t.me} \cdot y_{wt}}{10 \cdot N_A} \cdot \frac{1-\epsilon}{\epsilon} \cdot (+k_{42}^f \cdot [H_2\underset{*}{O}] - k_{42}^r \cdot P_{H_2O} \cdot [*]);$$

$$\frac{dn_{CO_2}}{dt} = \frac{n_{tot}^{in} \cdot R \cdot T}{P} \cdot \frac{\rho_{cat} \cdot C_{t.me} \cdot S_{t.me} \cdot y_{wt}}{10 \cdot N_A} \cdot \frac{1-\epsilon}{\epsilon} \cdot (+k_{58}^f \cdot [\underset{*}{O}=C=\underset{*}{O}] - k_{58}^r \cdot P_{CO_2} \cdot [*]^2);$$

$$\frac{dn_{C_3H_8}}{dt} = \frac{n_{tot}^{in} \cdot R \cdot T}{P} \cdot \frac{\rho_{cat} \cdot C_{t.me} \cdot S_{t.me} \cdot y_{wt}}{10 \cdot N_A} \cdot \frac{1-\epsilon}{\epsilon} \cdot (-k_1^f \cdot P_{C_3H_8} \cdot [*] - k_1^r \cdot [CH_3CH_2\underset{*}{C}H_3] - \ldots);$$

$$\frac{dn_{C_3H_6}}{dt} = \frac{n_{tot}^{in} \cdot R \cdot T}{P} \cdot \frac{\rho_{cat} \cdot C_{t.me} \cdot S_{t.me} \cdot y_{wt}}{10 \cdot N_A} \cdot \frac{1-\epsilon}{\epsilon} \cdot (+k_{18}^f \cdot [CH_3\underset{*}{C}H=\underset{*}{C}H_2] - k_{18}^r \cdot P_{C_3H_6} \cdot [*]^2);$$

…

where

$[*],[CH_3CH_2\underset{*}{C}H_3],[CH_3CH_2\underset{***}{C}H_2],[\underset{*}{H}]$, ... - surface fractions of intermediates;

$n_{C_3H_8}, n_{C_3H_6}, n_{H_2}$ - moles of components in the gas-phase; other symbols are described in Chapter 8.5 . The complete set of equations is given in the Matlab code in Chapter 8.6.3 .

The CSTR equation is described in Chapter 8.5 , the similar equation is also used in [50], [51].

3.2 THERMODYNAMICS OF MOLECULES AND RADICALS

3.2.1 CALCULATION OF ENTHALPIES OF FREE RADICALS

We use here the group additivity method ([58], [45] pp. 275-359, [66], [67]) for calculation of enthalpies and entropies for some of the radicals (as we don't have enough necessary data from the database [11]). This method is based on the idea that the enthalpy of the molecule or radical can be found as the summary of specific contributions of groups constituting the molecule. A group is a polyvalent atom together with its monovalent ligands and connections to neighbour polyvalent atoms. For example the functional group CH_3- in molecules CH_3-CH_2... and CH_3-CH=... will give different additivity contributions: C-$(H)_3$(C) and C-$(H)_3(C_d)$ appropriately.

The basic equation for chemical bond dissociation in gas phase:

$$D(R_1-R_2)=\Delta H_f^0(\dot{R}_1)+\Delta H_f^0(\dot{R}_2)-\Delta H_f^0(R_1R_2), \qquad (3.2.1.1)$$

where R_1R_2 - gas phase molecule or radical, R_1˙ and R_2˙ - radicals in reaction:

$$R_1R_2 \rightarrow \dot{R}_1+\dot{R}_2 \qquad (3.2.1.2)$$

For calculation of enthalpy of formation we use here the formula of first approximation of the method, taking the influence of free valence on all groups in the radical to be equal ([58], p. 150):

$$\Delta H_f^0(\dot{R}) = \{\dot{B}\} + \sum_{i=1}^{n-1} \{\dot{A}_i\}, \qquad (3.2.1.3)$$

where {*B*} - contribution of the group containing free valence, {A_i} - contributions of other groups, *n* - the number of groups in modelled radical.

We also use the approximation that the GAVs of groups are independent on the type of C atoms which the group is connected to. For example for the group -CH_2- we have:

{C-$(H)_2(C)_2$}≡{C-$(H)_2(C)(C)_d$}≡{C-$(H)_2(C)(C)_t$}≡{C-$(H)_2(C)(\dot{C})$}.

For C:-(H)(C), C:-$(C)_2$ were chosen values characteristic for the triplet state. For radicals containing unsaturated bond the following formula is used:

$$\Delta H_f^0(\dot{B} - A_1 = A_2) = \{\dot{B}\} + \sum_{i=1}^{n-1} \{\dot{A}_i\} + E_s(C=C-\dot{C}), \qquad (3.2.1.4)$$

where E_s(C=C-Ċ) - stabilisation energy ([58], p.158).

Using the GAVs from [59], we use the only approximation that for additivity groups that differs only in neighbour C-atom type ((C) ↔ (Ċ)) values are close, and we make summation of GAVs of appropriate groups. This approximation is based on a comparison of given GAVs.

According to the approach in [58] enthalpies are calculated as in the following example (resulting numbers are in Table 3.1.1):

$$\Delta H_f^0(CH_3\dot{C}HCH_3) = \{\dot{C}-(H)(C)_2\} + 2\cdot\{C-(H)_3(C)\} = 154.60 + 2\cdot(-41.04) = 72.52\left[\frac{kJ}{mol}\right],$$

$$\Delta H_f^0(CH_3\dot{C}H\dot{C}H_2) = \{\dot{C}-(H)(C)_2\} + \{\dot{C}-(H)_2(C)\} + \{C-(H)_3(C)\} = \qquad (3.2.1.5)$$

$$154.60 + 148.49 + (-41.04) = 262.05\left[\frac{kJ}{mol}\right].$$

According to GAVs from [59] enthalpies are calculated as is in the following example (resulting numbers are in Table 3.1.1):

$$\Delta H_f^0(CH_3\dot{C}HCH_3)=\{\dot{C}-(H)(C)_2\}+2\cdot\{C-(H)_3(\dot{C})\}=171.5+2\cdot(-41.8)=87.9\left[\frac{kJ}{mol}\right],$$
$$\Delta H_f^0(\dot{C}(O)OH)=\{\dot{C}O-(O)\}+\{O-(H)(\dot{C}O)\}=50.2+(-242.7)=-192.5\left[\frac{kJ}{mol}\right]. \quad (3.2.1.6)$$

Group additivity values are listed in the Table 3.2.1.1.

Table 3.2.1.1: Group additivity values.

Radical groups	Group additivity values, [kJ/mol]	
	From [58]	From [59]
$\dot{C}$-$(H)_2(C)$	148.49	160.7
$\dot{C}$-$(H)(C)_2$	154.60	171.5
$\dot{C}$-$(H)_2(O)$	98.8	
$\dot{O}$-(C)	37.57	62.8
$\dot{O}$-(O)		74.1
$\dot{O}$-(CO)		9.2
$\dot{C}O$-(C)	22.01	31.8
$\dot{C}O$-(O)	−39.75	50.2
$\dot{C}O$-(H)		41.8
CO-(H)($\dot{O}$)		−134.3
CO-(C)(O)	−175.6	
CO-(H)(C)	−135.9	
O-(H)(C)	−175.27	
O-(H)($\dot{C}$)		−158.6
O-(H)($\dot{C}O$)		−242.7
$\dot{C}_d$-(H)(C_d)	248.8	273.2
$\dot{C}_d$-(C_d)(C)	174.8	
$\dot{C}$-$(H)_2(C_d)$		108.4
$\dot{C}$-(H)(C)(C_d)		109.6
$\dot{C}$-$(H)_2(C_t)$		109.2
$\dot{C}$-(H)(C)(C_t)		119.2
$\dot{C}_t$-C_t		451.9

Radical groups	Group additivity values, [kJ/mol]	
	From [58]	From [59]
$C\text{-}(H)_3(C)$	−41.04	
$C\text{-}(H)_3(\dot{C})$		−41.8
$C\text{-}(H)_3(\dot{O})$		−41.8
$C\text{-}(H)_2(C)_2$	−21.76	
$C\text{-}(H)_2(C)(\dot{C})$		−20.9
$C_d\text{-}(H)_2(C_d)$	27.2	
$C_d\text{-}(H)(C_d)(C)$	35.6	
$C_d\text{-}(H)(C_d)(\dot{C})$		36.0
$C_d\text{-}(C)(C_d)(\dot{C})$		42.7
$C_t\text{-}(H)(C_t)$	107.9	
$C_t\text{-}(C_t)(C)$	117.7	
$C_t\text{-}(C_t)(\dot{C})$		114.2
$C\text{:-}(C)_2^{si}$	257.9	
$C\text{:-}(C)_2^{tr}$	377.9	
$C\text{:-}(H)(C)^{si}$	353.6	
$C\text{:-}(H)(C)^{tr}$	383.8	
$E_s(C{=}C\text{-}\dot{C})$	−52.0	
$E_s(C{\equiv}C\text{-}\dot{C})$	−36.5	

Calculation of GAVs in sources [58] and [59] was based on enthalpies of formation listed in it, as well as on modifications of group additivity method used there.

^{si} - singlet; ^{tr} - triplet; C_d - C atom participating in double bond; C_t - C atom participating in triple bond.

Values for enthalpies in [58] are smaller than appropriate values in other sources approximately by 15~25 kJ/mol, as well as values given by calculations based on this source. Thus we use enthalpies (see Table 3.1.1) from the first column, because we can get values for a wide range of temperatures, for the rest of molecules - from the second column, then - from last column right side (calculated values) and finally - from the last column left side.

3.2.2 CALCULATION OF ENTROPIES OF FREE RADICALS

For the calculation of entropies of molecules and radicals (as we do not have all the necessary data in [10]) we use the Difference - Method [45].

For some of the radicals that we need there are calculated values in [45] (p. 326):

S^0 ($CH_3CH{=}\dot{C}H$) = 269.3 [kJ/mol];

S^0 ($HC(O)\dot{O}$) = 253.7 [kJ/mol].

Calculation of $S^0(CH_3C{:}H)$ ([45], pp. 330-335) is as follows:

$$S^0(CH_3\ddot{C}H)=S^0(CH_3\dot{C}H_2)+\Delta S^0_m+\Delta S^0_v+\Delta S^0_{i.rot}+\Delta S^0_e+\Delta S^0_\sigma+\Delta S^0_{V_0}+\Delta S_{rot} \quad , \qquad (3.2.2.1)$$

$$\Delta S^0_m = \frac{3\cdot R}{2}\cdot\ln\left(\frac{M_{CH_3\ddot{C}H}}{M_{CH_3\dot{C}H_2}}\right)=12.47\cdot\ln\left(\frac{28.05}{29.06}\right)=-0.44\left[\frac{kJ}{mol}\right] \quad ,$$

$$\Delta S^0_v=-S^0(C-H)_{3000}-S^0\left(\begin{array}{c}C\\ \wedge\\ HH\end{array}\right)_{1450}-S^0\left(\begin{array}{c}C\\ \wedge\\ HC\end{array}\right)_{1150}=-0.33\left[\frac{kJ}{mol}\right] \quad ,$$

$$\Delta S_{rot}=\frac{1}{2}\cdot R\cdot\ln\left\{\frac{I_A\cdot I_B\cdot I_C(CH_3\ddot{C}H)}{I_A\cdot I_B\cdot I_C(CH_3\dot{C}H_2)}\right\}=\frac{1}{2}\cdot R\cdot\ln\left\{\frac{4.265\cdot 20.618\cdot 21.577}{5.385\cdot 22.451\cdot 23.671}\right\}=-1.71\left[\frac{kJ}{mol}\right] \quad ,$$

$$\Delta S^0_{i.rot}=\frac{1}{2}\cdot R\cdot\ln\left(\frac{I_{r(CH_3\ddot{C}H)}}{I_{r(CH_3\dot{C}H_2)}}\right)\approx-1.26\left[\frac{kJ}{mol}\right] \quad , \qquad (3.2.2.2)$$

$$\Delta S^0_\sigma=R\cdot\ln\frac{\sigma(CH_3\dot{C}H_2)}{\sigma(CH_3\ddot{C}H)}=R\cdot\ln\frac{6}{3}=5.8\left[\frac{kJ}{mol}\right] \quad ,$$

$$\Delta S^0_{V_0}=-S^0_{intr}(\dot{C}H_2-\infty)=-22.6\left[\frac{kJ}{mol}\right] \quad ,$$

$$\Delta S^0_e=R\cdot\ln(g_e)=R\cdot\ln(3)=9.13\left[\frac{kJ}{mol}\right].$$

$$S^0(CH_3\ddot{C}H)=S^0(CH_3\dot{C}H_2)+\sum\Delta S^0_{corrections}=247.118-11.41=235.71\left[\frac{kJ}{mol}\right]. \qquad (3.2.2.3)$$

Terms in formulas (3.2.2.1), (3.2.2.2) are:

ΔS^{o}_{m} - mass correction for translation partition function,

ΔS^{o}_{υ} - vibration correction,

ΔS^{o}_{rot} - rotational correction,

$\Delta S^{o}_{i.rot}$ - the difference in internal rotation,

ΔS^{o}_{σ} - change in symmetry,

ΔS^{o}_{V0} - change in rotational barriers,

ΔS^{o}_{e} - electronic degeneracy.

The difference in internal rotation $\Delta S^{o}_{i.rot}$ for $CH_3C{:}H/CH_3\dot{C}H_2$ was taken to be equal to the difference for $CH_3\dot{C}H_2/CH_3CH_3$ from [45].

$S = n_{unpaired}/2$, where $n_{unpaired}$ is the number of unpaired electrons, the degeneracy g_e of such a state is $g_e = (2S+1)$ [68].

The principal moments of inertia of the molecule for $CH_3CH_2C{:}H$ are I_A = 14.307, I_B = 52.796, I_C = 60.492; for $CH_3CH_2\dot{C}H2$ - I_A = 16.113, I_B = 55.048, I_C = 63.187 ; for $CH_3C{:}H$ - I_A = 4.265, I_B = 20.618, I_C = 21.577; $CH_3\dot{C}H_2$ - I_A = 5.385, I_B = 22.451, I_C = 23.671; CH_3CH_3 - I_A = 6.606, I_B = 24.916, I_C = 24.917. The principal moments of inertia are calculated in ChemBio3D program [69].

The σ - rotational symmetry number or external symmetry number for the molecule is calculated by the method described in [70]. For the calculation was used the GAP program [71] - a system for computational discrete algebra, especially for Computational Group Theory. Molecules in Figs. 3.2.2.1 - 3.2.2.3 where constructed in the ChemBio3D by using appropriate ~.mol files which were taken from the NIST database [10].

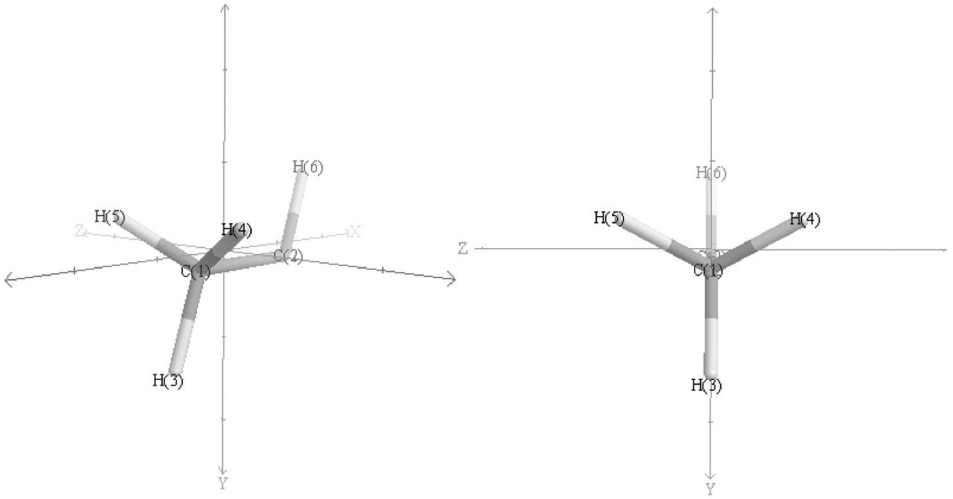

Fig. 3.2.2.1: The molecule $CH_3C{:}H$

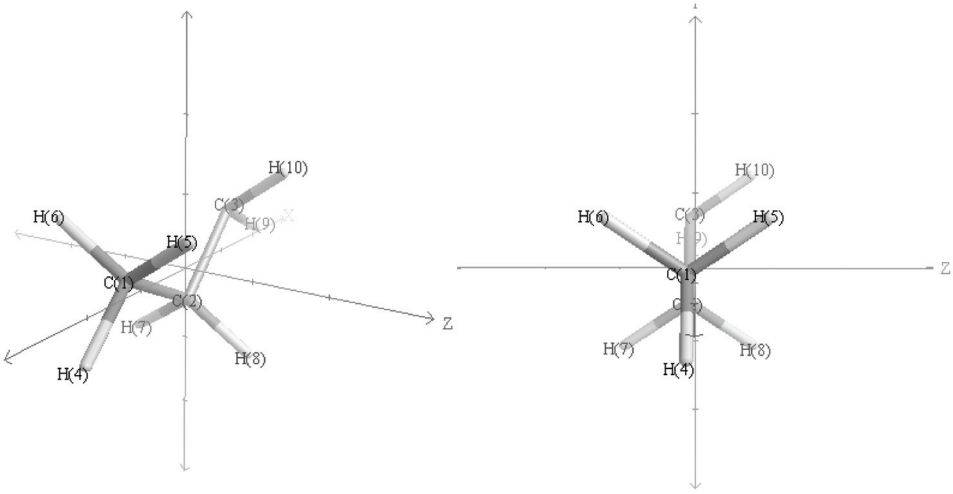

Fig. 3.2.2.2: The molecule $CH_3CH_2\dot{C}H_2$

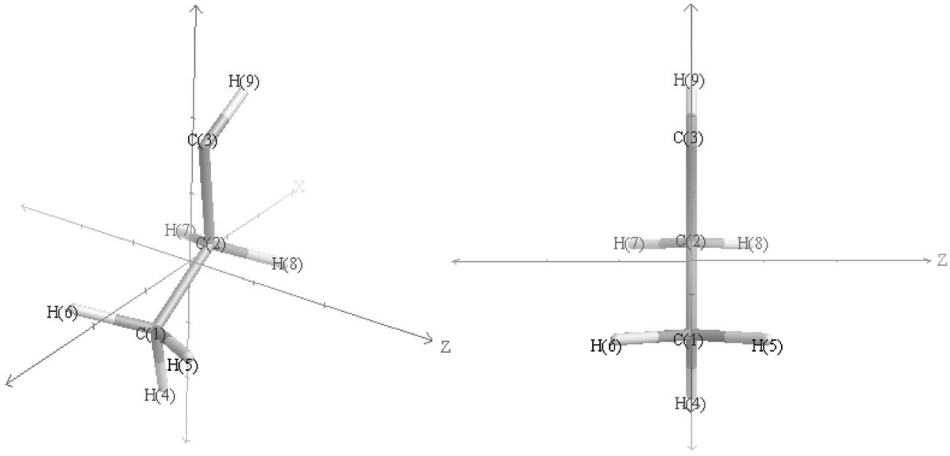

Fig. 3.2.2.3: The molecule $CH_3CH_2C{:}H$

Figs. 3.2.2.1 - 3.2.2.3 were used to determine the symmetry groups of the molecules. The rotational symmetry numbers were calculated in GAP (for details see Ch. 8.2.1 in Appendix).

The same procedure was used for calculation of the entropy of $CH_3CH_2C{:}H$ (for details see Ch. 8.2.2):

$$S^0(CH_3CH_2\ddot{C}H) = S^0(CH_3CH_2\dot{C}H_2) + \sum \Delta S^0_{corrections} = 279.18\left[\frac{kJ}{mol}\right]. \quad (3.2.2.4)$$

Entropies for $CH_3CH_2C{:}H$ and $CH_3C{:}H$ at different temperatures used in model simulation are calculated as $S_{CH3CH2C:H}(T) = S_{CH3CH2CH2}(T) + \Delta S^o_{corrections}$.

For $CH_3CH{=}\dot{C}H$ and $HC(O)\dot{O}$ we find $\Delta S^o_{corrections} = S^0(CH_3CH{=}\dot{C}H) - S^0(CH_3CH{=}CH2) = 269.3 - 266.668 = 2.63$ [kJ/mol]; $\Delta S^o_{corrections} = S^0(HC(O)\dot{O}) - S^0(HC(O)OH) = 253.7 - 248.99 = 4.71$ [kJ/mol]. These $\Delta S^o_{corrections}$ are used to calculate entropies for $CH_3CH{=}\dot{C}H$ and $HC(O)\dot{O}$ at different temperatures in the same manner as for $CH_3CH_2C{:}H$ and $CH_3C{:}H$.

4 EXPERIMENTAL WORK

4.1 PREPARATION AND CHARACTERISATION OF CATALYSTS

The catalysts tested during this work were not prepared by the author. The description of preparation procedures as well as main characteristics of the catalysts are given below.

4.1.1 PLATINUM-TIN ON HYDROTALCITE

The catalyst used was a platinum-tin on a hydrotalcite support HT50. This catalyst was synthesised during previous work [8], the preparation and characterization has been described there, as well some tests that were done. The catalyst was prepared by depositing the metals on a support by aqueous incipient wetness impregnation. The catalyst was dried at 100 ℃ for at least 12 hours and then calcined in air for 4 hours at 600 ℃, with a heating rate of 4 ℃/min. As the support was used a commercial hydrotalcite carrier (HT50) with 50.7 wt% of MgO and 49.3 wt% Al_2O_3, giving a ratio of $Al^{3+}/(Al^{3+}+Mg^{2+})$ of 0.46, supplied by CONDEA Chemie GmbH. The catalyst was made by consecutive impregnations, where the hydrotalcite was first impregnated with Sn using $SnCl_2 \cdot 2H_2O$ and then with Pt using $H_2PtCl_6 \cdot 6H_2O$, the loadings were 1.1wt% Pt, 2.0wt% Sn. The catalyst was sieved to a particle diameter range of 106-250 μm after calcination.

The catalyst was characterized using volumetric H_2-chemisorption, N_2-sorption, temperature programmed reduction (TPR) and X-ray diffraction (XRD) [8]. Barret-Joyner-Halenda (BJH) calculation scheme and Broekhoff-de Boer algorithm were used for calculation the pore volume and pore diameter correspondingly. For calculation the metallic surface area and crystallite size the following assumption was used: all metallic particles are spherical and the surface of the particle consists of equal fractions of (111), (110) and (100) crystal planes. A summary of the results from characterization of the catalyst PtSn/Ht50 is given in Table 4.1.1.1.

Table 4.1.1.1: Surface area, pore volume and pore diameter as determined by N_2-sorption; dispersion and crystallite size as calculated from chemisorption for PtSn/HT50 catalyst.

SSA, [m^2/g]	Pore volume, [cm^3/g]	Average pore diameter, [nm]	Dispersion, [%]; total H_2 ads.	Metallic surface area, [m^2/g_{sample}]	Metallic surface area, [m^2/g_{metal}]	Crystallite size, [nm]
140	0.20	3.6	29	0.71	70.8	4.0

The catalyst (PtSn/HT50 with 1.1 wt% of Pt and 2wt% of Sn) was used for a series of experiments performed for a composition-property diagram construction.

4.1.2 PLATINUM ON HYDROTALCITE

The preparation and characterisation of platinum catalysts were performed by Virginie Herauville as part of her master project. The catalysts were prepared by a method based on the polyol process [72].

A series of catalyst was prepared and tested at similar conditions. Three types of supports were used, HT30 (30 wt% of MgO and 70 wt% Al_2O_3), HT63 (63 wt% of MgO and 37 wt% Al_2O_3), HT70 (70 wt% of MgO and 30 wt% Al_2O_3). The hydrotalcites used were produced by Sasol Germany GmbH company (a successor of company CONDEA Chemie GmbH - supplier of hydrotalcites for PtSn catalyst). Catalysts with two different concentrations (1 wt% and 2 wt%) of Pt were prepared with every support (6 variants).

To prepare the catalysts, the precursor chloroplatinic acid hexahydrate ($H_2PtCl_6 \cdot 6H_2O$; SIGMA-ALDRICH) was dissolved into ethylene glycol. The chloroplatinic acid hexahydrate crystals were stirred for 30 minutes in ethylene glycol under argon flow, at room temperature. The support and water were added. The solution was heated till 110 ℃ using an oil bath. When the constant temperature was reached, the solution was left under argon flow with reflux during 3 hours, in order to ensure the full reduction of the platinum. After that, the catalysts were filtered under vacuum (using water pump) and washed with a distilled water. They were dried at 70 ℃ overnight in air flow. Finally, the catalysts were calcined for 4 hours, with a heating rate of 4 ℃/min

until 600 ℃. (The oven used was a controller P320 by Nabertherm). The calcination took place in air.

All six variants of Pt/HT catalyst were checked for activity (see the testing procedure below), and one of them (1wt%Pt/HT63) was chosen for experiments similar to experiments performed for PtSn/HT50 catalyst (with 1.1 wt% of Pt). The catalyst 1wt %Pt/HT63 was sieved to a particles diameter inferior to 106 μm and it was characterised by XRD, volumetric H_2-chemisorption and N_2-sorption (BET-analysis).

The XRD analyses were performed with a Dfocus 8 equipment using CuKα radiation, and a Lynxeye detector. The wavelength was 1.5406 nm. For each sample, the scans were performed with an angle 2Θ in the range from 5° to 70°, a step of 0.02° and a step time of 0.5 s. The powders were analysed without rotation. The software EVA was used for phase identification.

For the BET analysis, about 100 mg of catalyst was used. Prior the analysis, the samples were degassed at least 8 hours in a sample degas system (VacPrep 061). The temperature used for degassing was 250 ℃. After degassing, the weight of the samples was measured again. The surface area measurements were done with the device TriStar 3000. The nitrogen adsorption isotherms at 77.3 K were used for calculating the various surface areas, applying the BET equation. The cross-section of the nitrogen molecule used for calculation was 0.162 nm^2.

Volumetric chemisorption of hydrogen was performed on a Micrometric ASAP 2020. The purpose of the chemisorption analysis is to determine the number of active sites on the catalyst. Prior to the experiment, the catalyst was reduced in situ in a H_2 flow, with a heating rate of 10 ℃/min up to 500 ℃. Then, the sample was evacuated during 30 min in He flow at 120 ℃. A leak test was performed. Finally, the temperature was decreased to 34 ℃ before the analysis. The weight of the catalyst used for the experiment was 0.148 g. The pressure range for the measurements was 81-207 mmHg. The assumption that the H/Pt ratio is 1:1 was used. Consequently, the spillover was neglected.

The results of characterisation are given in Table 4.1.2.1.

Table 4.1.2.1: Surface area as determined by N_2-sorption; dispersion and crystallite size as calculated from chemisorption for Pt/HT63 catalyst.

SSA, [m^2/g]	Dispersion, [%]; total H_2 ads.	Metallic surface area [m^2/g_{sample}]	Metallic surface area, [m^2/g_{metal}]	Crystallite size, [nm]
136	55	1.36	136.1	2.0

The results shown in Table 4.1.2.1 are very similar to appropriate results shown for a similar catalyst (Pt/HT50 (1 wt% of Pt)) in [8].

4.2 EXPERIMENTAL SET-UP AND REACTION CONDITIONS

4.2.1 EXPERIMENTAL SET-UP

The experimental setup (Fig. 4.2.1.1) is equipped with a fixed-bed quartz reactor (U-form, with an inner diameter of 4 mm) placed in an electrical furnace (Fig. 4.2.1.2). The catalyst (0.075 or 0.15 g) was placed between quartz wool wads in one arm of the U-tube reactor, allowing for feed gas preheating in the other arm. The total gas flow was 50 ml/min. The flow of propane was fixed (10 ml/min), flows of air and hydrogen were varied, the balance being He. The experiments where done between 350 and 650 ℃ at 1 atm. Prior to the experiments the catalyst was reduced in situ in flowing H_2/He (H_2:10 ml/min, He:30 ml/min) at 500 ℃ for 2 hours.

The product gas mixture was analysed by gas chromatography (C_3H_8, C_3H_6, C_1-C_2 hydrocarbons, H_2, N_2, O_2, CO, CO_2, He) using an Agilent 3000A Micro GC based on N_2 as an internal standard. Three columns with TCD detectors were used for detection of different components.

Mass balances were used to calculate water content. The experimental runs lasted approximately 9 hours. After 2 hours of reduction in H_2/He flow at 500 ℃ the temperature in the furnace was decreased to 350 ℃ and the reactant gas mixture was fed to the reactor. After 10 min on stream the product gas was analysed 5 to 7 times. Typically, the 3 last analyses were used for calculation of the average values of the composition. Subsequently the temperature was increased to 400 ℃ and after 10 min

the gas composition was again analysed several times in the same manner. In this way the reaction was studied at temperatures in the range 350~500 ℃ with 50 ℃ steps and in the range 500~650 ℃ with step of 25 ℃. In addition other experiments were carried out using the same procedure but with a different feed gas: H_2+O_2 (1:1); H_2+O_2 (1:1) without catalyst but with quartz wool in the reactor; H_2+O_2+C_3H_8 without catalyst but with quartz wool.

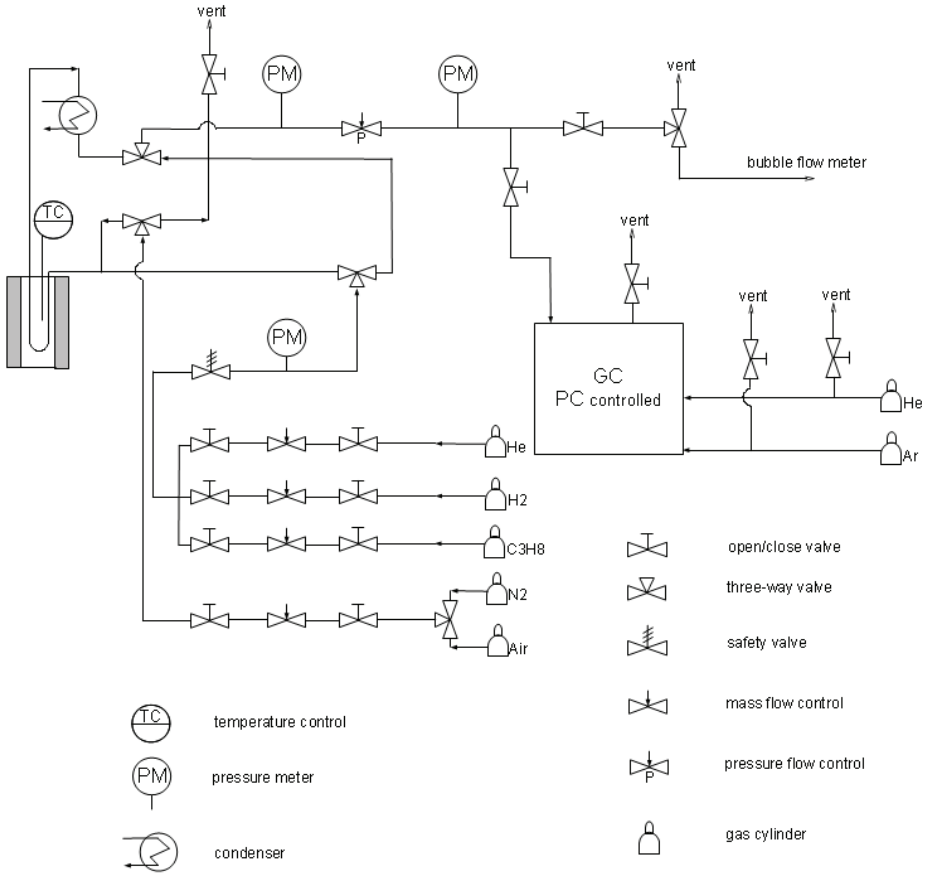

Fig. 4.2.1.1: Schematic drawing of the set-up used in experiments.

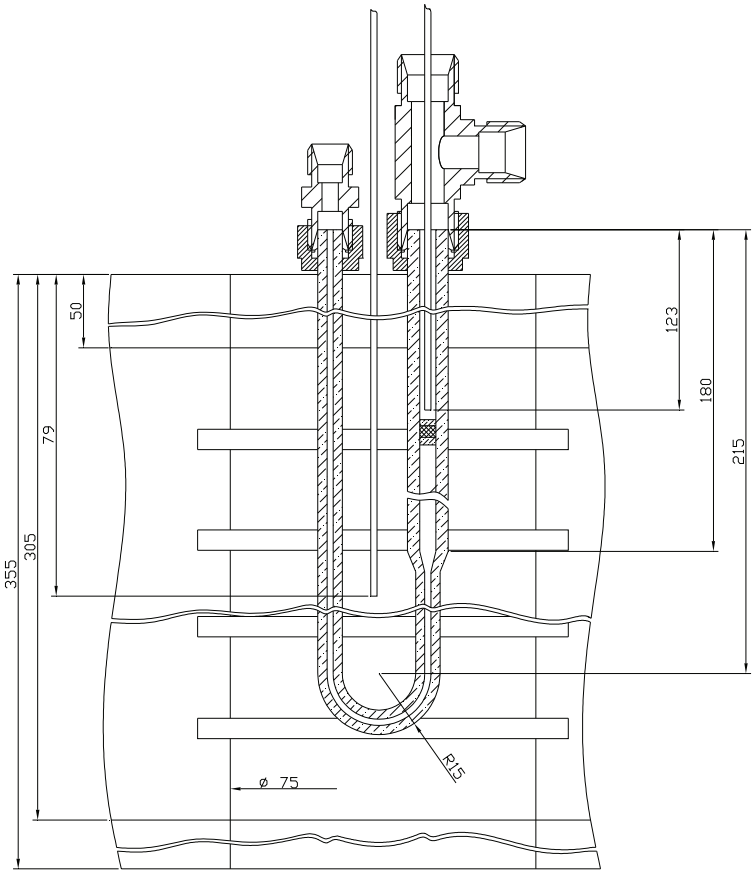

Fig. 4.2.1.2: Schematic drawing of the U-tube reactor and its placement in the oven.

4.2.2 COMPOSITION-PROPERTY DIAGRAMS

The detected products of the reaction are C_3H_6, H_2, CO, CO_2 and in some cases lighter hydrocarbons (C_1-C_2). H_2O is not detected, the selectivity and yield are determined by difference, assuming no other O-containing products are formed. The selectivity and yields were defined in terms of C and O mass balances. We study the properties of the

3-component mixture (C_3H_8, H_2, O_2) at different temperatures, varying composition of the feed gas mixture (as properties we define here the yields of the reaction products). At every temperature level these properties depend only on the ratio between the components. Thus we study in this experiment the properties (the result of the reaction) of a gas mixture. The results depend only on the ratio between the feed gas components. In this case "composition-property" diagrams are often used. The factorial space for the system is a regular simplex - equilateral triangle. Every point in the triangle represents a particular composition of the reaction mixture, this composition is expressed in molar fractions of components. The vertexes of the triangle correspond to pure substances, and the sides correspond to binary systems. The property (y) is usually represented by a projection of the lines of equal value to the plane of concentrational triangle. It is assumed that the studied property is a continuous function of its arguments and that this function can be represented by a reliable polynomial equation.

We build composition-property diagrams for catalysts PtSn/HT50 and Pt/HT63 at temperatures 525~650 ℃. For the gas-phase reaction (without catalyst) diagrams are built for 600 and 650 °. The diagrams are the following: propane conversion, yields of products. For gas-phase reaction the diagram describing oxygen conversion is also constructed. For compounds with low yields (CH_4 and sometimes C_2- compounds) the diagrams are not built because of low quality of polynomials fitting procedures.

For the description of the response surfaces polynomials of the third order are used. Taking into consideration the normalizing condition for the sum of variables (4.2.2.1) (molar fractions of mixture components - O_2, C_3H_8, H_2 in our case),

$$\sum_{i=1}^{3} x_i = 1 \qquad (4.2.2.1)$$

the polynomial of third order for three variables can be transformed to a reduced polynomial (4.2.2.2) ([73], p. 271):

$$y=\beta_1\cdot x_1+\beta_2\cdot x_2+\beta_3\cdot x_3+\beta_{12}\cdot x_1\cdot x_2+\beta_{13}\cdot x_1\cdot x_3+\beta_{23}\cdot x_2\cdot x_3+\gamma_{12}\cdot x_1\cdot x_2\cdot(x_1-x_2)+ \\ +\gamma_{13}\cdot x_1\cdot x_3\cdot(x_1-x_3)+\gamma_{23}\cdot x_2\cdot x_3\cdot(x_2-x_3)+\beta_{123}\cdot x_1\cdot x_2\cdot x_3; \qquad (4.2.2.2)$$

The chosen conditions of the experiments as well as the limitations of the experimental setup allowed us to vary the fractions of components only in limited ranges: $[O_2] \in [0, 0.45]$, $[C_3H_8] \in [0.21, 1]$, $[H_2] \in [0, 0.79]$ for the PtSn catalyst. The experimental points are shown in the plot in Fig. 4.2.2.1*a*.

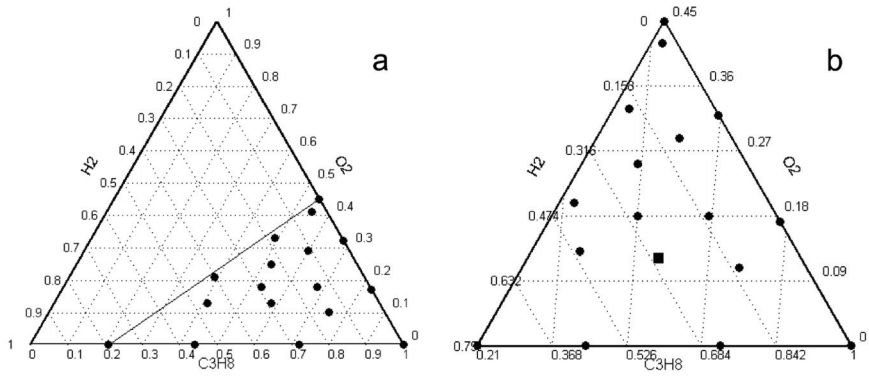

Fig. 4.2.2.1: a) composition diagram with experimental points, for experiment with PtSn catalyst, in right corner. Vertexes of new triangle ($[O_2]$:$[C_3H_8]$:$[H_2]$): 45:55:0; 0:100:0; 0:21:79. b) rescaled triangle (with one point for control purposes (18:68:14)). Point (13:58:30) is measured twice for dispersion calculation.

As we study properties of the system in a limited area of the variables, and in order to use plans aimed for studying complete diagrams, we need to make a renormalization of the plot. The compositions in the new vertexes are taken as selfstanding pseudocomponents z_i, so that for the area of the local simplex shown in the plot in Fig. 4.2.2.1*b* the condition in (4.2.2.3) holds [73]:

$$\sum_{i=1}^{3} z_i = 1 \qquad (4.2.2.3)$$

The planning of the experiments is made in the coordinate system of pseudocomponents. Experimental points on the rescaled diagram are shown on Fig. 4.2.2.1*b* . For convenience the subscripts under the axes are made in real components values.

Relation between variables x and pseudo-variables z ([73], p. 291):

$$\begin{aligned} z_1 &= z_1^{(1)} + x_2 \cdot \left(z_1^{(2)} - z_1^{(1)} \right) + x_3 \cdot \left(z_1^{(3)} - z_1^{(1)} \right); \\ z_2 &= z_2^{(1)} + x_2 \cdot \left(z_2^{(2)} - z_2^{(1)} \right) + x_3 \cdot \left(z_2^{(3)} - z_2^{(1)} \right); \\ z_3 &= 1 - z_1 - z_2 ; \end{aligned} \qquad (4.2.2.4)$$

where z_1,z_2,z_3 - composition in a new system; $x_i^{(j)}$ - amount of i-th component in j-th vertex (vertex of pseudo-triangle) in real coordinate system; $z_i^{(j)}$ - amount of pseudo-component z_i in vertexes of initial triangle. $x_1^{(1)}$ is $x_{O2}^{(up)}$, $x_1^{(2)}$ - $x_{O2}^{(right)}$, $x_1^{(3)}$ - $x_{O2}^{(left)}$; $x_2^{(1)}$ - $x_{C3H8}^{(up)}$, $x_2^{(2)}$ - $x_{C3H8}^{(right)}$, $x_2^{(3)}$ - $x_{C3H8}^{(left)}$; $x_3^{(1)}$ - $x_{H2}^{(up)}$, $x_3^{(2)}$ - $x_{H2}^{(right)}$, $x_3^{(3)}$ - $x_{H2}^{(left)}$.

$z_i^{(j)}$ can be found by solving 2 systems of equations:

$$\begin{aligned} x_1^{(1)} \cdot z_1^{(1)} + x_2^{(1)} \cdot z_1^{(2)} + x_3^{(1)} \cdot z_1^{(3)} &= 1 \\ x_1^{(2)} \cdot z_1^{(1)} + x_2^{(2)} \cdot z_1^{(2)} + x_3^{(2)} \cdot z_1^{(3)} &= 0 \\ x_1^{(3)} \cdot z_1^{(1)} + x_2^{(3)} \cdot z_1^{(2)} + x_3^{(3)} \cdot z_1^{(3)} &= 0 \end{aligned} \quad ; \quad \begin{aligned} x_1^{(1)} \cdot z_2^{(1)} + x_2^{(1)} \cdot z_2^{(2)} + x_3^{(1)} \cdot z_2^{(3)} &= 0 \\ x_1^{(2)} \cdot z_2^{(1)} + x_2^{(2)} \cdot z_2^{(2)} + x_3^{(2)} \cdot z_2^{(3)} &= 1 \\ x_1^{(3)} \cdot z_2^{(1)} + x_2^{(3)} \cdot z_2^{(2)} + x_3^{(3)} \cdot z_2^{(3)} &= 0 \end{aligned} \qquad (4.2.2.5)$$

Thus for our data (Fig. 4.2.2.2, Table 4.2.2.1):

$$\begin{aligned} x_1^{(1)} &= 0.45; \quad x_2^{(1)} = 0.55; \quad x_3^{(1)} = 0; \\ x_1^{(2)} &= 0; \quad x_2^{(2)} = 1; \quad x_3^{(2)} = 0; \\ x_1^{(3)} &= 0; \quad x_2^{(3)} = 0.21; \quad x_3^{(3)} = 0.79; \end{aligned} \qquad (4.2.2.6)$$

Solving systems of equations (4.2.2.5) we find the amounts (fractions) of the pseudo-components:

$$\begin{aligned} z_1^{(1)} &= 2.22; \quad z_1^{(2)} = 0; \quad z_1^{(3)} = 0; \\ z_2^{(1)} &= -1.22; \quad z_2^{(2)} = 1; \quad z_2^{(3)} = -0.27; \end{aligned} \qquad (4.2.2.7)$$

Solving the system of equations (4.2.2.4) we fill in the columns for *z* in Table 4.2.2.1:

Table 4.2.2.1: Data for composition diagram.

Experiment №	x_1 , $[O_2]$, %	x_2 , $[C_3H_8]$, %	x_3 , $[H_2]$, %	z_1	z_2	z_3	Yield C_3H_6, at 600°C
1	0	100	0	0	1.0	0	0.10
3	18	53	29	0.40	0.23	0.37	0.39
8	29	60	11	0.64	0.22	0.14	0.28
6	21	39	41	0.44	0.04	0.52	0.37
2	13	41	46	0.29	0.13	0.58	0.33
4	18	68	14	0.40	0.42	0.18	0.33
7	25	52	23	0.56	0.15	0.29	0.31
12	13	58	30	0.27	0.35	0.38	0.36 (0.37*)
5	17	83	0	0.38	0.62	0	0.27
9	32	68	0	0.71	0.29	0	0.29
14	10	75	14	0.24	0.58	0.18	0.37
13	41	55	3	0.93	0.03	0.04	0.29
10	0	44	56	0	0.29	0.71	0.20
11	45	55	0	1.0	0	0	0.23
15	0	72	28	0	0.65	0.35	0.15
16	0	21	79	0	0	1.0	0.22
17	33	49	18	0.73	0.04	0.23	0.33

* - repeated measurement

The result of experiment number 4 (Table 4.2.2.1) and repeated measurement of experiment number 12 were not used for coefficients fitting, but in the model validity check.

The coefficients of regression (4.2.2.2) in coordinates of pseudocomponents were calculated by means of the MATLAB `"nlinfit"` function (nonlinear least-squares regression), based on 16 experimental points. The propene yield dependence on the gas mixture composition at 600 ℃ over PtSn/HT50 catalyst was determined. As a result of this procedure we have a fitted reduced polynomial of third order in pseudocomponents:

$$y = 0.2569 \cdot z_1 + 0.0976 \cdot z_2 + 0.2209 \cdot z_3 + 0.4549 \cdot z_1 \cdot z_2 + 0.4354 \cdot z_1 \cdot z_3 + 0.0899 \cdot z_2 \cdot z_3 - \\ - 0.5311 \cdot z_1 \cdot z_2 \cdot (z_1 - z_2) - 0.2182 \cdot z_1 \cdot z_3 \cdot (z_1 - z_3) + 0.1342 \cdot z_2 \cdot z_3 \cdot (z_2 - z_3) + 1.6490 \cdot z_1 \cdot z_2 \cdot z_3 ; \qquad (4.2.2.8)$$

A plot of this equation is shown on Fig. 4.2.2.2*a*.

Having now found the coefficients of the regression equation it is necessary to make a statistical analysis of the results: to check the adequacy of the model and find the confidence intervals for the values predicted by the model. The F-test and the the Student's t-test were used ([74] pp.47, [73] pp.282). Both methods confirmed that the equation represents the results adequately (see the procedure and results in appendices, Ch. 8.7).

Confidence intervals for the function are different in different points of the simplex ([73], p. 282):

$$y = \hat{y} \pm \Delta ; \\ \Delta = t_{\alpha ll, f} \cdot \sqrt{\frac{s_y^2 \cdot \xi}{m}} ; \qquad (4.2.2.9)$$

where $\hat{y}$ - value calculated by fitted polynomial (shown on Fig. 4.2.2.2*a*), $\pm\Gamma$ - the confidence interval (shown on Fig. 4.2.2.2*b*).

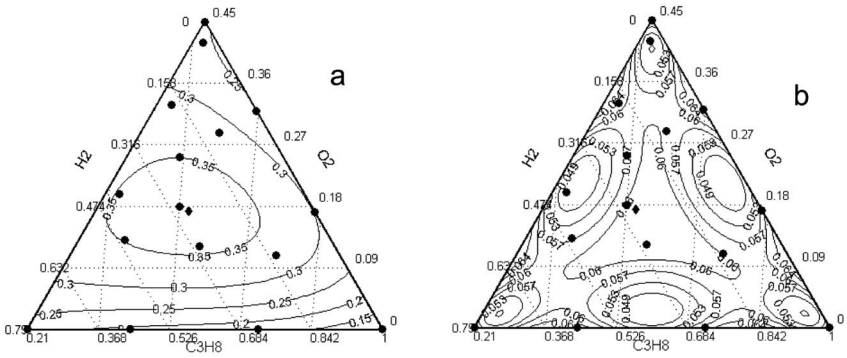

Fig. 4.2.2.2: Plot of $\hat{y}$ - value of the property (propene yield), calculated by the polynomial (a); and plot of Δ - the confidence intervals for the values predicted by the polynomial (b). Plots are built with using data from Table 8.7.3 and m = 2, l = 1.

For practical use it is more convenient to transform equation (4.2.2.8) back to the initial coordinate system:

$$y = 0.1 + 2.54 \cdot x_1 + 0.44 \cdot x_3 + 0.59 \cdot x_1 \cdot x_3 - 10.09 \cdot x_1^2 - 0.79 \cdot x_3^2 - 0.87 \cdot x_1^2 \cdot x_3 - 1.78 \cdot x_1 \cdot x_3^2 + \\ + 11.62 \cdot x_1^3 + 0.55 \cdot x_3^3; \quad \textit{(4.2.2.10)}$$

Here the interdependence of variables (4.2.2.1) gives the possibility of expressing equation (4.2.2.10) in various ways. The computer algebra system MAXIMA [75] can be used for making such transformations.

Since the polynomial fits the experimental values in a sufficient manner we include the control point into fitting procedure and get an equation describing the dependence of the C_3H_6 yield on the composition of the feed (Fig. 5.1.2.2*d*).

Similar expressions can be developed for the fitting of the yields of the other products at every temperature.

For experiments with platinum and experiments without catalyst we first prepare the plan of experiments following the procedure described above. We start with pseudo-variables (in Table 4.2.2.2), and using transformation rules (4.2.2.7), (4.2.2.6), (4.2.2.4) we find real variables - mole fractions of components (Table 4.2.2.2). In this case coordinates of some of the experimental points (the mole fractions of the feed gas mixture components) will be different of points for the experiment with platinum-tin catalyst but compositions in vertexes of the triangle will be the same. Thus the factorial spaces for all systems (experiments with PtSn, Pt and gas-phase) are planned to be identical.

Table 4.2.2.2: The plan of experiments for building the composition diagram for experiments with Pt/HT catalyst.

Experiment №	x_1 , $[O_2]$, %	x_2 , $[C_3H_8]$, %	x_3 , $[H_2]$, %	z_1	z_2	z_3
1	0.45	0.55	0	1	0	0
2	0	1	0	0	1	0
3	0	0.21	0.79	0	0	1
4	0.3	0.7	0	2/3	1/3	0
5	0.15	0.85	0	1/3	2/3	0
6	0	0.74	0.26	0	2/3	1/3
7	0	0.47	0.53	0	1/3	2/3
8	0.3	0.44	0.26	2/3	0	1/3
9	0.15	0.32	0.53	1/3	0	2/3
10	0.15	0.59	0.26	1/3	1/3	1/3
11	0.32	0.57	0.12	0.7	0.15	0.15
12	0.07	0.81	0.12	0.15	0.7	0.15
13	0.07	0.38	0.55	0.15	0.15	0.7
14	0.2	0.68	0.12	0.45	0.4	0.15
15	0.07	0.62	0.32	0.15	0.45	0.4
16	0.18	0.46	0.36	0.4	0.15	0.45
17	0.23	0.58	0.2	0.5	0.25	0.25

* - repeated measurement

After running the experiments with Pt/HT63 catalyst we get real values for the components concentrations and build composition diagrams using these real values. The fractions of components in real and pseudo-variables are given in Table 4.2.2.3. Values used for transformations real ↔ pseudo variables becomes (4.2.2.11), (4.2.2.12):

$$\begin{aligned} &x_1^{(1)}=0.44;\quad x_2^{(1)}=0.56;\quad x_3^{(1)}=0;\\ &x_1^{(2)}=0;\quad x_2^{(2)}=1;\quad x_3^{(2)}=0;\\ &x_1^{(3)}=0;\quad x_2^{(3)}=0.16;\quad x_3^{(3)}=0.84; \end{aligned} \tag{4.2.2.11}$$

$$\begin{aligned} &z_1^{(1)}=2.27;\quad z_1^{(2)}=0;\quad z_1^{(3)}=0;\\ &z_2^{(1)}=-1.27;\quad z_2^{(2)}=1;\quad z_2^{(3)}=-0.19; \end{aligned} \tag{4.2.2.12}$$

Table 4.2.2.3: Data for composition diagram (result of experiments with Pt/HT catalyst).

Experiment №	x_1 , $[O_2]$, %	x_2 , $[C_3H_8]$, %	x_3 , $[H_2]$, %	z_1	z_2	z_3
1	0.44	0.56	0.00	1.00	0	0
2	0.00	1.00	0.00	0	1.00	0
3	0.00	0.19	0.81	0	0.04	0.96
4	0.30	0.70	0.00	0.68	0.32	0
5	0.15	0.85	0.00	0.34	0.66	0
6	0.00	0.71	0.29	0	0.65	0.35
7	0.00	0.41	0.59	0	0.30	0.70
8	0.30	0.45	0.25	0.68	0.02	0.30
9	0.15	0.30	0.55	0.34	0	0.65
10	0.16	0.57	0.27	0.36	0.31	0.32
11	0.33	0.60	0.07	0.75	0.17	0.08
12	0.08	0.82	0.10	0.18	0.70	0.12
13	0.07	0.34	0.59	0.16	0.14	0.70
14	0.21	0.71	0.08	0.48	0.43	0.10
15	0.08	0.59	0.33	0.18	0.43	0.39
16	0.18	0.45	0.37	0.41	0.15	0.44
17	0.22	0.60	0.18	0.50	0.29	0.21

The experimental points are shown on the plot in Fig. 4.2.2.3*a*, a rescaled triangle is presented in Fig. 4.2.2.3*b*.

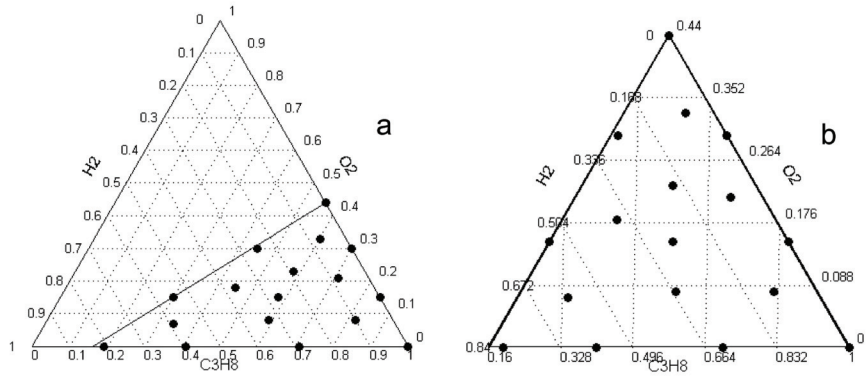

Fig. 4.2.2.3: The experimental plan. a) - composition diagram with experimental points, for experiment with Pt catalyst. Vertexes of new triangle ([O_2]:[C_3H_8]:[H_2]): 44:56:0; 0:100:0; 0:16:84. b) - rescaled triangle.

For experiments using Pt we had some technical issues and two groups of results - experiments carried out at 0.3~0.5 atm pressure drop and at 1.5~1.8 atm pressure drop. Some of the experiments were remeasured, because we aimed to build diagrams for conditions with low pressure. Still a few experiments were not remeasured and it was necessary to make an assumption about some of the results at low pressure - a re-evaluation of results at high pressure simulate results at low pressure. The possibility of such rough estimation follows from comparison of available results for pairs low-high pressure experiments as well as from comparison of results for experiments with similar ratios between components (i.e. with small difference in reaction conditions, thus comparable results). It is seen that the difference for propane conversion (Fig. 8.8.1) and for yields of the products for high and low pressure at temperatures 350~575 ℃ is small. But for temperatures 600~650 ℃ we see a sharp increase in the conversion and yields for experiments at high pressure. We can not use these high pressure results together with low pressure results in construction of compositional diagrams for temperatures 600, 625 and 650 ℃, but we determine approximate deltas and make a correction on results of high pressure drop (adjust to expected results at low pressure drop). The correction procedure is described in appendices, Ch. 8.8

We need to correct results of four measurements (4, 8, 9, 14) of 17 for temperatures 600-650 °C. We make the correction of yields of products by the same procedure.

Some observations, made from a comparison of experiments that differed in pressure drop are as follows. For experiment 7 (high pressure drop) we can see that at 350 °C C_2H_6 and CH_4 are produced in a ratio 1:1 mainly which is in accordance with these being formed in the hydrogenolysis reaction (2.1.17). With increasing of temperature the ratio between C_2H_6 and CH_4 is changing, with growth in the CH_4 amount and a corresponding decrease in the C_2H_6 amount, and production of propene is also increasing, this may be connected with shift to reaction (2.1.18) and dehydrogenation reaction (2.1.1).

For Pt in all experiments with higher pressures the production of CH_4 is higher and production of CO/CO_2 is lower in comparison to appropriate experiments with low pressure drop.

For systems without oxygen in the feed the influence of pressure was not observable (exp. 3 and 7).

4.2.3 THE EFFECT OF CATALYST COMPOSITION

The activity of six Pt catalysts (their compositions are shown in Table 4.2.3.1) was checked at similar conditions (T = 350~650 °C):

	C3H8	H2	Air	He	Total
Feed flow, [ml/min]	10	5.7	15	19.3	50

For the catalysts with 1 wt% of Pt the loading of 0.15 [g] was used, for the catalysts with 2 wt% of Pt the loading of 0.075 [g] was used. Different loadings were used in order to compare the catalysts activity per mass of active element.

Table 4.2.3.1: Composition of platinum catalysts and the catalyst loading for screening experiments.

Label	HT30	HT63	HT70	1 wt% Pt	2 wt% Pt	Loading, [g]
1%Pt/HT30	✓			✓		0.150
2%Pt/HT30	✓				✓	0.075
1%Pt/HT63		✓		✓		0.150
2%Pt/HT63		✓			✓	0.075
1%Pt/HT70			✓	✓		0.150
2%Pt/HT70			✓		✓	0.075

One catalyst (Pt/HT63 with 1 wt% of Pt) was chosen for a series of experiments similar to experiments performed for PtSn/HT50 catalyst (with 1.1 wt% of Pt).

4.2.4 LONG-TERM EXPERIMENT

An experiment using the PtSn catalyst with constant temperature and long time on stream was performed. The aim of the experiment is to determine the stability of catalyst activity. The feed gas composition was $[O_2]:[C_3H_8]:[H_2]$ = 20:50:30; O_2 flow is 3.8 ml/min, C_3H_8 flow is 9.7 ml/min, H_2 flow is 5.8 ml/min and temperature was 600 °C. The experiment lasted 10 hours, then the catalyst was reactivated by consequent air and hydrogen treatment, and the experiment was repeated. The second run lasted 9 hours.

4.2.5 EXPERIMENTS WITHOUT A CATALYST

The same experimental plan as for experiments with the platinum catalyst (Table 4.2.2.2) is also used for the experiment without a catalyst. Measurements are made at temperatures 600 and 650 ℃. The reactor contained the quarts wool without any catalyst (the amount of quarts wool here is the same as in experiments with the catalysts). After running the experiments real values for the components concentrations are gotten and the composition diagrams are built using these real values. The fractions of components in real and pseudo-variables are given in

Table 4.2.5.1. Values used for transformations real ↔ pseudo variables becomes (4.2.5.1), (4.2.5.2):

$$\begin{aligned} &x_1^{(1)}=0.45\,; \quad x_2^{(1)}=0.55\,; \quad x_3^{(1)}=0\,; \\ &x_1^{(2)}=0\,; \quad x_2^{(2)}=1\,; \quad x_3^{(2)}=0\,; \\ &x_1^{(3)}=0\,; \quad x_2^{(3)}=0.16\,; \quad x_3^{(3)}=0.84\,; \end{aligned} \tag{4.2.5.1}$$

$$\begin{aligned} &z_1^{(1)}=2.22\,; \quad z_1^{(2)}=0\,; \quad z_1^{(3)}=0\,; \\ &z_2^{(1)}=-1.22\,; \quad z_2^{(2)}=1\,; \quad z_2^{(3)}=-0.19\,; \end{aligned} \tag{4.2.5.2}$$

Table 4.2.5.1: Data for composition diagram (result of experiments without catalyst).

Experiment №	x_1 , $[O_2]$, %	x_2 , $[C_3H_8]$, %	x_3 , $[H_2]$, %	z_1	z_2	z_3
1	0.44	0.56	0.00	1.00	0	0
2	0.00	1.00	0.00	0	1.00	0
4	0.31	0.69	0.00	0.70	0.30	0
5	0.15	0.85	0.00	0.34	0.66	0
6	0.00	0.71	0.29	0	0.66	0.34
7	0.00	0.40	0.60	0	0.29	0.71
8	0.31	0.45	0.24	0.70	0.01	0.28
9	0.16	0.30	0.54	0.36	0	0.64
10	0.16	0.58	0.26	0.36	0.33	0.31
11	0.34	0.61	0.05	0.77	0.17	0.06
12	0.08	0.92	0.00	0.18	0.82	0
13	0.08	0.33	0.59	0.18	0.12	0.70
14	0.22	0.72	0.06	0.50	0.43	0.07
15	0.07	0.60	0.33	0.16	0.45	0.39
16	0.14	0.47	0.39	0.32	0.22	0.46
17	0.24	0.59	0.17	0.55	0.25	0.20

The experimental points are shown on the plot in Fig. 4.2.5.1*a*, a rescaled triangle is in Fig. 4.2.5.1*b*.

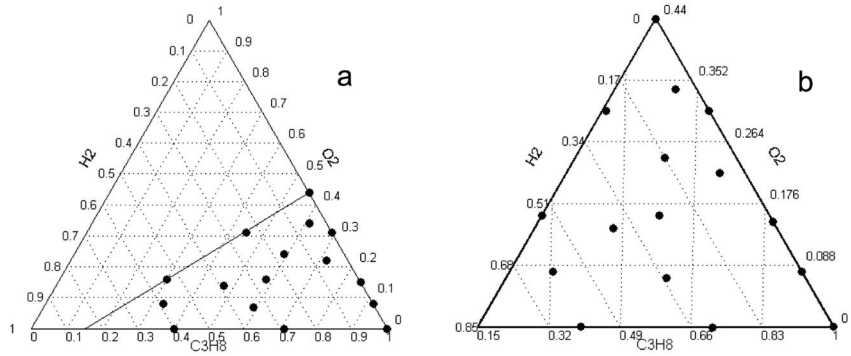

Fig. 4.2.5.1: The plan of experiment. a) - composition diagram with experimental points, for experiment without catalyst. Vertexes of new triangle ([O2]:[C3H8]:[H2]): 44:56:0; 0:100:0; 0:15:85. b) - rescaled triangle.

5 RESULTS AND DISCUSSION

5.1 PLATINUM-TIN CATALYST

5.1.1 LONG-TERM EXPERIMENT

In order to study the catalyst stability a long-term experiment was performed. Since coke formation is expected to be a key feature it is important that the conditions give a reasonable propane conversion.

The initial feed mixture contains helium, hydrogen, propane and air (total flow 50 ml/min), where $[O_2]:[C_3H_8]:[H_2]$ = 20:50:30; O_2 flow is 3.8 ml/min, C_3H_8 flow is 9.7 ml/min, H_2 flow is 5.8 ml/min. The experiment is performed at 600 °C in two runs. The first run lasted 10.5 hours with GC measurements every 0.5 hrs in between 0 and 2.5 hrs of experiment and then every hour. After the last measurement the feed composition was changed (propane flow was stopped and He flow increased to keep constant total flow). One GC measurement of the gas flow reacted without propane was made. The system was kept in flowing $He/H_2/O_2$ overnight. Then the catalyst was tested again at the same initial conditions as in the first run for 8.5 hrs.

In Fig. 5.1.1.1 the propane and hydrogen conversions (*a*) as well as propylene yield (*b*) for both runs are shown.

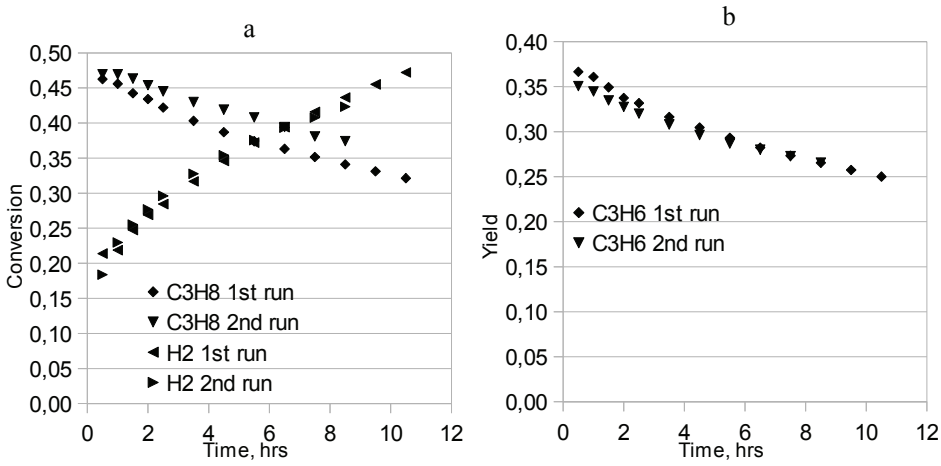

Fig. 5.1.1.1: Propane conversion and hydrogen conversion for first and second runs in a long-term experiment (a). Propylene yield for first and second runs in a long-term experiment (b).

The propane conversion decreased from 46% to 32% over 10 hrs in the first run. After the He flushing the conversion in the second run started at the same level and decreased with approximately the same rate. The oxygen conversion was complete in both runs. The hydrogen conversion was identical in both runs and increased with time from initially around 22% to ~46% after 10 hours on stream.

The selectivity for propylene was constant at 78% during the first run and at 72% in the second run. Other product selectivities were: CO, C_2H_6 ~1%; CO_2, CH_4 4~5%; C_2H_4 slowly grew from 3 to 6%. In the second run selectivities for co-products were similar to the ones in the first run. Oxygen selectivities towards H_2O, CO, CO_2 were identical in both runs (for H_2O 84%, CO ~3%, CO_2 ~13%). In Fig. 5.1.1.2 the time dependency of the yields of oxygen-containing products are shown.

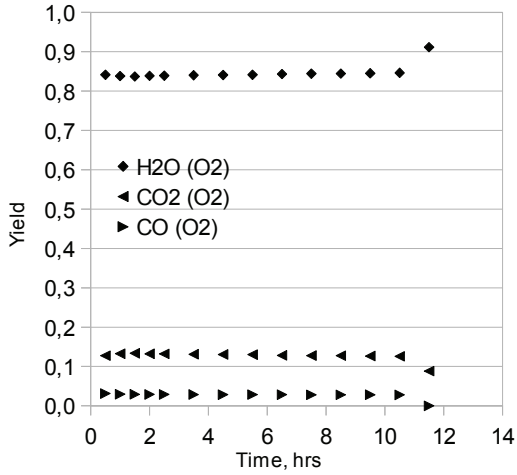

Fig. 5.1.1.2: Yields of CO, CO_2, H_2O (oxygen balance) in a long-term experiment. The last point is for feed mixture without propane.

The last point on the plot in Fig. 5.1.1.2 depicts the analysis after the propane flow was stopped, the flow of inert helium was increased to keep the total flow constant at 50 ml/min. Without feeding any carbon containing compounds into the reactor CO_2 was still produced, but the yield of CO_2 decreased from 13% (when propane was in the feed mixture) to 9% (without propane), and the CO production stopped. The hydrogen conversion became complete.

This picture can be explained as follows. During the propane dehydrogenation experiment the rate of formation of coke precursors on the surface is higher than the rate of oxidation of these precursors (or hydrogenation of it) removing it from the surface. The precursors oxidation reaction gives CO_2. Thus the CO detected is produced from C_xH_ys directly and not through coke precursors deposited on the catalyst surface.

The hydrogen conversion grew constantly with time but this is not visible in the yields of C-containing products. Hydrogen from feed and from dehydrogenation both participated in water production (as the amount of hydrogen in the feed was not enough for production of the estimated amount of water). At the same time in the measurement without propane in a feed, the hydrogen conversion became complete,

thus also hydrogen from coke precursors participated in water production. The hydrogen conversion increase in time was connected to grow of coke precursors on the catalyst surface (or/and grow of the fraction of hydrogen in coke precursors).

5.1.2 COMPOSITION-PROPERTY DIAGRAMS FOR PLATINUM-TIN CATALYST

In order to study the influence of the composition of feed gas on the results of reaction we construct the "composition-property" diagrams. As we have a 3-component mixture (C_3H_8, H_2, O_2) we use simplex diagrams. The studied properties are fitted by polynomials and plotted on diagrams as contour lines.

5.1.2.1 READING DIAGRAMS

First some information on how to read the diagrams. All lines of specific ratios (e.g. stoichiometric ratio) of two components go through the vertex of triangle related to the third component (e.g. the stoichiometric line of H_2 to O_2 goes through the vertex where C_3H_8 is 100%); if the contour lines of a property are parallel to the coordinate lines of one of the components (for the same level of a component the change in the property is minimal), this component determines (has the highest influence on) this property.

If contour lines of a property are parallel to a line representing a specific ratio (e.g. stoichiometric ratio) of two components (e.g. A and B, and we look and the area with excess of B), it can mean that the property is dependent on the amount of B after complete consumption of A (which occurs on the stoichiometric line). This is a sign of selective processes. First B is selectively used for processes involving component A, and the property plotted on the diagram has (in the area of excess of A) a complex dependence on the ratio of components or is determined by the lack of B, and after the stoichiometric line the excess of B starts to determine the property. As long as all three components (A, B, C) are connected through relation (4.2.2.1), the dependence can be more complex. For the case described above, the property after consumption of A can be dependent either on B or on C ([C] = Const-[B]) or on specific ratio B:C (keeping A

constant, i. e. moving along A value, we go from the stoichiometric line to a line of the property parallel to the stoichiometric line, and thus we make a step in the B value; we have related step in C, $[C_{step}] = 1 - [A_{const}] - [B_{step}]$).

In order to make a correct conclusion it is necessary to take into consideration the nature of chemical processes presumably running in the appropriate concentrational area (the described situation occurs in case with water - Fig. 5.1.2.4). For cases with strong dependence of the property on the component which is expected to be in a shortage in the area under consideration, one can propose the dependence of the property on the product of this component.

For a more detailed analysis of the form of property surfaces on the simplex diagrams it is necessary to compare diagrams constructed using the same data, but with a different sequence of components along the perimeter of the diagram (e.g. $H_2 \longrightarrow O_2 \longrightarrow C_3H_8$ and $O_2 \longrightarrow H_2 \longrightarrow C_3H_8$). For example the line representing the stoichiometric ratio between H_2 and O_2 on the simplex used in this work ($O_2 \longrightarrow H_2 \longrightarrow C_3H_8$ counter-clockwise) is going through the vertex with 100% of propane and this vertex is adjacent to the O_2 side, whereas for simplex $H_2 \longrightarrow O_2 \longrightarrow C_3H_8$ it is adjacent to H_2 side. Thus the property function will be different (reflected in some manner).

A complex dilution effect can have an influence on the results. We can see such effect in [17] (see Ch. 2.2), but it does not have an influence on the form of the responces curves there, but mainly on the value of responces. The propane flow in our case is always constant (10 ml/min), whereas H_2 and O_2 flows are varied, so the dillution can possibly be concerned with H_2 and O_2 (this will give rise to some differences for the form of the responses from composition to composition).

5.1.2.2 DIAGRAMS DISCUSSION (PLATINUM-TIN CATALYST)

Figs. 5.1.2.1~5.1.2.8 show the compositional diagrams for experiments with PtSn catalyst, with three varying components - gas phase fractions of oxygen, propane and hydrogen in the initial mixture in the feed to the reactor. The contour lines represent the isolevel lines of the response surface with numbers indicating the actual values of

the plotted responses (propane conversion, yields of products - C_3H_6, H_2O, CO, CO_2, CH_4 - at temperatures 525, 550, 575, 600, 625, 650 ℃; yields of C_2H_4, C_2H_6, at temperatures 600, 625, 650 ℃). The dashed line is drawn parallel to fractions of oxygen and hydrogen related stoichiometrically according to the reaction of hydrogen oxidation ($[O_2]$:$[H_2]$=1:2). The maximum of the response function is indicated by a diamond marker (◆), experimental points are shown by filled circles.

The propane conversion is shown on Fig. 5.1.2.1. The form of the surface (fitted function) of conversion should reflect the sum of surfaces of yields of the main products. Thus the analysis of it is more complicated.

For low temperatures the propane conversion is dependent on either hydrogen concentration or on some specific ratio between H_2 and propane. Especially on plots Fig. 5.1.2.1*c* and Fig. 5.1.2.1*d* we see a certain dependency on the ratio H_2:C_3H_8 - the altitude (ridge line of a surface) follows an imaginary line of a H_2/C_3H_8 specific ratio (which should intersect the point of 100% O_2). Whatever the ratio exactly is, the angle of this imaginary line is changed with temperature with a decrease of propane fraction in this ratio. On plots Fig. 5.1.2.1*a~d* we see a dependence of the maximum altitude on the H_2/C_3H_8 ratio and already on Fig. 5.1.2.1*e* it is mainly dependent on the H_2 concentration and on Fig. 5.1.2.1*f* the dependence on H_2/O_2 ratio is observed (the altitude is parallel to the line of H_2:O_2 ≈1:1 ratio).

For all temperatures the maximum in conversion lays in the area of oxygen excess (over the water stoichiometric line). For temperatures up to 600 ℃ (Fig. 5.1.2.1*a~d*) the highest conversion tend to be in the area of maximum oxygen concentration. For higher temperatures the maximum conversion lies in areas with lower propane concentrations. This means that for lower temperatures oxygen-assisted processes play the largest role in propane conversion, whereas at high temperatures some other processes have similar selectivities as oxygen-assisted processes (e.g. cracking, dehydrogenation). At 625, 650 ℃ we have byproducts CH_4, C_2H_4, C_2H_6 produced together with CO, CO_2 in addition to main product - propylene.

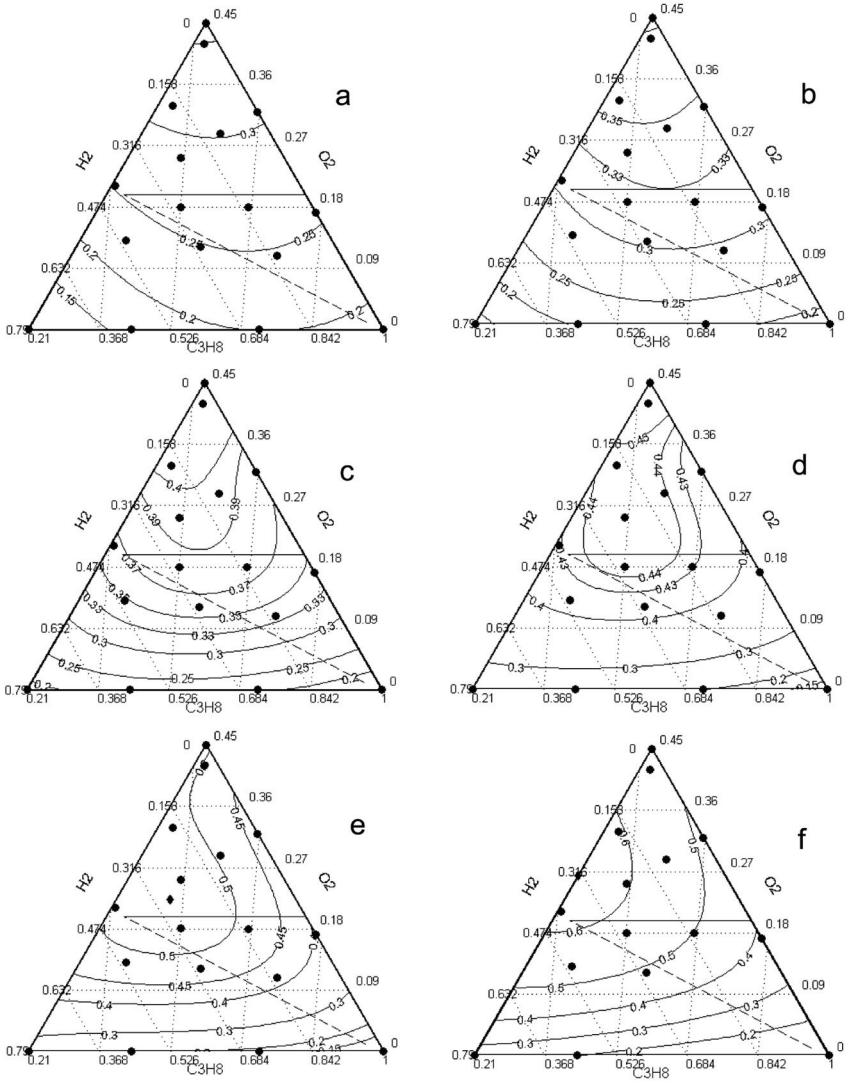

Fig. 5.1.2.1: C_3H_8 conversion at temperatures: a) 525 ℃, b) 550 ℃, c) 575 ℃, d) 600 ℃, e) 625 ℃, f) 650 ℃. The dashed line represents the stoichiometry 1:2 for the $[O_2]$:$[H_2]$ in the feed. The solid horizontal line represents the fraction 0.2 for the oxygen in the feed.

The propylene yields are shown on Fig. 5.1.2.2. The maximum propylene yield for all temperatures is close to a fraction of oxygen around 0.17. With increasing temperature the maximum moves from an area with high concentration of propane at low T

($[C_3H_8] \approx 0.6$, $[H_2] \approx 0.2$) to an area with a high concentration of hydrogen ($[C_3H_8] \approx 0.25$, $[H_2] \approx 0.55$) at high temperature.

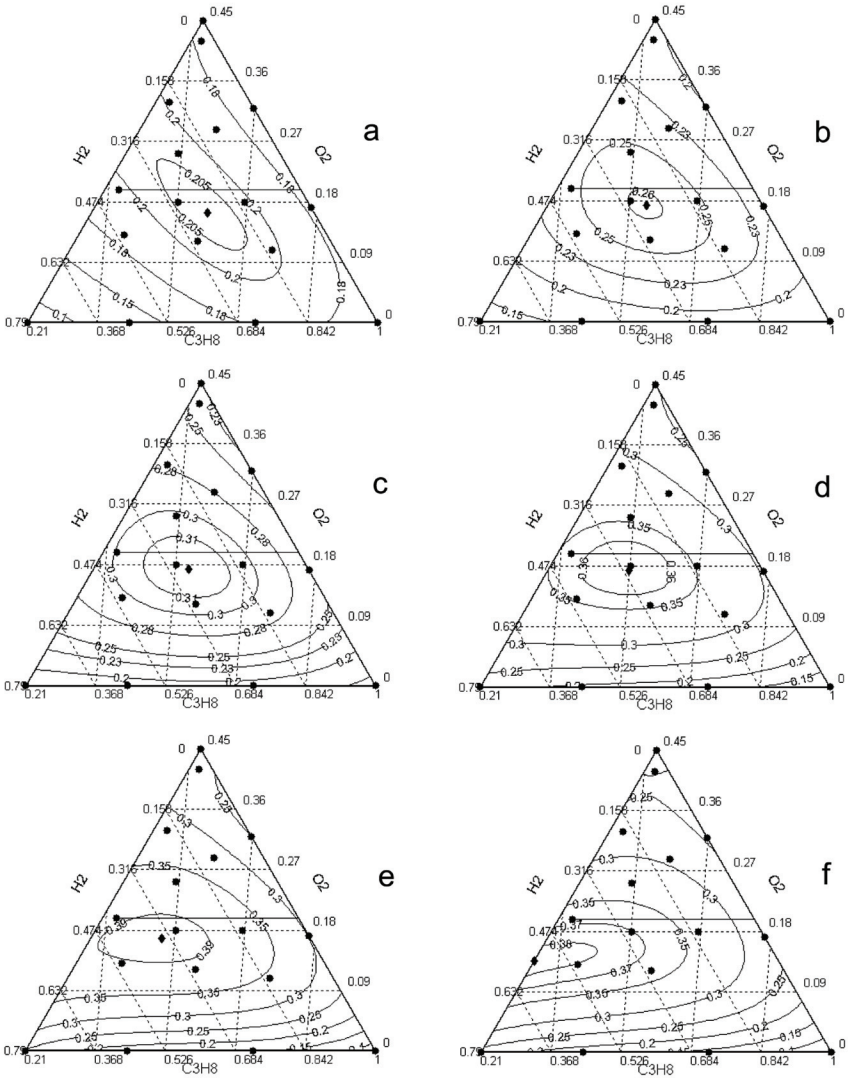

Fig. 5.1.2.2: Yield of propylene at temperatures: a) 525 ℃, b) 550 ℃, c) 575 ℃, d) 600 ℃, e) 625 ℃, f) 650 ℃. The solid horizontal line represents the fraction 0.2 for the oxygen in the feed.

The isolevel lines in Fig. 5.1.2.2*a* are close to parallel with the lines describing the hydrogen fraction, but in Fig. 5.1.2.2*f* describing experiments at 650 °C the isolevel lines are aligned with the lines representing the oxygen fractions. This corresponds to a stronger influence of the hydrogen concentration on the yield at lower temperatures and of the oxygen concentration at higher temperatures. A straight solid line is drawn parallel to the 0.2 fraction of oxygen, this is the line describing an autothermal process where half of all the hydrogen in the system is oxidized. But the dehydrogenation of propane is not complete and therefore hydrogen produced by dehydrogenation is not completely available for the water production reaction (see below), thus it is necessary to have a lower concentration of oxygen for an autothermal process to take place. We can see the maximum of propylene production laying along the line of 17% oxygen concentration.

The influence of the hydrogen concentrations at low temperature (in the area with lack of hydrogen) on the propene yield over PtSn can also mean that the influence is actually from the product of it - water. At the same time from the plots for water yields (Fig. 5.1.2.3) we see that water is dependent not only on hydrogen, but also on the H_2/C_3H_8 ratio. This mean that propene formation at low temperature is correlated with the water amount, specifically with water that is formed from hydrogen in the feed.

From the plots of the yield of water (Fig. 5.1.2.3) we can see that it strongly depends on the H_2/O_2 ratio. The dashed stoichiometric lines of oxygen and hydrogen fractions divide the plots into two areas. Below the water stoichiometric line (excess of hydrogen) there is a plateau at 100 % yield. Above the water stoichiometric line, with increasing distance from the line, the water yield decreases. The isolevel lines are parallel to the water stoichiometric line, which means that in the area of lack of the hydrogen the amount of water formed is determined by the available hydrogen. If propane was influencing the water production, the isolevel lines would be placed at a different angle to the water stoichiometric line (propane would give additional hydrogen for the reaction). But if it did not have an influence (dependency only on hydrogen), the isolevel lines would be parallel to the hydrogen concentrations. It

means that water formation is related to propane concentration not through hydrogen (from dehydrogenation for water production) but through CO_x formation (CO_x and H_2O are correlated through competition for oxygen). Surfaces on Fig. 5.1.2.3 show that the ratio H_2/C_3H_8 determines the water yield.

The water production is not correlated to propene yield (Fig. 5.1.2.3), hydrogen from dehydrogenation is not converted to water (or possibly only a small and *constant* part of it). This is similar to results in [32], where 90% of the oxygen was used to form H_2O from H_2 introduced but only 5% of oxygen was used to form H_2O from H_2 resulting from propane dehydrogenation (when the feed contained only C_3H_8 and O_2).

We interpret this to indicate that the water in this system is produced mainly from hydrogen that is fed to the reactor, combusted in the gas phase or in the very beginning of catalyst bed.

The change in the water yield with the temperature has the following features: the lowest level of the yield is located at the same area for all temperatures, whereas the plateau of high yield becomes more narrow. The selectivity towards water in the area of hydrogen excess depends on the temperature to a grater degree than does the selectivity in the area of oxygen excess.

At 650 ℃ in the left part of the diagram the yield isolevel lines become parallel to the oxygen levels. They start to be more dependent on the oxygen concentration. The yield of water is correlated to yields of CO (Fig. 5.1.2.4) and CO_2, (Fig. 5.1.2.5). At high temperatures the formation of these compounds compete strongly for oxygen.

If we have little inlet hydrogen, oxygen reacts preferably with carbon compounds producing CO_2 and CO and much less water.

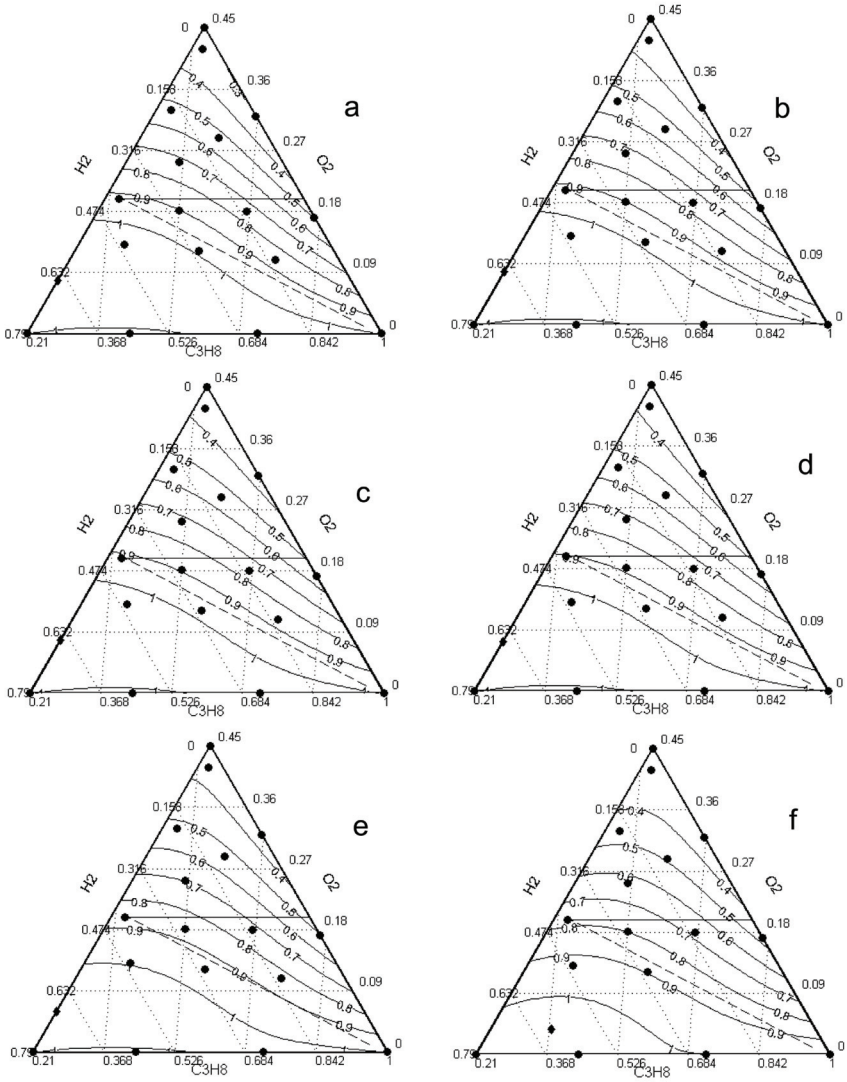

Fig. 5.1.2.3: Yield of H_2O (based on O_2) at temperatures: a) 525 ℃, b) 550 ℃, c) 575 ℃, d) 600 ℃, e) 625 ℃, f) 650 ℃. The solid horizontal line represents the fraction 0.2 for the oxygen in the feed.

From the diagrams for CO and CO_2 yields, Figs. 5.1.2.4 and 5.1.2.5 respectively, we can see that the CO_x-yield is dependent on the relation between concentrations of oxygen and hydrogen at low temperatures. CO and CO_2 is produced in higher yields when

oxygen is in excess compared to hydrogen. Almost no CO/CO_2 is produced below the stoichiometric line.

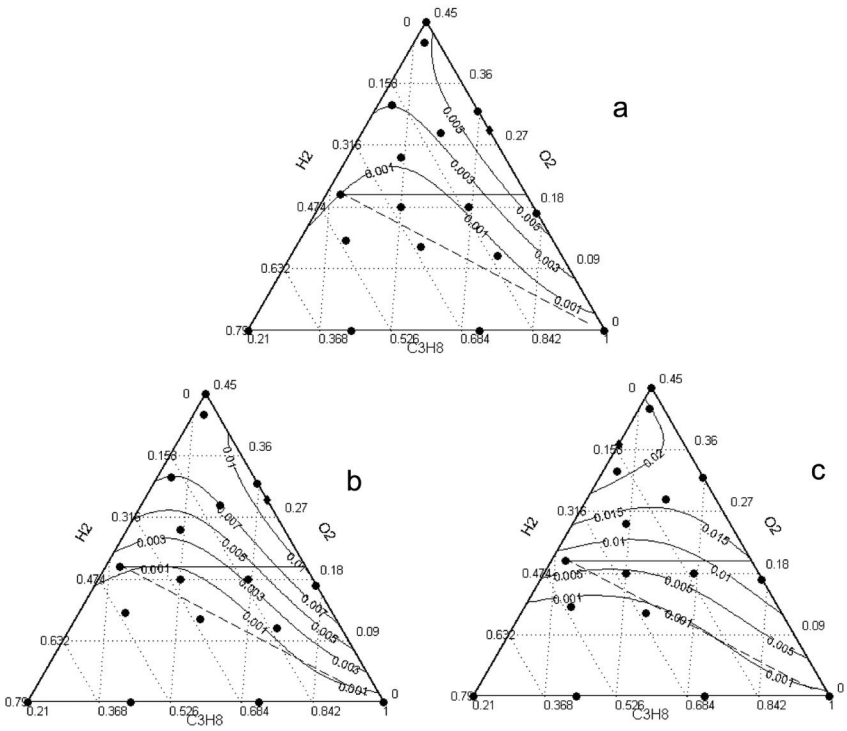

Fig. 5.1.2.4: Yield of CO (C_3H_8) at temperatures: a) 600 ℃, b) 625 ℃, c) 650 ℃. The dashed line represents the stoichiometry 1:2 for the $[O_2]$:$[H_2]$ in the feed. The solid horizontal line represents the fraction 0.2 for the oxygen in the feed.

Taking into consideration that water is mainly formed from hydrogen supplied in the feed, it is clear that CO/CO_2 are formed by the oxygen left after hydrogen combustion and water does not participate in CO/CO_2 production at low temperatures. The close correlation between the yield of CO and the stoichiometric line ($[CO] \propto [O_2]:[H_2]$) shows that CO is formed competitively with H_2O and subsequent to H_2O. Thus we can imagine concentration isolevel lines of CO determined by the yield of CO to be parallel to the water stoichiometric line. It is also evident that the levels of CO_2 yield lie at a certain angle to the water stoichiometric line (or CO concentrations).

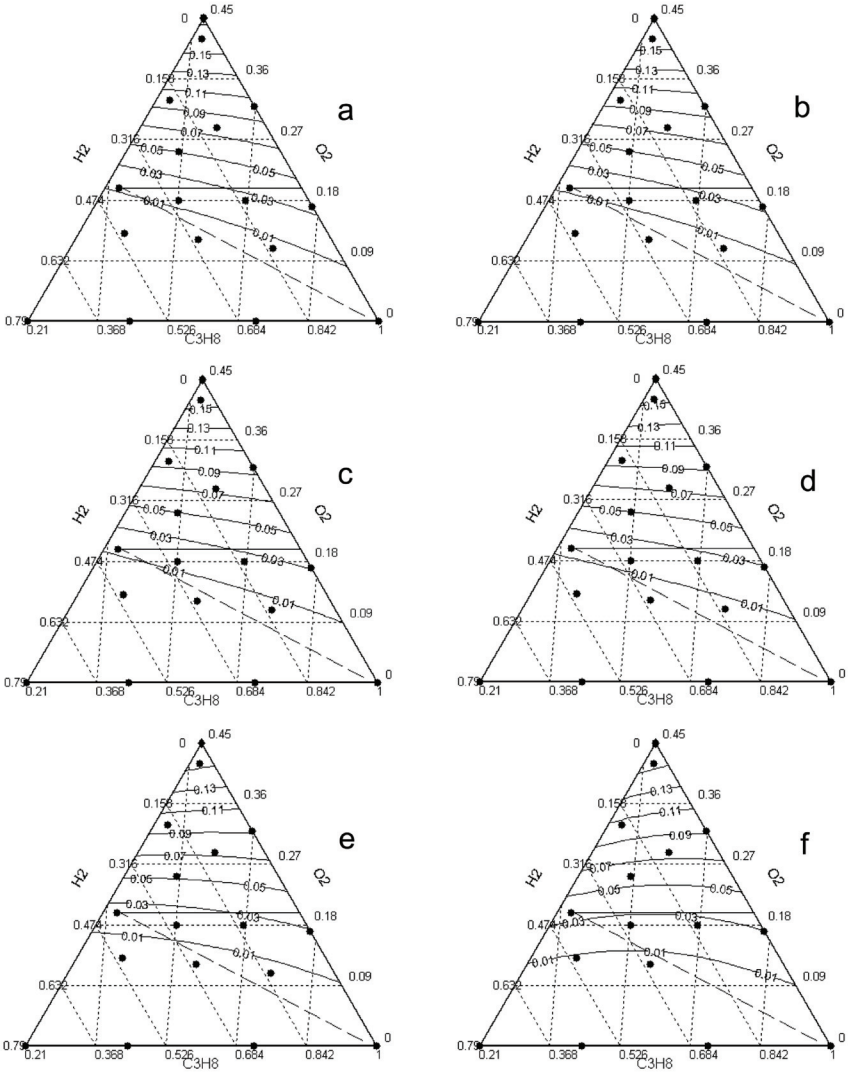

Fig. 5.1.2.5: Yield of CO_2 (C_3H_8) at temperatures: a) 525 ℃, b) 550 ℃, c) 575 ℃, d) 600 ℃, e) 625 ℃, f) 650 ℃. The dashed line represents the stoichiometry 1:2 for the $[O_2]$:$[H_2]$ in the feed. The solid horizontal line represents the fraction 0.2 for the oxygen in the feed.

Making the assumption that CO_2 is formed mainly from CO by the reaction:

$$CO+\frac{1}{2}O_2\rightarrow CO_2 \qquad (5.1.2.1)$$

we see that the ratio between [CO] and $[O_2]$ is 2:1 - the same as for $[H_2]$:$[O_2]$. Thus we can construct a line on the plot of CO_2 yield, which is the stoichiometric line of (5.1.2.1). As $[CO] \propto [O_2]:[H_2]$ = 1:2 and $[CO_2] \propto [O_2]:[CO]$ = 1:2, $[CO2] \propto [O_2]:[H_2]$ = 1:4. The isolevel lines of CO_2 yield appears to be in very close correlation with this line of oxygen - hydrogen ratio 1:4. Thus the assumption about the main route of CO_2 formation is reliable. At higher temperatures the yield of CO and CO_2 depends on the oxygen concentration.

On Fig. 5.1.2.6 plots for yields of C_2H_4 are shown.

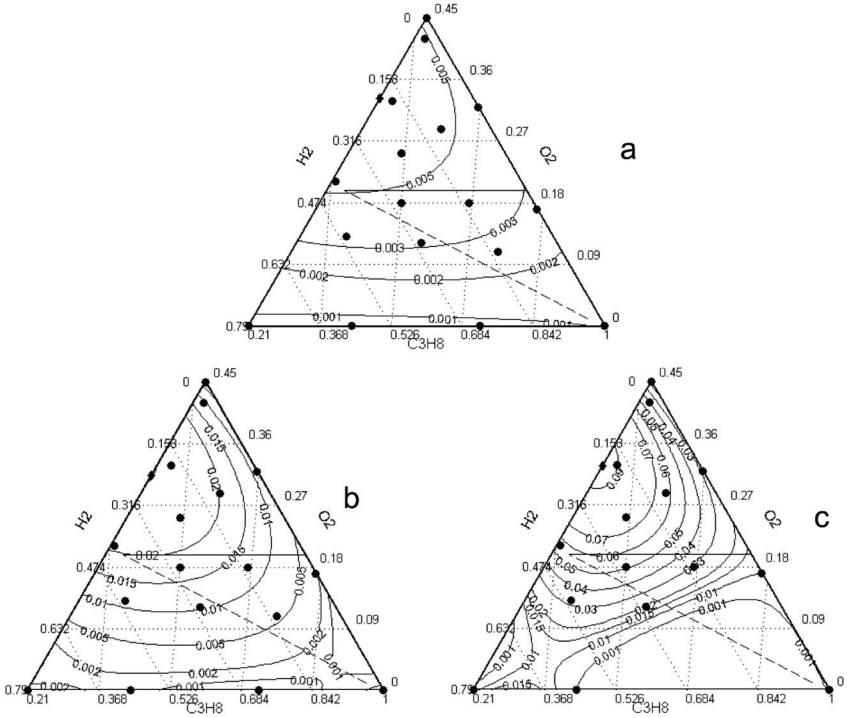

Fig. 5.1.2.6: Yields of C_2H_4 (C_3H_8) at temperatures: a) 600 ℃, b) 625 ℃, c) 650 ℃. The dashed line represents the stoichiometry 1:2 for the $[O_2]$:$[H_2]$ in the feed. The solid horizontal line represents the fraction 0.2 for the oxygen in the feed.

We see here that the yield in the area of hydrogen excess is determined mainly by the oxygen concentration (the more oxygen available, the higher is the ethene yield),

whereas in the area of oxygen excess the hydrogen concentration determines the yield (the higher the hydrogen concentration, the higher is the ethene yield). The border between the two areas is shifted to over the stoichiometric line (the altitude is along $[H_2]$:$[O_2]$ ≈1:1), with the maximum in the area of high oxygen concentrations (over the water stoichiometric line) and low propane concentrations.

On Fig. 5.1.2.7 yields for ethane are shown. We can see here that the isolevel lines are drawn along some O_2/C_3H_8 ratio (they are in average perpendicular to the water stoichiometric line). However, with increasing distance from the water stoichiometric line the influence of hydrogen in the oxygen excess area and oxygen in the hydrogen excess area are seen.

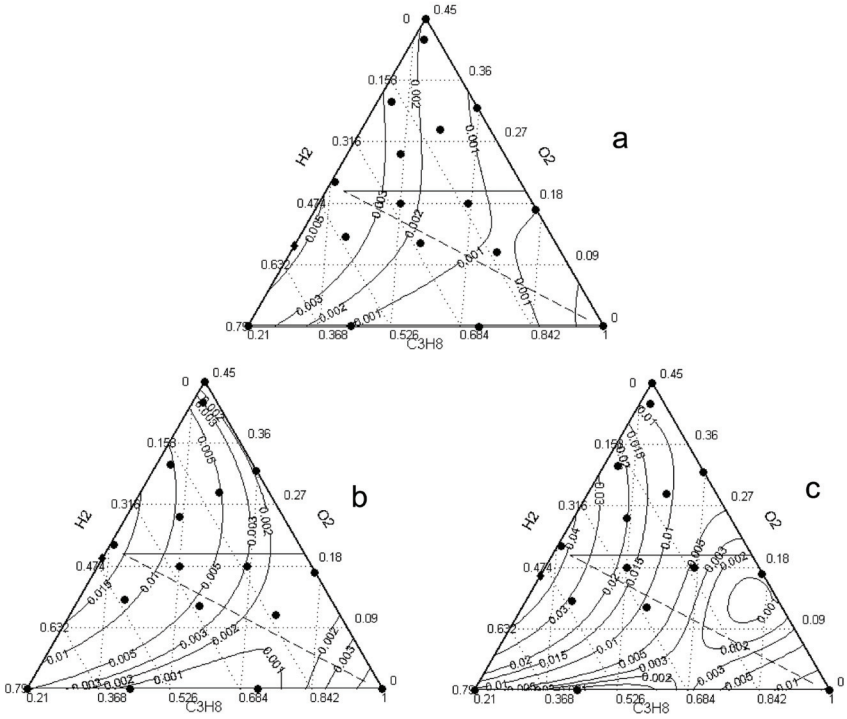

Fig. 5.1.2.7: Yields of C_2H_6 (C_3H_8) at temperatures: a) 600 ℃, b) 625 ℃, c) 650 ℃. The dashed line represents the stoichiometry 1:2 for the $[O_2]$:$[H_2]$ in the feed. The solid horizontal line represents the fraction 0.2 for the oxygen in the feed.

The maximum of the ethane yield lays right on the water stoichiometric line in the area of low propane concentrations. The form of the surface (function) of yield is similar for temperatures 600~650 °C, the values are higher for higher temperatures.

Plots for methane on Fig. 5.1.2.8 do not give much of reliable information, the form of surfaces is complex (the yield level is low and its value can include big errors). But we can see some trends. With increasing temperature the maximum yield moves from the upper part of the oxygen side to the upper part of the hydrogen side whereas the minimum moves from the middle part of the propane side to right side of propane side. The isolevel lines are crossing the water stoichiometric line at high angle and they are parallel (in average) to some ratio of O_2 and C_3H_8 (the ratio between components O_2 and C_3H_8 determines the methane yield).

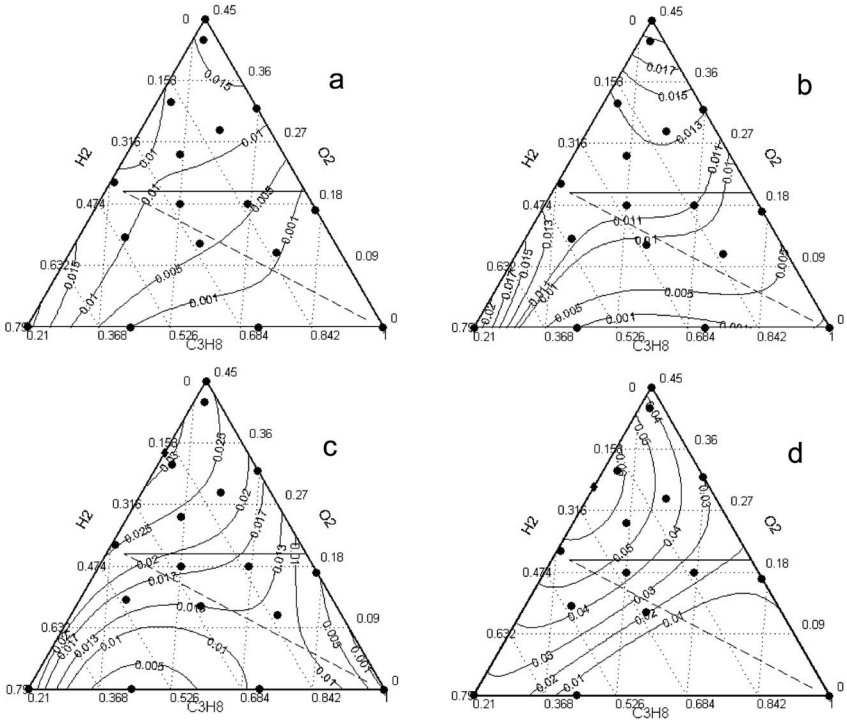

Fig. 5.1.2.8: Yields of CH_4 (C_3H_8) at temperatures: a) 575 ℃, b) 600 ℃, c) 625 ℃, d) 650 ℃. The dashed line represents the stoichiometry 1:2 for the $[O_2]$:$[H_2]$ in the feed. The solid horizontal line represents the fraction 0.2 for the oxygen in the feed.

Generalizing the information from the plots we can infer that we get the maximum water production at an excess of hydrogen when there is no production of CO, CO_2, whereas the maximum of propylene production lays in the area of oxygen excess and it is accompanied by formation of CO, CO_2 and water. Thus, we can identify three main competitive processes - combustion of hydrogen giving heat and shifting equilibrium, burning of C from the catalyst surface preventing catalyst deactivation, and burning of hydrocarbons. At low temperatures we have a high selectivity towards water formation and we need excess of oxygen to remove carbon from the catalyst in order to have a high yield of propylene. At low temperatures when deposition of C on the catalyst is expected to be low, we see that the propene yield is dependent on hydrogen concentrations, i.e. on the water production process, whereas at higher temperatures the propene yield is dependent on oxygen concentrations. Thus we can see that the optimum of the process is in the area between the two lines - H_2-O_2 stoichiometric line and 20% oxygen concentration. Below the stoichiometric line water is selectively produced and there is not enough oxygen for cleaning the catalyst surface, above 20% oxygen concentration oxygen is in excess and hydrocarbons are oxidized to a large extent, giving CO/CO_2.

If we want to have the auto thermal regime we need to feed hydrogen to the mixture or introduce oxygen somewhere in the middle of reactor when we already have hydrogen produced from dehydrogenation. Still it is possible that introduction of the oxygen in the middle of reactor will not improve the situation much (e.g in the case when oxygen-carbon reactions are faster than oxygen-hydrogen reaction).

To confirm of the conclusions and for a better determination of the optimal reaction conditions it is necessary to carry out the same analysis for experiments with feed gas mixtures $H_2O_{(g)}$+H_2+C_3H_8 and $H_2O_{(g)}$+O_2+C_3H_8 to identify the effect of H_2O on the reactions.

5.2 PLATINUM CATALYST

5.2.1 THE EFFECT OF CATALYST COMPOSITION

In order to compare the newly prepared Pt catalyst with the available PtSn catalyst the preparation procedure as well as materials used for preparation should be the same for both catalysts. As all the chemicals and materials are new (especially the hydrotalcite support HT63 compared to HT50 which was used with PtSn and is not produced any more now) a screening of Pt catalysts was done.

The screening experimental work on Pt catalysts of different composition (Table 4.2.3.1) was performed. The aim was to check their activities and compare it with the activities of identical catalysts in [8].

Comparing results for the catalysts with different compositions it is possible to conclude that the activities are similar. The conversion of propane follows similar trend for all catalysts in the range of temperatures 350~600 °C and reaches ~20%. Then the temperature dependence is steeper up till ~45~55% at 650 °C.

We can say the same for propane selectivities and oxygen selectivities. All catalysts gave the same picture. The selectivities change with temperature (350~600 °C) following the same trends (propene and CO_2 have highest values of propane selectivities among all products). At around 600 °C the trends for all selectivities change. CH_4, C_2H_4 and CO become more important products. It appears that the cracking processes start around this temperature.

All tested catalysts showed comparable activity, furthermore the activity is comparable to the activity for a similar catalyst in [8]. One of the catalysts (1%Pt/HT63) was therefore chosen to be compared with the platinum-tin catalyst (1.1%Pt2%Sn/HT50). The catalyst with similar content of Pt and similar support type was chosen and used for the experiments aimed for construction of composition-property diagrams.

5.2.2 COMPOSITION-PROPERTY DIAGRAMS FOR THE PLATINUM CATALYST

The propane conversion (Fig. 5.2.2.1) over the Pt/HT catalyst shows the same trends for all temperatures. The form of the function surface is the same and increases at higher temperatures. The lowest conversion (a valley) is placed along the water stoichiometric line. At low concentrations of propane the isolevel lines are perpendicular to the water stoichiometric line, subsequently they are parallel to a fixed O_2/C_3H_8 ratio line and the conversion is dependent on the O_2/C_3H_8 ratio. In areas near the axes the other components have an influence. Along the O_2 axis (diminishing H_2 concentration) the isolevel lines are parallel to oxygen values lines - the conversion depends mostly on the oxygen pressure; along the C_3H_8 axis (diminishing O_2 concentration) the isolevel lines are parallel to H_2 value lines - the conversion depends mostly on hydrogen. The maximum conversion is close to the water stoichiometric line in the area of low propane concentration.

The propene yield is shown in Fig. 5.2.2.2. For the Pt catalyst we see a more complex surface than for the PtSn catalyst. This can indicate that several independent processes have an influence, depending on temperature and ratio of components. In case of PtSn we see a more clear picture, indicating that some of the processes are more dominant than others.

For propene yields on Pt we can see that along the stoichiometric ratio line the yield remains relatively stable (along lines parallel to the stoichiometry line). Below the water stoichiometric line (area of excess hydrogen) the levels of the yield rise with increasing distance to the stoichiometric line. The surface above the line (excess oxygen) is more complex (a saddle point is present here). In any case moving away from the water line leads to lower yields.

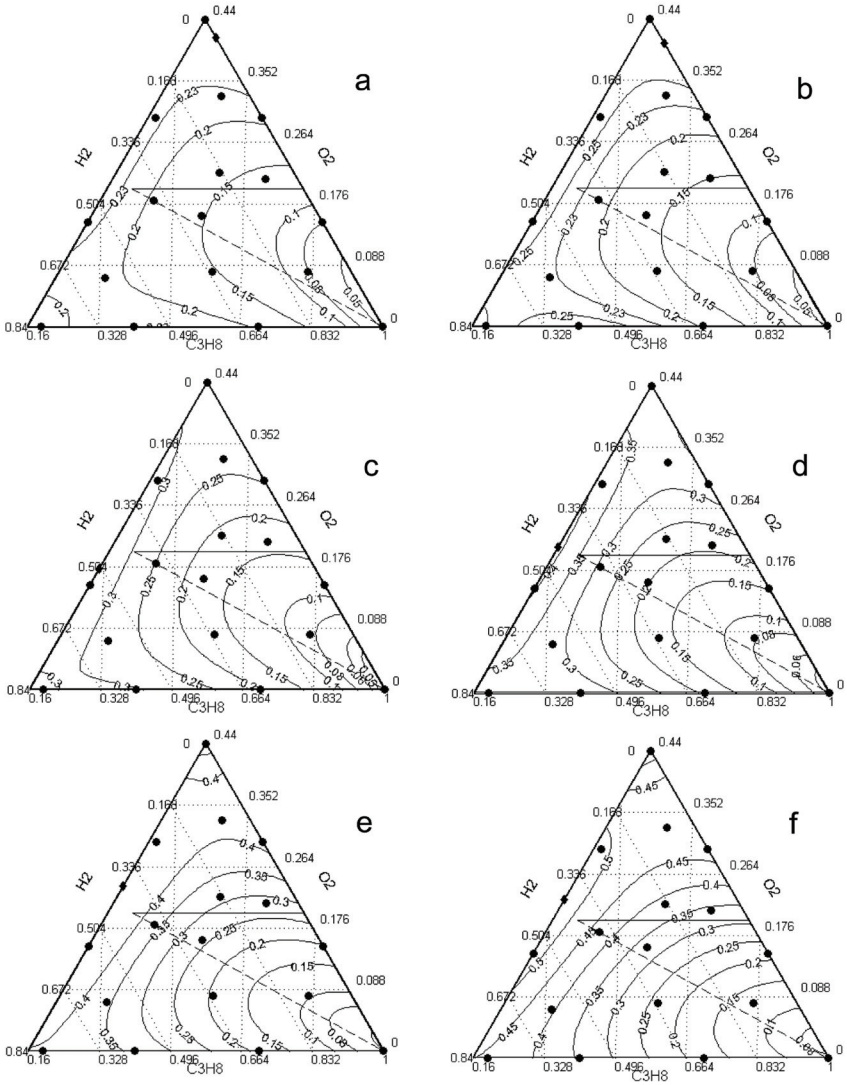

Fig. 5.2.2.1: Conversion of propane over Pt/HT63 at temperatures: a) 525 ℃, b) 550 ℃, c) 575 ℃, d) 600 ℃, e) 625 ℃, f) 650 ℃. The dashed line represents the stoichiometry 1:2 for the [O_2]:[H_2] in the feed. The solid horizontal line represents the fraction 0.2 for the oxygen in the feed.

For temperatures 575~650 ℃ (Fig. 5.2.2.2*c~f*) we see a valley in the yield above the water stoichiometric line, approximately along the line of O_2/H_2 ratio 1:1. Basically the

isolevel lines are placed parallel to the water stoichiometric line and thus are strongly dependent on the H_2/C_3H_8 ratio.

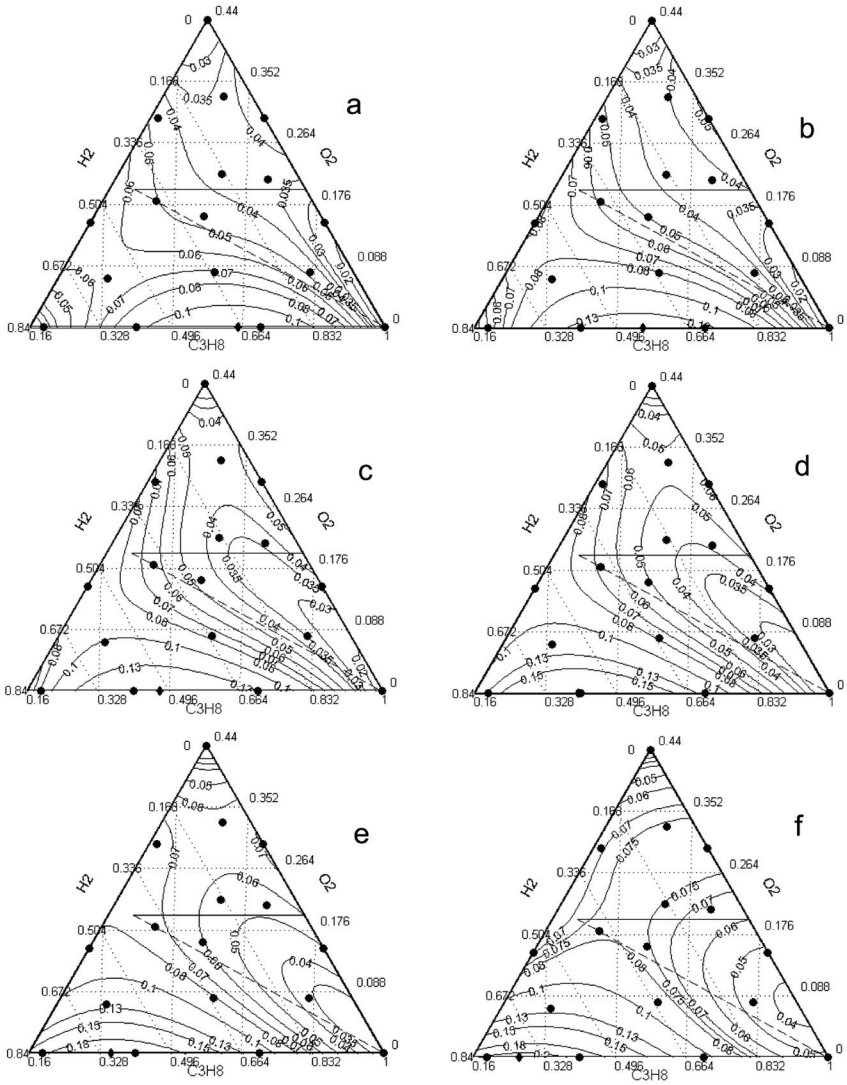

Fig. 5.2.2.2: Yield of propylene at temperatures: a) 525 ℃, b) 550 ℃, c) 575 ℃, d) 600 ℃, e) 625 ℃, f) 650 ℃. The dashed line represents the stoichiometry 1:2 for the [O_2]:[H_2] in the feed. The solid horizontal line represents the fraction 0.2 for the oxygen in the feed.

For both Pt and PtSn catalysts we see that the result is more stable along the stoichiometric line with a shift of the optimum to the hydrogen excess area. It could

therefore also for this system be of interest to make experiments with feed mixtures H_2O-H_2-C_3H_8.

In Fig. 5.2.2.3 the yield of water is plotted.

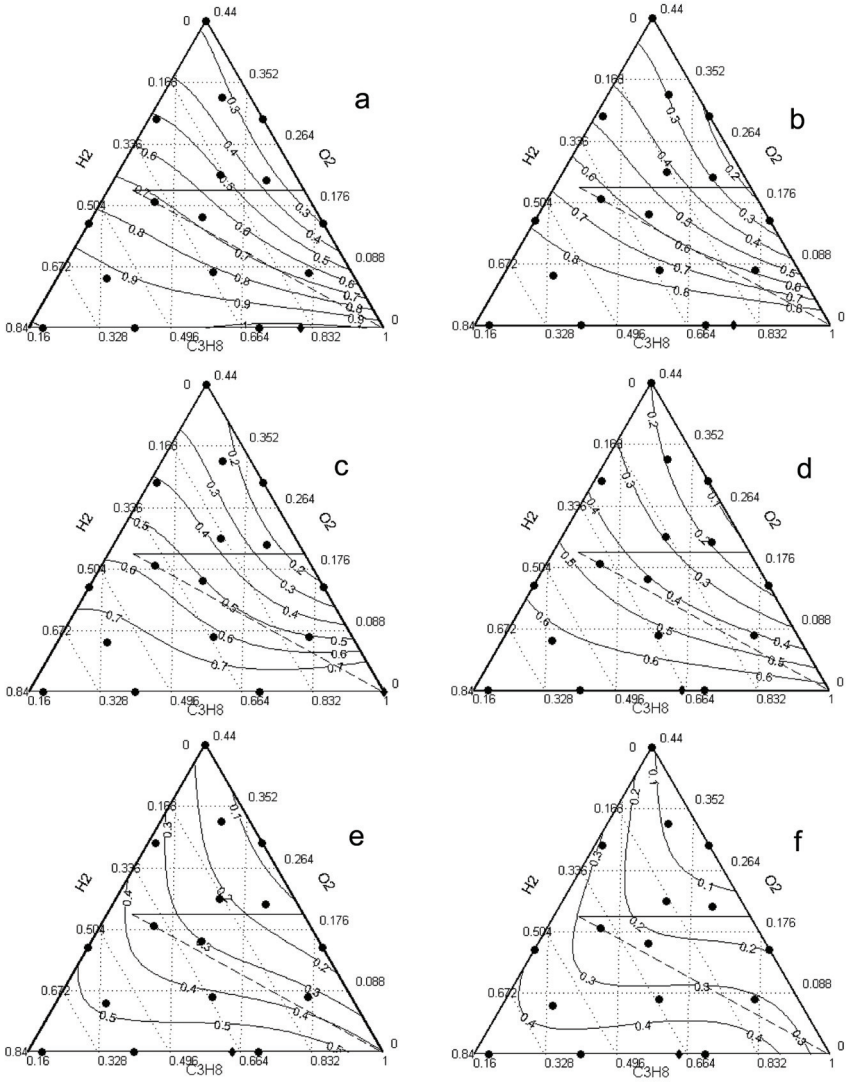

Fig. 5.2.2.3: Yields of H_2O (based on O_2) at temperatures: a) 525 ℃, b) 550 ℃, c) 575 ℃, d) 600 ℃, e) 625 ℃, f) 650 ℃. The dashed line represents the stoichiometry 1:2 for the $[O_2]$:$[H_2]$ in the feed. The solid horizontal line represents the fraction 0.2 for the oxygen in the feed.

At low temperatures (*a-c*) it behaves in a similar way as the water yield over the PtSn catalyst. But there is a small difference. For PtSn catalyst the yield was influenced by H_2/C_3H_8 ratio, whereas for Pt this is correct only for the central part of the diagram but along the oxygen axis the water yield is dependent on the hydrogen concentration.

For high temperatures (Fig. 5.2.2.3*e, f*) we see a change in the function surface, there is a valley in the water yield that follows a O_2/C_3H_8 ratio. Above this line (along the left side of the diagram) the yield is dependent on propane concentration (less propane - higher water yield), below this line the water yield depends on oxygen concentration (at high propane concentrations, less oxygen - higher water yield). This can be interpreted as a high correlation between water production and CO_x products formation.

The CO yield is shown in Fig. 5.2.2.4. At low temperatures (*a*, *b*) the CO yield is determined by O_2/C_3H_8 ratio (the valley lays along the line of a fixed ratio O_2/C_3H_8). But at temperatures 575~650 °C the CO yield is mainly dependent on the oxygen concentration. The amount of CO produced over Pt is higher than over PtSn, and the shape of the surface for these two are different. This indicates that different mechanisms are involved in the CO production over Pt and PtSn catalysts.

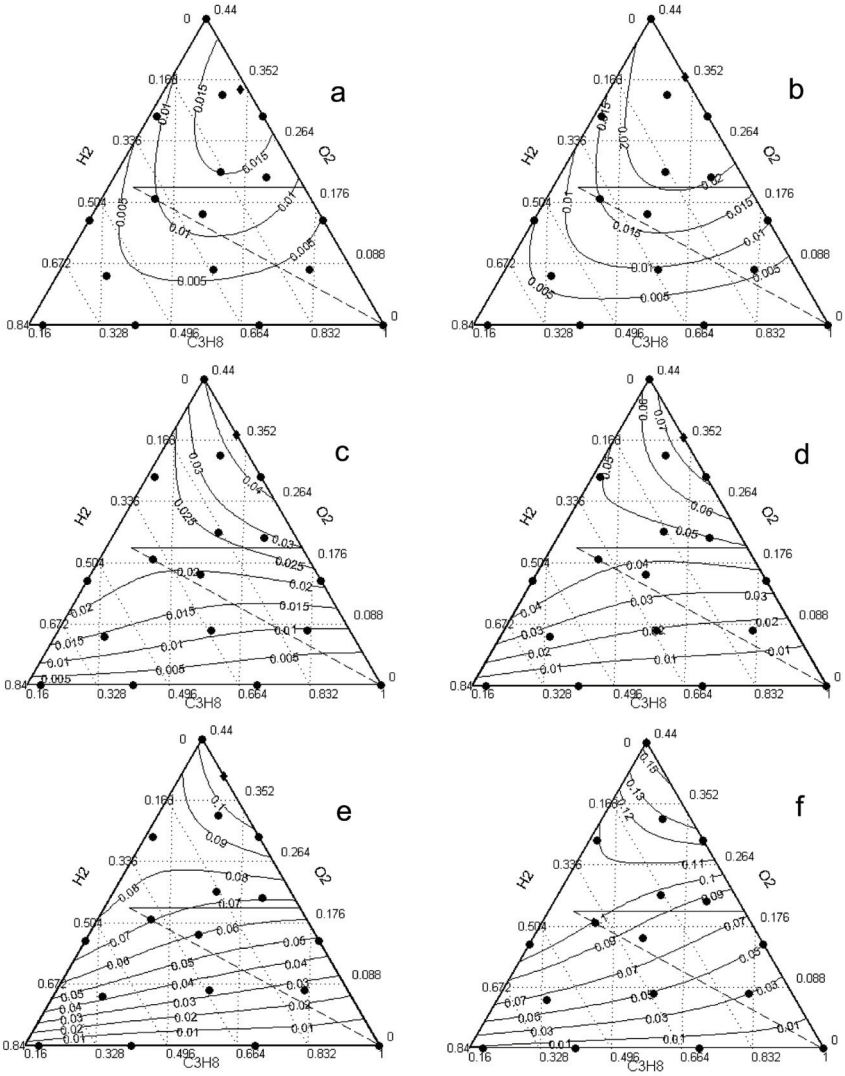

Fig. 5.2.2.4: Yields of CO (based on C_3H_8) at temperatures: a) 525 ℃, b) 550 ℃, c) 575 ℃, d) 600 ℃, e) 625 ℃, f) 650 ℃. The dashed line represents the stoichiometry 1:2 for the $[O_2]$:$[H_2]$ in the feed. The solid horizontal line represents the fraction 0.2 for the oxygen in the feed.

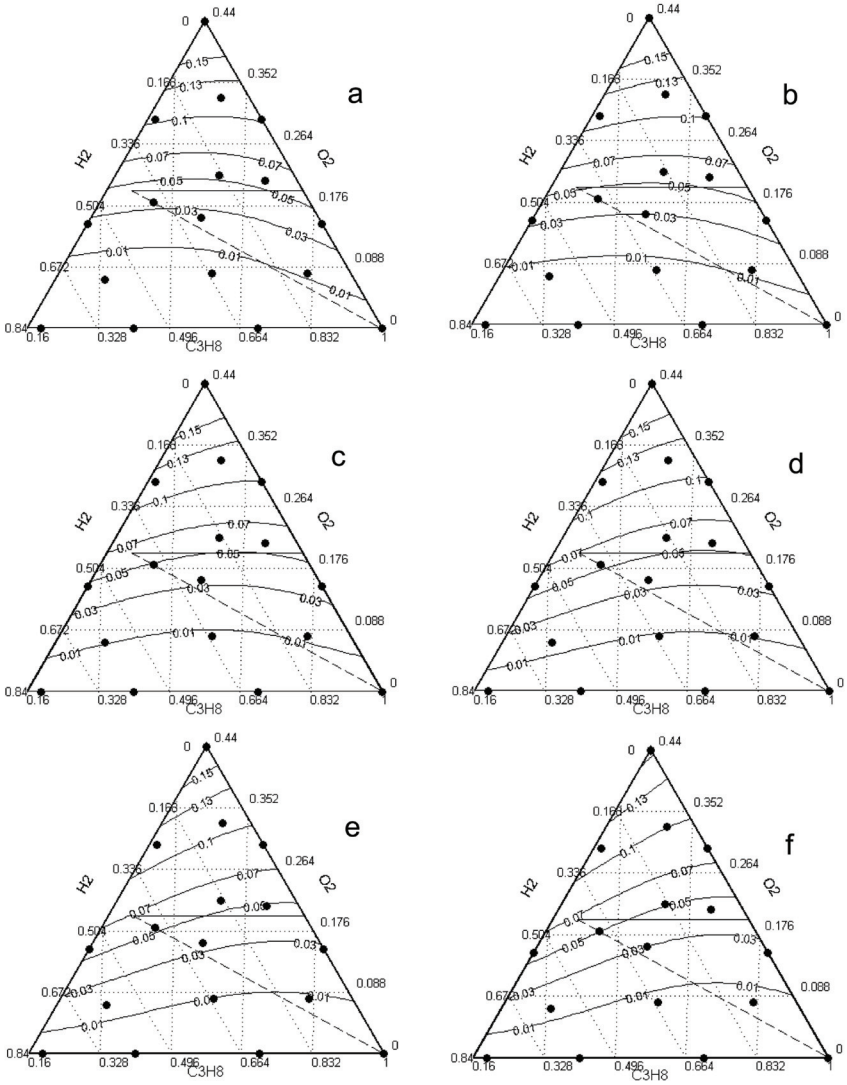

Fig. 5.2.2.5: Yields of CO_2 (based on C_3H_8) at temperatures: a) 525 ℃, b) 550 ℃, c) 575 ℃, d) 600 ℃, e) 625 ℃, f) 650 ℃. The dashed line represents the stoichiometry 1:2 for the $[O_2]$:$[H_2]$ in the feed. The solid horizontal line represents the fraction 0.2 for the oxygen in the feed.

In Fig. 5.2.2.5 the CO_2 yield is shown. Yields for all temperatures look similar. In plots *a*, *b* the yield can be seen to be mainly dependent on the oxygen concentrations, whereas at high temperatures (plots *c*~*d*) it is dependent on the O_2/C_3H_8 ratio. The amount of

produced CO_2 over Pt is similar to the amount produced over PtSn. There is almost no difference between the surfaces and amounts in the area above the water stoichiometric line (oxygen excess), whereas below it the production of CO_2 over Pt is higher. Nevertheless it is possible to conclude that the mechanism of CO_2 formation over Pt and PtSn is the same.

In Fig. 5.2.2.6 the ethene yield is shown. The surface is complex, but still some trends are detectable. At temperatures 525~550 °C (*a*, *b*) the isolevel lines of yield of C_2H_4 lay along the lines of hydrogen concentration - its concentration plays an important role. At 575 °C this changes, and at 575~650 °C the yields are parallel to the oxygen concentrations.

In Fig. 5.2.2.7 the ethane yield is shown. At low concentrations of propane (~<50%) the yield at all temperatures is mainly dependent on propane concentration. Possibly (looking at the angle of isolevel lines), at low temperatures (*a*) it is dependent on H_2/C_3H_8 ratio (little fraction of hydrogen), at high temperatures (*d~f*) it is dependent on O_2/C_3H_8 ratio (with little fraction of oxygen). The minimum is observed at high propane concentrations and with increasing temperature it is localised in the area with high propane concentration and stoichiometric ratio of H_2 and O_2 (along the water stoichiometric line). The picture observed here can indicate the following processes. The ethene is expected to be produced via propane cracking and consequently the ethane is produced from ethene hydrogenation. For low propane concentrations there is enough hydrogen for the hydrogenation and the ethane yield is dependent on availability of propane. For high propane concentrations oxygen and hydrogen play their separate important roles in the process. The minimum of ethane yield is along the water stoichiometric line where water is produced and there is no hydrogen or oxygen left. A similar picture is observed for the methane yield (Fig. 5.2.2.8). The described behaviour can signify that we have here the Pt-catalysed hydrogenolysis process (2.1.17).

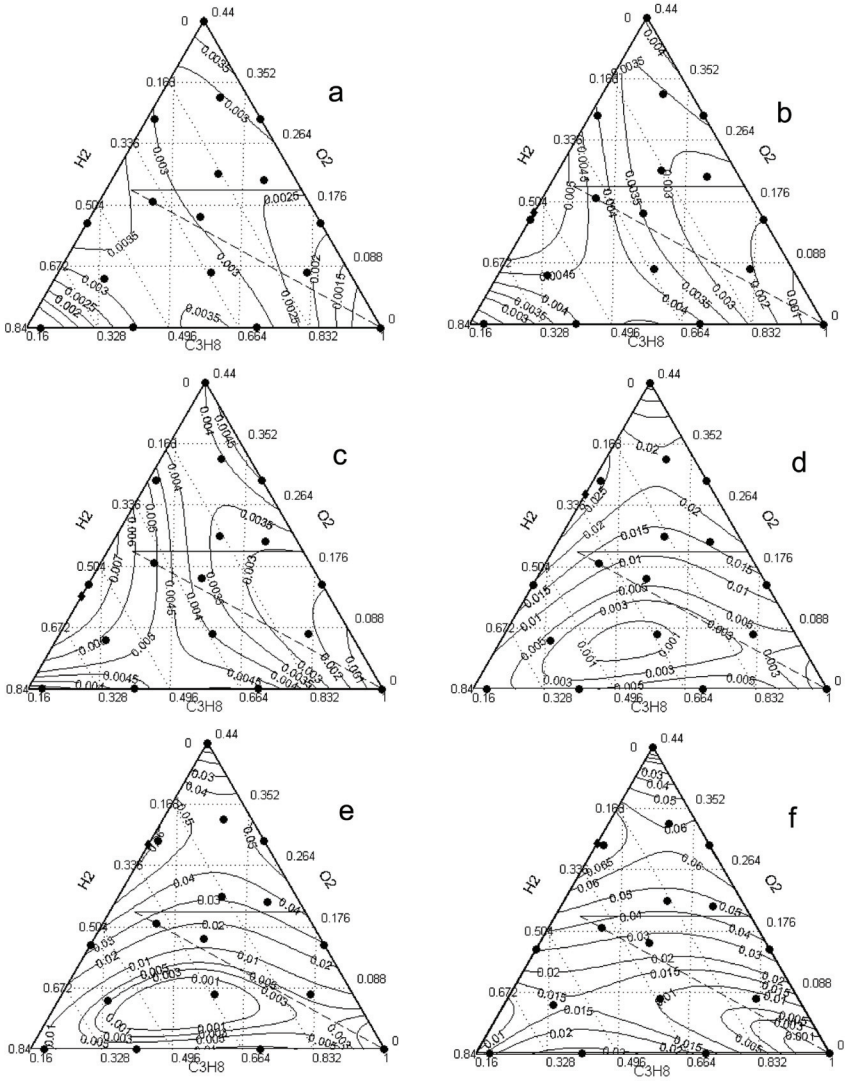

Fig. 5.2.2.6: Yields of C_2H_4 (based on C_3H_8) at temperatures: a) 525 ℃, b) 550 ℃, c) 575 ℃, d) 600 ℃, e) 625 ℃, f) 650 ℃. The dashed line represents the stoichiometry 1:2 for the $[O_2]$:$[H_2]$ in the feed. The solid horizontal line represents the fraction 0.2 for the oxygen in the feed.

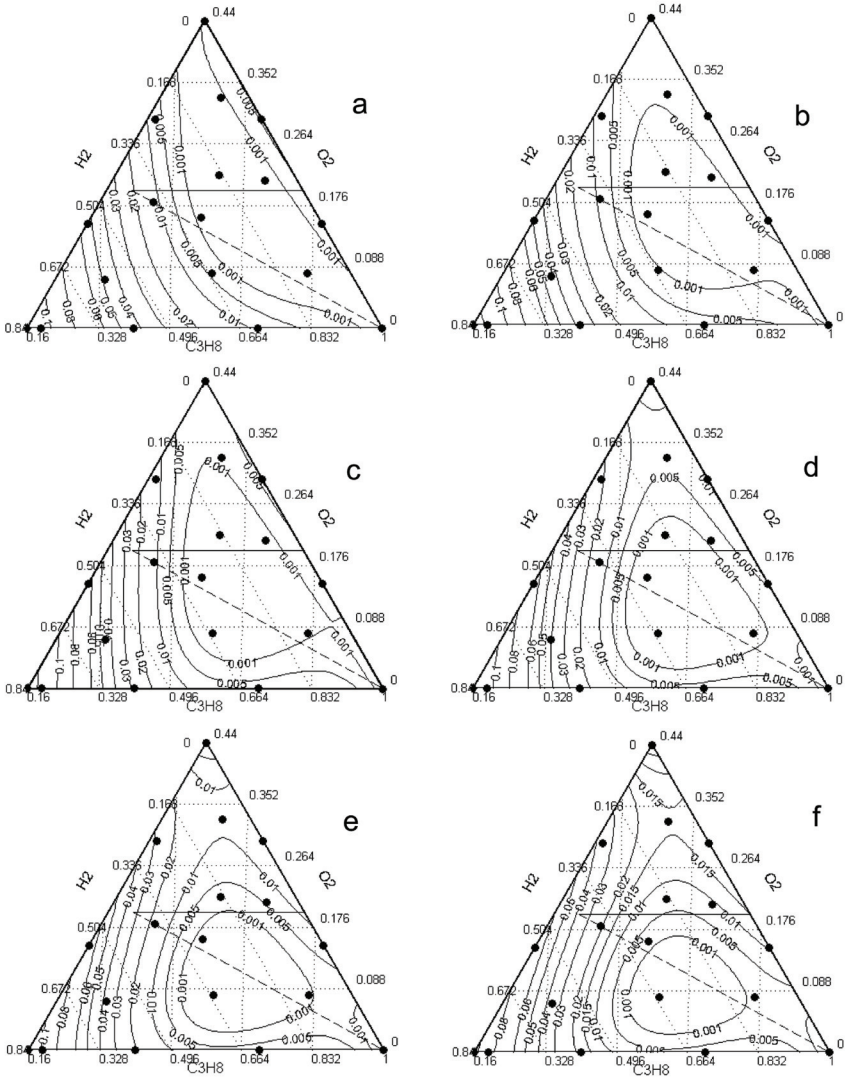

Fig. 5.2.2.7: Yields of C_2H_6 (based on C_3H_8) at temperatures: a) 525 ℃, b) 550 ℃, c) 575 ℃, d) 600 ℃, e) 625 ℃, f) 650 ℃. The dashed line represents the stoichiometry 1:2 for the $[O_2]$:$[H_2]$ in the feed. The solid horizontal line represents the fraction 0.2 for the oxygen in the feed.

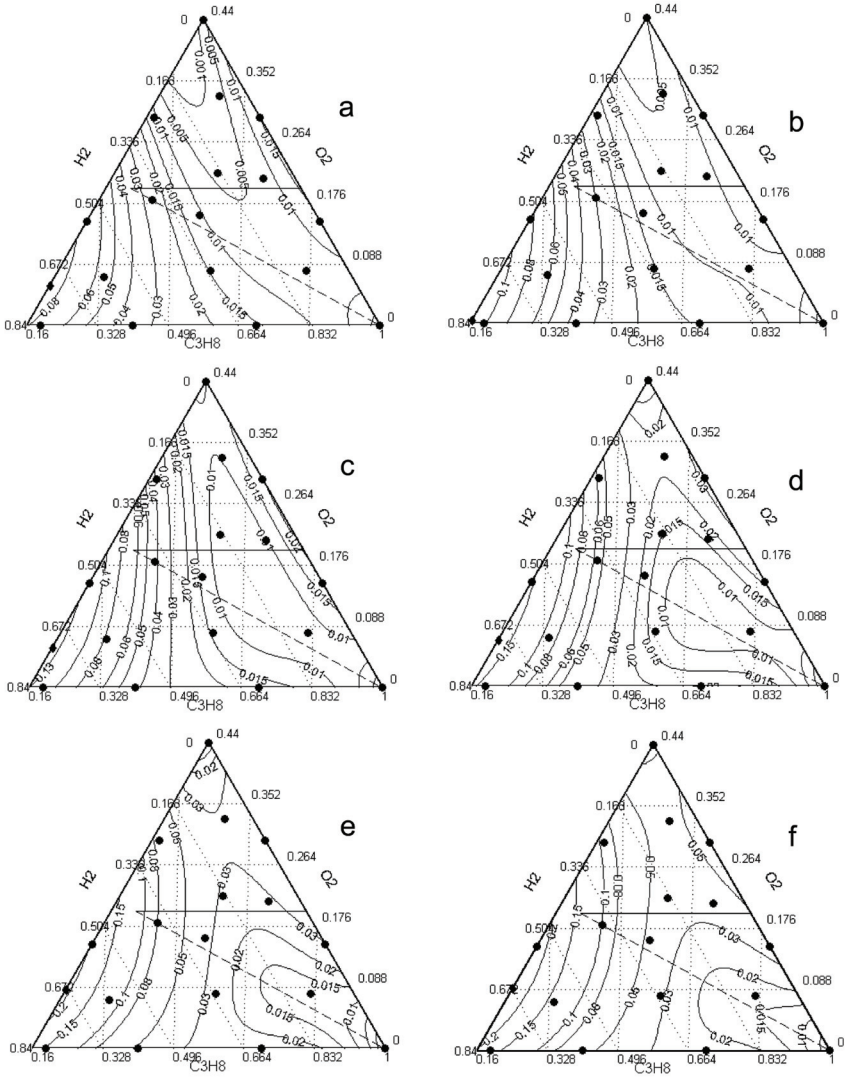

Fig. 5.2.2.8: Yields of CH_4 (based on C_3H_8) at temperatures: a) 525 ℃, b) 550 ℃, c) 575 ℃, d) 600 ℃, e) 625 ℃, f) 650 ℃. The dashed line represents the stoichiometry 1:2 for the $[O_2]$:$[H_2]$ in the feed. The solid horizontal line represents the fraction 0.2 for the oxygen in the feed.

The methane yield is shown in Fig. 5.2.2.8. It is similar to the yield of ethane. Although the influence of hydrogen concentrations on methane yield is higher (isolevel lines are parallel to the line of a certain ratio H_2/C_3H_8, where the importance of hydrogen decreases with temperature increase). The minimum of methane yield follows the

minimum of ethane yield (at high propane concentrations, on the water stoichiometric line), indicating a common formation mechanism.

5.3 REACTION WITHOUT A CATALYST

A set of experiments without a catalyst was performed in order to check the influence of non-catalytic reactions on the results. All experimental procedures were similar to procedures for experiments with Pt and PtSn catalysts. The quarts wool (that keeps the catalyst bed in experiments with the catalysts) was placed in the reactor in the same amount but without a catalyst.

5.3.1 HYDROGEN COMBUSTION AND DEHYDROGENATION OF PROPANE

Hydrogen combustion without a catalyst was performed at temperatures 25~225 °C for feed mixture $[O_2]:[H_2] \approx 50:50$ (5.6 and 5.2 ml/min appropriately, with inert (helium), 50 ml/min total flow). Fig. 5.3.1.1 shows the hydrogen conversion. We can see that the reaction between H_2 and O_2 at these conditions ignites around 200 °C.

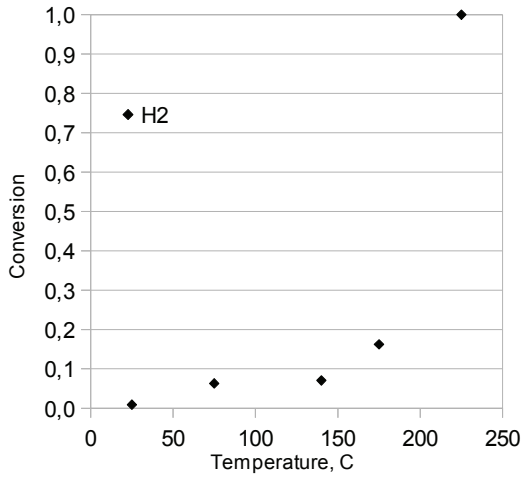

Fig. 5.3.1.1: Hydrogen conversion in the experiment without a catalyst. $[O_2]:[H_2] \approx 50:50$.

The dehydrogenation and hydrogen combustion reaction was performed without a catalyst at temperatures 350~650 °C for feed mixture $[O_2]:[C_3H_8]:[H_2]$ = 24:46:30 (4.9, 9.4 and 6.2 ml/min, with helium, 50 ml/min total flow).

Propane conversion is shown in Fig. 5.3.1.2*a*, yields of products in Fig. 5.3.1.2*b*. Propane conversion constantly grow till 2% at 600 ℃, and then jump to 8% at 650 ℃. The two main products of the reaction are CO_2 and propene. The selectivity towards propene is increasing with the temperature increase. At 650 ℃ some of the products proceed with their trend of change in yields (CO_2, CH_4, C_2H_6), while other products change more abruptly, this is true for C_3H_6, C_2H_4, CO (which appears only at this temperature).

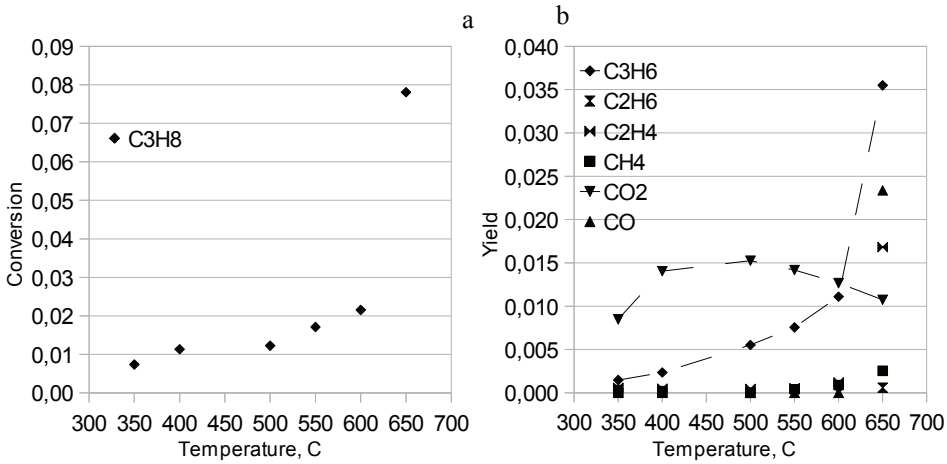

Fig. 5.3.1.2: Propane conversion (a) and yields of products (b) dependent on temperature. Reaction without a catalyst with $[O_2]:[C_3H_8]:[H_2]$ = 24:46:30.

In Fig. 5.3.1.3 the yields of oxygen-containing products are shown. The oxygen conversion was not complete at 350 °C (78%) and at 400 °C it was 95%. The oxygen selectivity towards water is ~90%.

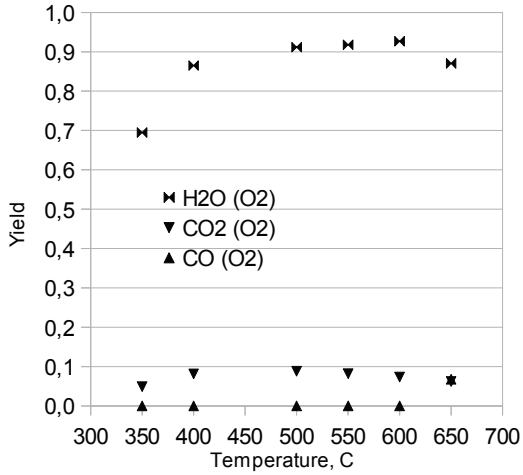

Fig. 5.3.1.3: Yields of oxygen-containing products (based on oxygen balance) dependent on temperature. Reaction without a catalyst with [O_2]:[C_3H_8]:[H_2] = 24:46:30.

The selectivity towards CO_2 is following the same trend across the temperature range (slightly decreasing with increasing temperature). CO appears only at 650 ℃ and its appearance is not accompanied by a change in the CO_2 yield, but is clearly linked to H_2O formation. The oxygen conversion was complete at high temperatures, hydrogen combustion started around 200 ℃, it means that water was a reagent for CO production (it can indicate a steam reforming process (2.1.19)), since there was no competition from C_xH_y and H_2 for oxygen.

5.3.2 FLOW RATES INFLUENCE

To test the influence of residence time in a reactor the mixtures with the same ratio of components, but different flow rates were tested. The ratio of components was [O_2]:[C_3H_8]:[H_2] ≈ 19:44:37. The feed rates were 50, 100, 150 and 200 ml/min. The temperature was 575 ℃. In each case, O_2 and H_2 were completely consumed. C_2H_4 was produced, but CH_4 and C_2H_6 were not. Propane conversion as well as yields of products are shown in Fig. 5.3.2.1*a* and *b* appropriately. The yields of oxygen-containing products are shown in Fig. 5.3.2.2.

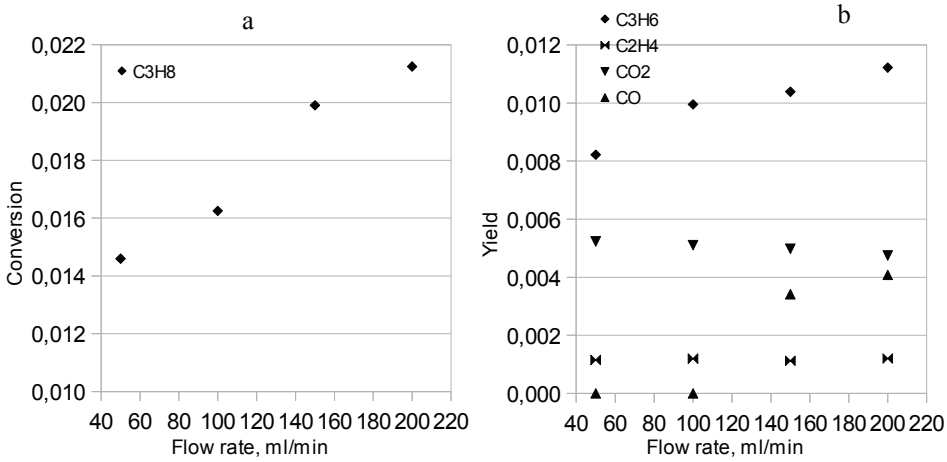

Fig. 5.3.2.1: Propane conversion (a) and yields of products (based on C_3H_8) (b) dependent on flow rate. Reaction without a catalyst with $[O_2]:[C_3H_8]:[H_2] \approx$ 19:44: 37 at 575 ℃.

Propane conversion is increasing with flow increase, the propene yield is also increasing while CO_2 yield is decreasing. At flows 150 and 200 ml/min CO appears in the outlet and it is increasing with flow increase.

In Fig. 5.3.2.2 we see that when CO appeared, CO_2 did not decrease correspondingly, but H_2O decreased. It can indicate that we have a reaction … CO ⟶ … ⟶ H_2O that is not completed at high flow rates. CO is an intermediate product in a route of water production. For the case when water is produced via CO, the decrease of oxygen selectivity towards H_2O in favour of CO with the growth of temperature can be interpreted as decrease of CO selectivity towards water.

The change in propene yield can be connected with the change in CO_2 yield (ratio between changes in flows is a factor of 2.85 which is close to 3). Thus CO_2 is produced from propene and at higher flow rates (small reaction time) this reaction is less completed. CO_2 production is not connected much with CO production.

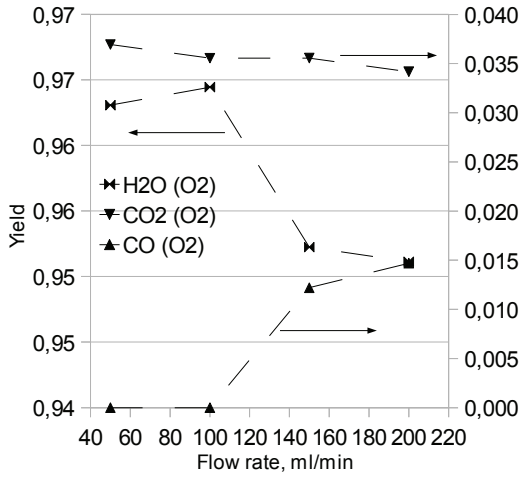

Fig. 5.3.2.2: Yields of oxygen-containing products (based on oxygen balance) dependent on flow rate. Reaction without a catalyst with $[O_2]:[C_3H_8]:[H_2] \approx 19:44:37$ at 575 °C.

5.3.3 COMPOSITION-PROPERTY DIAGRAMS FOR REACTION WITHOUT A CATALYST

The propane conversion and yields of the main products for reaction without a catalyst were lower than for a catalysed reaction. The fitted surfaces (functions) of these properties are more complex. The reason for this can be the higher complexity of the reaction mechanism (i.e. no dominant mechanisms but a system of competing reactions), or a higher influence of the experimental errors. Nevertheless it is possible to see the main trends for the propane conversion and yields of products.

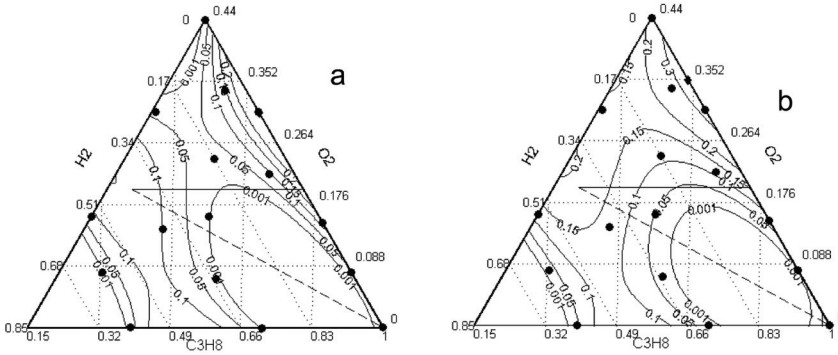

Fig. 5.3.3.1: Propane conversion in the experiment without a catalyst at temperatures: a) 600 ℃, b) 650 ℃. The dashed line represents the stoichiometry 1:2 for the [O_2]:[H_2] in the feed. The solid horizontal line represents the fraction 0.2 for the oxygen in the feed.

The propane conversion is shown in Fig. 5.3.3.1. The isolevel lines are mainly parallel to lines of hydrogen concentrations, thus the amount of hydrogen has an influence on the propane conversion. The highest conversion is at low concentration of hydrogen and high concentration of oxygen. The minimum is observed on the water stoichiometric line at high concentrations of propane.

The propene yield is shown in Fig. 5.3.3.2. The propene yield is also strongly dependent on hydrogen concentrations.

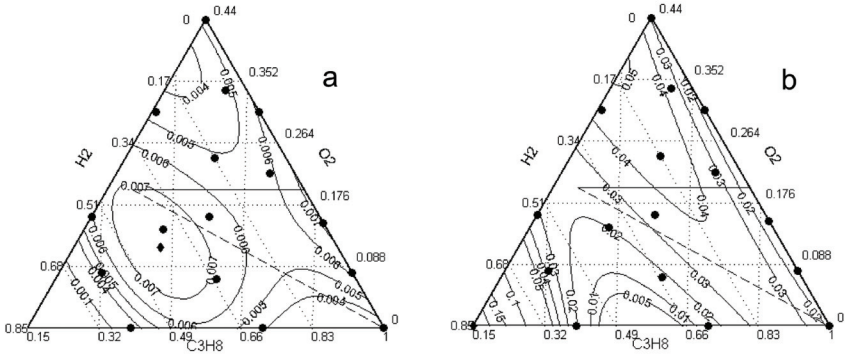

Fig. 5.3.3.2: Yield of C_3H_6 in the experiment without a catalyst at temperatures: a) 600 ℃, b) 650 ℃. The dashed line represents the stoichiometry 1:2 for the [O_2]:[H_2] in the feed. The solid horizontal line represents the fraction 0.2 for the oxygen in the feed.

The water yield is shown in Fig. 5.3.3.3. The surface for the yield of water without a catalyst is almost identical to the water yield in the reaction over PtSn catalyst (Fig. 5.1.2.3).

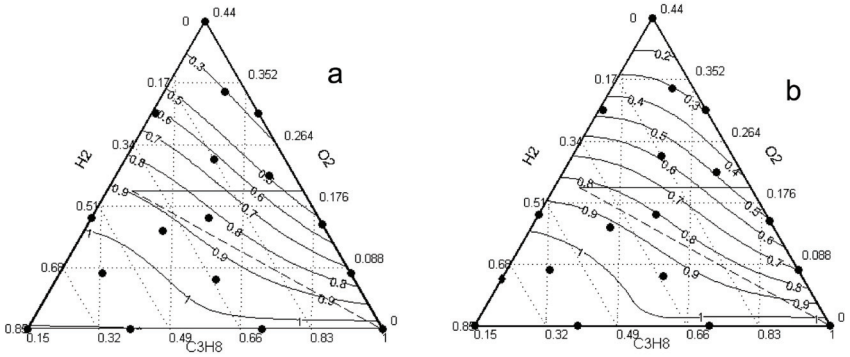

Fig. 5.3.3.3: Yield of H_2O in the experiment without a catalyst at temperatures: a) 600 ℃, b) 650 ℃. The dashed line represents the stoichiometry 1:2 for the $[O_2]$:$[H_2]$ in the feed. The solid horizontal line represents the fraction 0.2 for the oxygen in the feed.

The CO_2 yield is shown in Fig. 5.3.3.4. It depends mainly on oxygen concentrations (as isolovel lines are in average parallel to lines of oxygen concentrations).

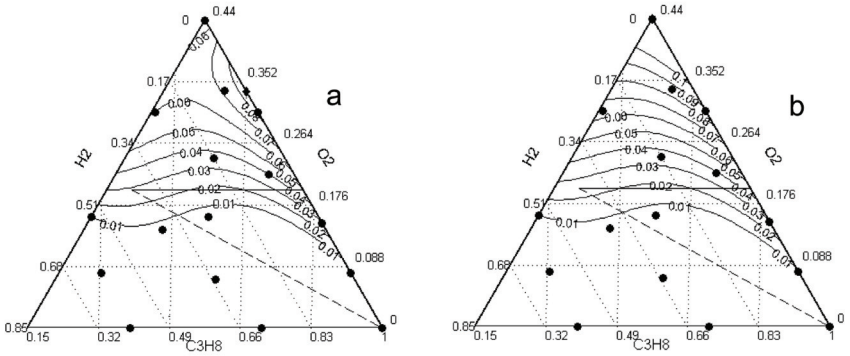

Fig. 5.3.3.4: Yield of CO_2 in the experiment without a catalyst at temperatures: a) 600 ℃, b) 650 ℃. The dashed line represents the stoichiometry 1:2 for the $[O_2]$:$[H_2]$ in the feed. The solid horizontal line represents the fraction 0.2 for the oxygen in the feed.

The yield is comparable with the CO_2 yield in the reaction over PtSn, whereas over Pt the CO_2 yield is higher. For reactions in gas phase and over PtSn the CO_2 yield is

almost absent below the water stoichiometric line (excess of hydrogen), whereas for Pt the situation is different.

The CO yield is shown in Fig. 5.3.3.5. CO appeared only at 650 °C. In the area of low propane concentrations the yield of CO is dependent on O_2/C_3H_8 ratio (the isolevel lines becomes parallel to line of O_2/C_3H_8 ratio). In the area of high propane concentrations the yield is dependent on H_2/O_2 ratio. The altitude lays along the line of H_2:O_2 ≈ 1:1 ratio.

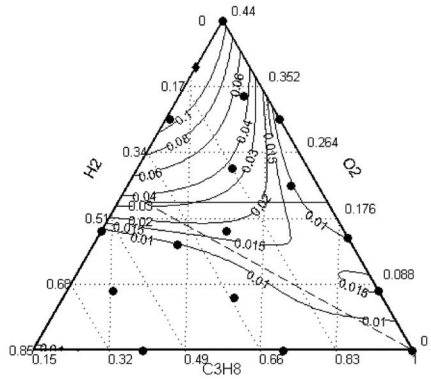

Fig. 5.3.3.5: Yield of CO in the experiment without a catalyst at temperature 650 °C. The dashed line represents the stoichiometry 1:2 for the [O_2]:[H_2] in the feed. The solid horizontal line represents the fraction 0.2 for the oxygen in the feed.

Without a catalyst, the oxygen conversion was not complete. O_2 conversion is shown in Fig. 5.3.3.6. Minimum conversion is at high oxygen concentrations, the maximum of conversion is at low oxygen concentration. The valley lays parallel to the line of H_2/C_3H_8 ratio.

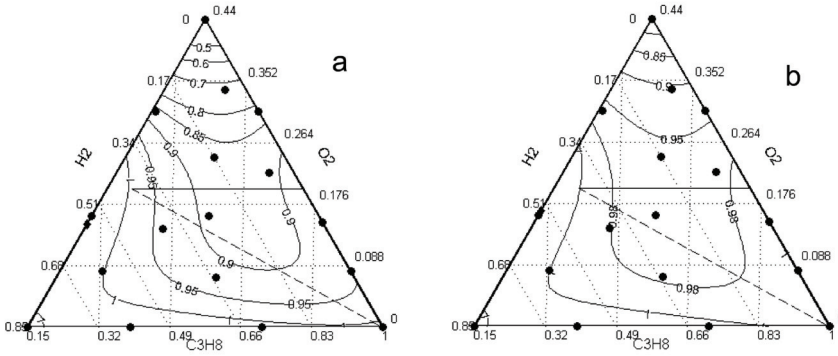

Fig. 5.3.3.6: O_2 conversion in the experiment without a catalyst at temperatures: a) 600 ℃, b) 650 ℃. The dashed line represents the stoichiometry 1:2 for the $[O_2]$:$[H_2]$ in the feed. The solid horizontal line represents the fraction 0.2 for the oxygen in the feed.

Concerning the oxygen conversion it is necessary to point to some issues regarding the experimental plan used. We can see here some disadvantages of the chosen experimental plan. There is no oxygen conversion (the experimental result) at experimental points which lay on the propane axis (this axis corresponds to the mixtures of hydrogen and propane, the oxygen concentration here is zero). Meanwhile in the area along the propane axis (very close to it) where oxygen tends to zero, we would expect the highest conversion of oxygen (having the high hydrogen concentration and the low oxygen concentration). In order to fit the proper polynomial function we have to substitute 100% oxygen conversion for the experiments at points on the propane axis (at these points we had only hydrogen and propane in a feed and oxygen conversion is thus absent). In a fitting procedure (see code in Ch. 8.6.4) we substitute 1 instead of 0 in a file with the experimental results for three points (0.00 0.71 0.29; 0.00 0.40 0.60; 0.00 1.00 0.00) laying on the propane axis. The same is done for the H_2O yield.

Here we see some inconvenience of the experimental plan used. On the sides of the diagrams we have two-compound systems, whereas inside the diagram we have three-compound systems (mixtures of two compounds or three compounds). Properties (functions) that we determine (conversions and yields as a result of reaction) are not just the result of interactions of the pairs of compounds. We have a complex system

(reaction mechanism) with a number of intermediate compounds, we have several different possibilities for interaction between the three main compounds. It is possible, that improved diagrams could be built if the experimental plan includes only the experimental points with all three components (all experiments are done with oxygen, propane and hydrogen in a feed). In this case the simplex diagram is a rescaled triangle where all points - in vertexes, on sides of the diagram and inside of the diagram - represent mixtures of three components (hydrogen, oxygen and propane).

In the reaction without a catalyst the C_2H_4 and CH_4 appeared only at 650 ℃ but with very low yield. The yields were of similar level therefore the C_2H_4 and CH_4 could be produced in the cracking reaction (2.1.16).

Making some summation on the experiments over Pt, PtSn catalysts and an experiment without a catalyst: the experiments with only H_2-O_2 with and without catalyst showed that the reaction between hydrogen and oxygen occurs on the catalyst at temperatures below 100 ℃ and without the catalyst the reaction occurs at approximately 200 ℃ at these flow rates.

In the experiments with $[O_2]=0$ the catalyst deactivation was observed, at higher concentrations of hydrogen the deactivation was less severe, whereas at higher concentrations of propane it was more severe. This is best seen on the plots of the propane conversion on PtSn (Fig. 5.1.2.1). At temperatures 600~650 ℃ and propane concentration above ~60% the propane conversion on the propane axis (bottom side of the diagram) slowly decreases with the temperature increase. Whereas for the propane concentrations below ~60% the decrease in the conversion is less marked. This trend is worse for the Pt catalyst as deactivation of the catalyst was faster. The influence of the hydrogen concentration is in agreement with the idea of hydrogenation of the carbonaceous deposits formed on the catalyst surface. Higher amount of hydrogen provides greater surface coverages by hydrogen atoms and suppresses the process of coke precursor formation and its polymerisation [76].

The results indicate that reaction between oxygen and hydrogen occurs in the gas-phase or in the inlet part of the catalyst bed. Oxygen transformation is very selective

towards water production. The water and CO yields are different for the Pt (Figs. 5.2.2.3, 5.2.2.4) and PtSn (Figs. 5.1.2.3, 5.1.2.4) catalysts, whereas the CO_2 yield is almost not dependent on the catalyst (Figs. 5.2.2.5, 5.1.2.5).

The H_2O yield is similar for the reaction on PtSn (Fig. 5.1.2.3) and the reaction without a catalyst (Fig. 5.3.3.3), whereas for the Pt catalyst it is different (Fig. 5.2.2.3). At temperatures below 500 ℃ the water yield is similar for the catalysts, but with the temperature increase the water yield for Pt catalyst decrease fast. It can be explained as follows: water adsorbs on the Pt and participates in further reactions, whereas on the PtSn it does not adsorb and does not participate in other reactions. This is in agreement with [28] (see Ch. 2.4).

5.4 MODEL SIMULATIONS

The result of the model simulation is described in this chapter. Estimation of the model parameters was described in Chapter 3 , the Matlab code used for the model simulation is given in Chapter 8.6.3 . Some details of the model are described here; results of the tuned model simulation and non-tuned model simulation are given in subchapters.

In the basic recommendations of the UBI-QEP method ([43]) it is proposed to describe the adsorption of molecules such as $CH_3\dot{C}H_2$ on a hollow site ($CH_3C^{***}H_2$). Adsorption of this molecule on a bridge site ($C^*H_3C^{***}H_2$) is not usually taken into consideration. However the formalism of the method allows to perform the calculation of adsorption energies in both cases. It is recommended to use additional information about possible forms of adsorbates and make a choice of these forms before starting using UBI-QEP calculations.

At the same time there are some possibilities to use the method for recognition of the most preferable forms of adsorbates. We can assume that the value of the adsorption energy is a criterion for the stability of adsorbates, and by comparing stabilities of different adsorbates we can choose one as more preferable. In the calculations presented in Table 8.2.3.1 we can see some regularity: hydrocarbon molecules have much smaller adsorption energy for a bridge site than for adsorption on one contact

atom; mono-radicals of saturated hydrocarbons have also smaller adsorption energy for a bridge site; mono-radicals of unsaturated hydrocarbons have already smaller adsorption energy for adsorption on one contact atom; di-radicals of both saturated and unsaturated hydrocarbons have smaller adsorption energy for adsorption on one contact atom. The appropriate data is shown in Table 5.4.1 (the data is selected from Table 8.2.3.1).

Possibly, a more detailed search could reveal correlation between ratios of Q_a, Q_b and D_{ab} and possibilities for the existence of a specific form of adsorbates.

Table 5.4.1: Regularities in the adsorption energies for different types of adsorbates.

One contact atom	Q_{AB} [kJ/mol]	Bridge site	Q_{AB} [kJ/mol]
$CH_3CH_2\underset{*}{C}H_3$	71.9	$CH_3\underset{*}{C}H_2\underset{*}{C}H_3$	11.3
$CH_3CH_2\underset{***}{C}H_2$	164.2	$CH_3\underset{*}{C}H_2\underset{***}{C}H_2$	112.3
$CH_3CH_2\underset{***}{C}H$	289.6	$CH_3\underset{*}{C}H_2\underset{***}{C}H$	320.0
$CH_3CH=\underset{*}{C}H_2$	75.6	$CH_3\underset{*}{C}H=\underset{*}{C}H_2$	11.8
$CH_3CH=\underset{***}{C}H$	179.7	$CH_3\underset{*}{C}H=\underset{***}{C}H$	202.5
$\underset{*}{C}H_3CH_3$	71.7	$\underset{*}{C}H_3\underset{*}{C}H_3$	10.8
$CH_3\underset{***}{C}H_2$	163.2	$\underset{*}{C}H_3\underset{***}{C}H_2$	115.1
$CH_3\underset{***}{C}H$	293.3	$\underset{*}{C}H_3\underset{***}{C}H$	323.7
$\underset{*}{C}H_2=CH_2$	75.9	$\underset{*}{C}H_2=\underset{*}{C}H_2$	11.3
$CH_2=\underset{***}{C}H$	180.7	$\underset{*}{C}H_2=\underset{***}{C}H$	210.1
$CH_2=\underset{***}{C}$	298.1	$\underset{*}{C}H_2=\underset{***}{C}$	512.8

In our model we use two different types of active sites and we can expect this to have some influence of the probabilities of adsorption of species adsorbed on different sites on the simulated kinetics. At the same time the model does not take this factor into

consideration. Big molecules like propane influence the neighbouring binding sites through screening. But hydrogen atoms can occupy binding sites without being affected by the screening effect (mechanism with non-competitive adsorption sites, [42], pp.119-123).

We describe the surface mechanism utilising the idea that every atom (approaching the surface from gas phase) can form three connections while forming binding sites. The asterisk (*) in the mechanism depicts the $\frac{1}{3}^{rd}$ of surface atom ability to form connection. Three asterisks (3*) may depict three such abilities from three different atoms forming one adsorption hollow site.

Different molecules utilise different numbers of surface atoms while forming adsorbates, thus the term "surface fraction" needs some adjustments. Surface fractions (that are used in rate equations) of species adsorbed on different amount of active sites should be written in terms of $N^{molec}{}_A/N^{sites}{}_{Tot}$ but not in $N^{sites}{}_A/N^{sites}{}_{Tot}$ (see code in Ch. 8.6.3).

The results from the model simulations are only to some extent comparable with the result from experiments since not all of the experimental conditions were described as parts of the model.

The energy balance (heat balance) is not taken into consideration; time and mass flow characteristics are not identical for the model and experiment. The reported result of an experiments is a steady state result, when in time of the operation (minutes or dozens of minutes with gas flow of 50 ml/min) the concentrations of the compounds (gas-phase and surface concentrations) have been well equilibrated. We assume that the steady-state concentrations are dependent on the place in the reactor (have a certain profile along the reactor axe), but at certain point these are constant during some measurable time (minutes).

In principle the model describes only one pass of an initial gas through the reactor, moreover the volume of passed gas equals the free volume of one CSTR. As the PFR reactor is described as a row of ten CSTRs, the free volume of one CSTR is calculated,

the gas of this volume is taken and consequently passed through the row of CSTRs (the volume of reacted feed gas is $\frac{1}{10}^{nth}$ of the PFR reactor free volume).

For one pass of initial gas, in every CSTR the portion of gas is only once, the initial state of the surface is - a free surface, and final state of the surface is not similar to appropriate state in experiment. In order to get a similar state, we repeat the pass many times, taking the initial state of the surface in last pass equal to final state of the surface in previous pass, until the state of the surface to establish a constant. The repeating procedure is a time consuming process (computing time for simulation of the model with one pass takes ~4 min (~0.033 s of simulated reaction time); with three passes ~6 min (~0.099 s of simulated reaction time); ten passes take ~10 min (~0.33 s of simulated reaction time); 100 passes take ~100 min(~3.3 s of simulated reaction time)).

The results of the simulations were compared and the following decision was made: the results for three passes are identical to results of 100 passes, thus three passes is enough for establishing the steady state in a short-time operation in the model.

The result of the model simulation using three passes of the initial mixture is shown below. Calculations are done for different gas compositions in the models with non-tuned and tuned model parameters. Three types of plots are given: propane conversion, surface fractions and gas-phase fractions of compounds at the end of the reactor; propane conversion, surface fractions and gas-phase fractions of compounds at 1^{st}, 5^{th} CSTRs (stages) and end of the reactor; oxygen conversion, propylene yield and water yield (based on oxygen) at the end of the reactor.

The conversion after every CSTR is calculated based on initial amount of the compounds being in the very beginning, thus the conversion of e.g. 5^{th} stage is the conversion after 5 stages but not the conversion in the 5^{th} stage. Whereas the surface fraction is a surface fraction in 5^{th} CSTR and gas-phase fraction is a fraction after 5^{th} stage.

Parameters being used in the reactor equation (8.5.14) are shown in Table 5.4.2.

Table 5.4.2: Pt catalyst parameters for the model.

Parameter	Symbol	Value
Weight fraction of metal in a catalyst used in experiments	ywt	0.01
Approximate volume of pores in a catalyst, measured in [8]	Vpor	$0.17 \cdot 10^{-3}$ [m^3/kg]
Metallic surface area per mass of the sample from Table 4.1.2.1	StMe	$1.36 \cdot 10^{3}$ [m^2/kg]
Concentration, surface atoms per surface area, calculated by (8.5.9) with a lattice constant from Table 8.1.2.2	CtMe	$1.5 \cdot 10^{19}$ [$1/m^2$]
Catalyst density, calculated by (8.5.5)	pCat	2141 [kg/m^3]
Hydrotalcite density	Dhdrtlc	2122 [kg/m^3]
Mass of the catalyst used in experiments	mcat	$0.15 \cdot 10^{-3}$ [kg]
50 ml/min total flow of feed gas mixture	V0	$50 \cdot 10^{-6}/60$ [m^3/s]

5.4.1 NON TUNED MODEL

First we plot the results of the model simulation without any fine tuning of the model parameters (preexponentials). The simulation results for different initial gas compositions are shown. Figs. 5.4.1.1, 5.4.1.2, 5.4.1.3 show results for feed gas with 20% of propane and 80% of N_2. Figs. 5.4.1.4, 5.4.1.5 are for for feed gas with 20% of propane, 20% of O_2 and 60% of N_2. Figs. 5.4.1.6, 5.4.1.7 are for feed gas with 20% of propane, 20% of O_2, 20% of H_2 and 40% of N_2. Figs. 5.4.1.8, 5.4.1.9 are for feed gas with 20% of propane, 20% of H_2 and 60% of N_2. Figs. 5.4.1.10, 5.4.1.11 are for feed gas with 20% of O_2, 20% of H_2 and 60% of N_2.

The non tuned model gives a relatively good result. It reveals some important features of the system that can be used for fine tuning of model parameters.

The reaction of pure propane (Fig. 5.4.1.1, 5.4.1.2, 5.4.1.3) is active, complete propane conversion occur at 400~450 °C, propylene has a relatively stable yield whereas yields

of other products change with temperature. The amount of methane produced is highest, the ethane and ethene yields are lower than that of propene and methane.

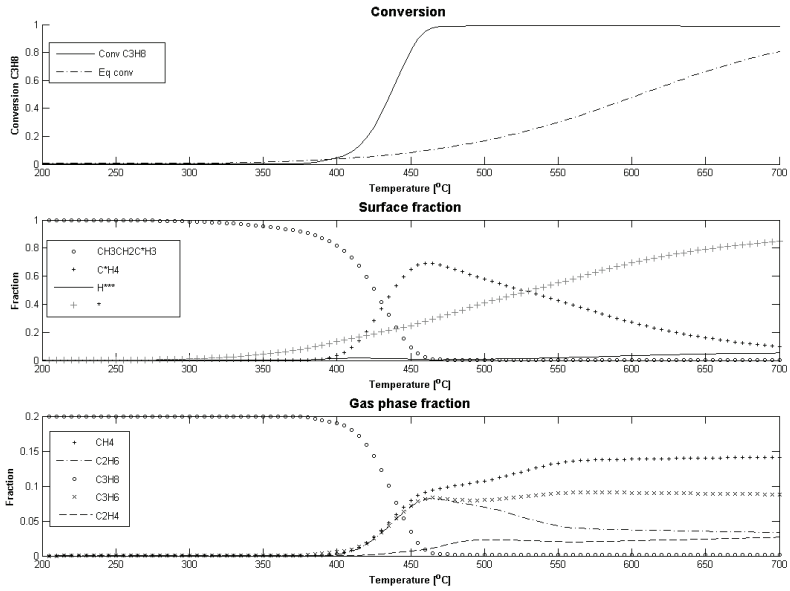

Fig. 5.4.1.1: Result of the model simulation. Gas composition: 20% propane, 80% N_2; 50 ml/min total flow. The conversion plot shows the modelled propane conversion and theoretical equilibrium conversion of propane in pure propane dehydrogenation reaction.

The behaviour is qualitatively close to experimental observations, apart from the high propane conversion at low temperature and high yield of methane in the model simulation. The coke formation is not shown by the model whereas a real catalyst deactivates due to coke formation (it is possible that coke formation is not predicted because of very short time of operation in a model (~0.1 s) compared to long time of operation in the real system). The real system gives much lower propane conversion.

The conversion of propane is high at temperatures that are lower than expected, this can be tuned by adjustment of the preexponentials for adsorption-desorption steps of propane and/or other compounds.

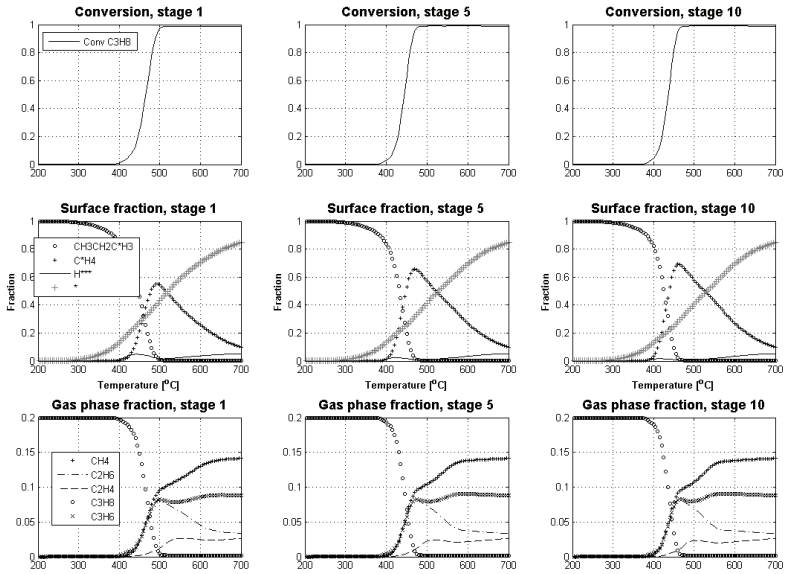

Fig. 5.4.1.2: Result of the model simulation. Gas composition: 20% propane, 80% N_2; 50 ml/min total flow. Conversion of propane, surface and gas-phase fractions of compounds after 1st, 5th and 10th stages.

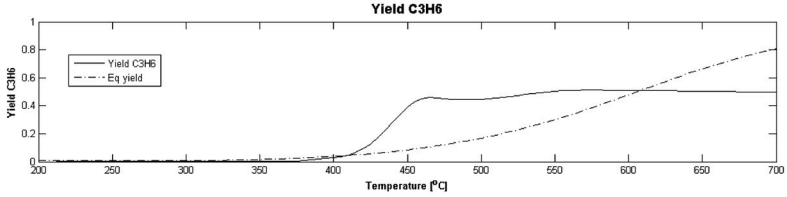

Fig. 5.4.1.3: Result of the model simulation. Gas composition: 20% propane, 80% N_2; 50 ml/min total flow. The modelled yield of propene in comparison to equilibrium yield of propene in pure propane dehydrogenation reaction.

Propane dehydrogenation in the presence of oxygen (Figs. 5.4.1.4, 5.4.1.5) shows very low process activity. At temperatures below 350~400 °C, where propane is inactive

(according to Fig. 5.4.1.1), propane occupies part of the surface. At higher temperature oxygen occupies the whole surface, propane can not adsorb and react. At 600~700 °C oxygen start to free the surface and we see a small activity of propane and a small water production.

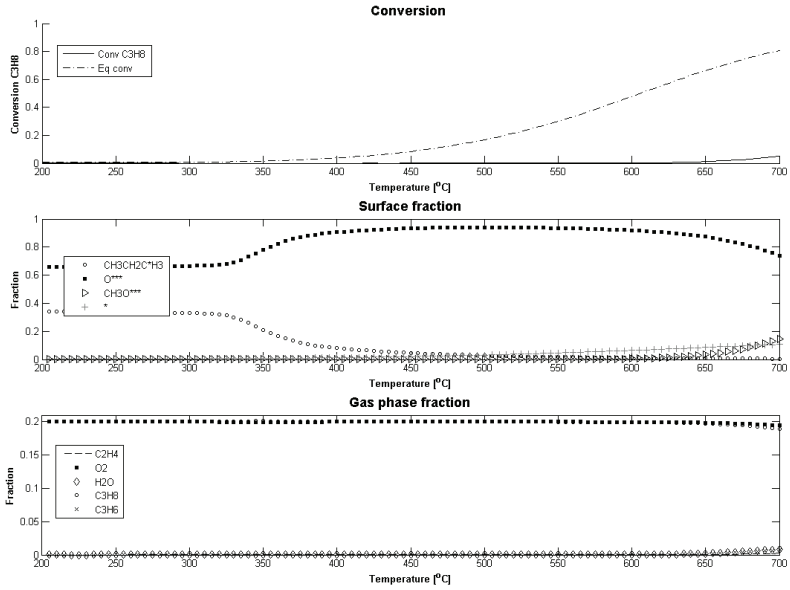

Fig. 5.4.1.4: Result of the model simulation. Gas composition: 20% propane, 20% O_2, 60% N_2; 50 ml/min total flow. The conversion plot shows the modelled propane conversion and theoretical equilibrium conversion of propane in pure propane dehydrogenation reaction.

Thus the competition for the surface between reagents plays an important role in modelling the reaction. The predicted oxygen adsorption is too strong. Relation between reaction rates of the adsorption-desorption reactions of reagents can be adjusted by tuning the preexponentials in appropriate rate constants.

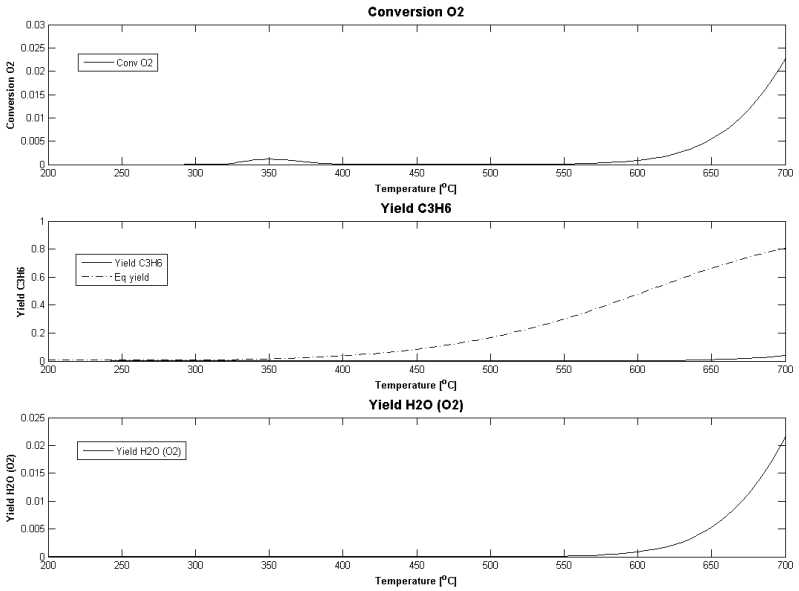

Fig. 5.4.1.5: Result of the model simulation. Gas composition: 20% propane, 20% O_2, 60% N_2; 50 ml/min total flow. The modelled yield of propene and equilibrium yield of propene in pure propane dehydrogenation reaction.

Propane dehydrogenation in the presence of hydrogen and oxygen (Figs. 5.4.1.6, 5.4.1.7) shows similar activity as dehydrogenation in presence of only oxygen. We see intensive water production at 300~350 ℃ consuming all the hydrogen present in feed mixture. Further behaviour of the system is identical to one in the previous case. The surface is occupied by oxygen and this prevents reactions of propane until ~600 ℃. The gas phase consists of water, oxygen and propane.

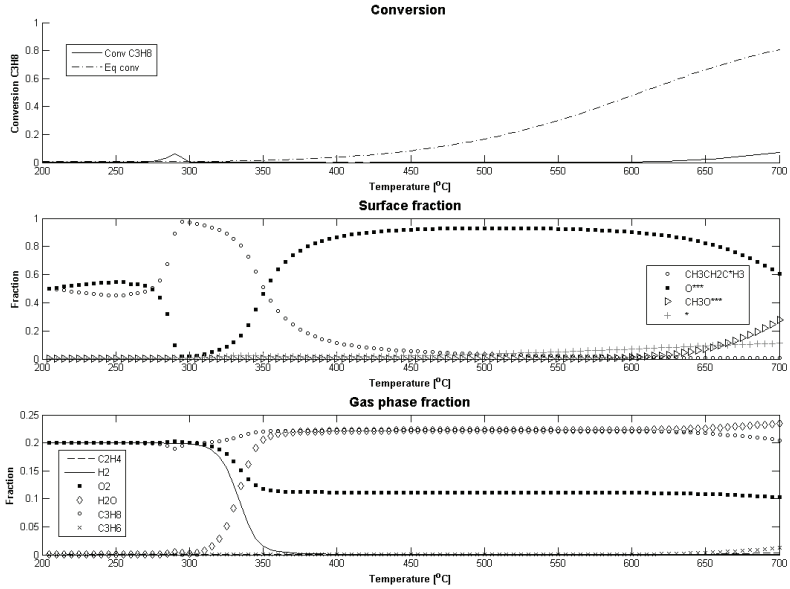

Fig. 5.4.1.6: Result of the model simulation. Gas composition: 20% propane, 20% O_2, 20% H_2, 40% N_2; 50 ml/min total flow. The conversion plot shows the modelled propane conversion and theoretical equilibrium conversion of propane in pure propane dehydrogenation reaction.

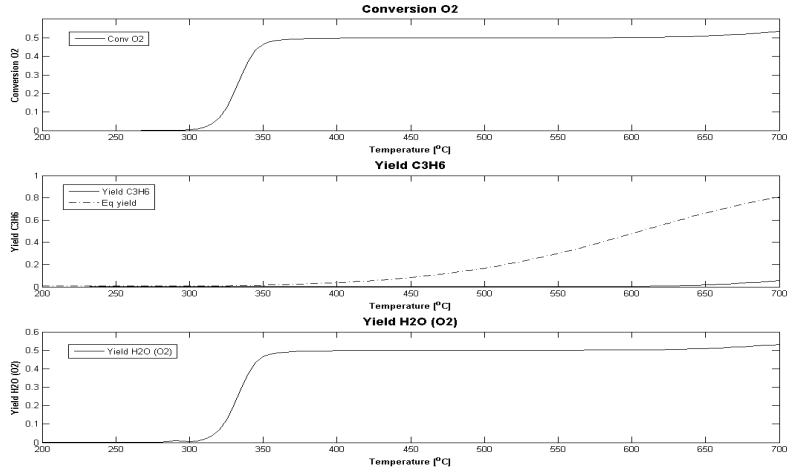

Fig. 5.4.1.7: Result of the model simulation. Gas composition: 20% propane, 20% O_2, 20% H_2, 40% N_2; 50 ml/min total flow. The modelled yield of propene and equilibrium yield of propene in pure propane dehydrogenation reaction.

Propane dehydrogenation in the presence of hydrogen (Fig. 5.4.1.8, 5.4.1.9) shows the expected changes in the result of simulation. Comparing it with results for only propane reaction (Fig. 5.4.1.1) we see an increase in production of saturated hydrocarbons (CH_4, C_2H_6). The full conversion of propane in the presence of hydrogen occur later (at ~500 °C, Fig. 5.4.1.8) than without hydrogen (~450 °C, Fig. 5.4.1.1). In both cases the maximum conversion of propane is connected with the downhill of the surface fraction of hydrogen. In the range of temperatures, where the maximum conversion is reached, there is a free surface space, thus the shift of the conversion maximum is not due to competition for free surface sites.

For the propane-hydrogen mixture the full conversion of propane occurred only when all hydrogen was consumed, thus the delay in appearance of full propane conversion is connected to equilibrium effect.

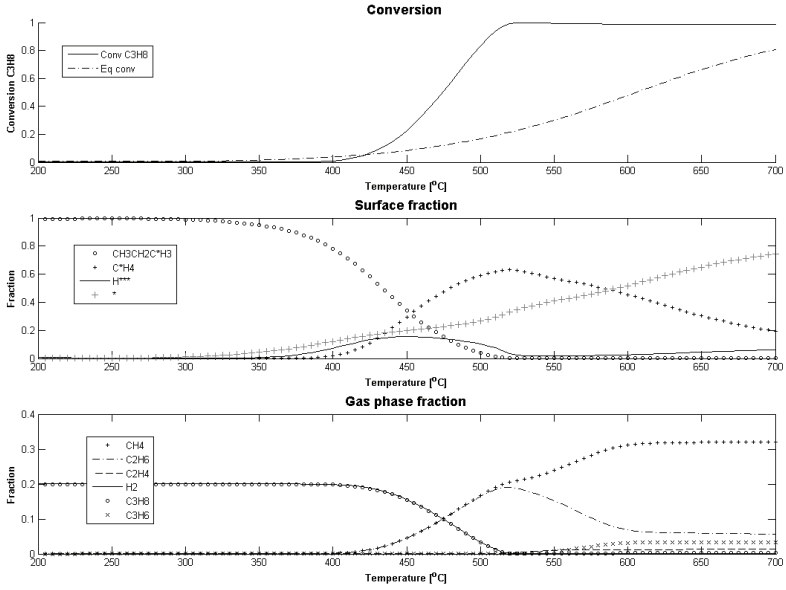

Fig. 5.4.1.8: Result of the model simulation. Gas composition: 20% propane, 20% H_2, 60% N_2; 50 ml/min total flow. The conversion plot shows the modelled propane conversion and theoretical equilibrium conversion of propane in pure propane dehydrogenation reaction.

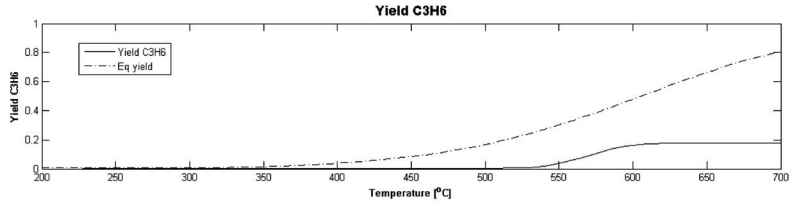

Fig. 5.4.1.9: Result of the model simulation. Gas composition: 20% propane, 20% H_2, 60% N_2; 50 ml/min total flow. The modelled yield of propene and equilibrium yield of propene in pure propane dehydrogenation reaction.

The hydrogen combustion reaction without presence of propane was also simulated (Figs. 5.4.1.10, 5.4.1.11). Full hydrogen combustion occur at 150~300 °C, the catalyst surface is mainly covered with oxygen in the whole range of temperatures.

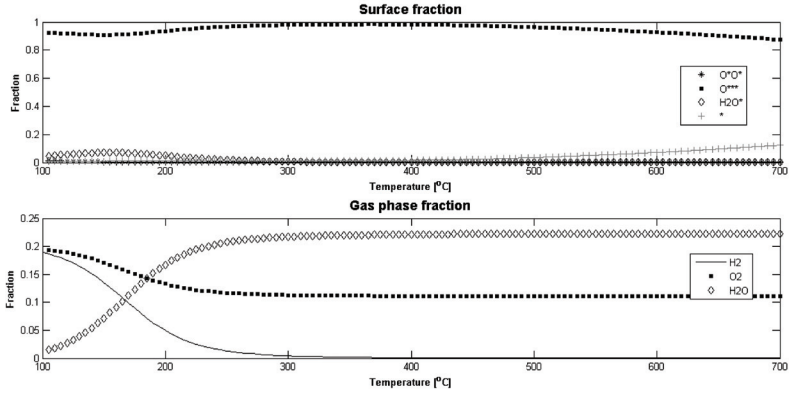

Fig. 5.4.1.10: Result of the model simulation. Gas composition: 20% O_2, 20% H_2, 60% N_2; 50 ml/min total flow.

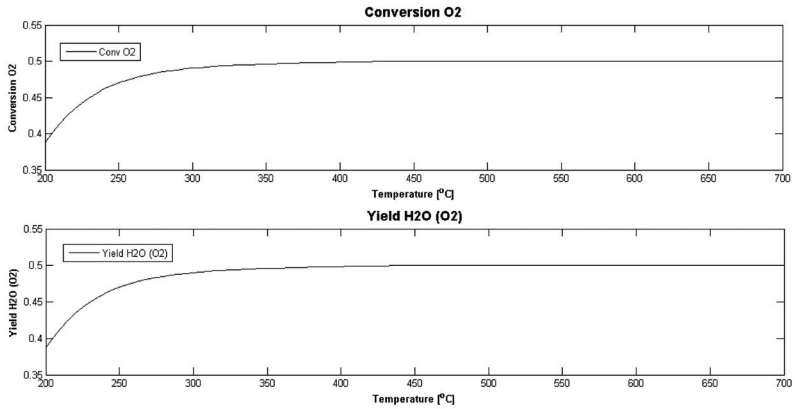

Fig. 5.4.1.11: Result of the model simulation. Gas composition: 20% O_2, 20% H_2, 60% N_2; 50 ml/min total flow. Oxygen conversion and water yield.

Out of interest the model was also checked for the WGS reaction. The initial gas composition was 20% H_2O, 20% CO, 60% N_2. The catalyst used in this case was Cu (appropriate atomic binding energies (Table 8.1.2.3) and lattice parameter (Table 8.1.2.2) were used (shown in Table 5.4.1.1), the rest parameters are similar to ones for Pt catalyst (Table 5.4.2)).

Table 5.4.1.1: Cu catalyst parameters for the model.

Parameter	Symbol	Value
Atomic binding energy C-Cu	QoC	301.2 [kJ/mol]
Atomic binding energy H-Cu	QoH	140.6 [kJ/mol]
Atomic binding energy O-Cu	QoO	258.6 [kJ/mol]
Concentration, surface atoms per surface area, calculated by (8.5.9) with a lattice constant from Table 8.1.2.2	CtMe	$1.8 \cdot 10^{19}$ [$1/m^2$]
Catalyst density, calculated by (8.5.5)	pCat	2138 [kg/m^3]

The result is shown on Fig. 5.4.1.12, the simulated dependence of gas phase composition on temperature is in principle comparable (qualitatively) with results shown for model simulation in [50], [51] (our result is shifted to lower temperatures).

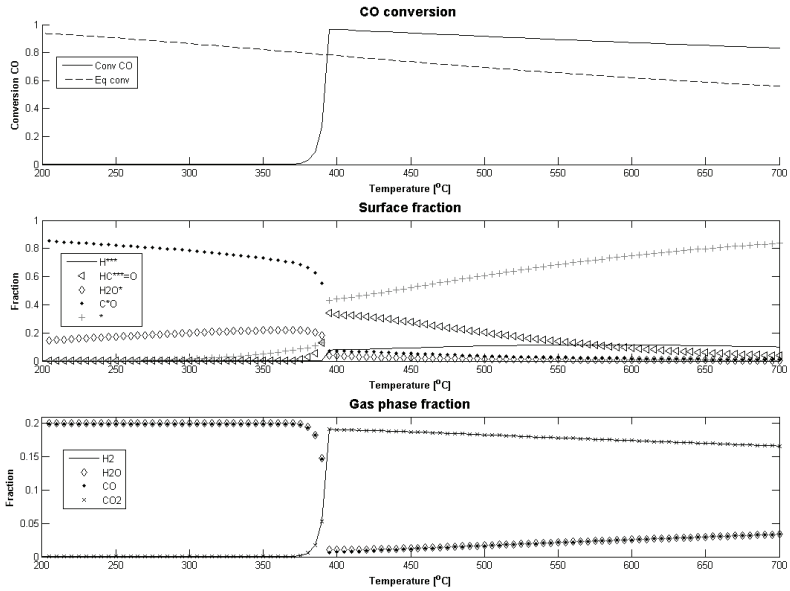

Fig. 5.4.1.12: Result of the model simulation. Gas composition: 20% H_2O, 20% CO, 60% N_2; 50 ml/min total flow. The conversion plot shows the modelled CO conversion and theoretical equilibrium conversion of CO in WGS reaction.

The model simulation of the WGS over the Pt catalyst at these conditions shows almost no activity for the reaction.

5.4.2 TUNED MODEL

In order to tune the model for better convergence with experimental observations it is necessary to adjust some of the model parameters. The preexponentials in rate equations are often (e.g. in [52], [14] and others) adjusted as these are determined using the least precise approach (for proper usage of TST the geometrics of intermediates should be known, but usually different assumptions are used).

Preexponentials in the model are calculated following TST, the adjustment is made by multiplying the calculated preexponential by an adjustment coefficient K_A ($A_{adjusted} = A_{calc} \cdot K_A$).

Based on the results for the non-tuned model it is possible to conclude that the ratio between rates of adsorption-desorption reactions of reactants plays an important role in determining the result of the overall process. Thus the preexponentials for some of the adsorption-desorption steps were adjusted.

The developed model does not cover all the features of the modelled real system, thus it is not justified to try to reach the full quantitative agreement between model and experiment by mathematical adjustment. We consider it more important to show a qualitative agreement between the model and experimental observations.

Taking into consideration the fact that the oxygen coverage of the catalyst surface suppressed the hydrocarbon reactions, first, the oxygen preexponential was adjusted. In order to keep the overall thermodynamic consistency fairly correct the preexponentials of water and hydrogen were adjusted as well. K_A=10 for oxygen desorption, for hydrogen adsorption and water adsorption.

The result of such adjustment is shown on Figs. 5.4.2.1, 5.4.2.2 - hydrogen combustion occur at temperatures below 100 °C (it is shifted to the expected lower temperature compared to the non tuned model Figs. 5.4.1.10, 5.4.1.11).

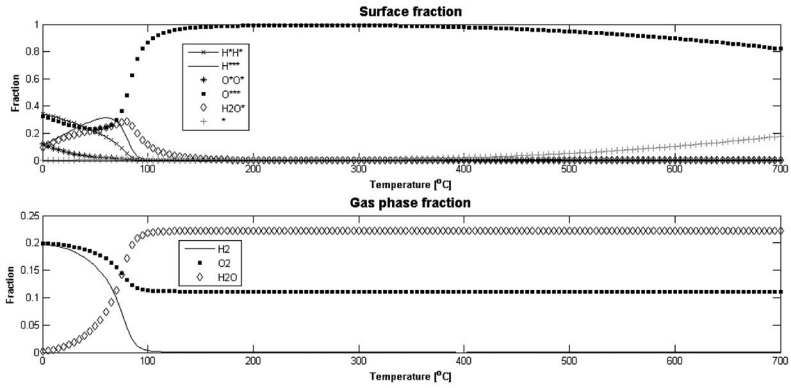

Fig. 5.4.2.1: Result of the tuned model simulation. Gas composition: 20% O_2, 20% H_2, 60% N_2; 50 ml/min total flow.

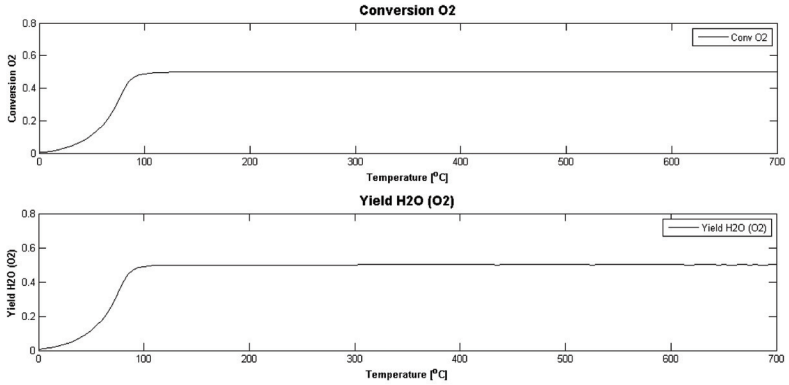

Fig. 5.4.2.2: Result of the tuned model simulation. Gas composition: 20% O_2, 20% H_2, 60% N_2; 50 ml/min total flow.

As the methane yield in the non-tuned model was higher than expected according to experimental observations (and higher than the propylene yield, that is opposite to experimental observations), the preexponential for methane adsorption was increased by 100 (K_A=100) and preexponential for the propylene desorption was increased by 10 (K_A=10). In order to to keep the overall thermodynamic consistency fairly correct the preexponential for propane adsorption was increased by 10 (K_A=10). Adjusted preexponentials are shown in Table 5.4.2.1 (at 298.15 K).

Table 5.4.2.1: Adjusted preexponentials.

Reaction	Direction	Adjusted preexp. A at 298.15 K
R35. $O_2 + 2^* \leftrightarrow O^*O^*$	reverse	$1.6887 \cdot 10^{14}$
R33. $H_2 + 2^* \leftrightarrow H^*H^*$	forward	$1.2323 \cdot 10^{8}$
R42. $H_2O^* \leftrightarrow H_2O + ^*$	forward	$1.6887 \cdot 10^{14}$
R1. $CH_3CH_2CH_3 + ^* \leftrightarrow CH_3CH_2C^*H_3$	forward	$1.2045 \cdot 10^{6}$
R18. $CH_3C^*H=C^*H_2 \leftrightarrow CH_3CH=CH_2 + 2^*$	forward	$1.6887 \cdot 10^{14}$
R26. $C^*H_4 \leftrightarrow CH_4 + ^*$	reverse	$5.4892 \cdot 10^{7}$

Plots, similar to those built in Chapter 5.4.1 , but constructed using adjusted preexponentials are shown on Figs. 5.4.2.3~5.4.2.10.

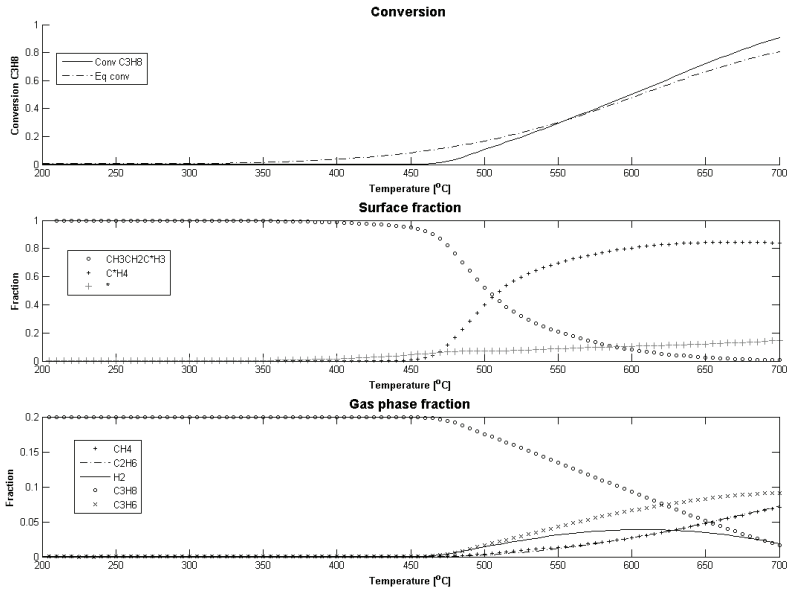

Fig. 5.4.2.3: Result of the tuned model simulation. Gas composition: 20% propane, 80% N_2; 50 ml/min total flow. The conversion plot shows the modelled propane conversion and theoretical equilibrium conversion of propane in pure propane dehydrogenation reaction.

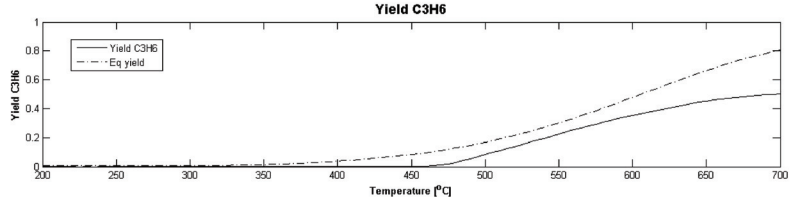

Fig. 5.4.2.4: Result of the tuned model simulation. Gas composition: 20% propane, 80% N_2; 50 ml/min total flow. The modelled yield of propene and equilibrium yield of propene in pure propane dehydrogenation reaction.

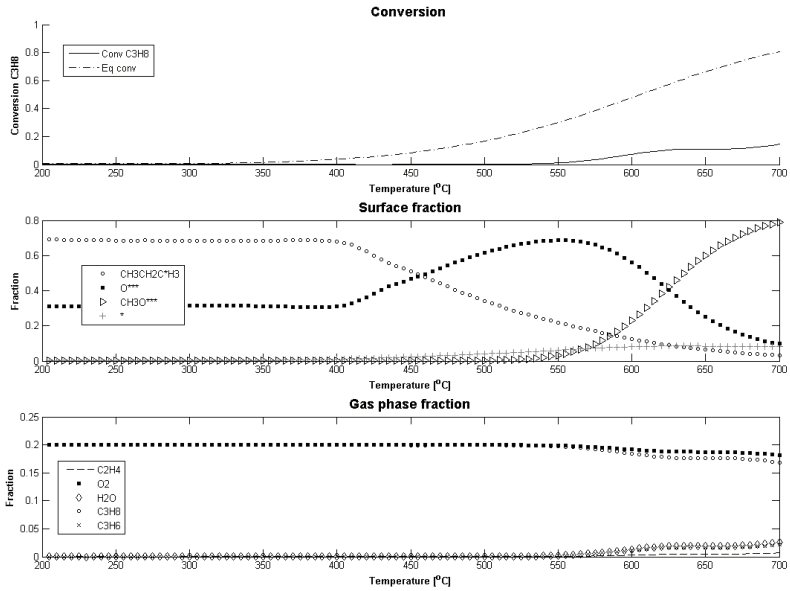

Fig. 5.4.2.5: Result of the tuned model simulation. Gas composition: 20% propane, 20% O_2, 60% N_2; 50 ml/min total flow. The conversion plot shows the modelled propane conversion and theoretical equilibrium conversion of propane in pure propane dehydrogenation reaction.

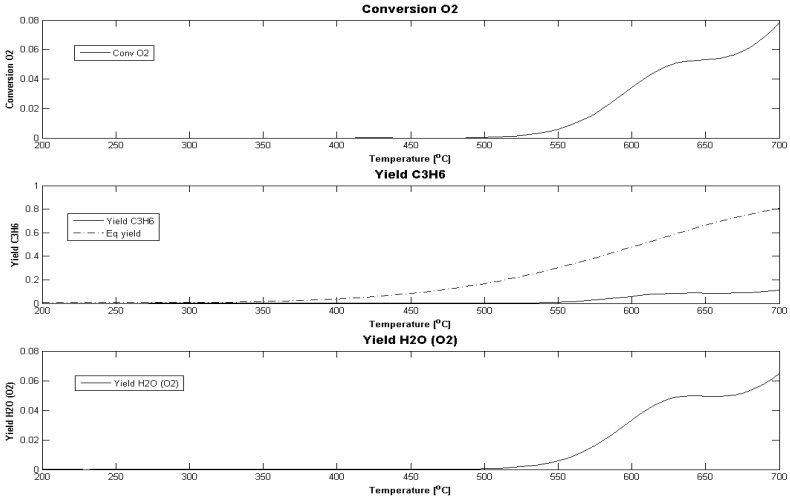

Fig. 5.4.2.6: Result of the tuned model simulation. Gas composition: 20% propane, 20% O_2, 60% N_2; 50 ml/min total flow.

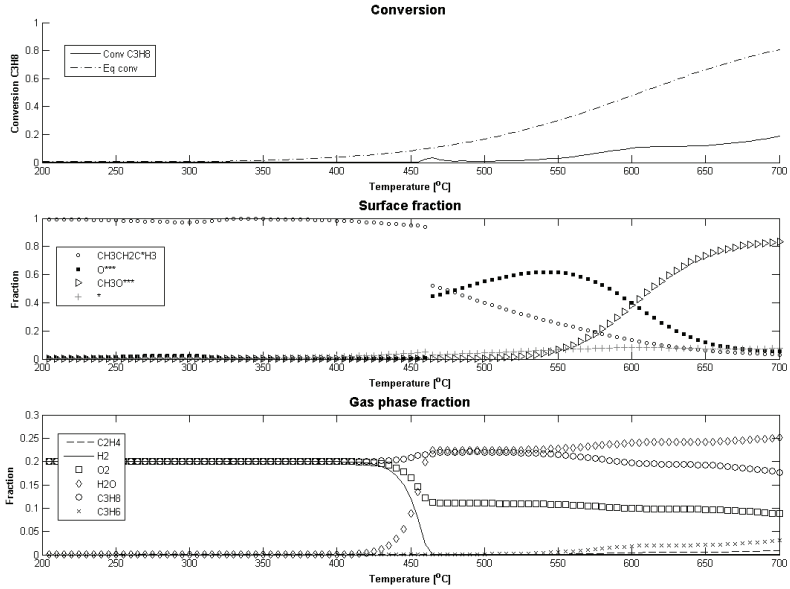

Fig. 5.4.2.7: Result of the tuned model simulation. Gas composition: 20% propane, 20% O_2, 20% H_2, 40% N_2; 50 ml/min total flow. The conversion plot shows the modelled propane conversion and theoretical equilibrium conversion of propane in pure propane dehydrogenation reaction.

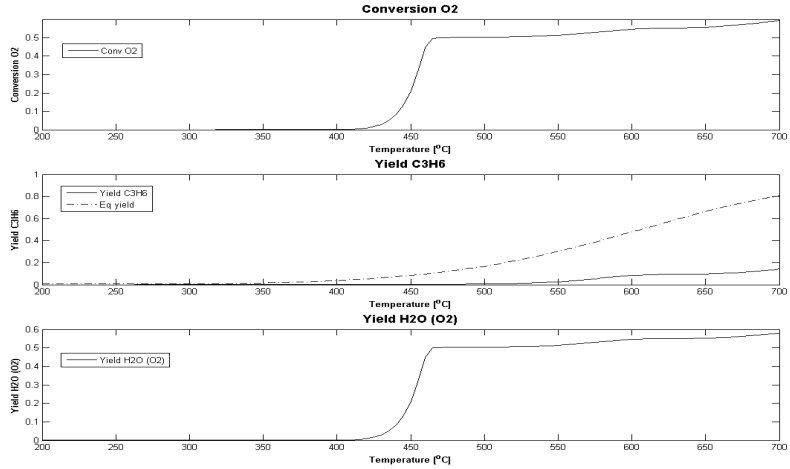

Fig. 5.4.2.8: Result of the tuned model simulation. Gas composition: 20% propane, 20% O_2, 20% H_2, 40% N_2; 50 ml/min total flow.

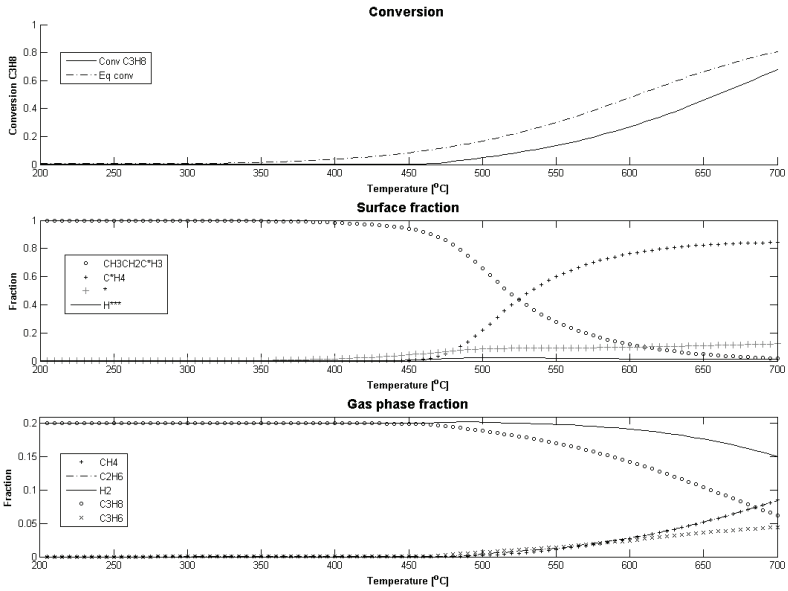

Fig. 5.4.2.9: Result of the tuned model simulation. Gas composition: 20% propane, 20% H_2, 60% N_2; 50 ml/min total flow. The conversion plot shows the modelled propane conversion and theoretical equilibrium conversion of propane in pure propane dehydrogenation reaction.

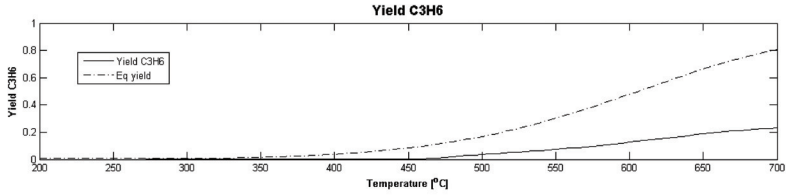

Fig. 5.4.2.10: Result of the tuned model simulation. Gas composition: 20% propane, 20% H_2, 60% N_2; 50 ml/min total flow. The modelled yield of propene and equilibrium yield of propene in pure propane dehydrogenation reaction.

Further tuning of parameters does not make sense since the model still does not cover all the features of a real system. For example all the energetics is described related to fcc (111) metal catalyst surface, whereas the surface of round metal particles is

expected to consist of fractions of (111), (110) and (100) lattices ([42], p. 124); coverage dependence of adsorption is not taken into consideration, nor is the heat balance.

We see the activity in WGS reaction (Fig. Ошибка: источник перёкрестной ссылки не найден), it means that connection $CO \leftrightarrow CO_2$ in the model is described fairly well, whereas we do not see production of CO_x and coke from propane (while we see production of CH_4, C_2H_4, C_2H_6), this can mean that the route $C_xH_y \rightarrow CO_z$ is not described correctly in the model.

The model describes well some common experimental and theoretical observations and tends: adding hydrogen gives rise to hydrogenation products; with mixtures O_2-H_2-C_3H_8, O_2-C_3H_8 the production of C_2H_4 is usually increasing while the formation of C_2H_6 is decreasing with temperature.

6 CONCLUSIONS

The dehydrogenation reaction of propane was studied. The reaction gas mixture composed of propane, oxygen and hydrogen was tested over PtSn/HT and Pt/HT catalysts. This work consisted of two parts: experimental work and modelling work. The experimental work was performed on a dedicated set-up using a simplex planning, where the concentrations of reactants were varied. Some interesting process features for the reaction H_2+O_2+C_3H_8 over PtSn/HT, Pt/HT catalysts and empty reactor were identified using this method.

The hydrogen below the stoichiometric concentration (for reaction of water production) can be selectively combusted over both catalysts. There is a difference between hydrogen premixed in the feed and hydrogen formed in the reaction. Premixed (feed) hydrogen reacts rapidly with oxygen, either upstream of the catalyst bed (in gas-phase) or in the initial part of the bed. The hydrogen formed in the reaction does not see any oxygen (the oxygen is consumed since oxidation reactions are fast).

It is possible to suggest that the water formed at the beginning of the catalyst bed participates (is consumed) in further surface reactions. This process is more important on Pt than on PtSn. Thus the water selectivity for the overall process is lower for Pt than for PtSn catalyst.

Using the simplex plan it was found that there is more than one route to production for each of the products - H_2O and CO_2. One route to CO_2 formation is from propene, another route is production from coke precursors. One route for the production of H_2O is direct hydrogen oxidation, another route incorporates CO as an intermediate compound. In addition the formation of water from coke precursors was also observed.

CO_2 production is not correlated with CO production, whereas the correlation between CO production and H_2O production was observed.

The PtSn catalyst is more selective to propene and water than the Pt catalyst. Pt is more active for production of CO_2, CO, C_2H_6, CH_4, especially at temperatures up to 600 °C (in comparison with PtSn whose activity for these products is very low). At

higher temperatures the results (products distribution) for both catalysts are similar to gas phase reaction (increase in byproducts CO, C_2H_4, CH_4, C_2H_6,), whereas the Pt is still more active for hydrogenation reactions producing CH_4, C_2H_6 and for oxidation reactions producing CO, CO_2.

The maximum rate of formation of CO, CO_2 promotes the stability of the catalyst and coincides with the maximum in propene production over PtSn catalyst. For the Pt catalyst oxidation reactions are so fast that the positive effect of stabilisation of the catalyst is overlapped by negative effect of propene oxidation.

The ratio between H_2 and O_2 fed to the reactor plays a significant role in the outcome of reaction. For different compounds and for both catalyst we can see some features in intensity of production connected with the water production stoichiometric line. On the other hand the specific oxygen concentration of 20% (the necessary amount for the autothermal regime) is playing a role only for PtSn/HT. The only obvious influence of this concentration is observed for propene yield over PtSn catalyst. The maximum yield was at ~17% of O_2 in the whole range of temperatures. This can be an indication that the autothermal regime take place for the process over PtSn catalyst (when hydrogen for combustion is added to the feed).

The optimal mixture content for highest yield of propylene at relevant industrial temperatures (550-625 ℃) over PtSn was found to be: O_2 – 17%, C_3H_8 – 57~50%, H_2 – 26~33%. For Pt it was: O_2 – 0%, C_3H_8 – 55~35%, H_2 – 45~65%.

The model constructed in this work describes the surface reactions with the compounds adsorbed on an adsorption sites of complex configuration. The simulation results for different compositions of the gas mixture reacting on Pt were plotted.

The model describes qualitatively well the experimental observations. The simulation showed a high influence of the adsorptive properties of compounds and coverage effects on the result of reaction.

The model is generalized - it can be used in further work with different input parameters in order to check the behaviour of the reaction mixture with:

- Different compositions of initial mixture ($[O_2]$, $[C_3H_8]$, ... $\in [0, 1]$);
- Different catalysts (Pt, Pd, Au, Cu...);
- Different parameters of the catalyst, flow rates, dilution by inert gas.

7 FURTHER WORK

It is possible to improve some of the approaches used in this work or make additional research in order to get more complete description of the reacting system H_2+O_2+C_3H_8.

For the model:

- Introduce into model diffusion barriers along the surface and surface coverage dependence of Q_{AB} (UBI-QEP has this formalism);
- Using methods of calculation of the heat capacities, find it and calculate the temperature dependencies of entropies that are not available from databases;
- Improve calculation procedures for enthalpies, entropies (using molecular dynamics [58], [59], [77]);
- Describe the catalyst surface as set of kinks, steps (different crystal planes) and prepare mechanisms for every such crystal plane;
- Improve the reactor model by adding the description of mass-transfer in the bulk of flow and in the surface layer, as well as the heat-transfer in a catalyst layer;
- having the energy balance and temperature calculated for every CSTR (that are calculated in a row modelling PFR), make the recalculation of all energetic parameters of the reactions in between the CSTRs;
- Having possibility to use supercomputer and having optimised the way of solving the system of differential equations it can be possible to exclude the step of choose of only part of equations based on activation energies. This can give better description of the system also because of the fact that with change in temperature the activation energies change and relation between activation energies of some of the reactions can change. This can lead us to different working mechanisms at different temperatures;
- Sensitivity analysis of the model parameters;
- Extending model by introducing additional iteration cycle in order to introduce into the model the time axe (varying amount of elementary volumes of feed gas running through the reactor consequently). This would give the description of dynamic time-dependent change of gas-phase and surface concentrations.

For the experimental part:

- Check the dehydrogenation reaction in a system $H_2O(g)/Air/C_3H_8$ or $H_2O(g)/H_2/C_3H_8$ instead of $H_2/Air/C_3H_8$;
- Use different plan of experiments - where all points of the simplex contain all three components and most possible variations of components are used (e.g. every component varies in range 5~95%);

- Use the reactor with the reactor volume limited by volume of the catalyst bed (to exclude possibility of intensive gas-phase reactions);
- Test the system where feed mixture comes into the catalyst bed by two different lines - one with oxygen (air) and second with all other components (to exclude the gas-phase reactions of oxygen in preheating step).

BIBLIOGRAPHY

[1] US Energy information administration: Country analysis - Norway, http://www.eia.gov (2011)

[2] Statistisk sentralbyrå, http://www.ssb.no (2012)

[3] , Melding til Stortinget (2010-2011): En næring for framtida - om petroleumsvirksomheten. - Oslo: Olje- og energidepartement, 2011. - 164 p.

[4] Natural gas, http://www.statoil.com (2012)

[5] P. Eisele, R. Killpack, "Propene", Ullmann's Encyclopedia of Industrial Chemistry, Electronic Release, chap. 4.3. - Weinheim: Wiley-VCH, 2005. - p.

[6] R.A. Meyers, edt., Handbook of petrochemicals production processes. - New York: McGraw-Hill, 2005. - 300 p.

[7] L. Låte, Oxygen-assisted conversion of propane over metal and metal-oxide catalysts. PhD Thesis, NTNU 2002:48. (2002)

[8] H. Dyrbeck, Selective catalytic oxidation of hydrogen and oxygen-assisted conversion of propane. PhD thesis, NTNU 2007:194. (2007)

[9] L. Bednarova, Study of supported Pt-Sn catalysts for propane dehydrogenation. PhD Thesis, NTNU 2002:47. (2002)

[10] NIST Chemistry WebBook. NIST Standard Reference Database Number 69, http://webbook.nist.gov/chemistry/form-ser.html (2012)

[11] ThermoBuild, NASA Glenn thermodynamic database, http://www.grc.nasa.gov/WWW/CEAWeb/ceaThermoBuild.htm (2012)

[12] P.R. Norton, Chapter 2 The hydrogen-oxygen reaction on metal surfaces, in Vol.4 Fundamental studies of heterogeneous catalysis, in The chemical physics of solid surfaces and heterogeneous catalysis (edited by D.A. King, D.P. Woodruff). - Oxford: Elsevier, 1982. - 27-72 p.

[13] W.R. Williams, C.M. Marks, L.D. Schmidt, Steps in the Reaction H2 + O2 = H2O on Pt: OH Desorption at High Temperatures. J. Phys. Chem. 96 (1992) 5922-5931.

[14] Y.K. Park, P. Aghalayam, D.G. Vlachos, A Generalized Approach for Predicting Coverage-Dependent Reaction Parameters of Complex Surface Reactions: Application to H2 Oxidation over Platinum. J. Phys. Chem. A 103 (1999) 8101-8107.

[15] O. Deutschmann, R. Schmidt, F. Behrendt, J. Warnatz, Numerical modelling of catalytic ignition. Conference proceedings, The combustion institute, 1996. - 1747-1754 p.

[16] P.-A. Bui, D.G. Vlachos, P.R. Westmoreland, Modeling Ignition of Catalytic Reactors with Detailed Surface Kinetics and Transport: Oxidation of H2/Air Mixtures over Platinum Surfaces. Ind. Eng. Chem. Res. 36 (1997) 2558-2567.

[17] Fernandes N.E., Park Y.K., Vlachos D.G., The autothermal behavior of platinum catalyzed hydrogen oxidation: experiments and modeling. Combustion and Flame 118 (1999) 164-178.

[18] M. De Falco et al. (eds.), Membrane Reactors for Hydrogen Production Processes, Ch. 9 Alkanes Dehydrogenation. - London: Springer-Verlag, 2011. - 183-200 p.

[19] STAR process, Overview, http://www.uhde.eu/competence/technologies/gas-technologies/152/overview.html (2012)

[20] D. Sanfilippo, F. Buonomo, G. Fusco, Fluidized bed reactors for paraffins dehydrogenation. Chemical Engineering Science 47, No. 9-11 (1992) 2313-2318.

[21] M. Larsson, M. Hulten, E.A. Blekkan, B. Andersson, The Effect of Reaction Conditions and Time on Stream on the Coke Formed during Propane Dehydrogenation. J. Catal. 164 (1996) 44–53.

[22] Q. Li, Z. Sui, X. Zhou, Y. Zhu, J. Zhou, D. Chen, Coke Formation on Pt–Sn/Al2O3 Catalyst in Propane Dehydrogenation: Coke Characterization and Kinetic Study. Top. Catal. 54 (2011) 888–896.

[23] A. Beretta, P. Forzatti, E. Ranzi, Production of Olefins via Oxidative Dehydrogenation of Propane in Autothermal Conditions. J. Catal. 184 (1999) 469–478.

[24] C. Yokoyama, S.S. Bharadwaj, L.D. Schmidt, Platinum-tin and platinum-copper catalysts for autothermal oxidativedehydrogenation of ethane to ethylene. Catal. Letters 38 (1996) 181-188.

[25] E.V. Kondratenko, N. Steinfeldt, M. Baerns, Transient and steady state investigation of selective and non-selective reaction pathways in the oxidative dehydrogenation of propane over supported vanadia catalysts. Phys. Chem. Chem. Phys. 8 (2006) 1624–1633.

[26] R.K. Grasselli, D.L. Stern, J.G. Tsikoyiannis, Catalytic dehydrogenation (DH) of light paraffins combined with selective hydrogen combustion (SHC): I. DH->SHC->DH catalysts in series (co-fed process mode). Appl. Catal. A: Gen. 189 (1999) 1-8.

[27] R.K. Grasselli, D.L. Stern, J.G. Tsikoyiannis, Catalytic dehydrogenation (DH) of light paraffins combined withselective hydrogen combustion (SHC): II. DH+SHC catalysts physically mixed (redox process mode). Appl. Catal. A: Gen. 189 (1999) 9-14.

[28] L. Låte, J.-I. Rundereim, E.A. Blekkan, Selective combustion of hydrogen in the presence of hydrocarbons1. Pt-based catalysts. Appl. Catal. A: Gen. 262 (2004) 53–61.

[29] R. Ramos, M.P. Pina, M. Menendez, J. Santamaria, G.S. Patience, Oxidative Dehydrogenation of Propane to Propene, 2: Simulation of a Commercial Inert Membrane Reactor Immersed in a Fluidized Bed. The Canadian Journal of Chemical Engineering 79 (2001) 902-912.

[30] K. Chen, A. Khodakov, J. Yang, A.T. Bell, E. Iglesia, Isotopic Tracer and Kinetic Studies of Oxidative Dehydrogenation Pathways on Vanadium Oxide Catalysts. J. Catal. 186 (1999) 325–333.

[31] J. Beckers, G. Rothenberg, Ce0.95Cr0.05O2 and Ce0.97Cu0.03O2: active, selective and stable catalysts for selective hydrogen combustion. Dalton Trans. (2009) 5673-5682.

[32] Waku T., Biscardi J.A., Iglesia E., Catalytic dehydrogenation of alkanes on Pt/Na-[Fe]ZSM5 and staged O2 introduction for selective H2 removal. J. Catal. 222 (2004) 481-492.

[33] O. Czuprat, J. Caro, V.A. Kondratenko, E.V. Kondratenko, Dehydrogenation of propane with selective hydrogen combustion: A mechanistic study by transient analysis of products. Catalysis Communications 11 (2010) 1211–1214.

[34] S. Kannan, Catalytic applications of hydrotalcite-like materials and their derived forms. Catalysis Surveys from Asia 10 (2006) 117-137.

[35] Product information: Hydrotalcite PURAL MG, http://www.sasoltechdata.com/tds/pural-mg.pdf (2012)

[36] Y. Kuang, L. Zhao, S. Zhang, F. Zhang, M. Dong, S. Xu, Morphologies, Preparations and Applications of Layered Double Hydroxide Micro-/Nanostructures. Materials 3 (2010) 5220-5235.

[37] J.A. van Bokhoven, J.C.A.A. Roelofs, K.P. de Jong, D.C. Koningsberger, Unique Structural Properties of the Mg±Al Hydrotalcite Solid Base Catalyst: An In Situ Study Using Mg and Al K-Edge XAFS during Calcination and Rehydration. Chem. Eur. J. 7, No. 6 (2001) 1258-1265.

[38] M.R. Othman, Z. Helwani, Martunus, W.J.N. Fernando, Synthetic hydrotalcites from different routes and their application as catalysts and gas adsorbents: a review. Appl. Organometal. Chem. 23 (2009) 335–346.

[39] Mukhlenov I.P., Averbukh A.Ya., Tumarkina E.S., Furmer I.E., Common chemical technology (in Russian). - Moscow: «Vysshaya shkola», 1984. - 256 p.

[40] Edt. L.S. Polak, The application of computational mathematics in the chemical and physical kinetics (in Russian). - Moskva: Nauka, 1969. - 279 p.

[41] Chorkendorff I., Niemantsverdriet J.W., Concepts of modern catalysis and kinetics. - Weinheim: WILEY-VCH, 2003. - 452 p.

[42] Dumesic J.A., Rudd D.F., Aparicio L.M., Rekoske J.E., Trevino A.A., The Microkinetics of Heterogeneous Catalysis. - Washington: ACS Professional Reference Book, 1993. - 315 p.

[43] Shustorovich E., Sellers H., The UBI-QEP method: a practical theoretical approach to understanding chemistry on transition metal surfaces. Surface Science Reports 31 (1998) 1-119.

[44] Sellers H., Modeling the kinetics of large sets of reactions on metal surfaces. Russian Journal of Phisical Chemistry B 1/4 (2007) 386-402.

[45] O'Neal H.E., Benson S.W., Free radicals / Ed. J. K. Kochi. Vol. 2. - N.Y.: Wiley, 1973. - 275-359 p.

[46] E.B. Smith, Basic chemical thermodynamics. 4th ed. - Oxford: Clarendon press, 1990. - 166 p.

[47] Kudryashov I.V., Karetnikov G.S., The book of examples and problems in physical chemistry. - Moskva: Vysshaya shkola, 1991. - 527 p.

[48] H. Sellersl, E. Shustorovich, Intrinsic activation barriers and coadsorption effects for reactions on metal surfaces: unified formalism within the UBI-QEP approach. Surface Science 504 (2002) 167-182.

[49] Shustorovich E.M., Zeigarnik A.V, The UBI-QEP treatment of polyatomic molecules without bond-energy partitioning. Surface Science 527 (2003) 137-148.

[50] Fishtik I., Datta R., A UBI-QEP microkinetic model for the water-gas shift reaction on Cu(111). Surface Science 512 (2002) 229-254.

[51] Zeigarnik A.V., Callaghan C., Datta R., Fishtik I., Shustorovich E., Prediction of comparative catalytic activity in the series of single crystalline surfaces in a water-gas shift reaction. Kinetics and Catalysis 46/4 (2005) 509-515.

[52] A.B. Mhadeshwar, D.G. Vlachos, A thermodynamically consistent surface reaction mechanism for CO oxidation on Pt. Combustion and Flame 142 (2005) 289–298.

[53] S. Storsæter, D. Chen, A. Holmen, Microkinetic modelling of the formation of C1 and C2 products in the Fischer–Tropsch synthesis over cobalt catalysts. Surface Science 600 (2006) 2051–2063.

[54] I.V. Kuz'min, A.V. Zeigarnik, Microkinetic Modeling of Ethane Hydrogenolysis on Metals. Kinetics and Catalysis 45, No. 4 (2004) 561–568.

[55] P. Stoltze, Microkinetic simulation of catalytic reactions. Progress in Surface Science 65 (2000) 65-150.

[56] A.B. Mhadeshwar, D.G. Vlachos, A Catalytic Reaction Mechanism for Methane Partial Oxidation at Short Contact Times, Reforming, and Combustion, and for

Oxygenate Decomposition and Oxidation on Platinum. Ind. Eng. Chem. Res. 46 (2007) 5310-5324.

[57] M. Salciccioli, Y. Chen, D. G. Vlachos, Microkinetic Modeling and Reduced Rate Expressions of Ethylene Hydrogenation and Ethane Hydrogenolysis on Platinum. Ind. Eng. Chem. Res. 50(1) (2011) 28-40.

[58] Orlov Yu.D., Lebedev Yu.A., Saifullin I.Sh., Thermochemistry of organic free radicals (in Russian). - Moscow: Nauka, 2001. - 304 p.

[59] Luo Yu-Ran, Comprehensive handbook of chemical bond energies. - Boca Raton, FL: CRC Press, 2007. - p.

[60] Lide David R., CRC Handbook of Chemistry and Physics. - Boca Raton, FL: Taylor and Francis, 2008. - 2388 p.

[61] Database of thermodinamical properties of individual substances IVTANTHERMO, http://www.chem.msu.su/rus/handbook/ivtan (2012)

[62] E.T. Denisov, T.G. Denisova, T.S. Pokidova, Handbook of free radical initiators. - New Jersey: Wiley-Interscience, 2003. - 879 p.

[63] Ming-Lei Yang, Yi-An Zhu, Chen Fan, Zhi-Jun Sui, De Chen, Xing-Gui Zhou, Density functional study of the chemisorption of C1, C2 and C3 intermediates in propane dissociation on Pt(111). Journal of Molecular Catalysis A: Chemical 321 (2010) 42-49.

[64] Vincent R.S., Lindstedt R.P., Malik N.A., Reid I.A.B., Messenger B.E., The chemistry of ethane dehydrogenation over a supported platinum catalyst. Journal of Catalysis 260 (2008) 37-64.

[65] N.S. Zefirov, S.I. Kuchanov, The theory of graphs in chemistry. - Novosibirsk: Nauka, 1988. - 305 p.

[66] R. Sumathi, H.H. Carstensen, W. H. Green, Reaction Rate Prediction via Group Additivity Part 1: H Abstraction from Alkanes by H and CH3. J. Phys. Chem. A 105 (2001) 6910-6925.

[67] R. Sumathi, H.H. Carstensen, W. H. Green, Reaction Rate Prediction via Group Additivity, Part 2: H-Abstraction from Alkenes, Alkynes, Alcohols, Aldehydes, and Acids by H Atoms. J. Phys. Chem. A 105 (2001) 8969-8984.

[68] K.K. Irikura, D.J. Frurip, Eds., In "Computational Thermochemistry: Prediction and Estimation of Molecular Thermodynamics" (ACS Symposium Series 677). - Washington: ACS, 1998. - Appendix B p.

[69] ChemBio3D Ultra 12.0 by CambridgeSoft, http://www.cambridgesoft.com/software/chembio3d/default.aspx (2012)

[70] M.K. Gilson, K.K. Irikura, Symmetry Numbers for Rigid, Flexible, and Fluxional Molecules: Theory and Applications. J. Phys. Chem. B 114 (2010) 16 304–16 317.

[71] GAP - Groups, Algorithms, Programming - a System for Computational Discrete Algebra, http://www.gap-system.org/ ()

[72] Z. Zhou, S. Wang, W. Zhou, G. Wang, L. Jiang, W. Li, S. Song, J. Liu, G. Suna, Q. Xin, Novel synthesis of highly active Pt/C cathode electrocatalyst for direct methanol fuel cell. Chem. Com. (2003) 394–395.

[73] S.L. Akhnazarova, V.V. Kafarov, Methods of the experiments optimization in chemical technology (In Russian). - Moskva: Vysshaya shkola, 1985. - 327 p.

[74] I.M. Agayants, Handbook of statistical tasks. Part III (in Russian). - Moskva: MITHT im. M.V. Lomonosova, 2007. - 79 p.

[75] Computer algebra system Maxima, http://maxima.sourceforge.net (2012)

[76] G.C. Bond, Metal-Catalysed Reactions of Hydrocarbons. - USA: Springer, 2005. - 688 p.

[77] J.B. Pedley, R.D. Naylor, S.P. Kirby, Thermochemical data of organic compounds. - Oxford: Chapman and Hall, 1986. - 792 p.

[78] Green D. W., Perry R. H., Perry's Chemical Engineers' Handbook (8th Edition). - New York: McGraw-Hill, 2008. - 2851 p.

[79] Rohsenow, Warren M.; Hartnett, James P.; Cho, Young I., Handbook of Heat Transfer (3rd Edition). - : McGraw-Hill, 1998. - 1473 p.

[80] M. Balonis, F.P. Glasser, The densitiy of cement phases worksheets. - Aberdeen: University of Aberdeen, 2009. - 61 p.

[81] Hellwege K.-H., Hellwege A. M., Landolt-Börnstein - Group III Condensed Matter. Numerical Data and Functional Relationships in Science and Technology. - Berlin: Springer-Verlag, 1961. - p.

[82] L. Nykänen, K. Honkala, Density functional theory study on propane and propene adsorption on Pt(111) and PtSn alloy surfaces. J. Phys. Chem. C 115(19) (2011) 9578-9586.

[83] Shustorovich E.M., Zeigarnik A.V, The UBI-QEP Method: Basic Formalism and Applications to Chemisorption Phenomena on Transition Metal Surfaces. Chemisorption Energetics. Russian Journal of Physical Chemistry 80-1 (2006) 4-30.

[84] P. Aghalayam, Y. K. Park, D.G. Vlachos, Construction and Optimization of Complex Surface-Reaction Mechanisms. AIChE Journal Vol. 46, No. 10 (2000) 2017-2029.

[85] Bronshtein I.N., Semendyayev K.A., Handbook of Mathematics. - Moskva: Nauka, 1986. - 544 p.

[86] Perry Robert H., Perry's chemical engineers' handbook. - New York: McGraw-Hill, 1999. - 2582 p.

[87] Naval Research Laboratory. Center for Computational Materials Science , http://cst-www.nrl.navy.mil/lattice/struk/a1.html (2011)

[88] F. Delannay (edt.), Characterization of heterogeneous catalysts. - New York: Marcel Dekker, 1984. - 409 p.

[89] Ternary Plots (Matlab functions), http://www.mathworks.com/matlabcentral/fileexchange/7210-ternary-plots (2012)

[90] I.M. Agayants, Handbook of statistical tasks. Part II (in Russian). - Moskva: MITHT im. M.V. Lomonosova, 2007. - 77 p.

[91] K.I. Sakodynskiy, V.V. Brazhnikov, S.A. Volkov and others, Analytical chromatography (in Russian). - Moskva: Khimiya, 1993. - 464 p.

[92] A.Yu. Zakgeim, General chemical technology (in Russian). - Moskva: Logos, 2009. - 304 p.

8 APPENDICES

8.1 REFERENCE DATA

8.1.1 CONVERSION FACTORS AND CONSTANTS

From [60], 1-38 ~ 1-40, 1-46:

1 psi = 6894.757 Pa

1 bar = 100 000 Pa

1 atm = 101 325 Pa

1 kcal/mol = 4.184 kJ/mol

1 eV = 96.4853 kJ/mol

t, ℃ = T, °K - 273.15

Gas constant, R = 8.314472 $\frac{Pa \cdot m^3}{K \cdot mol}$

Boltzmann constant, $k_B = 1.380658 \cdot 10^{-23}$ [J/K]

Plank constant, $h = 6.6262755 \cdot 10^{-34}$ [J·s]

Avogadro constant, $N_A = 6{,}022141\,793 \cdot 10^{23}$ [1/mol]

8.1.2 PHYSICAL PROPERTIES

Table 8.1.2.1: Density (kg/m³) of selected elements as a function of temperature ([78], p. 2-125, [79], p. 2.47).

Temp.,	**Element**													
K°	**Al**	**Be**	**Cr**	**Cu**	**Au**	**Ir**	**Fe**	**Pb**	**Mo**	**Ni**	**Pt**	**Pd**	**Ag**	**Zn**
50	2736	3650	7160	9019	19 490	22 600	7910	11 570	10 260	8960	21 570	12 110	10 620	7280
100	2732	3640	7155	9009	19 460	22 580	7900	11 520	10 260	8950	21 550	12 100	10 600	7260
150	2726	3630	7150	8992	19 420	22 560	7890	11 470	10 250	8940	21 530	12 090	10 575	7230

200	2719	3620	7145	8973	19 380	22 540	7880	11 430	10 250	8930	21 500	12 070	10 550	7200
250	2710	3610	7140	8951	19 340	22 520	7870	11 380	10 250	8910	21 470	12 050	10 520	7170
300	2701	3600	7135	8930	19 300	22 500	7860	11 330	10 240	8900	21 450	12 030	10 490	7135
400	2681	3580	7120	8885	19 210	22 450	7830	11 230	10 220	8860	21 380	11 980	10 430	7070
500	2661	3555	7110	8837	19 130	22 410	7800	11 130	10 210	8820	21 330	11 940	10 360	7000
600	2639	3530	7080	8787	19 040	22 360	7760	11 010	10 190	8780	21 270	11 890	10 300	6935
800	2591		7040	8686	18 860	22 250	7690	10 430	10 160	8690	21 140	11 790	10 160	6430

Mean density of hydrotalcites $Mg_{2x}Al_2(OH)_{4x+4}CO_3 \cdot nH_2O$ [80]: 2122 [kg/m^3].

Table 8.1.2.2: Structures of elements ([81], Table 2.1).

Element	Space group	Lattice constants, [Å]	Formula units in the unit cell
Ag	Fm3m	a = 4.08626	4
Au	Fm3m	a = 4.07833	4
Cu	Fm3m	a = 3.6147	4
Ir	Fm3m	a = 3.8389	4
Ni	Fm3m	a = 3.5238	4
Pd	Fm3m	a = 3.8908	4
Pt	Fm3m	a = 3.9240	4

Table 8.1.2.3: Suggested UBI-QEP values of atomic binding energies Q_{0A} [kcal/mol] on fcc(111) surfaces ([43],p.31, [49], p.146).

Atom\Metal	Cu	Ag	Au	Ni	Pd	Pt
H	33.6	31.2	27.06	37.8	37.2	36.6
O	61.8	48.0	45.0	69.0	52.3	51.0
N	69.0	60.0	58.2	81.0	78.0	69.6
C	72.0	66.2	65.0	102.6	96.0	90.0
S	52.6	46.8	48.0	67.2	57.0	55.2

8.2 REACTION ENERGETICS

8.2.1 ROTATIONAL SYMMETRY NUMBERS

The code used in GAP program [71] for calculation of the rotational symmetry numbers of molecules (see Ch. 3.2.2):

```
gap> torsion := PermList( [1,2,4,5,3,6] );
       (3,4,5)
gap> CH3CH := Group(torsion);
       Group([ (3,4,5) ])
gap> Order(CH3CH);
       3
------------
gap> torsion1 := PermList( [1,2,3,5,6,4,7,8,9,10] );
       (4,5,6)
gap> torsion2 := PermList( [1,2,3,4,5,6,7,8,10,9] );
       (9,10)
gap> CH3CH2CH2 := Group(torsion1, torsion2);
       Group([ (4,5,6), (9,10) ])
gap> Order(CH3CH2CH2);
       6
------------
gap> torsion := PermList( [1,2,3,5,6,4,7,8,9] );
       (4,5,6)
gap> CH3CH2CH := Group(torsion);
       Group([ (4,5,6) ])
gap> Order(CH3CH2CH);
       3
------------
```

8.2.2 ENTROPY CALCULATION

Calculation of the entropy of $CH_3CH_2C{:}H$ (see Ch. 3.2.2):

$$\Delta S_m^0 = \frac{3\cdot R}{2}\cdot\ln\left(\frac{M_{CH_3CH_2\ddot{C}H}}{M_{CH_3CH_2\dot{C}H_2}}\right)=12.47\cdot\ln\left(\frac{42.08}{43.09}\right)=-0.3\left[\frac{kJ}{mol}\right],$$

$$\Delta S_v^0=-S^0(C-H)_{3000}-S^0\left(\begin{matrix}C\\ \wedge\\ H\ H\end{matrix}\right)_{1450}-S^0\left(\begin{matrix}C\\ \wedge\\ H\ C\end{matrix}\right)_{1150}=-0.33\left[\frac{kJ}{mol}\right],$$

$$\Delta S_{rot}=\frac{1}{2}\cdot R\cdot\ln\left\{\frac{I_A\cdot I_B\cdot I_C(CH_3CH_2\ddot{C}H)}{I_A\cdot I_B\cdot I_C(CH_3CH_2\dot{C}H_2)}\right\}=\frac{1}{2}\cdot R\cdot\ln\left\{\frac{14.307\cdot 52.796\cdot 60.492}{16.113\cdot 55.048\cdot 63.187}\right\}=-0.85\left[\frac{kJ}{mol}\right], \quad (8.2.2.1)$$

$$\Delta S_{i.rot}^0=\frac{1}{2}\cdot R\cdot\ln\left(\frac{I_{r(CH_3CH_2\ddot{C}H)}}{I_{r(CH_3CH_2\dot{C}H_2)}}\right)\approx-1.26\left[\frac{kJ}{mol}\right],$$

$$\Delta S_\sigma^0=R\cdot\ln\frac{\sigma(CH_3CH_2\dot{C}H_2)}{\sigma(CH_3CH_2\ddot{C}H)}=R\cdot\ln\frac{6}{3}=5.8\left[\frac{kJ}{mol}\right],$$

$$\Delta S_{V_0}^0=-S_{intr}^0(\dot{C}H_2-\infty)=-22.6\left[\frac{kJ}{mol}\right],$$

$$\Delta S_e^0=R\cdot\ln(g_e)=R\cdot\ln(3)=9.13\left[\frac{kJ}{mol}\right].$$

$$S^0(CH_3CH_2\ddot{C}H)=S^0(CH_3CH_2\dot{C}H_2)+\sum\Delta S_{corrections}^0=289.586-10.41=279.18\left[\frac{kJ}{mol}\right] \quad (8.2.2.2)$$

8.2.3 HEATS OF ADSORPTION

Table 8.2.3.1 Heats of molecular chemisorption.

Molecule	Calculation, with ΔH_f^0 from Table 3.1.1, Q_{0A} from Table 8.1.2.3	Q_{AB} [kJ/mol]
$CH_3\underset{*}{C}H_2CH_3$	site: on-top; coordination: mono-C $D_{AB}=2\cdot\Delta H_f^0(H)+2\cdot\Delta H_f^0(\dot{C}H_3)+\Delta H_f^0(C)-$ $-\Delta H_f^0(CH_3CH_2CH_3)=$ $=2\cdot 218.0+2\cdot 146.7+716.67-(-104.7)=1550.8\left[\frac{kJ}{mol}\right]$ weak binding, (2.6.4.2):	73.6

	$Q_{0A}=Q_{0C}=376.56\left[\frac{kJ}{mol}\right]$ $Q_{AB}=\frac{376.56^2}{376.56+1550.8}=73.6\left[\frac{kJ}{mol}\right]$	
$CH_3CH_2\underset{*}{C}H_3$	site: on-top; coordination: mono-C $D_{AB}=3\cdot\Delta H_f^0(H)+\Delta H_f^0(CH_3\dot{C}H_2)+\Delta H_f^0(C)-$ $-\Delta H_f^0(CH_3CH_2CH_3)=$ $=3\cdot 218.0+118.7+716.67-(-104.7)=1594.1\left[\frac{kJ}{mol}\right]$ weak binding, (2.6.4.2): $Q_{0A}=Q_{0C}=376.56\left[\frac{kJ}{mol}\right]$ $Q_{AB}=\frac{376.56^2}{376.56+1594.1}=71.9\left[\frac{kJ}{mol}\right]$	71.9
$CH_3\underset{*}{C}H_2\underset{*}{C}H_3$	site: bridge; coordination: di-C pseudo-atom A = CH_3-$\dot{C}H_2$; site: on-top; binding: weak pseudo-atom B = $\dot{C}H_3$; site: on-top; binding: weak $D_{AB}=D_{CH_3CH_2-CH_3}=\Delta H_f^0(CH_3\dot{C}H_2)+\Delta H_f^0(\dot{C}H_3)-$ $-\Delta H_f^0(CH_3CH_2CH_3)=$ $=118.7+146.7-(-104.7)=370.1\left[\frac{kJ}{mol}\right]$ From (2.6.4.11):	11.3, [8.7-35.7 [82]], [5.8 [63] (no pref. site)]

$$D_{iA}=D_{CH_3\dot{C}H_2}=2\cdot\Delta H_f^0(H)+\Delta H_f^0(\dot{C}H_3)+\Delta H_f^0(C)-$$
$$-\Delta H_f^0(CH_3\dot{C}H_2)=$$
$$=2\cdot 218.0+146.7+716.67-118.7=1180.7\left[\frac{kJ}{mol}\right]$$

$$Q_{0a}=Q_{0b}=Q_{0C}=376.56\left[\frac{kJ}{mol}\right]$$

$$Q_{0A}=Q_{CH_3\dot{C}H_2}=\frac{376.56^2}{376.56+1180.7}=91.1\left[\frac{kJ}{mol}\right]$$

$$D_{iB}=D_{\dot{C}H_3}=3\cdot\Delta H_f^0(H)+\Delta H_f^0(C)-\Delta H_f^0(\dot{C}H_3)=$$
$$=3\cdot 218.0+716.67-146.7=1224.0\left[\frac{kJ}{mol}\right]$$

$$Q_{0B}=Q_{\dot{C}H_3}^{wk}=\frac{376.56^2}{376.56+1224.0}=88.6\left[\frac{kJ}{mol}\right]$$

From (2.6.4.9), (2.6.4.10):

$$a=\frac{91.1^2\cdot(91.1+2\cdot 88.6)}{(91.1+88.6)^2}=69.0\left[\frac{kJ}{mol}\right]$$

$$b=\frac{88.6^2\cdot(88.6+2\cdot 91.1)}{(91.1+88.6)^2}=65.8\left[\frac{kJ}{mol}\right]$$

From (2.6.4.8):

	$Q_{AB}=\frac{69.0\cdot 65.8\cdot(69.0+65.8)+370.1\cdot(69.0-65.8)^2}{69.0\cdot 65.8+370.1\cdot(69.0+65.8)}=$ $=11.3\left[\frac{kJ}{mol}\right]$	
$CH_3CH_2\underset{***}{C}H_2$	site: hollow; coordination: mono-C $D_{AB}=2\cdot\Delta H_f^0(H)+\Delta H_f^0(CH_3\dot{C}H_2)+\Delta H_f^0(C)-$ $-\Delta H_f^0(CH_3CH_2\dot{C}H_2)=$ $=2\cdot 218.0+118.7+716.67-100.5=1170.9\left[\frac{kJ}{mol}\right]$ medium binding, (2.6.4.5): $Q_{0A}=Q_{0C}=376.56\left[\frac{kJ}{mol}\right]$ (2.6.4.1): $Q_A=Q_C=376.56\cdot\left(2-\frac{1}{3}\right)=627.6\left[\frac{kJ}{mol}\right]$ $Q_{AB}=\frac{1}{2}\cdot\left(\frac{376.56^2}{\frac{376.56}{3}+1170.9}+\frac{627.6^2}{627.6+1170.9}\right)=164.2\left[\frac{kJ}{mol}\right]$	164.2, [181.4 [63] (on-top)]
$CH_3\underset{***}{C}HCH_3$	site: hollow; coordination: mono-C $D_{AB}=\Delta H_f^0(H)+2\cdot\Delta H_f^0(\dot{C}H_3)+\Delta H_f^0(C)-$ $-\Delta H_f^0(CH_3\dot{C}HCH_3)=$ $=218.0+2\cdot 146.7+716.67-93.3=1134.8\left[\frac{kJ}{mol}\right]$ medium binding, (2.6.4.5):	168.0, [160.2 [63] on-top]

	$Q_{0A}=Q_{0C}=376.56\left[\frac{kJ}{mol}\right]$, $Q_{A}=Q_{C}=627.6\left[\frac{kJ}{mol}\right](see\ above)$ $Q_{AB}=\frac{1}{2}\cdot\left(\frac{376.56^2}{\frac{376.56}{3}+1134.8}+\frac{627.6^2}{627.6+1134.8}\right)=168.0\left[\frac{kJ}{mol}\right]$	
$\underset{***}{CH_3}\underset{*}{CHCH_3}$	site: bridge; coordination: di-C pseudo-atom A = CH_3-C:H; site: hollow; binding: medium pseudo-atom B = $\dot{C}H_3$; site: on-top; binding: weak $D_{AB}=D_{CH_3\dot{C}H-CH_3}=\Delta H_f^0(CH_3\ddot{C}H)+\Delta H_f^0(\dot{C}H_3)-$ $-\Delta H_f^0(CH_3\dot{C}HCH_3)=$ $=366.1+146.7-93.3=419.5\left[\frac{kJ}{mol}\right]$ From (2.6.4.11): $D_{iA}=D_{CH_3\ddot{C}H}=\Delta H_f^0(H)+\Delta H_f^0(\dot{C}H_3)+\Delta H_f^0(C)-$ $-\Delta H_f^0(CH_3\ddot{C}H)=$ $=218.0+146.7+716.67-366.1=715.3\left[\frac{kJ}{mol}\right]$ $Q_{0a}=Q_{0b}=Q_{0C}=376.56\left[\frac{kJ}{mol}\right]$,	125.1

	$Q_a = Q_C = 627.6\left[\frac{kJ}{mol}\right] (see\ above)$ $Q_{0A} = Q^{mdm}_{CH_3\dot{C}H} = \frac{1}{2}\cdot\left(\frac{376.56^2}{\frac{376.56}{3}+715.3}+\frac{627.6^2}{627.6+715.3}\right) = 231.0\left[\frac{kJ}{mol}\right]$ $D_{iB} = D_{\dot{C}H_3} = 1224.0\left[\frac{kJ}{mol}\right] (see\ above)$ $Q_{0B} = Q^{wk}_{\dot{C}H_3} = 88.6\left[\frac{kJ}{mol}\right] (see\ above)$ From (2.6.4.9), (2.6.4.10): $a = \frac{231.0^2\cdot(231.0+2\cdot 88.6)}{(231.0+88.6)^2} = 213.2\left[\frac{kJ}{mol}\right]$ $b = \frac{88.6^2\cdot(88.6+2\cdot 231.0)}{(231.0+88.6)^2} = 42.3\left[\frac{kJ}{mol}\right]$ $Q_{AB} = \frac{213.2\cdot 42.3\cdot(213.2+42.3)+419.5\cdot(213.2-42.3)^2}{213.2\cdot 42.3+419.5\cdot(213.2+42.3)} =$ $= 125.3\left[\frac{kJ}{mol}\right]$	
$CH_3\underset{***}{C}CH_3$	site: hollow; coordination: mono-C $D_{AB} = 2\cdot\Delta H^0_f(\dot{C}H_3)+\Delta H^0_f(C)-\Delta H^0_f(CH_3\ddot{C}CH_3) =$ $= 2\cdot 146.7+716.7-295.8 = 714.3\left[\frac{kJ}{mol}\right]$ strong binding, (2.6.4.4):	293.5, [334.8 [63] site: n=2]

	$Q_A = Q_C = 627.6\left[\frac{kJ}{mol}\right](see\ above)$ $Q_{AB} = \frac{627.6^2}{627.6+714.3} = 293.5\left[\frac{kJ}{mol}\right]$	
$CH_3\underset{***}{C}\underset{*}{C}H_3$	Impossible to calculate because of lack $\Delta H_f^0(CH_3C)$	
$CH_3\underset{*}{C}H_2\underset{***}{C}H_2$	site: bridge; coordination: di-C pseudo-atom A = CH_3-$\dot{C}H_2$; site: on-top; binding: weak pseudo-atom B = C:H_2; site: hollow; binding: medium $D_{AB} = D_{CH_3CH_2-\dot{C}H_2} = \Delta H_f^0(CH_3\dot{C}H_2) + \Delta H_f^0(\ddot{C}H_2) -$ $- \Delta H_f^0(CH_3CH_2\dot{C}H_2) =$ $= 118.7 + 390.4 - 100.5 = 408.6\left[\frac{kJ}{mol}\right]$ From (2.6.4.11): $D_{iA} = D_{CH_3\dot{C}H_2} = 1180.7\left[\frac{kJ}{mol}\right](see\ above)$ $Q_{0a} = Q_{0b} = Q_{0C} = 376.56\left[\frac{kJ}{mol}\right]$ $Q_{0A} = Q^{wk}_{CH_3\dot{C}H_2} = 91.1\left[\frac{kJ}{mol}\right](see\ above)$ $D_{iB} = D_{\dot{C}H_2} = 2\cdot\Delta H_f^0(H) + \Delta H_f^0(C) - \Delta H_f^0(\ddot{C}H_2) =$ $= 2\cdot 218.0 + 716.67 - 390.4 = 762.3\left[\frac{kJ}{mol}\right]$	112.3

	$Q_b = Q_C = 627.6\left[\frac{kJ}{mol}\right] (see\ above)$ $Q_{0B} = Q_{\dot{C}H_2}^{mdm} = \frac{1}{2}\cdot\left(\frac{376.56^2}{\frac{376.56}{3}+762.3} + \frac{627.6^2}{627.6+762.3}\right) = 221.6\left[\frac{kJ}{mol}\right]$ From (2.6.4.9), (2.6.4.10): $a = \frac{91.1^2\cdot(91.1+2\cdot221.6)}{(91.1+221.6)^2} = 45.3\left[\frac{kJ}{mol}\right]$ $b = \frac{221.6^2\cdot(221.6+2\cdot91.1)}{(91.1+221.6)^2} = 202.8\left[\frac{kJ}{mol}\right]$ $Q_{AB} = \frac{45.3\cdot202.8\cdot(45.3+202.8)+408.6\cdot(45.3-202.8)^2}{45.3\cdot202.8+408.6\cdot(45.3+202.8)} = 112.3\left[\frac{kJ}{mol}\right]$	
$CH_3CH=\underset{*}{C}H_2$	site: on-top; coordination: mono-C $D_{AB} = 2\cdot\Delta H_f^0(H) + \Delta H_f^0(CH_3\ddot{C}H) + \Delta H_f^0(C) -$ $- \Delta H_f^0(CH_3CH=CH_2) =$ $= 2\cdot218.0 + 366.1 + 716.67 - 20.0 = 1498.8\left[\frac{kJ}{mol}\right]$ weak binding, (2.6.4.2): $Q_{0A} = Q_{0C} = 376.56\left[\frac{kJ}{mol}\right]$ $Q_{AB} = \frac{376.56^2}{376.56+1498.8} = 75.6\left[\frac{kJ}{mol}\right]$	75.6
	site: on-top; coordination: mono-C	77.6

$CH_3\underset{*}{C}H=CH_2$	$D_{AB}=\Delta H_f^0(H)+\Delta H_f^0(\dot{C}H_3)+\Delta H_f^0(C)+\Delta H_f^0(\ddot{C}H_2)-$ $-\Delta H_f^0(CH_3CH=CH_2)=$ $=218.0+146.7+716.67+390.4-20.0=1451.8\left[\frac{kJ}{mol}\right]$ weak binding, (2.6.4.2): $Q_{0A}=Q_{0C}=376.56\left[\frac{kJ}{mol}\right]$ $Q_{AB}=\frac{376.56^2}{376.56+1451.8}=77.6\left[\frac{kJ}{mol}\right]$	
$CH_3\underset{*}{C}H=\underset{*}{C}H_2$	site: bridge; coordination: di-C pseudo-atom A = CH_3-C:H; site: on-top; binding: weak pseudo-atom B = C:H_2; site: on-top; binding: weak $D_{AB}=D_{CH_3CH=(CH_2)}=\Delta H_f^0(CH_3\ddot{C}H)+\Delta H_f^0(\ddot{C}H_2)-$ $-\Delta H_f^0(CH_3CH=CH_2)=$ $=366.1+390.4-20.0=736.5\left[\frac{kJ}{mol}\right]$ From (2.6.4.11): $D_{iA}=D_{CH_3\ddot{c}H}=715.3\left[\frac{kJ}{mol}\right](see\ above)$ $Q_{0a}=Q_{0b}=Q_{0C}=376.56\left[\frac{kJ}{mol}\right]$ $Q_{0A}=Q^{wk}_{CH_3\ddot{c}H}=\frac{376.56^2}{376.56+715.3}=129.9\left[\frac{kJ}{mol}\right]$	11.8, [40.5-80.1 [82]]

	$D_{iB} = D_{\dot{C}H_2} = 762.3 \left[\frac{kJ}{mol}\right] (see\ above)$ $Q_{0B} = Q^{wk}_{\dot{C}H_2} = \frac{376.56^2}{376.56 + 762.3} = 124.5 \left[\frac{kJ}{mol}\right]$ From (2.6.4.9), (2.6.4.10): $a = \frac{129.9^2 \cdot (129.9 + 2 \cdot 124.5)}{(129.9 + 124.5)^2} = 98.8 \left[\frac{kJ}{mol}\right]$ $b = \frac{124.5^2 \cdot (124.5 + 2 \cdot 129.9)}{(129.9 + 124.5)^2} = 92.0 \left[\frac{kJ}{mol}\right]$ $Q_{AB} = \frac{98.8 \cdot 92.0 \cdot (98.8 + 92.0) + 736.5 \cdot (98.8 - 92.0)^2}{98.8 \cdot 92.0 + 736.5 \cdot (98.8 + 92.0)} = 11.8 \left[\frac{kJ}{mol}\right]$	
$\overset{*}{C}H_3CH=CH_2$	site: on-top; coordination: mono-C $D_{AB} = 3 \cdot \Delta H^0_f(H) + \Delta H^0_f(CH_2 = \dot{C}H) + \Delta H^0_f(C) -$ $- \Delta H^0_f(CH_3CH = CH_2) =$ $= 3 \cdot 218.0 + 299.7 + 716.67 - 20.0 = 1650.4 \left[\frac{kJ}{mol}\right]$ weak binding, (2.6.4.2): $Q_{0A} = Q_{0C} = 376.56 \left[\frac{kJ}{mol}\right]$ $Q_{AB} = \frac{376.56^2}{376.56 + 1650.4} = 70.0 \left[\frac{kJ}{mol}\right]$	70

$CH_3\overset{*}{C}H=\overset{***}{C}H$	site: bridge; coordination: di-C pseudo-atom A = CH_3-C:H; site: on-top; binding: weak pseudo-atom B = C:H; site: hollow; binding: medium $D_{AB}=D_{CH_3CH=(\dot{C}H)}=\Delta H_f^0(CH_3\ddot{C}H)+\Delta H_f^0(CH)-$ $-\Delta H_f^0(CH_3CH=\dot{C}H)=$ $=366.1+597.4-267=696.5\left[\frac{kJ}{mol}\right]$ From (2.6.4.11): $D_{iA}=D_{CH_3\dot{C}H}=715.3\left[\frac{kJ}{mol}\right](see\ above)$ $Q_{0a}=Q_{0b}=Q_{0C}=376.56\left[\frac{kJ}{mol}\right]$ $Q_{0A}=Q_{CH_3\dot{C}H}^{wk}=\frac{376.56^2}{376.56+715.3}=129.9\left[\frac{kJ}{mol}\right]$ $D_{iB}=D_{\dot{C}H}=\Delta_f H^0(H)+\Delta_f H^0(C)-$ $-\Delta_f H^0(CH)=218.0+716.7-597.4=337.3\left[\frac{kJ}{mol}\right]$ $Q_b=Q_C=627.6\left[\frac{kJ}{mol}\right](see\ above)$ $Q_{0B}=Q_{\dot{C}H}^{mdm}=\frac{1}{2}\cdot\left(\frac{376.56^2}{\frac{376.56}{3}+337.3}+\frac{627.6^2}{627.6+337.3}\right)=357.3\left[\frac{kJ}{mol}\right]$ From (2.6.4.9), (2.6.4.10):	202.5

	$a=\frac{129.9^2\cdot(129.9+2\cdot357.3)}{(129.9+357.3)^2}=60.0\left[\frac{kJ}{mol}\right]$ $b=\frac{357.3^2\cdot(357.3+2\cdot129.9)}{(129.9+357.3)^2}=331.9\left[\frac{kJ}{mol}\right]$ $Q_{AB}=\frac{60\cdot331.9\cdot(60+331.9)+696.5\cdot(60-331.9)^2}{60\cdot331.9+696.5\cdot(60+331.9)}=202.5\left[\frac{kJ}{mol}\right]$	
$CH_3CH=\underset{***}{CH}$	site: hollow; coordination: mono-C $D_{AB}=\Delta_f H^0(H)+\Delta_f H^0(CH_3\ddot{C}H)+\Delta_f H^0(C)-$ $-\Delta_f H^0(CH_3CH=\dot{C}H)=$ $=218.0+366.1+716.67-267=1033.8\left[\frac{kJ}{mol}\right]$ medium binding, (2.6.4.5): $Q_{0A}=Q_{0C}=376.56\left[\frac{kJ}{mol}\right]$, $Q_A=Q_C=627.6\left[\frac{kJ}{mol}\right](see\ above)$ $Q_{AB}=\frac{1}{2}\cdot\left(\frac{376.56^2}{\frac{376.56}{3}+1033.8}+\frac{627.6^2}{627.6+1033.8}\right)=179.7\left[\frac{kJ}{mol}\right]$	179.7
$CH_3CH_2\underset{***}{CH}$	site: hollow; coordination: mono-C	289.6, [372.4 [63] site: n=2]

	$D_{AB}=\Delta_f H^0(H)+\Delta_f H^0(CH_3\dot{C}H_2)+\Delta_f H^0(C)-$ $-\Delta_f H^0(CH_3CH_2\ddot{C}H)=$ $=218.0+118.7+716.67-321=732.4\left[\frac{kJ}{mol}\right]$ strong binding, (n = 3) (2.6.4.4): $Q_A=Q_C=627.6\left[\frac{kJ}{mol}\right](see\ above)$ $Q_{AB}=\frac{627.6^2}{627.6+732.4}=289.6\left[\frac{kJ}{mol}\right]$	
$CH_3\underset{*}{C}H_2\underset{***}{C}H$	site: bridge; coordination: di-C pseudo-atom A = CH_3-$\dot{C}H_2$; site: on-top; binding: weak pseudo-atom B = CH; site: hollow; binding: strong $D_{AB}=D_{CH_3CH_2-\ddot{C}H}=\Delta_f H^0(CH_3\dot{C}H_2)+\Delta_f H^0(CH)-$ $-\Delta_f H^0(CH_3CH_2\ddot{C}H)=$ $=118.7+597.4-321=395.1\left[\frac{kJ}{mol}\right]$ From (2.6.4.11): $D_{iA}=D_{CH_3\dot{C}H_2}=1180.7\left[\frac{kJ}{mol}\right](see\ above)$ $Q_{0a}=Q_{0C}=376.56\left[\frac{kJ}{mol}\right]$ $Q_{0A}=Q^{wk}_{CH_3\dot{C}H_2}=91.1\left[\frac{kJ}{mol}\right](see\ above)$	320.0

	$D_{iB} = D_{C\,H} = 337.3\left[\frac{kJ}{mol}\right]\,(see\ above)$ $Q_b = Q_C = 627.6\left[\frac{kJ}{mol}\right]\,(see\ above)$ $Q_{0B} = Q_{C\,H}^{stg} = \frac{627.6^2}{627.6+337.3} = 408.2\left[\frac{kJ}{mol}\right]$ From (2.6.4.9), (2.6.4.10): $a = \frac{91.1^2\cdot(91.1+2\cdot408.2)}{(91.1+408.2)^2} = 30.2\left[\frac{kJ}{mol}\right]$ $b = \frac{408.2^2\cdot(408.2+2\cdot91.1)}{(91.1+408.2)^2} = 394.6\left[\frac{kJ}{mol}\right]$ $Q_{AB} = \frac{30.2\cdot394.6\cdot(30.2+394.6)+395.1\cdot(30.2-394.6)^2}{30.2\cdot394.6+395.1\cdot(30.2+394.6)} = 320.0\left[\frac{kJ}{mol}\right]$	
$CH_3CH_2C_{***}$	Impossible to calculate because of lack $\Delta H_f^0(CH_3CH_2C)$	343.5 [63]
$CH_3C_{*}H_2C_{***}$	Impossible to calculate because of lack $\Delta H_f^0(CH_3CH_2C)$	
$CH_3C_{***}HC_{***}H_2$	site: bridge; coordination: di-C pseudo-atom A = CH_3-C:H; site: hollow; binding: medium pseudo-atom B = C:H_2; site: hollow; binding: medium	52.6, 89.7 [63]

	$D_{AB}=D_{CH_3\dot{C}H-\dot{C}H_2}=\Delta_f H^0(CH_3\ddot{C}H)+\Delta_f H^0(\ddot{C}H_2)-$ $-\Delta_f H^0(CH_3\dot{C}H\dot{C}H_2)=$ $=366.1+390.4-290.4=466.1\left[\frac{kJ}{mol}\right]$ From (2.6.4.11): $D_{iA}=D_{CH_3\dot{\mathbf{C}}H}=715.3\left[\frac{kJ}{mol}\right](see\ above)$ $Q_{0A}=Q^{mdm}_{CH_3\dot{\mathbf{C}}H}=231.0\left[\frac{kJ}{mol}\right](see\ above)$ $D_{iB}=D_{\dot{\mathbf{C}}H_2}=762.3\left[\frac{kJ}{mol}\right](see\ above)$ $Q_{0B}=Q^{mdm}_{\dot{\mathbf{C}}H_2}=221.6\left[\frac{kJ}{mol}\right](see\ above)$ From (2.6.4.9), (2.6.4.10): $a=\frac{231.0^2\cdot(231.0+2\cdot221.6)}{(231.0+221.6)^2}=175.6\left[\frac{kJ}{mol}\right]$ $b=\frac{221.6^2\cdot(221.6+2\cdot231.0)}{(231.0+221.6)^2}=163.9\left[\frac{kJ}{mol}\right]$ $Q_{AB}=\frac{175.6\cdot163.9\cdot(175.6+163.9)+466.1\cdot(175.6-163.9)^2}{175.6\cdot163.9+466.1\cdot(175.6+163.9)}=52.6\left[\frac{kJ}{mol}\right]$	
	site: bridge; coordination: di-C pseudo-atom A = CH_3-C:H; site: hollow; binding: medium	165.8, [298.1

$CH_3\underset{***}{C}H\underset{***}{C}H$	pseudo-atom B = CH; site: hollow; binding: strong $D_{AB}=D_{CH_3\dot{C}H-\ddot{C}H}=\Delta_f H^0(CH_3\ddot{C}H)+\Delta_f H^0(CH)-$ $-\Delta_f H^0(CH_3\dot{C}H\ddot{C}H)=$ $=366.1+597.4-497.4=466.1\left[\frac{kJ}{mol}\right]$ From (2.6.4.11): $D_{iA}=D_{CH_3\check{C}H}=715.3\left[\frac{kJ}{mol}\right](see\ above)$ $Q_{0A}=Q^{mdm}_{CH_3\check{C}H}=231.0\left[\frac{kJ}{mol}\right](see\ above)$ $D_{iB}=D_{\check{C}H}=337.3\left[\frac{kJ}{mol}\right](see\ above)$ $Q_{0B}=Q^{stg}_{\check{C}H}=408.2\left[\frac{kJ}{mol}\right](see\ above)$ From (2.6.4.9), (2.6.4.10): $a=\frac{231.0^2\cdot(231.0+2\cdot408.2)}{(231.0+408.2)^2}=136.8\left[\frac{kJ}{mol}\right]$ $b=\frac{408.2^2\cdot(408.2+2\cdot231.0)}{(231.0+408.2)^2}=354.9\left[\frac{kJ}{mol}\right]$ $Q_{AB}=\frac{136.8\cdot354.9\cdot(136.8+354.9)+466.1\cdot(136.8-354.9)^2}{136.8\cdot354.9+466.1\cdot(136.8+354.9)}=165.8\left[\frac{kJ}{mol}\right]$	[63] A: on-top, B: n=2]

$CH_3\underset{******}{C}\,C\,H_2$	Impossible to calculate because of lack $\Delta H_f^0(CH_3C)$	[275.9 [63] A: n=2, B:on-top]
$CH_3\underset{******}{C}\,C\,H$	Impossible to calculate because of lack $\Delta H_f^0(CH_3C)$	201.7 [63] A: n=2, B: n=2]
$CH_3\underset{***}{C}\,H\,\underset{***}{C}$	Impossible to calculate because of lack $\Delta H_f^0(CH_3CHC)$	218.1 [63] A: on-top B: hollow
$CH_3\underset{******}{C}\,C$	Impossible to calculate because of lack $\Delta H_f^0(CH_3CC)$	446.7 [63] A: n=2, B: hollow
$\underset{*}{H}-\underset{*}{H}$	site: bridge; coordination: di-H (every H ontop) ([51], p. 510; [43], p.32-33) $D_{AB}=\Delta H_f^0(H)+\Delta H_f^0(H)-\Delta H_f^0(H_2)$ $=218.0+218.0-0=436\left[\frac{kJ}{mol}\right]$ $Q_{0A}=Q_{0H}=153.1\left[\frac{kJ}{mol}\right]$ From (2.6.4.3): $Q_{A_2}=\frac{9\cdot 153.1^2}{6\cdot 153.1+16\cdot 436}=26.7\left[\frac{kJ}{mol}\right]$	26.7, 26.8 [64], 26.8 [51]
$\underset{***}{H}$	site: hollow; coordination: mono-H	255.2, 255 [64],

	$Q_{0A}=Q_{0H}=153.1\left[\frac{kJ}{mol}\right]$ From (2.6.4.1) (n=3): $Q_A=Q_H=153.1\cdot\left(2-\frac{1}{3}\right)=255.2\left[\frac{kJ}{mol}\right]$	263.4 [63], 278 [57]
$\underset{*}{O}-\underset{*}{O}$	site: bridge; coordination: di-O (every O on-top) ([43], p. 54) $D_{AB}=\Delta H_f^0(O)+\Delta H_f^0(O)-\Delta H_f^0(O_2)$ $=249.2+249.2-0=498.4\left[\frac{kJ}{mol}\right]$ $Q_{0A}=Q_{0O}=213.4\left[\frac{kJ}{mol}\right]$ From (2.6.4.3): $Q_{A_2}=\frac{9\cdot 213.4^2}{6\cdot 213.4+16\cdot 498.4}=44.3\left[\frac{kJ}{mol}\right]$	44.3, 44.3 [64]
$\underset{***}{O}$	site: hollow; coordination: mono-O $Q_{0A}=Q_{0O}=213.4\left[\frac{kJ}{mol}\right]$ From (2.6.4.1): $Q_A=Q_O=213.4\cdot\left(2-\frac{1}{3}\right)=355.7\left[\frac{kJ}{mol}\right]$	355.7, 356 [64]
$\underset{***}{OH}$	site: hollow; coordination: mono-O ([83]; [43], p. 54)	161.1, [247 [64] adj. exp.],

	$D_{AB}=\Delta H_f^0(H)+\Delta H_f^0(O)-\Delta H_f^0(OH)$ $=218.0+249.2-37.3=429.9\left[\frac{kJ}{mol}\right]$ $Q_A=Q_O=355.7\left[\frac{kJ}{mol}\right](see\ above)$ strong binding, (2.6.4.4): $Q_{AB}=\frac{355.7^2}{355.7+429.9}=161.1\left[\frac{kJ}{mol}\right]$	161.5 [51]
H_2O *	site: on-top; coordination: mono-O ([83]; [43], pp. 38, 54) $D_{AB}=D_{H_2O}=2\cdot\Delta H_f^0(H)+\Delta H_f^0(O)-\Delta H_f^0(H_2O)$ $=2\cdot 218.0+249.2+241.8=927\left[\frac{kJ}{mol}\right]$ weak binding, (2.6.4.2): $Q_{0A}=Q_{0O}=213.4\left[\frac{kJ}{mol}\right]$ $Q_{AB}=\frac{213.4^2}{213.4+927}=39.9\left[\frac{kJ}{mol}\right]$	39.9, 40.2 [64], 40.1 [51]
C ***	site: hollow; coordination: mono-C ([43], p. 31) $Q_A=Q_C=627.6\left[\frac{kJ}{mol}\right](see\ above)$	627.6, [623-653 [82]], 687.9 [63], 628 [64], 692 [57]
	site: hollow, coordination: mono-C ([48], p.171)	408.2,

$C\,H$ ***	$D_{AB}=D_{\mathbf{C}\,H}=337.3\left[\frac{kJ}{mol}\right](see\ above)$ strong binding $Q_{AB}=Q^{stg}_{\mathbf{C}\,H}=408.2\left[\frac{kJ}{mol}\right](see\ above)$	642.6 [63], 407 [64], 646 [57]
$C\,H_2$ ***	site: hollow, coordination: mono-C ([48], p.171) $D_{AB}=D_{\ddot{\mathbf{C}}\,H_2}=762.3\left[\frac{kJ}{mol}\right](see\ above)$ strong binding, (2.6.4.4): $Q_A=Q_C=627.6\left[\frac{kJ}{mol}\right](see\ above)$ $Q_{AB}=Q^{stg}_{\ddot{\mathbf{C}}\,H_2}=\frac{627.6^2}{627.6+762.3}=283.4\left[\frac{kJ}{mol}\right]$	283.4, [391.7 [63] site: n=2], 283 [64], 445 [57]
$C\,H_3$ ***	site: hollow, coordination: mono-C ([43], p. 38) $D_{AB}=D_{\dot{\mathbf{C}}\,H_3}=1224.0\left[\frac{kJ}{mol}\right](see\ above)$ medium binding, (2.6.4.5): $Q_{0A}=Q_{0C}=376.56\left[\frac{kJ}{mol}\right]$,	158.9, [192.0 [63] on-top], 159 [64], 220 [57]

	$Q_A = Q_C = 627.6\left[\frac{kJ}{mol}\right] (see\ above)$ $Q_{AB} = Q_{\dot{C}H_3}^{mdm} = \frac{1}{2}\cdot\left(\frac{376.56^2}{\frac{376.56}{3}+1223.9} + \frac{627.6^2}{627.6+1223.9}\right) = 158.9\left[\frac{kJ}{mol}\right]$	
$\underset{*}{C}H_4$	site: on-top; coordination: mono-C $D_{AB} = 4\cdot\Delta_f H^0(H) + \Delta_f H^0(C) - \Delta_f H^0(CH_4) =$ $= 4\cdot 218.0 + 716.67 - (-74.6) = 1663.3\left[\frac{kJ}{mol}\right]$ weak binding, (2.6.4.2): $Q_{0A} = Q_{0C} = 376.56\left[\frac{kJ}{mol}\right]$ $Q_{AB} = \frac{376.56^2}{376.56+1663.3} = 69.5\left[\frac{kJ}{mol}\right]$	69.5, [25.1 [64] adj. exp.]
$\underset{*}{C}H_3CH_3$	site: on-top; coordination: mono-C $D_{AB} = 3\cdot\Delta_f H^0(H) + \Delta_f H^0(C) + \Delta_f H^0(\dot{C}H_3) -$ $-\Delta_f H^0(CH_3CH_3) = 3\cdot 218.0 + 716.67 + 146.7 - (-83.9) =$ $= 1601.3\left[\frac{kJ}{mol}\right]$ weak binding, (2.6.4.2): $Q_{0A} = Q_{0C} = 376.56\left[\frac{kJ}{mol}\right]$	71.7

	$Q_{AB}=\frac{376.56^2}{376.56+1601.3}=71.7\left[\frac{kJ}{mol}\right]$	
$\overset{*}{C}H_3\overset{*}{C}H_3$	site: bridge; coordination: di-C pseudo-atoms A = B = $\dot{C}H_3$; site: on-top; binding: weak $D_{AB}=D_{CH_3-CH_3}=2\cdot\Delta_f H^0(\dot{C}H_3)-\Delta_f H^0(CH_3CH_3)=$ $=2\cdot 146.7-(-83.9)=377.3\left[\frac{kJ}{mol}\right]$ From (2.6.4.11): $D_{iA}=D_{iB}=D_{\dot{C}H_3}=1224.0\left[\frac{kJ}{mol}\right](see\ above)$ $Q_{0A}=Q_{0B}=Q^{wk}_{\dot{C}H_3}=88.6\left[\frac{kJ}{mol}\right](see\ above)$ From (2.6.4.3): $Q_{A_2}=\frac{9\cdot 88.6^2}{6\cdot 88.6+16\cdot 377.3}=10.8\left[\frac{kJ}{mol}\right]$ weak? $Q_{A_2}=\frac{9\cdot 158.9^2}{6\cdot 158.9+16\cdot 377.3}=32.5\left[\frac{kJ}{mol}\right]$ medium?	10.8, [36.1 [64] A: n=2]
$CH_3\overset{***}{C}H_2$	site: hollow; coordination: mono-C ([48], p.182) $D_{AB}=D_{CH_3\dot{C}H_2}=1180.7\left[\frac{kJ}{mol}\right](see\ above)$ medium binding, (2.6.4.5):	163.2, [177.5 [63] on-top], 163 [64], 243 [57]

	$Q_{0A}=Q_{0C}=376.56\left[\frac{kJ}{mol}\right]$, $Q_{A}=Q_{C}=627.6\left[\frac{kJ}{mol}\right](see\ above)$ $Q_{AB}=Q^{mdm}_{CH_3\dot{C}H_2}=\frac{1}{2}\cdot\left(\frac{376.56^2}{\frac{376.56}{3}+1180.7}+\frac{627.6^2}{627.6+1180.7}\right)=163.2\left[\frac{kJ}{mol}\right]$	
$\overset{*}{C}H_3\overset{***}{C}H_2$	site: bridge; coordination: di-C pseudo-atom A = $\dot{C}H_3$; site: on-top; binding: weak pseudo-atom B = C:H_2; site: hollow; binding: medium $D_{AB}=D_{CH_3-\dot{C}H_2}=\Delta_f H^0(\dot{C}H_3)+\Delta_f H^0(\ddot{C}H_2)-$ $-\Delta_f H^0(CH_3\dot{C}H_2)=146.7+390.4-118.7=418.4\left[\frac{kJ}{mol}\right]$ From (2.6.4.11): $D_{iA}=D_{\dot{C}H_3}=1224.0\left[\frac{kJ}{mol}\right](see\ above)$ $Q_{0A}=Q^{wk}_{\dot{C}H_3}=88.6\left[\frac{kJ}{mol}\right](see\ above)$ $D_{iB}=D_{\dot{C}H_2}=762.3\left[\frac{kJ}{mol}\right](see\ above)$	115.1

	$Q_{0B} = Q^{mdm}_{\dot{C}H_2} = 221.6 \left[\frac{kJ}{mol}\right] (see\ above)$ From (2.6.4.9), (2.6.4.10): $a = \frac{88.6^2 \cdot (88.6 + 2 \cdot 221.6)}{(88.6 + 221.6)^2} = 43.4 \left[\frac{kJ}{mol}\right]$ $b = \frac{221.6^2 \cdot (221.6 + 2 \cdot 88.6)}{(88.6 + 221.6)^2} = 203.5 \left[\frac{kJ}{mol}\right]$ $Q_{AB} = \frac{43.4 \cdot 203.5 \cdot (43.4 + 203.5) + 418.4 \cdot (43.4 - 203.5)^2}{43.4 \cdot 203.5 + 418.4 \cdot (43.4 + 203.5)} = 115.1 \left[\frac{kJ}{mol}\right]$	
$CH_3\underset{***}{C}H$	site: hollow; coordination: mono-C $D_{AB} = D_{CH_3\dot{C}H} = 715.3 \left[\frac{kJ}{mol}\right] (see\ above)$ strong binding, (2.6.4.4): $Q_A = Q_C = 627.6 \left[\frac{kJ}{mol}\right] (see\ above)$ $Q_{AB} = Q^{stg}_{CH_3\dot{C}H} = \frac{627.6^2}{627.6 + 715.3} = 293.3 \left[\frac{kJ}{mol}\right]$	293.3, [368.6 [63] site: n=2], [294 [64] site: n=2]
$\underset{*}{C}H_3\underset{***}{C}H$	site: bridge; coordination: di-C pseudo-atom A = $\dot{C}H_3$; site: on-top; binding: weak pseudo-atom B = CH; site: hollow; binding: strong	323.7

	$D_{AB}=D_{CH_3-\ddot{C}H}=\Delta_f H^0(\dot{C}H_3)+\Delta_f H^0(CH)-$ $-\Delta_f H^0(CH_3\ddot{C}H)=146.7+597.4-366.1=378.0\left[\frac{kJ}{mol}\right]$ From (2.6.4.11): $D_{iA}=D_{\dot{C}H_3}=1224.0\left[\frac{kJ}{mol}\right](see\ above)$ $Q_{0A}=Q^{wk}_{\dot{C}H_3}=88.6\left[\frac{kJ}{mol}\right](see\ above)$ $D_{iB}=D_{CH}=337.3\left[\frac{kJ}{mol}\right](see\ above)$ $Q_{0B}=Q^{stg}_{CH}=408.2\left[\frac{kJ}{mol}\right](see\ above)$ From (2.6.4.9), (2.6.4.10): $a=\frac{88.6^2\cdot(88.6+2\cdot408.2)}{(88.6+408.2)^2}=28.8\left[\frac{kJ}{mol}\right]$ $b=\frac{408.2^2\cdot(408.2+2\cdot88.6)}{(88.6+408.2)^2}=395.2\left[\frac{kJ}{mol}\right]$ $Q_{AB}=\frac{28.8\cdot395.2\cdot(28.8+395.2)+378.0\cdot(28.8-395.2)^2}{28.8\cdot395.2+378.0\cdot(28.8+395.2)}=323.7\left[\frac{kJ}{mol}\right]$	
CH_3C_{***}	Impossible to calculate because of lack $\Delta H_f^0(CH_3C)$	563.6 [57], 571.2

		[63], [405 [64] hollow]
$\overset{*}{C}H_3\overset{***}{C}$	Impossible to calculate because of lack $\Delta H_f^0(CH_3C)$	
$\overset{***}{C}H_2\overset{***}{C}H_2$	site: bridge; coordination: di-C pseudo-atoms A = B = C:H$_2$; site: hollow; binding: medium $D_{AB}=D_{\dot{C}H_2-\dot{C}H_2}=2\cdot\Delta_f H^0(\ddot{C}H_2)-\Delta_f H^0(\dot{C}H_2\dot{C}H_2)=$ $=2\cdot390.4-321.4=459.4\left[\frac{kJ}{mol}\right]$ $D_{iA}=D_{iB}=D_{\dot{\mathbf{C}}H_2}=762.3\left[\frac{kJ}{mol}\right](see\ above)$ $Q_{0A}=Q_{0B}=Q^{mdm}_{\dot{\mathbf{C}}H_2}=221.6\left[\frac{kJ}{mol}\right](see\ above)$ From (2.6.4.3): $Q_{A_2}=\frac{9\cdot221.6^2}{6\cdot221.6+16\cdot459.4}=50.9\left[\frac{kJ}{mol}\right]$	50.9, [46.1 [64] A: n=2]
$\overset{***}{C}H_2\overset{***}{C}H$	site: bridge; coordination: di-C pseudo-atom A = C:H$_2$; site: hollow; binding: medium pseudo-atom B = CH; site: hollow; binding: strong $D_{AB}=D_{\dot{C}H_2-\ddot{C}H}=\Delta_f H^0(\ddot{C}H_2)+\Delta_f H^0(CH)-$ $-\Delta_f H^0(\dot{C}H_2\ddot{C}H)=390.4+597.4-532.3=455.5\left[\frac{kJ}{mol}\right]$ From (2.6.4.11):	173.0, [129 [64] adj. exp.], 346 [57]

	$D_{iA} = D_{\ddot{C}H_2} = 762.3\left[\frac{kJ}{mol}\right](see\ above)$ $Q_{0A} = Q^{mdm}_{\ddot{C}H_2} = 221.6\left[\frac{kJ}{mol}\right](see\ above)$ $D_{iB} = D_{CH} = 337.3\left[\frac{kJ}{mol}\right](see\ above)$ $Q_{0B} = Q^{stg}_{CH} = 408.2\left[\frac{kJ}{mol}\right](see\ above)$ From (2.6.4.9), (2.6.4.10): $a = \frac{221.6^2 \cdot (221.6 + 2 \cdot 408.2)}{(221.6 + 408.2)^2} = 128.5\left[\frac{kJ}{mol}\right]$ $b = \frac{408.2^2 \cdot (408.2 + 2 \cdot 221.6)}{(221.6 + 408.2)^2} = 357.7\left[\frac{kJ}{mol}\right]$ $Q_{AB} = \frac{128.5 \cdot 357.7 \cdot (128.5 + 357.7) + 455.5 \cdot (128.5 - 357.7)^2}{128.5 \cdot 357.7 + 455.5 \cdot (128.5 + 357.7)} = 173.0\left[\frac{kJ}{mol}\right]$	
$C\ H\ C\ H$ *** ***	site: bridge; coordination: di-C pseudo-atoms A = B = CH; site: hollow; binding: strong $D_{AB} = D_{\ddot{C}H-\ddot{C}H} = 2 \cdot \Delta_f H^0(CH) - \Delta_f H^0(\ddot{C}H\ddot{C}H) =$ $= 2 \cdot 597.4 - 767.6 = 427.2\left[\frac{kJ}{mol}\right]$	161.5, [134 [64] adj. exp.]

	$D_{iA} = D_{iB} = D_{C\,H} = 337.3 \left[\frac{kJ}{mol}\right] (see\ above)$ $Q_{0A} = Q_{0B} = Q_{C\,H}^{stg} = 408.2 \left[\frac{kJ}{mol}\right] (see\ above)$ From (2.6.4.3): $Q_{A_2} = \frac{9 \cdot 408.2^2}{6 \cdot 408.2 + 16 \cdot 427.2} = 161.5 \left[\frac{kJ}{mol}\right]$	
$\underset{***}{C}\,H_2\,\underset{***}{C}$	Impossible to calculate because of lack $\Delta H_f^0(CH_2C)$	
$\underset{***}{C}\,H\,\underset{***}{C}$	Uncertain specie	
$\underset{*}{C}\,H \equiv \underset{*}{C}\,H$	site: bridge; coordination: di-C pseudo-atoms A = B = CH; site: on-top; binding: weak $D_{AB} = D_{C\,H \equiv C\,H} = 2 \cdot \Delta_f H^0(CH) - \Delta_f H^0(C\,H \equiv C\,H) =$ $= 2 \cdot 597.4 - 228.2 = 966.6 \left[\frac{kJ}{mol}\right]$ $D_{iA} = D_{iB} = D_{C\,H} = 337.3 \left[\frac{kJ}{mol}\right] (see\ above)$ $Q_{0A} = Q_{0B} = Q_{C\,H}^{wk} = \frac{376.56^2}{376.56 + 337.3} = 198.6 \left[\frac{kJ}{mol}\right]$ From (2.6.4.3):	21.3, 95 [64]

	$Q_{A_2}=\frac{9\cdot 198.6^2}{6\cdot 198.6+16\cdot 966.6}=21.3\left[\frac{kJ}{mol}\right]$	
$CH\equiv \underset{***}{C}$	site: hollow; coordination: mono-C $D_{AB}=D_{CH\equiv\dot{C}}=\Delta_f H^0(CH)+\Delta_f H^0(C)-\Delta_f H^0(CH\equiv\dot{C})=$ $=597.4+716.7-566.2=747.9\left[\frac{kJ}{mol}\right]$ medium binding, (2.6.4.5): $Q_{0A}=Q_{0C}=376.56\left[\frac{kJ}{mol}\right]$, $Q_A=Q_C=627.6\left[\frac{kJ}{mol}\right](see\ above)$ $Q_{AB}=Q_{CH\equiv\dot{C}}=\frac{1}{2}\cdot\left(\frac{376.56^2}{\frac{376.56}{3}+747.9}+\frac{627.6^2}{627.6+747.9}\right)=224.4\left[\frac{kJ}{mol}\right]$	224.4, [287 [64] on-top]
$\underset{*}{C}\,H\equiv \underset{***}{C}$	site: bridge; coordination: di-C pseudo-atom A = CH; site: on-top; binding: weak pseudo-atom B = C; site: hollow; binding: medium $D_{AB}=D_{CH\equiv\dot{C}}=747.9\left[\frac{kJ}{mol}\right](see\ above)$ From (2.6.4.11): $D_{iA}=D_{\mathbf{C}H}=337.3\left[\frac{kJ}{mol}\right](see\ above)$	422.0

	$Q_{0a}=Q_{0C}=376.56\left[\frac{kJ}{mol}\right]$ $Q_{0A}=Q_{C\,H}^{wk}=198.6\left[\frac{kJ}{mol}\right](see\ above)$ $Q_b=Q_C=627.6\left[\frac{kJ}{mol}\right](see\ above)$ $Q_{0B}=Q_C=627.6\left[\frac{kJ}{mol}\right](see\ above)$ From (2.6.4.9), (2.6.4.10): $a=\frac{198.6^2\cdot(198.6+2\cdot627.6)}{(198.6+627.6)^2}=84.0\left[\frac{kJ}{mol}\right]$ $b=\frac{627.6^2\cdot(627.6+2\cdot198.6)}{(198.6+627.6)^2}=591.3\left[\frac{kJ}{mol}\right]$ $Q_{AB}=\frac{84.0\cdot591.3\cdot(84.0+591.3)+455.5\cdot(84.0-591.3)^2}{84.0\cdot591.3+455.5\cdot(84.0+591.3)}=422.0\left[\frac{kJ}{mol}\right]$	
$C\equiv C$ *** ***	site: bridge; coordination: di-C pseudo-atoms A = B = C; site: hollow; binding: medium $D_{AB}=D_{\dot{C}\equiv\dot{C}}=2\cdot\Delta_f H^0(C)-\Delta_f H^0(\dot{C}\equiv\dot{C})=$ $=2\cdot716.7-830.5=602.9\left[\frac{kJ}{mol}\right]$	264.3

	$Q_{0A}=Q_{0B}=Q_C=627.6\left[\frac{kJ}{mol}\right](see\ above)$ From (2.6.4.3): $Q_{A_2}=\frac{9\cdot 627.6^2}{6\cdot 627.6+16\cdot 602.9}=264.3\left[\frac{kJ}{mol}\right]$	
$\overset{*}{C}H_2=\overset{*}{C}H_2$	site: bridge; coordination: di-C pseudo-atoms A = B = C:H_2; site: on-top; binding: weak $D_{AB}=D_{CH_2=CH_2}=2\cdot\Delta_f H^0(\ddot{C}H_2)-\Delta_f H^0(CH_2=CH_2)=$ $=2\cdot 390.4-52.5=728.3\left[\frac{kJ}{mol}\right]$ $D_{iA}=D_{iB}=D_{\dot{C}H_2}=762.3\left[\frac{kJ}{mol}\right](see\ above)$ $Q_{0A}=Q_{0B}=Q^{wk}_{\dot{C}H_2}=124.5\left[\frac{kJ}{mol}\right](see\ above)$ From (2.6.4.3): $Q_{A_2}=\frac{9\cdot 124.5^2}{6\cdot 124.5+16\cdot 728.3}=11.3\left[\frac{kJ}{mol}\right]$ weak $Q_{A_2}=\frac{9\cdot 221.6^2}{6\cdot 221.6+16\cdot 728.3}=34.0\left[\frac{kJ}{mol}\right]$ medium	11.3, [29.3 [64] on-top]
$\overset{*}{C}H_2=CH_2$	site: on-top; coordination: mono-C	75.9

	$D_{AB}=D_{\mathbf{C}H_2=CH_2}=2\cdot\Delta_f H^0(H)+\Delta_f H^0(\ddot{C}H_2)+\Delta_f H^0(C)-$ $-\Delta_f H^0(CH_2=CH_2)=2\cdot 218.0+390.4+716.7-52.5=$ $=1490.6\left[\frac{kJ}{mol}\right]$ weak binding, (2.6.4.2): $Q_{0A}=Q_{0C}=376.56\left[\frac{kJ}{mol}\right]$ $Q_{AB}=\frac{376.56^2}{376.56+1490.6}=75.9\left[\frac{kJ}{mol}\right]$	
$CH_2=\underset{***}{C}H$	site: hollow; coordination: mono-C $D_{AB}=D_{CH_2=\dot{C}H}=\Delta_f H^0(H)+\Delta_f H^0(\ddot{C}H_2)+\Delta_f H^0(C)-$ $-\Delta_f H^0(CH_2=\dot{C}H)=218.0+390.4+716.7-299.7=$ $=1025.4\left[\frac{kJ}{mol}\right]$ medium binding, (2.6.4.5): $Q_{0A}=Q_{0C}=376.56\left[\frac{kJ}{mol}\right]$, $Q_A=Q_C=627.6\left[\frac{kJ}{mol}\right](see\ above)$ $Q_{AB}=Q_{CH_2=\dot{C}H}=\frac{1}{2}\cdot\left(\frac{376.56^2}{\frac{376.56}{3}+1025.4}+\frac{627.6^2}{627.6+1025.4}\right)=180.7\left[\frac{kJ}{mol}\right]$	180.7, [184 [64] on-top]

$\overset{*}{C}H_2=\overset{***}{C}H$	site: bridge; coordination: di-C pseudo-atom A = C:H$_2$; site: on-top; binding: weak pseudo-atom B = CH; site: hollow; binding: medium $D_{AB}=D_{CH_2=\dot{C}H}=\Delta_f H^0(\ddot{C}H_2)+\Delta_f H^0(CH)-$ $-\Delta_f H^0(CH_2=\dot{C}H)=390.4+597.4-299.7=688.1\left[\frac{kJ}{mol}\right]$ From (2.6.4.11): $D_{iA}=D_{\dot{\mathbf{C}}H_2}=762.3\left[\frac{kJ}{mol}\right](see\ above)$ $Q_{0A}=Q^{wk}_{\dot{\mathbf{C}}H_2}=124.5\left[\frac{kJ}{mol}\right](see\ above)$ $D_{iB}=D_{\mathbf{C}H}=337.3\left[\frac{kJ}{mol}\right](see\ above)$ $Q_{0B}=Q^{mdm}_{\mathbf{C}H}=357.3\left[\frac{kJ}{mol}\right](see\ above)$ From (2.6.4.9), (2.6.4.10): $a=\frac{124.5^2\cdot(124.5+2\cdot357.3)}{(124.5+357.3)^2}=56.0\left[\frac{kJ}{mol}\right]$ $b=\frac{357.3^2\cdot(357.3+2\cdot124.5)}{(124.5+357.3)^2}=333.4\left[\frac{kJ}{mol}\right]$	210.1

	$Q_{AB}=\frac{56\cdot 333.4\cdot(56+333.4)+688.1\cdot(56-333.4)^2}{56\cdot 333.4+688.1\cdot(56+333.4)}=210.1\left[\frac{kJ}{mol}\right]$	
$CH_2{=}\underset{***}{C}$	site: hollow; coordination: mono-C $D_{AB}=D_{CH_2=\dot{\underset{\cdot}{C}}}=\Delta_f H^0(\ddot{C}H_2)+\Delta_f H^0(C)-$ $-\Delta_f H^0(CH_2=\dot{C})=390.4+716.7-414.8=692.3\left[\frac{kJ}{mol}\right]$ strong binding, (2.6.4.4): $Q_A=Q_C=627.6\left[\frac{kJ}{mol}\right](see\ above)$ $Q_{AB}=Q_{CH_2=\dot{\underset{\cdot}{C}}}=\frac{627.6^2}{627.6+693.3}=298.1\left[\frac{kJ}{mol}\right]$	298.1, [299 [64] n=2], 448 [57]
$\underset{*}{C}H_2{=}\underset{***}{C}$	site: bridge; coordination: di-C pseudo-atom A = C:H_2; site: on-top; binding: weak pseudo-atom B = C; site: hollow; binding: strong $D_{AB}=D_{CH_2=\ddot{C}}=\Delta_f H^0(\ddot{C}H_2)+\Delta_f H^0(C)-$ $-\Delta_f H^0(CH_2=\ddot{C})=390.4+716.7-414.8=692.3\left[\frac{kJ}{mol}\right]$ From (2.6.4.11): $D_{iA}=D_{\dot{\underset{\cdot}{C}}H_2}=762.3\left[\frac{kJ}{mol}\right](see\ above)$ $Q_{0A}=Q^{wk}_{\dot{\underset{\cdot}{C}}H_2}=124.5\left[\frac{kJ}{mol}\right](see\ above)$	512.8

	$Q_{0B}=Q_C=627.6\left[\frac{kJ}{mol}\right](see\ above)$ From (2.6.4.9), (2.6.4.10): $a=\frac{124.5^2\cdot(124.5+2\cdot627.6)}{(124.5+627.6)^2}=37.8\left[\frac{kJ}{mol}\right]$ $b=\frac{627.6^2\cdot(627.6+2\cdot124.5)}{(124.5+627.6)^2}=610.4\left[\frac{kJ}{mol}\right]$ $Q_{AB}=\frac{37.8\cdot610.4\cdot(37.8+610.4)+692.3\cdot(37.8-610.4)^2}{37.8\cdot610.4+692.3\cdot(37.8+610.4)}=512.8\left[\frac{kJ}{mol}\right]$	
$\underset{*}{C}O$	site: on-top; coordination: mono-C ([43], pp. 31,54) $D_{AB}=\Delta H_f^0(C)+\Delta H_f^0(O)-\Delta H_f^0(CO)$ $=716.7+249.2-(-110.5)=1076.4\left[\frac{kJ}{mol}\right]$ weak binding, (2.6.4.2) $Q_{0A}=Q_{0C}=376.56\left[\frac{kJ}{mol}\right]$ $Q_{AB}=\frac{376.56^2}{376.56+1076.4}=97.6\left[\frac{kJ}{mol}\right]$	97.6, [134 [64] site: n=2; adj. exp.], [133.8 [51] adj. exp.]
$\underset{*}{O}=C=\underset{*}{O}$	Following the calculation procedure from [51]: The $\underset{*}{O}=C=\underset{*}{O}$ fragment is replaced by the $\underset{*}{O}\cdots\underset{*}{O}$ fragment.	15.2, [15.1 [64] site: n=2]

	$D_{AB}=\Delta H_f^0(C)+2\cdot\Delta H_f^0(O)-\Delta H_f^0(CO_2)$ $=716.7+2\cdot249.2-(-393.5)=1608.6\left[\frac{kJ}{mol}\right]$ site: bridge; coordination: di-O (every O on-top), (2.6.4.3): $Q_{0A}=Q_{0O}=213.4\left[\frac{kJ}{mol}\right]$ $Q_{A2}=\frac{9\cdot213.4^2}{6\cdot213.4+16\cdot1608.6}=15.2\left[\frac{kJ}{mol}\right]$	
CH_3O_{***}	site: hollow; coordination: mono-O ([43], p.38) $D_{AB}=\Delta H_f^0(O)+\Delta H_f^0(\dot{C}H_3)-\Delta H_f^0(CH_3\dot{O})$ $=249.2+146.7-13.0=382.9\left[\frac{kJ}{mol}\right]$ strong binding, (2.6.4.4): $Q_A=Q_O=355.7\left[\frac{kJ}{mol}\right](see\ above)$ $Q_{AB}=\frac{355.7^2}{355.7+382.9}=171.3\left[\frac{kJ}{mol}\right]$	171.3, [173 [64] on-top]
$C_{***}H_2O_{***}$	site: bridge; coordination: C, O pseudo-atom A = C:H_2; site: on-top; binding: medium pseudo-atom B = O; site: hollow; binding: strong $D_{AB}=D_{\dot{C}H_2-\dot{O}}=\Delta_f H^0(\ddot{C}H_2)+\Delta_f H^0(O)$- $-\Delta_f H^0(\dot{C}H_2\dot{O})=390.4+249.2-188.7=450.9\left[\frac{kJ}{mol}\right]$	128.0

	From (2.6.4.11): $D_{iA} = D_{\dot{C}H_2} = 762.3\left[\frac{kJ}{mol}\right](see\ above)$ $Q_{0A} = Q^{mdm}_{\dot{C}H_2} = 221.6\left[\frac{kJ}{mol}\right](see\ above)$ $Q_{0B} = Q_O = 355.7\left[\frac{kJ}{mol}\right](see\ above)$ From (2.6.4.9), (2.6.4.10): $a = \frac{221.6^2 \cdot (221.6 + 2 \cdot 355.7)}{(221.6 + 355.7)^2} = 137.5\left[\frac{kJ}{mol}\right]$ $b = \frac{355.7^2 \cdot (355.7 + 2 \cdot 221.6)}{(221.6 + 355.7)^2} = 303.3\left[\frac{kJ}{mol}\right]$ $Q_{AB} = \frac{137.5 \cdot 303.3 \cdot (137.5 + 303.3) + 450.9 \cdot (137.5 - 303.3)^2}{137.5 \cdot 303.3 + 450.9 \cdot (137.5 + 303.3)} = 128.0\left[\frac{kJ}{mol}\right]$	
$H\overset{***}{C}=O$	site: hollow; coordination: mono-C $D_{AB} = D_{H\dot{C}=O} = \Delta_f H^0(H) + \Delta_f H^0(\ddot{O}) + \Delta_f H^0(C)$- $-\Delta_f H^0(H\dot{C}=O) = 218.0 + 249.2 + 716.7 - 42.4 = 1141.5\left[\frac{kJ}{mol}\right]$ medium binding, (2.6.4.5): $Q_{0A} = Q_{0C} = 376.56\left[\frac{kJ}{mol}\right]$,	167.3 [167 [64] on-top]

	$Q_A = Q_C = 627.6\left[\frac{kJ}{mol}\right] (see\ above)$ $Q_{AB} = Q_{H\dot{C}=O} = \frac{1}{2}\cdot\left(\frac{376.56^2}{\frac{376.56}{3}+1141.5} + \frac{627.6^2}{627.6+1141.5}\right) = 167.3\left[\frac{kJ}{mol}\right]$	
$\underset{***}{C H_2 OH}$	site: hollow; coordination: mono-C $D_{AB} = D_{\dot{C}H_2OH} = 2\cdot\Delta_f H^0(H) + \Delta_f H^0(\dot{O}H) + \Delta_f H^0(C) -$ $-\Delta_f H^0(\dot{C}H_2OH) = 2\cdot 218.0 + 37.3 + 716.7 - (-17.0) = 1207\left[\frac{kJ}{mol}\right]$ medium binding, (2.6.4.5): $Q_{0A} = Q_{0C} = 376.56\left[\frac{kJ}{mol}\right]$, $Q_A = Q_C = 627.6\left[\frac{kJ}{mol}\right] (see\ above)$ $Q_{AB} = Q_{\dot{C}H_2OH} = \frac{1}{2}\cdot\left(\frac{376.56^2}{\frac{376.56}{3}+1207} + \frac{627.6^2}{627.6+1207}\right) = 160.6\left[\frac{kJ}{mol}\right]$	160.6 [160 [64] on-top]
$\underset{***}{H C OH}$	Impossible to calculate because of lack ΔH_f^0(HC:OH)	[200 [64] n=2]
$\underset{***}{HC(O)O}$	site: hollow; coordination: mono-O $D_{AB} = D_{HC(O)\dot{O}} = \Delta H_f^0(O) + \Delta H_f^0(H\dot{C}(O)) -$ $-\Delta H_f^0(HC(O)\dot{O}) = 249.2 + 42.4 - (-129.7) = 421.3\left[\frac{kJ}{mol}\right]$ strong binding, (2.6.4.4):	162.8, 180.7 [51]

	$Q_A = Q_O = 355.7\left[\frac{kJ}{mol}\right] (see\ above)$ $Q_{AB} = \frac{355.7^2}{355.7+421.3} = 162.8\left[\frac{kJ}{mol}\right]$	
$\overset{***}{C(O)OH}$	site: hollow; coordination: mono-C $D_{AB} = D_{\dot{C}(O)OH} = \Delta H_f^0(O) + \Delta H_f^0(C) + \Delta H_f^0(\dot{O}H) -$ $- \Delta H_f^0(\dot{C}(O)OH) = 249.2 + 716.7 + 37.3 - (-213.0) = 1216.2\left[\frac{kJ}{mol}\right]$ medium binding, (2.6.4.5): $Q_{0A} = Q_{0C} = 376.56\left[\frac{kJ}{mol}\right]$, $Q_A = Q_C = 627.6\left[\frac{kJ}{mol}\right] (see\ above)$ $Q_{AB} = Q_{\dot{C}(O)OH} = \frac{1}{2}\cdot\left(\frac{376.56^2}{\frac{376.56}{3}+1216.2} + \frac{627.6^2}{627.6+1216.2}\right) = 159.7\left[\frac{kJ}{mol}\right]$	159.7, [213 [64] on-top]

Adsorption heats can be different for a similar species for the bridge adsorbtion sites - Q^{wk} - weak binding, Q^{mdm} - medium binding Q^{stg} - strong binding (see explanation in a text). In the second column references to the literature where the same configuration of adsorbates is used are given in parentheses. In the third column the calculated values of heats of adsorption are given, as well as values from literature with references and notes on peculiars of adsorbate form used in the literature.

8.2.4 ELEMENTARY REACTIONS AND ACTIVATION BARRIERS

Table 8.2.4.1: Activation barriers for surface reactions, calculations are made using (2.6.4.12)-(3.1.2.2), with Q_{AB} from Table 8.2.3.1, D_{AB} from Table 3.1.2.

№	Reaction	Calculation	ΔE, [kJ/mol] frwrd	ΔE, [kJ/mol] rev.
	Adsorption			
1 R1	$CH_3CH_2CH_3 + * \rightarrow CH_3CH_2\underset{*}{C}H_3$	$\Delta E_f = 0$ $\Delta E_r = Q_{\underset{*}{C}H_3CH_2CH_3}$	0	71.9
2	$CH_3CH_2CH_3 + * \rightarrow CH_3\underset{*}{C}H_2CH_3$	$\Delta E_f = 0$ $\Delta E_r = Q_{CH_3\underset{*}{C}H_2CH_3}$	0	73.6
3 R2	$CH_3CH_2CH_3 + 2* \rightarrow CH_3\underset{*}{C}H_2\underset{*}{C}H_3$	$\Delta E_f = 0$ $\Delta E_r = Q_{CH_3\underset{*}{C}H_2\underset{*}{C}H_3}$	0	11.3
4 R33	$H_2 + 2* \rightarrow \underset{*}{H}\text{-}\underset{*}{H}$	$\Delta E_f = 0$ $\Delta E_r = Q_{\underset{*}{H-H}}$	0	26.7
5 R35	$O_2 + 2* \rightarrow \underset{*}{O}\text{-}\underset{*}{O}$	$\Delta E_f = 0$ $\Delta E_r = Q_{\underset{*}{O-O}}$	0	44.3
	Additional adsorption			
6 R3	$CH_3CH_2\underset{*}{C}H_3 + * \rightarrow CH_3\underset{*}{C}H_2\underset{*}{C}H_3$	$\Delta E_f = 71.9 - 11.3$ $\Delta E_r = 11.3 - 71.9$	60.6	0
7 R6	$CH_3CH_2\underset{***}{C}H_2 + * \rightarrow CH_3\underset{*}{C}H_2\underset{***}{C}H_2$	$\Delta E_f = 164.2 - 112.3$ $\Delta E_r = 112.3 - 164.2$	51.9	0
8	$CH_3CH_2\underset{***}{C}H + * \rightarrow CH_3\underset{*}{C}H_2\underset{***}{C}H$	$\Delta E_f = 289.6 - 320$ $\Delta E_r = 320 - 289.6$	0	30.4

№	Reaction	Calculation	ΔE, [kJ/mol] frwrd	ΔE, [kJ/mol] rev.
9	$CH_3\underset{***}{C}HCH_3 + * \rightarrow CH_3\underset{***}{C}H\underset{*}{C}H_3$	$\Delta E_f = 168.0 - 125.1$	42.9	
		$\Delta E_r = 125.1 - 168.0$		0
10	$CH_3\underset{*}{C}H_2CH_3 + * \rightarrow CH_3\underset{*}{C}H_2\underset{*}{C}H_3$	$\Delta E_f = 73.6 - 11.3$	62.3	
		$\Delta E_r = 11.3 - 73.6$		0
11	$CH_3\underset{***}{C}CH_3 + * \rightarrow CH_3\underset{***}{C}\underset{*}{C}H_3$	--	--	
		--		--
12	$CH_3CH_2\underset{***}{C} + * \rightarrow CH_3\underset{*}{C}H_2\underset{***}{C}$	--	--	
		--		--
13	$CH_3CH=\underset{*}{C}H_2 + * \rightarrow CH_3\underset{*}{C}H=\underset{*}{C}H_2$	$\Delta E_f = 75.6 - 11.8$	63.8	
		$\Delta E_r = 11.8 - 75.6$		0
14	$CH_3\underset{*}{C}H=CH_2 + * \rightarrow CH_3\underset{*}{C}H=\underset{*}{C}H_2$	$\Delta E_f = 77.6 - 11.8$	65.8	
		$\Delta E_r = 11.8 - 77.6$		0
15	$CH_3CH=\underset{***}{C}H + * \rightarrow CH_3\underset{*}{C}H=\underset{***}{C}H$	$\Delta E_f = 179.7 - 202.5$	0	
		$\Delta E_r = 202.5 - 179.7$		22.8
16	$CH_3\underset{*}{C}H_3 + * \rightarrow \underset{*}{C}H_3\underset{*}{C}H_3$	$\Delta E_f = 71.7 - 10.8$	60.9	
		$\Delta E_r = 10.8 - 71.7$		0
17	$CH_3\underset{***}{C}H_2 + * \rightarrow \underset{*}{C}H_3\underset{***}{C}H_2$	$\Delta E_f = 163.2 - 115.1$	48.1	
		$\Delta E_r = 115.1 - 163.2$		0
18	$CH_3\underset{***}{C}H + * \rightarrow \underset{*}{C}H_3\underset{***}{C}H$	$\Delta E_f = 293.3 - 323.7$	0	
		$\Delta E_r = 323.7 - 293.3$		30.4
19		$\Delta E_f = 75.9 - 11.3$	64.6	

№	Reaction	Calculation	ΔE, [kJ/mol] frwrd	rev.
	$\underset{*}{C}H_2{=}CH_2 + * \rightarrow \underset{*}{C}H_2{=}\underset{*}{C}H_2$	$\Delta E_r = 11.3 - 75.9$		0
20	$CH_3\underset{***}{C} + * \rightarrow \underset{*}{C}H_3\underset{***}{C}$	-- --	--	--
	Dissociation C-H			
21 R4	$CH_3CH_2\underset{*}{C}H_3 + 5* \rightarrow CH_3CH_2\underset{***}{C}H_2 + \underset{***}{H}$	$\Delta E_f = \frac{1}{2}\cdot\left(71.9+423.2-164.2-255.2+\frac{164.2\cdot255.2}{164.2+255.2}\right)$ $\Delta E_r = \frac{1}{2}\left(164.2+255.2-71.9-423.2+\frac{164.2\cdot255.2}{164.2+255.2}\right)$	87.8	12.1
22	$CH_3CH_2\underset{***}{C}H_2 + 3* \rightarrow CH_3CH_2\underset{***}{C}H + \underset{***}{H}$	$\Delta E_f = \frac{1}{2}\cdot\left(164.2+438.5-289.6-255.2+\frac{289.6\cdot255.2}{289.6+255.2}\right)$ $\Delta E_r = \frac{1}{2}\cdot\left(289.6+255.2-164.2-438.5+\frac{289.6\cdot255.2}{289.6+255.2}\right)$	96.8	38.9
23 R13	$CH_3CH_2\underset{***}{C}H_2 + 2* \rightarrow CH_3\underset{*}{C}H{=}\underset{*}{C}H_2 + \underset{***}{H}$	$\Delta E_f = \frac{1}{2}\left(164.2+407.9+408.6-736.5-11.8-255.2+\frac{11.8\cdot255.2}{11.8+255.2}\right)$ $\Delta E_r = \frac{1}{2}\left(736.5+11.8+255.2-164.2-407.9-408.6+\frac{11.8\cdot255.2}{11.8+255.2}\right)$	0	17.0
24	$CH_3CH_2\underset{***}{C}H + 3* \rightarrow CH_3CH_2\underset{***}{C} + \underset{***}{H}$	-- --	--	--
25	$CH_3\underset{*}{C}H_2CH_3 + 5* \rightarrow CH_3\underset{***}{C}HCH_3 + \underset{***}{H}$	$\Delta E_f = \frac{1}{2}\cdot\left(73.6+416-168-255.2+\frac{168\cdot255.2}{168+255.2}\right)$ $\Delta E_r = \frac{1}{2}\cdot\left(168+255.2-73.6-416+\frac{168\cdot255.2}{168+255.2}\right)$	83.9	17.5
26	$CH_3\underset{***}{C}HCH_3 + 3* \rightarrow CH_3\underset{***}{C}CH_3$	$\Delta E_f = \frac{1}{2}\cdot\left(168+420.5-293.5-255.2+\frac{293.5\cdot255.2}{293.5+255.2}\right)$ $\Delta E_r = \frac{1}{2}\left(293.5+255.2-168-420.5+\frac{293.5\cdot255.2}{293.5+255.2}\right)$	88.2	48.4
27 R5	$CH_3\underset{*}{C}H_2\underset{*}{C}H_3 + 5* \rightarrow CH_3\underset{*}{C}H_2\underset{***}{C}H_2 + \underset{***}{H}$	$\Delta E_f = \frac{1}{2}\cdot\left(11.3+423.2-112.3-255.2+\frac{112.3\cdot255.2}{112.3+255.2}\right)$ $\Delta E_r = \frac{1}{2}\left(112.3+255.2-11.3-423.2+\frac{112.3\cdot255.2}{112.3+255.2}\right)$	72.5	5.5
28 R11	$CH_3\underset{*}{C}H_2\underset{***}{C}H_2 + 3* \rightarrow CH_3\underset{*}{C}H_2\underset{***}{C}H + \underset{***}{H}$	$\Delta E_f = \frac{1}{2}\cdot\left(112.3+438.5-320-255.2+\frac{320\cdot255.2}{320+255.2}\right)$ $\Delta E_r = \frac{1}{2}\cdot\left(320+255.2-112.3-438.5+\frac{320\cdot255.2}{320+255.2}\right)$	58.8	83.2
29	$CH_3\underset{*}{C}H_2\underset{***}{C}H + 3* \rightarrow CH_3\underset{*}{C}H_2\underset{***}{C} + \underset{***}{H}$	-- --	--	--

№	Reaction	Calculation	ΔE, [kJ/mol] frwrd	ΔE, [kJ/mol] rev.
30	$CH_3\underset{*}{C}H_2\underset{***}{C}H_2 + 5* \rightarrow CH_3\underset{***}{C}H\underset{***}{C}H_2 + \underset{***}{H}$	$\Delta E_f=\frac{1}{2}\cdot\left(112.3+407.9-52.6-255.2+\frac{52.6\cdot255.2}{52.6+255.2}\right)$	128.0	
		$\Delta E_r=\frac{1}{2}\cdot\left(52.6+255.2-112.3-407.9+\frac{52.6\cdot255.2}{52.6+255.2}\right)$		0
31 R12	$CH_3\underset{*}{C}H_2\underset{***}{C}H_2 + * \rightarrow CH_3\underset{*}{C}H=\underset{*}{C}H_2 + \underset{***}{H}$	$\Delta E_f=\frac{1}{2}\cdot\left(112.3+407.9+408.6-736.5-11.8-255.2+\frac{11.8\cdot255.2}{11.8+255.2}\right)$	0	
		$\Delta E_r=\frac{1}{2}\cdot\left(736.5+11.8+255.2-112.3-407.9-408.6+\frac{11.8\cdot255.2}{11.8+255.2}\right)$		43.0
32	$CH_3\underset{***}{C}H\underset{***}{C}H_2 + 3* \rightarrow CH_3\underset{***}{C}H\underset{***}{C}H + \underset{***}{H}$	$\Delta E_f=\frac{1}{2}\cdot\left(52.6+425-165.8-255.2+\frac{165.8\cdot255.2}{165.8+255.2}\right)$	78.6	
		$\Delta E_r=\frac{1}{2}\cdot\left(165.8+255.2-52.6-425+\frac{165.8\cdot255.2}{165.8+255.2}\right)$		22.0
33 R15	$CH_3\underset{*}{C}H=\underset{*}{C}H_2 + 5* \rightarrow CH_3\underset{*}{C}H=\underset{***}{C}H + \underset{***}{H}$	$\Delta E_f=\frac{1}{2}\cdot\left(11.8+465-202.5-255.2+\frac{202.5\cdot255.2}{202.5+255.2}\right)$	66.0	
		$\Delta E_r=\frac{1}{2}\cdot\left(202.5+255.2-11.8-465+\frac{202.5\cdot255.2}{202.5+255.2}\right)$		46.9
34	$CH_3\underset{***}{C}H\underset{***}{C}H + 3* \rightarrow CH_3\underset{***}{C}H\underset{***}{C} + \underset{***}{H}$	--	--	
		--		--
35	$CH_3\underset{***}{C}H\underset{***}{C} + 3* \rightarrow CH_3\underset{******}{C}\underset{}{C} + \underset{***}{H}$	--	--	
		--		--
36	$CH_3\underset{***}{C}H\underset{***}{C}H_2 + 3* \rightarrow CH_3\underset{******}{C}\underset{}{C}H_2 + \underset{***}{H}$	$\Delta E_f=\frac{1}{2}\cdot\left(52.6+413-275.9-255.2+\frac{275.9\cdot255.2}{275.9+255.2}\right)$	33.5	
		$\Delta E_r=\frac{1}{2}\cdot\left(275.9+255.2-52.6-413+\frac{275.9\cdot255.2}{275.9+255.2}\right)$		99.0
37	$CH_3\underset{******}{C}\underset{}{C}H_2 + 3* \rightarrow CH_3\underset{******}{C}\underset{}{C}H + \underset{***}{H}$	$\Delta E_f=\frac{1}{2}\cdot\left(275.9+453.3-201.7-255.2+\frac{201.7\cdot255.2}{201.7+255.2}\right)$	192.5	
		$\Delta E_f=\frac{1}{2}\cdot\left(201.7+255.2-275.9-453.3+\frac{201.7\cdot255.2}{201.7+255.2}\right)$		0
38	$CH_3\underset{******}{C}\underset{}{C}H + 3* \rightarrow CH_3\underset{******}{C}\underset{}{C} + \underset{***}{H}$	--	--	
		--		--
39	$CH_3\underset{*}{C}H_2\underset{*}{C}H_3 + 5* \rightarrow CH_3\underset{***}{C}H\underset{*}{C}H_3 + \underset{***}{H}$	$\Delta E_f=\frac{1}{2}\cdot\left(11.3+416-125.1-255.2+\frac{125.1\cdot255.2}{125.1+255.2}\right)$	65.5	
		$\Delta E_r=\frac{1}{2}\cdot\left(125.1+255.2-11.3-416+\frac{125.1\cdot255.2}{125.1+255.2}\right)$		18.5
40	$CH_3\underset{***}{C}H\underset{*}{C}H_3 + 3* \rightarrow CH_3\underset{***}{C}\underset{*}{C}H_3 + \underset{***}{H}$	--	--	
		--		--
41	$CH_3\underset{***}{C}H\underset{*}{C}H_3 + 5* \rightarrow CH_3\underset{***}{C}H\underset{***}{C}H_2 + \underset{***}{H}$	$\Delta E_f=\frac{1}{2}\cdot\left(125.1+415.1-52.6-255.2+\frac{52.6\cdot255.2}{52.6+255.2}\right)$	138.0	
		$\Delta E_r=\frac{1}{2}\cdot\left(52.6+255.2-125.1-415.1+\frac{52.6\cdot255.2}{52.6+255.2}\right)$		0

№	Reaction	Calculation	ΔE, [kJ/mol] frwrd	ΔE, [kJ/mol] rev.
42	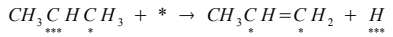	$\Delta E_f=\frac{1}{2}\cdot\left(125.1+415.1+419.5-736.5-11.8-255.2+\frac{11.8\cdot255.2}{11.8+255.2}\right)$	0	
		$\Delta E_r=\frac{1}{2}\cdot\left(736.5+11.8+255.2-125.1-415.1-419.5+\frac{11.8\cdot255.2}{11.8+255.2}\right)$		27.5
43		$\Delta E_f=\frac{1}{2}\cdot\left(320+394.4-165.8-255.2+\frac{165.8\cdot255.2}{165.8+255.2}\right)$	197.0	
		$\Delta E_r=\frac{1}{2}\cdot\left(165.8+255.2-320-394.4+\frac{165.8\cdot255.2}{165.8+255.2}\right)$		0
44 R16		$\Delta E_f=\frac{1}{2}\cdot\left(320+394.4+395.1-696.5-202.5-255.2+\frac{202.5\cdot255.2}{202.5+255.2}\right)$	34.1	
		$\Delta E_r=\frac{1}{2}\cdot\left(696.5+202.5+255.2-320-394.4-395.1+\frac{202.5\cdot255.2}{202.5+255.2}\right)$		78.8
45		$\Delta E_f=\frac{1}{2}\cdot\left(168+415.1+419.5-736.5-11.8-255.2+\frac{11.8\cdot255.2}{11.8+255.2}\right)$	5.2	
		$\Delta E_r=\frac{1}{2}\cdot\left(736.5+11.8+255.2-168-415.1-419.5+\frac{11.8\cdot255.2}{11.8+255.2}\right)$		6.1
46	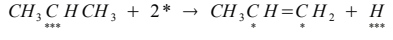	$\Delta E_f=\frac{1}{2}\cdot\left(165.8+441.3-201.7-255.2+\frac{201.7\cdot255.2}{201.7+255.2}\right)$	131.4	
		$\Delta E_r=\frac{1}{2}\cdot\left(201.7+255.2-165.8-441.3+\frac{201.7\cdot255.2}{201.7+255.2}\right)$		0
47	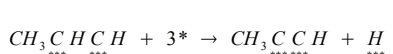	--	--	
		--		--
48		--	--	
		--		--
49 R49	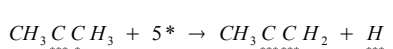	$\Delta E_f=\frac{1}{2}\cdot\left(163.2+465.4-293.3-255.2+\frac{293.3\cdot255.2}{293.3+255.2}\right)$	108.3	
		$\Delta E_r=\frac{1}{2}\cdot\left(293.3+255.2-163.2-465.4+\frac{293.3\cdot255.2}{293.3+255.2}\right)$		28.2
50		--	--	
		--		--
51		$\Delta E_f=\frac{1}{2}\cdot\left(115.1+465.4-323.7-255.2+\frac{323.7\cdot255.2}{323.7+255.2}\right)$	72.1	
		$\Delta E_r=\frac{1}{2}\cdot\left(323.7+255.2-115.1-465.4+\frac{323.7\cdot255.2}{323.7+255.2}\right)$		70.5
52		--	--	
		--		--
53		--	--	
		--		--
54		--	--	
		--		--

№	Reaction	Calculation	ΔE, [kJ/mol] frwrd	ΔE, [kJ/mol] rev.
55	$C_{*}H_2{=}C_{***} + 3* \rightarrow C_{*}H{\equiv}C_{***} + H_{***}$	$\Delta E_f = \frac{1}{2}\cdot\left(512.8+439+692.3-747.9-422-255.2+\frac{422\cdot255.2}{422+255.2}\right)$	189.0	
		$\Delta E_r = \frac{1}{2}\cdot\left(747.9+422+255.2-512.8-439-692.3+\frac{422\cdot255.2}{422+255.2}\right)$		0
56	$C_{***}H C_{***} + 3* \rightarrow C_{******}C + H_{***}$	--	--	
		--		--
57	$C_{*}H{\equiv}C_{***} + 5* \rightarrow C_{***}{\equiv}C_{***} + H_{***}$	$\Delta E_f = \frac{1}{2}\cdot\left(422+482.3-264.3-255.2+\frac{264.3\cdot255.2}{264.3+255.2}\right)$	257.3	
		$\Delta E_r = \frac{1}{2}\cdot\left(264.3+255.2-422-482.3+\frac{264.3\cdot255.2}{264.3+255.2}\right)$		0
58	$C_{*}H_3C_{***}H + 5* \rightarrow C_{***}H_2C_{***}H + H_{***}$	$\Delta E_f = \frac{1}{2}\cdot\left(323.7+384.2-173-255.2+\frac{173\cdot255.2}{173+255.2}\right)$	191.4	
		$\Delta E_r = \frac{1}{2}\cdot\left(173+255.2-323.7-384.2+\frac{173\cdot255.2}{173+255.2}\right)$		0
59	$C_{*}H_3C_{***}H + 3* \rightarrow C_{*}H_2{=}C_{***}H + H_{***}$	$\Delta E_f = \frac{1}{2}\cdot\left(323.7+384.2+378-688.1-210.1-255.2+\frac{210.1\cdot255.2}{210.1+255.2}\right)$	23.9	
		$\Delta E_r = \frac{1}{2}\cdot\left(688.1-210.1-255.2-323.7-384.2-378+\frac{210.1\cdot255.2}{210.1+255.2}\right)$		0
60	$C_{*}H_3C_{***}H_2 + 5* \rightarrow C_{***}H_2C_{***}H_2 + H_{***}$	$\Delta E_f = \frac{1}{2}\cdot\left(115.1+420.7-50.9-255.2+\frac{50.9\cdot255.2}{50.9+255.2}\right)$	136.1	
		$\Delta E_r = \frac{1}{2}\cdot\left(50.9+255.2-115.1-420.7+\frac{50.9\cdot255.2}{50.9+255.2}\right)$		0
61 R19	$CH_3C_{***}H_2 + 2* \rightarrow C_{*}H_2{=}C_{*}H_2 + H_{***}$	$\Delta E_f = \frac{1}{2}\left(163.2+420.7+418.4-728.3-11.3-255.2+\frac{11.3\cdot255.2}{11.3+255.2}\right)$	9.2	
		$\Delta E_r = \frac{1}{2}\left(728.3+11.3+255.2-163.2-420.7-418.4+\frac{11.3\cdot255.2}{11.3+255.2}\right)$		1.7
62	$C_{*}H_3C_{***}H_2 + * \rightarrow C_{*}H_2{=}C_{*}H_2 + H_{***}$	$\Delta E_f = \frac{1}{2}\left(115.1+420.7+418.4-728.3-11.3-255.2+\frac{11.3\cdot255.2}{11.3+255.2}\right)$	0	
		$\Delta E_r = \frac{1}{2}\left(728.3+11.3+255.2-115.1-420.7-418.4+\frac{11.3\cdot255.2}{11.3+255.2}\right)$		25.7
63	$C_{***}H_2C_{***}H_2 + 3* \rightarrow C_{***}H_2C_{***}H + H_{***}$	$\Delta E_f = \frac{1}{2}\cdot\left(50.9+428.9-173-255.2+\frac{173\cdot255.2}{173+255.2}\right)$	77.4	
		$\Delta E_r = \frac{1}{2}\cdot\left(173+255.2-50.9-428.9+\frac{173\cdot255.2}{173+255.2}\right)$		25.8
64 R28	$C_{*}H_2{=}C_{*}H_2 + 5* \rightarrow C_{*}H_2{=}C_{***}H + H_{***}$	$\Delta E_f = \frac{1}{2}\cdot\left(11.3+465.2-210.1-255.2+\frac{210.1\cdot255.2}{210.1+255.2}\right)$	63.2	
		$\Delta E_r = \frac{1}{2}\cdot\left(210.1+255.2-11.3-465.2+\frac{210.1\cdot255.2}{210.1+255.2}\right)$		52.0
65	$C_{***}H_2C_{***}H + 3* \rightarrow C_{***}H_2C_{***} + H_{***}$	--	--	
		--		--
66		$\Delta E_f = \frac{1}{2}\cdot\left(173+453.3-161.5-255.2+\frac{161.5\cdot255.2}{161.5+255.2}\right)$	154.3	

№	Reaction	Calculation	ΔE, [kJ/mol] frwrd	ΔE, [kJ/mol] rev.
	$\underset{***}{C}H_2\underset{***}{C}H + 3* \rightarrow \underset{***}{C}H\underset{***}{C}H + \underset{***}{H}$	$\Delta E_r=\frac{1}{2}\cdot\left(161.5+255.2-173-453.3+\frac{161.5\cdot255.2}{161.5+255.2}\right)$		0
67 R29	$\underset{*}{C}H_2=\underset{***}{C}H + * \rightarrow \underset{*}{C}H\equiv\underset{*}{C}H + \underset{***}{H}$	$\Delta E_f=\frac{1}{2}\left(210.1+464.7+688.1-966.6-21.3-255.2+\frac{21.3\cdot255.2}{21.3+255.2}\right)$	69.7	
		$\Delta E_r=\frac{1}{2}\left(966.6+21.3+255.2-210.1-464.7-688.1+\frac{21.3\cdot255.2}{21.3+255.2}\right)$		0
68	$\underset{***}{C}H\underset{***}{C}H + 3* \rightarrow \underset{***}{C}H\underset{***}{C} + \underset{***}{H}$	--	--	
		--		--
69	$\underset{*}{C}H\equiv\underset{*}{C}H + 5* \rightarrow \underset{*}{C}H\equiv\underset{***}{C} + \underset{***}{H}$	$\Delta E_f=\frac{1}{2}\cdot\left(21.3+556-422-255.2+\frac{422\cdot255.2}{422+255.2}\right)$	29.6	
		$\Delta E_r=\frac{1}{2}\cdot\left(422+255.2-21.3-556+\frac{422\cdot255.2}{422+255.2}\right)$		129.5
R30	$\underset{*}{C}H\equiv\underset{*}{C}H + 4* \rightarrow CH\equiv\underset{***}{C} + \underset{***}{H}$	$\Delta E_f=\frac{1}{2}\cdot\left(21.3+556-224.4-255.2+\frac{224.4\cdot255.2}{224.4+255.2}\right)$	108.6	
		$\Delta E_r=\frac{1}{2}\cdot\left(224.4+255.2-21.3-556+\frac{224.4\cdot255.2}{224.4+255.2}\right)$		10.9
70	$\underset{*}{C}H_3\underset{*}{C}H_3 + 5* \rightarrow \underset{*}{C}H_3\underset{***}{C}H_2 + \underset{***}{H}$	$\Delta E_f=\frac{1}{2}\cdot\left(10.8+420.6-115.1-255.2+\frac{115.1\cdot255.2}{115.1+255.2}\right)$	70.2	
		$\Delta E_r=\frac{1}{2}\cdot\left(115.1+255.2-10.8-420.6+\frac{115.1\cdot255.2}{115.1+255.2}\right)$		9.1
R22	$\underset{*}{C}H_3\underset{*}{C}H_3 + 4* \rightarrow CH_3\underset{***}{C}H_2 + \underset{***}{H}$	$\Delta E_f=\frac{1}{2}\cdot\left(10.8+420.6-163.2-255.2+\frac{163.2\cdot255.2}{163.2+255.2}\right)$	56.3	
		$\Delta E_r=\frac{1}{2}\cdot\left(163.2+255.2-10.8-420.6+\frac{163.2\cdot255.2}{163.2+255.2}\right)$		43.3
71	$CH_3\underset{*}{C}H_3 + 5* \rightarrow CH_3\underset{***}{C}H_2 + \underset{***}{H}$	$\Delta E_f=\frac{1}{2}\cdot\left(71.7+420.6-163.2-255.2+\frac{163.2\cdot255.2}{163.2+255.2}\right)$	86.7	
		$\Delta E_r=\frac{1}{2}\cdot\left(163.2+255.2-71.7-420.6+\frac{163.2\cdot255.2}{163.2+255.2}\right)$		12.8
72 R21	$\underset{***}{C}H_3 + 3* \rightarrow \underset{***}{C}H_2 + \underset{***}{H}$	$\Delta E_f=\frac{1}{2}\cdot\left(158.9+461.7-283.4-255.2+\frac{283.4\cdot255.2}{283.4+255.2}\right)$	108.1	
		$\Delta E_r=\frac{1}{2}\cdot\left(283.4+255.2-158.9-461.7+\frac{283.4\cdot255.2}{283.4+255.2}\right)$		26.1
73	$\underset{***}{C}H_2 + 3* \rightarrow \underset{***}{C}H + \underset{***}{H}$	$\Delta E_f=\frac{1}{2}\cdot\left(283.4+425-408.2-255.2+\frac{408.2\cdot255.2}{408.2+255.2}\right)$	101.0	
		$\Delta E_r=\frac{1}{2}\cdot\left(408.2+255.2-283.4-425+\frac{408.2\cdot255.2}{408.2+255.2}\right)$		56.0
74 R32	$\underset{***}{C}H + 3* \rightarrow \underset{***}{C} + \underset{***}{H}$	$\Delta E_f=\frac{1}{2}\cdot\left(408.2+337.3-627.6-255.2+\frac{627.6\cdot255.2}{627.6+255.2}\right)$	22.1	
		$\Delta E_r=\frac{1}{2}\cdot\left(627.6+255.2-408.2-337.3+\frac{627.6\cdot255.2}{627.6+255.2}\right)$		159.4

№	Reaction	Calculation	ΔE, [kJ/mol] frwrd	ΔE, [kJ/mol] rev.
75 R24	$C\underset{***}{H_3} + \underset{***}{H} \rightarrow \underset{*}{CH_4} + 5*$	$\Delta E_f = \frac{1}{2}\cdot\left(158.9+255.2-69.5-439.3+\frac{158.9\cdot 255.2}{158.9+255.2}\right)$	1.6	
		$\Delta E_r = \frac{1}{2}\cdot\left(69.5+439.3-158.9-255.2+\frac{158.9\cdot 255.2}{158.9+255.2}\right)$		96.3
	Dissociation C-C			
76	$CH_3CH_2\underset{***}{C} + 3* \rightarrow CH_3\underset{***}{C}H_2 + \underset{***}{C}$	--	--	
		--		--
77 R8	$CH_3\underset{*}{C}H_2\underset{*}{C}H_3 + 4* \rightarrow CH_3\underset{***}{C}H_2 + \underset{***}{C}H_3$	$\Delta E_f = \frac{1}{2}\cdot\left(11.3+370.1-163.2-158.9+\frac{163.2\cdot 158.9}{163.2+158.9}\right)$	69.9	
		$\Delta E_r = \frac{1}{2}\cdot\left(163.2+158.9-11.3-370.1+\frac{163.2\cdot 158.9}{163.2+158.9}\right)$		10.6
78 R10	$CH_3\underset{*}{C}H_2\underset{***}{C}H_2 + 2* \rightarrow CH_3\underset{***}{C}H_2 + \underset{***}{C}H_2$	$\Delta E_f = \frac{1}{2}\cdot\left(112.3+408.6-163.2-283.4+\frac{163.2\cdot 283.4}{163.2+283.4}\right)$	88.9	
		$\Delta E_r = \frac{1}{2}\cdot\left(163.2+283.4-112.3-408.6+\frac{163.2\cdot 283.4}{163.2+283.4}\right)$		14.6
79	$CH_3\underset{***}{C}H\underset{*}{C}H_3 + 2* \rightarrow CH_3\underset{***}{C}H + \underset{***}{C}H_3$	$\Delta E_f = \frac{1}{2}\cdot\left(125.1+419.5-293.3-158.9+\frac{293.3\cdot 158.9}{293.3+158.9}\right)$	97.7	
		$\Delta E_r = \frac{1}{2}\cdot\left(293.3+158.9-125.1-419.5+\frac{293.3\cdot 158.9}{293.3+158.9}\right)$		5.3
80	$CH_3\underset{*}{C}H_2\underset{***}{C} + 2* \rightarrow CH_3\underset{***}{C}H_2 + \underset{***}{C}$	--	--	
		--		--
81	$CH_3\underset{***}{C}H\underset{***}{C}H \rightarrow CH_3\underset{***}{C}H + \underset{***}{C}H$	$\Delta E_f = \frac{1}{2}\cdot\left(165.8+466.1-293.3-408.2+\frac{293.3\cdot 408.2}{293.3+408.2}\right)$	50.5	
		$\Delta E_r = \frac{1}{2}\cdot\left(293.3+408.2-165.8-466.1+\frac{293.3\cdot 408.2}{293.3+408.2}\right)$		120.1
82	$CH_3\underset{*}{C}H=\underset{***}{C}H + 2* \rightarrow CH_3\underset{***}{C}H + \underset{***}{C}H$	$\Delta E_f = \frac{1}{2}\cdot\left(202.5+696.5-293.3-408.2+\frac{293.3\cdot 408.2}{293.3+408.2}\right)$	184.1	
		$\Delta E_r = \frac{1}{2}\cdot\left(293.3+408.2-202.5-696.5+\frac{293.3\cdot 408.2}{293.3+408.2}\right)$		0
83	$CH_3\underset{*}{C}H=\underset{***}{C}H + 2* \rightarrow CH_3\underset{***}{C}H\underset{***}{C}H$	$\Delta E_f = 202.5+696.5-466.1-165.8$	267.1	
		$\Delta E_r = 466.1+165.8-202.5-696.5$		0
84	$CH_3\underset{***}{C}\underset{***}{C}H_2 \rightarrow CH_3\underset{***}{C} + \underset{***}{C}H_2$	--	--	
		--		--
85 R7	$CH_3CH_2\underset{*}{C}H_3 + 5* \rightarrow CH_3\underset{***}{C}H_2 + \underset{***}{C}H_3$	$\Delta E_f = \frac{1}{2}\cdot\left(71.9+370.1-163.2-158.9+\frac{163.2\cdot 158.9}{163.2+158.9}\right)$	100.2	
		$\Delta E_r = \frac{1}{2}\cdot\left(163.2+158.9-71.9-370.1+\frac{163.2\cdot 158.9}{163.2+158.9}\right)$		0
86		$\Delta E_f = \frac{1}{2}\cdot\left(73.6+370.1-163.2-158.9+\frac{163.2\cdot 158.9}{163.2+158.9}\right)$	101.1	

№	Reaction	Calculation	ΔE, [kJ/mol] frwrd	rev.
	$CH_3\underset{*}{C}H_2CH_3 + 5^* \rightarrow CH_3\underset{***}{C}H_2 + \underset{***}{C}H_3$	$\Delta E_r=\frac{1}{2}\cdot\left(163.2+158.9-73.6-370.1+\frac{163.2\cdot158.9}{163.2+158.9}\right)$		0
87 R9	$CH_3CH_2\underset{***}{C}H_2 + 3^* \rightarrow CH_3\underset{***}{C}H_2 + \underset{***}{C}H_2$	$\Delta E_f=\frac{1}{2}\cdot\left(164.2+408.6-163.2-283.4+\frac{163.2\cdot283.4}{163.2+283.4}\right)$	114.9	
		$\Delta E_r=\frac{1}{2}\cdot\left(163.2+283.4-164.2-408.6+\frac{163.2\cdot283.4}{163.2+283.4}\right)$		0
88	$CH_3\underset{***}{C}H\underset{***}{C}H_2 \rightarrow CH_3\underset{***}{C}H + \underset{***}{C}H_2$	$\Delta E_f=\frac{1}{2}\cdot\left(52.6+466.1-293.3-283.4+\frac{293.3\cdot283.4}{293.3+283.4}\right)$	43.1	
		$\Delta E_r=\frac{1}{2}\cdot\left(293.3+283.4-52.6-466.1+\frac{293.3\cdot283.4}{293.3+283.4}\right)$		101.1
89 R48	$CH_3\underset{*}{C}H=\underset{*}{C}H_2 + 4^* \rightarrow CH_3\underset{***}{C}H + \underset{***}{C}H_2$	$\Delta E_f=\frac{1}{2}\cdot\left(11.8+736.5-293.3-283.4+\frac{293.3\cdot283.4}{293.3+283.4}\right)$	157.9	
		$\Delta E_r=\frac{1}{2}\cdot\left(293.3+283.4-11.8-736.5+\frac{293.3\cdot283.4}{293.3+283.4}\right)$		0
90 R17	$CH_3\underset{*}{C}H=\underset{*}{C}H_2 + 5^* \rightarrow \underset{***}{C}H_3 + \underset{***}{C}H=\underset{*}{C}H_2$	$\Delta E_f=\frac{1}{2}\cdot\left(11.8+426.4-158.9-210.1+\frac{158.9\cdot210.1}{158.9+210.1}\right)$	79.8	
		$\Delta E_r=\frac{1}{2}\cdot\left(158.9+210.1-11.8-426.4+\frac{158.9\cdot210.1}{158.9+210.1}\right)$		10.6
91	$CH_3\underset{*}{C}H=CH_2 + 5^* \rightarrow CH_3\underset{***}{C}H\underset{***}{C}H_2$	$\Delta E_f=77.6+736.5-466.1-52.6$	295.4	
		$\Delta E_r=466.1+52.6-77.6-736.5$		0
92	$CH_3CH=\underset{*}{C}H_2 + 5^* \rightarrow CH_3\underset{***}{C}H\underset{***}{C}H_2$	$\Delta E_f=75.6+736.5-466.1-52.6$	293.4	
		$\Delta E_r=466.1+52.6-75.6-736.5$		0
93	$CH_3\underset{*}{C}H=\underset{*}{C}H_2 + 4^* \rightarrow CH_3\underset{***}{C}H\underset{***}{C}H_2$	$\Delta E_f=11.8+736.5-466.1-52.6$	229.6	
		$\Delta E_r=466.1+52.6-11.8-736.5$		0
94	$CH_3\underset{***}{C}\underset{*}{C}H_3 + 2^* \rightarrow CH_3\underset{***}{C} + \underset{***}{C}H_3$	--	--	
		--		--
95	$CH_3\underset{***}{C}CH_3 + 3^* \rightarrow CH_3\underset{***}{C} + \underset{***}{C}H_3$	--	--	
		--		--
96	$CH_3\underset{***}{C}HCH_3 + 3^* \rightarrow CH_3\underset{***}{C}H + \underset{***}{C}H_3$	$\Delta E_f=\frac{1}{2}\cdot\left(168+419.5-293.3-158.9+\frac{293.3\cdot158.9}{293.3+158.9}\right)$	119.2	
		$\Delta E_r=\frac{1}{2}\cdot\left(293.3+158.9-168.0-419.5+\frac{293.3\cdot158.9}{293.3+158.9}\right)$		0
97	$CH_3\underset{***}{C}\underset{***}{C}H \rightarrow CH_3\underset{***}{C} + \underset{***}{C}H$	--	--	
		--		--

№	Reaction	Calculation	ΔE, [kJ/mol] frwrd	rev.
98	$CH_3\underset{*}{C}H_2\underset{***}{C}H + 2* \rightarrow CH_3\underset{***}{C}H_2 + \underset{***}{C}H$	$\Delta E_f=\frac{1}{2}\cdot\left(320+395.1-163.2-408.2+\frac{163.2\cdot408.2}{163.2+408.2}\right)$	130.1	
		$\Delta E_r=\frac{1}{2}\cdot\left(163.2+408.2-320-395.1+\frac{163.2\cdot408.2}{163.2+408.2}\right)$		0
99	$CH_3CH_2\underset{***}{C}H + 3* \rightarrow CH_3\underset{***}{C}H_2 + \underset{***}{C}H$	$\Delta E_f=\frac{1}{2}\cdot\left(289.6+395.1-163.2-408.2+\frac{163.2\cdot408.2}{163.2+408.2}\right)$	114.9	
		$\Delta E_r=\frac{1}{2}\cdot\left(163.2+408.2-289.6-395.1+\frac{163.2\cdot408.2}{163.2+408.2}\right)$		1.6
100	$CH_3\underset{***}{C}H\underset{***}{C} \rightarrow CH_3\underset{***}{C}H + \underset{***}{C}$	--	--	
		--		--
101	$CH_3\underset{***}{\underset{***}{C}}C \rightarrow CH_3\underset{***}{C} + \underset{***}{C}$	--	--	
		--		--
102	$\underset{***}{C}H\underset{***}{C} \rightarrow \underset{***}{C}H + \underset{***}{C}$	--	--	
		--		--
103	$\underset{*}{C}H\equiv\underset{***}{C} + 2* \rightarrow \underset{***}{C}H + \underset{***}{C}$	$\Delta E_f=\frac{1}{2}\cdot\left(422+747.9-408.2-627.6+\frac{408.2\cdot627.6}{408.2+627.6}\right)$	190.7	
		$\Delta E_r=\frac{1}{2}\cdot\left(408.2+627.6-422-747.9+\frac{408.2\cdot627.6}{408.2+627.6}\right)$		56.6
104 R31	$CH\equiv\underset{***}{C} + 3* \rightarrow \underset{***}{C}H + \underset{***}{C}$	$\Delta E_f=\frac{1}{2}\cdot\left(224.4+747.9-408.2-627.6+\frac{408.2\cdot627.6}{408.2+627.6}\right)$	91.9	
		$\Delta E_r=\frac{1}{2}\cdot\left(408.2+627.6-224.4-747.9+\frac{408.2\cdot627.6}{408.2+627.6}\right)$		155.4
105 R23	$\underset{*}{C}H_3\underset{*}{C}H_3 + 4* \rightarrow \underset{***}{C}H_3 + \underset{***}{C}H_3$	$\Delta E_f=\frac{1}{2}\cdot\left(10.8+377.3-158.9-158.9+\frac{158.9\cdot158.9}{158.9+158.9}\right)$	74.9	
		$\Delta E_r=\frac{1}{2}\cdot\left(158.9+158.9-10.8-377.3+\frac{158.9\cdot158.9}{158.9+158.9}\right)$		4.6
106	$\underset{*}{C}H\equiv\underset{*}{C}H + 4* \rightarrow \underset{***}{C}H + \underset{***}{C}H$	$\Delta E_f=\frac{1}{2}\cdot\left(21.3+966.6-408.2-408.2+\frac{408.2\cdot408.2}{408.2+408.2}\right)$	187.8	
		$\Delta E_r=\frac{1}{2}\cdot\left(408.2+408.2-21.3-966.6+\frac{408.2\cdot408.2}{408.2+408.2}\right)$		16.3
107	$\underset{*}{C}H\equiv\underset{*}{C}H + 4* \rightarrow \underset{***}{C}H\underset{***}{C}H$	$\Delta E_f=21.3+966.6-427.2-161.5$	399.2	
		$\Delta E_r=427.2+161.5-21.3-966.6$		0
108 R20	$\underset{*}{C}H_2=\underset{*}{C}H_2 + 4* \rightarrow \underset{***}{C}H_2 + \underset{***}{C}H_2$	$\Delta E_f=\frac{1}{2}\cdot\left(11.3+728.3-283.4-283.4+\frac{283.4\cdot283.4}{283.4+283.4}\right)$	157.2	
		$\Delta E_r=\frac{1}{2}\cdot\left(283.4+283.4-11.3-728.3+\frac{283.4\cdot283.4}{283.4+283.4}\right)$		0
109		$\Delta E_f=\frac{1}{2}\cdot\left(75.9+728.3-283.4-283.4+\frac{283.4\cdot283.4}{283.4+283.4}\right)$	189.6	

№	Reaction	Calculation	ΔE, [kJ/mol] frwrd	rev.
	$\underset{*}{C}H_2{=}CH_2 + 4* \rightarrow \underset{***}{C}H_2 + \underset{***}{C}H_2$	$\Delta E_r{=}\frac{1}{2}\cdot\left(283.4{+}283.4{-}75.9{-}728.3{+}\frac{283.4\cdot283.4}{283.4+283.4}\right)$		0
110	$\underset{*}{C}H_2{=}CH_2 + 5* \rightarrow \underset{***}{C}H_2\underset{***}{C}H_2$	$\Delta E_f{=}75.9{+}728.3{-}459.4{-}50.9$	293.9	
		$\Delta E_r{=}459.4{+}50.9{-}75.9{-}728.3$		0
111	$\underset{*}{C}H_2{=}\underset{*}{C}H_2 + 4* \rightarrow \underset{***}{C}H_2\underset{***}{C}H_2$	$\Delta E_f{=}11.3{+}728.3{-}459.4{-}50.9$	229.3	
		$\Delta E_r{=}459.4{+}50.9{-}11.3{-}728.3$		0
112	$\underset{***}{C}H_2\underset{***}{C}H_2 \rightarrow \underset{***}{C}H_2 + \underset{***}{C}H_2$	$\Delta E_f{=}\frac{1}{2}\cdot\left(50.9{+}459.4{-}283.4{-}283.4{+}\frac{283.4\cdot283.4}{283.4+283.4}\right)$	42.6	
		$\Delta E_r{=}\frac{1}{2}\cdot\left(283.4{+}283.4{-}50.9{-}459.4{+}\frac{283.4\cdot283.4}{283.4+283.4}\right)$		99.1
113	$CH_3\underset{***}{C} + 3* \rightarrow \underset{***}{C}H_3 + \underset{***}{C}$	--	--	
		--		--
114	$\underset{*}{C}H_3\underset{***}{C}H + 2* \rightarrow \underset{***}{C}H_3 + \underset{***}{C}H$	$\Delta E_f{=}\frac{1}{2}\cdot\left(323.7{+}378{-}158.9{-}408.2{+}\frac{158.}{158.}\right.$	124.5	
		$\Delta E_r{=}\frac{1}{2}\cdot\left(158.9{+}408.2{-}323.7{-}378{+}\frac{158.9\cdot408.2}{158.9+408.2}\right)$		0
115	$\underset{*}{C}H_3\underset{***}{C} + 2* \rightarrow \underset{***}{C}H_3 + \underset{***}{C}$	--	--	
		--		--
116	$\underset{*}{C}H_3\underset{***}{C}H_2 + 2* \rightarrow \underset{***}{C}H_3 + \underset{***}{C}H_2$	$\Delta E_f{=}\frac{1}{2}\cdot\left(115.1{+}418.4{-}158.9{-}283.4{+}\frac{158.9\cdot283.4}{158.9+283.4}\right)$	96.5	
		$\Delta E_r{=}\frac{1}{2}\left(158.9{+}283.4{-}115.1{-}418.4{+}\frac{158.9\cdot283.4}{158.9+283.4}\right)$		5.3
117	$CH_3\underset{***}{C}H + 3* \rightarrow \underset{***}{C}H_3 + \underset{***}{C}H$	$\Delta E_f{=}\frac{1}{2}\cdot\left(293.3{+}378{-}158.9{-}408.2{+}\frac{158.9\cdot408.2}{158.9+408.2}\right)$	109.3	
		$\Delta E_r{=}\frac{1}{2}\cdot\left(158.9{+}408.2{-}293.3{-}378{+}\frac{158.9\cdot408.2}{158.9+408.2}\right)$		5.1
118	$\underset{*}{C}H_3CH_3 + 4* \rightarrow \underset{***}{C}H_3 + \underset{***}{C}H_3$	$\Delta E_f{=}\frac{1}{2}\cdot\left(71.7{+}377.3{-}158.9{-}158.9{+}\frac{158.9\cdot158.9}{158.9+158.9}\right)$	105.3	
		$\Delta E_r{=}\frac{1}{2}\cdot\left(158.9{+}158.9{-}71.7{-}377.3{+}\frac{158.9\cdot158.9}{158.9+158.9}\right)$		0
119	$CH_3\underset{***}{C}H_2 + 3* \rightarrow \underset{***}{C}H_3 + \underset{***}{C}H_2$	$\Delta E_f{=}\frac{1}{2}\cdot\left(163.2{+}418.4{-}158.9{-}283.4{+}\frac{158.9\cdot283.4}{158.9+283.4}\right)$	120.6	
		$\Delta E_r{=}\frac{1}{2}\cdot\left(158.9{+}283.4{-}163.2{-}418.4{+}\frac{158.9\cdot283.4}{158.9+283.4}\right)$		0
120	$\underset{***}{C}{-}\underset{***}{C} \rightarrow \underset{***}{C} + \underset{***}{C}$	--	--	
		--		--

№	Reaction	Calculation	ΔE, [kJ/mol] frwrd	ΔE, [kJ/mol] rev.
121	$\underset{***}{C}H_2\underset{***}{C}H \rightarrow \underset{***}{C}H_2 + \underset{***}{C}H$	$\Delta E_f=\frac{1}{2}\cdot\left(173+455.5-283.4-408.2+\frac{283.4\cdot 408.2}{283.4+408.2}\right)$	52.1	
		$\Delta E_r=\frac{1}{2}\cdot\left(283.4+408.2-173-455.5+\frac{283.4\cdot 408.2}{283.4+408.2}\right)$		115.2
122	$\underset{*}{C}H_2=\underset{***}{C}H + 2* \rightarrow \underset{***}{C}H_2 + \underset{***}{C}H$	$\Delta E_f=\frac{1}{2}\cdot\left(210.1+688.1-283.4-408.2+\frac{283.4\cdot 408.2}{283.4+408.2}\right)$	186.9	
		$\Delta E_r=\frac{1}{2}\cdot\left(283.4+408.2-210.1-688.1+\frac{283.4\cdot 408.2}{283.4+408.2}\right)$		0
123	$\underset{***}{C}H_2\underset{***}{C} \rightarrow \underset{***}{C}H_2 + \underset{***}{C}$	--	--	
		--		--
124	$\underset{***}{C}H\underset{***}{C}H \rightarrow \underset{***}{C}H + \underset{***}{C}H$	$\Delta E_f=\frac{1}{2}\cdot\left(161.5+427.2-408.2-408.2+\frac{408.2\cdot 408.2}{408.2+408.2}\right)$	0	
		$\Delta E_r=\frac{1}{2}\cdot\left(408.2+408.2-161.5-427.2+\frac{408.2\cdot 408.2}{408.2+408.2}\right)$		215.9
	Inner recombination C-H			
125	$CH_3\underset{***}{C}\underset{*}{C}H_3 + 2* \rightarrow CH_3\underset{***}{C}H\underset{***}{C}H_2$	--	--	
		--		--
126	$CH_3\underset{*}{C}H_2\underset{***}{C}H + 2* \rightarrow CH_3\underset{***}{C}H\underset{***}{C}H_2$	$\Delta E_f=320+394.4-425-52.6$	236.8	
		$\Delta E_r=425+52.6-320-394.4$		0
127	$CH_3\underset{***}{C}CH_3 + 3* \rightarrow CH_3\underset{***}{C}H\underset{***}{C}H_2$	$\Delta E_f=293.5+407.6-413-52.6$	235.5	
		$\Delta E_r=413+52.6-293.5-407.6$		0
128	$CH_3CH_2\underset{***}{C}H \rightarrow CH_3CH=\underset{*}{C}H_2 + 2*$	$\Delta E_f=289.6+395.1+394.4-736.5-465-75.6$	0	
		$\Delta E_r=736.5+465+75.6-289.6-395.1-394.4$		198.0
129	$CH_3CH_2\underset{***}{C}H + 3* \rightarrow CH_3\underset{***}{C}H\underset{***}{C}H_2$	$\Delta E_f=289.6+394.4-425-52.6$	206.4	
		$\Delta E_r=425+52.6-289.6-394.4$		0
130	$CH_3CH_2\underset{***}{C} + 3* \rightarrow CH_3\underset{***}{C}H\underset{***}{C}H$	--	--	
		--		--
131	$CH_3\underset{***}{C}CH_3 \rightarrow CH_3\underset{*}{C}H=CH_2 + 2*$	--	--	
		--		--
132	$CH_3\underset{***}{C}H\underset{***}{C}H \rightarrow CH_3\underset{***}{C}\underset{***}{C}H_2$	$\Delta E_f=165.8+441.3-453.3-275.9$	0	
		$\Delta E_r=453.3+275.9-165.8-441.3$		122.1
133		$\Delta E_f=168+415.1-438.5-164.2$	0	

№	Reaction	Calculation	ΔE, [kJ/mol] frwrd	ΔE, [kJ/mol] rev.
	$CH_3\underset{***}{C}H\,CH_3 \rightarrow CH_3CH_2\underset{***}{C}H_2$	$\Delta E_r = 438.5 + 164.2 - 168 - 415.1$		19.6
134 R14	$CH_3\underset{*}{C}H_2\underset{***}{C}H \rightarrow CH_3\underset{*}{C}H{=}\underset{*}{C}H_2 + 2*$	$\Delta E_f = 320 + 395.1 + 394.4 - 736.5 - 465 - 11.8$	0	
		$\Delta E_r = 736.5 + 465 + 11.8 - 320 - 395.1 - 394.4$		103.8
135	$CH_3\underset{*}{C}H_2\underset{***}{C} + 2* \rightarrow CH_3\underset{***}{C}H\underset{***}{C}H$	--	--	
		--		--
136	$CH_3\underset{***}{C}\underset{*}{C}H_3 \rightarrow CH_3\underset{*}{C}H{=}\underset{*}{C}H_2 + 2*$	--	--	
		--		--
137	$CH_3\underset{***}{C}H\underset{*}{C}H_3 \rightarrow CH_3\underset{*}{C}H_2\underset{***}{C}H_2$	$\Delta E_f = 125.1 + 415.1 - 407.9 - 112.3$	20.0	
		$\Delta E_r = 407.9 + 112.3 - 125.1 - 415.1$		0
138	$CH_3\underset{***}{C}H\underset{*}{C}H_3 \rightarrow CH_3CH_2\underset{***}{C}H_2 + *$	$\Delta E_f = 125.1 + 415.1 - 407.9 - 164.2$	0	
		$\Delta E_r = 407.9 + 164.2 - 125.1 - 415.1$		31.9
139	$CH_3\underset{***}{C}H\,CH_3 + * \rightarrow CH_3\underset{*}{C}H_2\underset{***}{C}H_2$	$\Delta E_f = 168 + 415.1 - 407.9 - 112.3$	62.9	
		$\Delta E_r = 407.9 + 112.3 - 168 - 415.1$		0
140	$CH_3\underset{***}{\underset{***}{C}}\underset{***}{C}H \rightarrow CH_3\underset{***}{C}H\underset{***}{C}$	--	--	
		--		--
141	$CH_3\underset{***}{C}H \rightarrow CH_2{=}\underset{*}{C}H_2 + 2*$	$\Delta E_f = 293.3 + 384.2 + 378 - 728.3 - 465.2 - 75.9$	0	
		$\Delta E_r = 728.3 + 465.2 + 75.9 - 293.3 - 384.2 - 378$		213.9
142	$CH_3\underset{***}{C}H + 3* \rightarrow \underset{***}{C}H_2\underset{***}{C}H_2$	$\Delta E_f = 293.3 + 384.2 - 428.9 - 50.9$	197.7	
		$\Delta E_r = 428.9 + 50.9 - 293.3 - 384.2$		0
143	$CH_3\underset{***}{C} + 3* \rightarrow \underset{***}{C}H_2\underset{***}{C}H$	--	--	
		--		--
144	$\underset{*}{C}H_3\underset{***}{C} + 2* \rightarrow \underset{***}{C}H_2\underset{***}{C}H$	--	--	
		--		--
145	$\underset{***}{C}H_2\underset{***}{C} \rightarrow \underset{***}{C}H\underset{***}{C}H$	--	--	
		--		--
146	$\underset{*}{C}H_3\underset{***}{C}H \rightarrow \underset{*}{C}H_2{=}\underset{*}{C}H_2 + 2*$	$\Delta E_f = 323.7 + 384.2 + 378 - 728.3 - 465.2 - 11.3$	0	
		$\Delta E_r = 728.3 + 465.2 + 11.3 - 323.7 - 384.2 - 378$		118.9

№	Reaction	Calculation	ΔE, [kJ/mol] frwrd	ΔE, [kJ/mol] rev.
147	$\underset{*}{CH_3}\underset{***}{CH} + 2* \rightarrow \underset{***}{CH_2}\underset{***}{CH_2}$	$\Delta E_f = 323.7 + 384.2 - 428.9 - 50.9$	228.1	
		$\Delta E_r = 428.9 + 50.9 - 323.7 - 384.2$		0
	Dissociation, recombination H-O, C-O			
148 R39	$\underset{***}{H} + \underset{***}{O} \rightarrow \underset{***}{OH} + 3*$	$\Delta E_f = \frac{1}{2}\cdot\left(255.2 + 355.7 - 161.1 - 429.9 + \frac{255.2\cdot 355.7}{255.2+355.7}\right)$	84.2	
		$\Delta E_r = \frac{1}{2}\cdot\left(161.1 + 429.9 - 255.2 - 355.7 + \frac{255.2\cdot 355.7}{255.2+355.7}\right)$		64.3
149 R40	$\underset{***}{H} + \underset{***}{OH} \rightarrow \underset{*}{H_2O} + 5*$	$\Delta E_f = \frac{1}{2}\cdot\left(255.2 + 161.1 - 39.9 - 497.1 + \frac{255.2\cdot 161.1}{255.2+161.1}\right)$	0	
		$\Delta E_r = \frac{1}{2}\cdot\left(39.9 + 497.1 - 255.2 - 161.1 + \frac{255.2\cdot 161.1}{255.2+161.1}\right)$		109.7
150 R38	$\underset{*}{H_2O} + \underset{***}{O} + 2* \rightarrow \underset{***}{OH} + \underset{***}{OH}$	$\Delta E_f = \frac{1}{2}\left(355.7 + 39.9 + 497.1 - 429.9 - 161.1*2 + \frac{161.1\cdot 161.1}{161.1+161.1}\right)$	110.6	
		$\Delta E_r = \frac{1}{2}\left(429.9 + 161.1*2 - 355.7 - 39.9 - 497.1 + \frac{161.1\cdot 161.1}{161.1+161.1}\right)$		0
151 R37	$\underset{*}{H}\text{-}\underset{*}{H} + \underset{***}{O} + * \rightarrow \underset{***}{OH} + \underset{***}{H}$	$\Delta E_f = \frac{1}{2}\cdot\left(26.7 + 355.7 + 436 - 429.9 - 255.2 - 161.1 + \frac{255.2\cdot 161.1}{255.2+161.1}\right)$	35.5	
		$\Delta E_r = \frac{1}{2}\left(429.9 + 255.2 + 161.1 - 26.7 - 355.7 - 436 + \frac{255.2\cdot 161.1}{255.2+161.1}\right)$		63.3
152 R41	$\underset{*}{H_2O} + \underset{***}{H} + * \rightarrow \underset{*}{H}\text{-}\underset{*}{H} + \underset{***}{OH}$	$\Delta E_f = \frac{1}{2}\cdot\left(39.9 + 255.2 + 497.1 - 436 - 26.7 - 161.1 + \frac{26.7\cdot 161.1}{26.7+161.1}\right)$	95.7	
		$\Delta E_r = \frac{1}{2}\left(436 + 26.7 + 161.1 - 39.9 - 255.2 - 497.1 + \frac{26.7\cdot 161.1}{26.7+161.1}\right)$		0
153 R52	$\underset{***}{C} + \underset{***}{O} \rightarrow \underset{*}{CO} + 5*$	$\Delta E_f = \frac{1}{2}\cdot\left(627.6 + 355.7 - 1076.4 - 97.6 + \frac{627.6\cdot 355.7}{627.6+355.7}\right)$	18.2	
		$\Delta E_r = \frac{1}{2}\cdot\left(1076.4 + 97.6 - 627.6 - 355.7 + \frac{627.6\cdot 355.7}{627.6+355.7}\right)$		208.9
154 R45	$\underset{*}{CO} + \underset{***}{CH_3} + 2* \rightarrow \underset{***}{CH_3O} + \underset{***}{C}$	$\Delta E_f = \frac{1}{2}\left(158.9 + 97.6 + 1076.4 - 382.9 - 171.3 - 627.6 + \frac{171.3\cdot 627.6}{171.3+627.6}\right)$	142.8	
		$\Delta E_r = \frac{1}{2}\left(382.9 + 171.3 + 627.6 - 158.9 - 97.6 - 1076.4 + \frac{171.3\cdot 627.6}{171.3+627.6}\right)$		0
155 R43	$\underset{***}{CH_3} + \underset{***}{O} \rightarrow \underset{***}{CH_3O} + 3*$	$\Delta E_f = \frac{1}{2}\cdot\left(158.9 + 355.7 - 171.3 - 382.9 + \frac{158.9\cdot 355.7}{158.9+355.7}\right)$	35.1	
		$\Delta E_r = \frac{1}{2}\cdot\left(171.3 + 382.9 - 158.9 - 355.7 + \frac{158.9\cdot 355.7}{158.9+355.7}\right)$		74.7
156	$\underset{***}{CH_2} + \underset{***}{O} \rightarrow \underset{***}{CH_2O}$	$\Delta E_f = \frac{1}{2}\cdot\left(283.4 + 355.7 - 450.9 - 128 + \frac{283.4\cdot 355.7}{283.4+355.7}\right)$	109.0	
		$\Delta E_r = \frac{1}{2}\cdot\left(450.9 + 128 - 283.4 - 355.7 + \frac{283.4\cdot 355.7}{283.4+355.7}\right)$		48.8
157		$\Delta E_f = \frac{1}{2}\cdot\left(408.2 + 355.7 - 804.2 - 167.3 + \frac{408.2\cdot 355.7}{408.2+355.7}\right)$	0	

№	Reaction	Calculation	ΔE, [kJ/mol] frwrd	rev.
R47	$\underset{***}{CH} + \underset{***}{O} \rightarrow \underset{***}{HC=O} + 3*$	$\Delta E_r = \frac{1}{2}\cdot\left(804.2+167.3-408.2-355.7+\frac{408.2\cdot 355.7}{408.2+355.7}\right)$		198.8
158	$CH_3\underset{***}{O} + 6* \rightarrow \underset{***}{CH_2}\underset{***}{O} + \underset{***}{H}$	$\Delta E_f = \frac{1}{2}\cdot\left(171.3+393.7-128-255.2+\frac{128\cdot 255.2}{128+255.2}\right)$	133.5	
		$\Delta E_r = \frac{1}{2}\cdot\left(128+255.2-171.3-393.7+\frac{128\cdot 255.2}{128+255.2}\right)$		0
159	$\underset{***}{CH_2}\underset{***}{O} \rightarrow \underset{***}{HC=O} + \underset{***}{H}$	--	--	
		--		--
160 R50	$\underset{***}{HC=O} + * \rightarrow \underset{*}{CO} + \underset{***}{H}$	$\Delta E_f = \frac{1}{2}\cdot\left(167.3+63.2+804.2-1076.4-97.6-255.2+\frac{97.6\cdot 255.2}{97.6+255.2}\right)$	0	
		$\Delta E_r = \frac{1}{2}\left(1076.4+97.6+255.2-167.3-63.2-804.2+\frac{97.6\cdot 255.2}{97.6+255.2}\right)$		232.5
161	$\underset{***}{CH_2}\underset{***}{O} + \underset{***}{H} \rightarrow \underset{***}{CH_2OH} + 6*$	$\Delta E_f = \frac{1}{2}\cdot\left(128+255.2-423.7-160.6+\frac{128\cdot 255.2}{128+255.2}\right)$	0	
		$\Delta E_r = \frac{1}{2}\cdot\left(423.7+160.6-128-255.2+\frac{128\cdot 255.2}{128+255.2}\right)$		143.2
162	$\underset{*}{CH}\equiv\underset{*}{CH} + \underset{***}{O} + * \rightarrow \underset{***}{CH} + \underset{***}{HC=O}$	$\Delta E_f = \frac{1}{2}\cdot\left(21.3+355.7+966.6-804.2-167.3-408.2+\frac{167.3\cdot 408.2}{167.3+408.2}\right)$	41.3	
		$\Delta E_r = \frac{1}{2}\left(804.2+167.3+408.2-21.3-355.7-966.6+\frac{167.3\cdot 408.2}{167.3+408.2}\right)$		77.4
163	$\underset{*}{CH_2}=\underset{*}{CH_2} + \underset{***}{O} + 4* \rightarrow \underset{***}{CH_2} + \underset{***}{CH_2O}$	$\Delta E_f = \frac{1}{2}\cdot\left(11.3+355.7+728.3-450.9-283.4-128+\frac{283.4\cdot 128}{283.4+128}\right)$	160.6	
		$\Delta E_r = \frac{1}{2}\left(450.9+283.4+128-11.3-355.7-728.3+\frac{283.4\cdot 128}{283.4+128}\right)$		0
164	$\underset{***}{CH_2OH} + 3* \rightarrow \underset{***}{CH_2} + \underset{***}{OH}$	$\Delta E_f = \frac{1}{2}\cdot\left(160.6+444.7-283.4-161.1+\frac{283.4\cdot 161.1}{283.4+161.1}\right)$	131.8	
		$\Delta E_r = \frac{1}{2}\cdot\left(283.4+161.1-160.6-444.7+\frac{283.4\cdot 161.1}{283.4+161.1}\right)$		0
165 R54	$\underset{***}{HC=O} + \underset{***}{O} \rightarrow \underset{***}{HC(O)O} + 3*$	$\Delta E_f = \frac{1}{2}\cdot\left(167.3+355.7-421.3-162.8+\frac{167.3\cdot 355.7}{167.3+355.7}\right)$	26.3	
		$\Delta E_r = \frac{1}{2}\cdot\left(421.3+162.8-167.3-355.7+\frac{167.3\cdot 355.7}{167.3+355.7}\right)$		87.4
166	$\underset{***}{HC=O} + \underset{***}{H} \rightarrow \underset{***}{HCOH} + 3*$	--	--	
		--		--
167	$\underset{***}{HCOH} + \underset{***}{H} \rightarrow \underset{***}{CH_2OH} + 3*$	--	--	
		--		--
168	$\underset{***}{HCOH} + 3* \rightarrow \underset{***}{CH} + \underset{***}{OH}$	--	--	
		--		--
169		$\Delta E_f = \frac{1}{2}\cdot\left(97.6+355.7+1076.4-2*804.3-15.2+\frac{97.6\cdot 355.7}{97.6+355.7}\right)$	0	

№	Reaction	Calculation	ΔE, [kJ/mol] frwrd	ΔE, [kJ/mol] rev.
R51	$C^{*}O + O^{***} \rightarrow O^{*}=C=O^{*} + 2*$	$\Delta E_r=\frac{1}{2}\left(2*804.3+15.2-97.6-355.7-1076.4+\frac{97.6\cdot 355.7}{97.6+355.7}\right)$		85.3
170	$CH_3C^{*}H=C^{*}H_2 + O^{***} + 4* \rightarrow CH_3C^{***}H + C^{***}H_2O^{***}$	$\Delta E_f=\frac{1}{2}\left(11.8+355.7+736.5-450.9-293.3-128+\frac{293.3\cdot 128}{293.3+128}\right)$	160.5	
		$\Delta E_r=\frac{1}{2}\left(450.9+293.3+128-11.8-355.7-736.5+\frac{293.3\cdot 128}{293.3+128}\right)$		0
171 R46	$CH_3C^{***}H + HC^{***}=O + * \rightarrow CH_3C^{*}H=C^{***}H + O^{***}$	$\Delta E_f=\frac{1}{2}\left(293.3+167.3+804.2-696.5-202.5-355.7+\frac{202.5\cdot 355.7}{202.5+355.7}\right)$	69.6	
		$\Delta E_r=\frac{1}{2}\left(696.5+202.5+355.7-293.3-167.3-804.2+\frac{202.5\cdot 355.7}{202.5+355.7}\right)$		59.5
	Other reactions			
172 R34	$H^{*}\text{-}H^{*} + 4* \rightarrow H^{***} + H^{***}$	$\Delta E_f=\frac{1}{2}\cdot\left(26.7+436-255.2-255.2+\frac{255.2\cdot 255.2}{255.2+255.2}\right)$	40.0	
		$\Delta E_r=\frac{1}{2}\cdot\left(255.2+255.2-26.7-436+\frac{255.2\cdot 255.2}{255.2+255.2}\right)$		87.6
173 R36	$O^{*}\text{-}O^{*} + 4* \rightarrow O^{***} + O^{***}$	$\Delta E_f=\frac{1}{2}\cdot\left(44.3+498.4-355.7-355.7+\frac{355.7\cdot 355.7}{355.7+355.7}\right)$	4.6	
		$\Delta E_r=\frac{1}{2}\cdot\left(355.7+355.7-44.3-498.4+\frac{355.7\cdot 355.7}{355.7+355.7}\right)$		173.3
174 R44	$CH_3^{***} + OH^{***} \rightarrow CH_3O^{***} + H^{***}$	$\Delta E_f=\frac{1}{2}\left(158.9+161.1+429.9-382.9-171.3-255.2+\frac{171.3\cdot 255.2}{171.3+255.2}\right)$	21.5	
		$\Delta E_r=\frac{1}{2}\left(382.9+171.3+255.2-158.9-161.1-429.9+\frac{171.3\cdot 255.2}{171.3+255.2}\right)$		81.0
175 R56	$HC(O)O^{***} + 2* \rightarrow O^{*}=C=O^{*} + H^{***}$	$\Delta E_f=\frac{1}{2}\left(162.8-46+421.3-530.4-15.2-255.2+\frac{15.2\cdot 255.2}{15.2+255.2}\right)$	0	
		$\Delta E_r=\frac{1}{2}\left(530.4+15.2+255.2-162.8+46-421.3+\frac{15.2\cdot 255.2}{15.2+255.2}\right)$		138.5
176	$C^{***}(O)OH + 2* \rightarrow O^{*}=C=O^{*} + H^{***}$	$\Delta E_f=\frac{1}{2}\left(159.7+138+37.3-530.4-15.2-255.2+\frac{15.2\cdot 255.2}{15.2+255.2}\right)$	0	
		$\Delta E_r=\frac{1}{2}\left(530.4+15.2+255.2-159.7-138-37.3+\frac{15.2\cdot 255.2}{15.2+255.2}\right)$		240.1
177 R55	$HC(O)O^{***} + * \rightarrow CO^{*} + OH^{***}$	$\Delta E_f=\frac{1}{2}\left(162.8-46+421.3-429.9-97.6-161.1+\frac{97.6\cdot 161.1}{97.6+161.1}\right)$	0	
		$\Delta E_r=\frac{1}{2}\left(429.9+97.6+161.1-162.8+46-421.3+\frac{97.6\cdot 161.1}{97.6+161.1}\right)$		105.6
178	$CO^{*} + H_2O^{*} + 4* \rightarrow C^{***}(O)OH + H^{***}$	$\Delta E_f=\frac{1}{2}\left(97.6+1076.4+39.9+497.1-1078.2-138-159.7-255.2+\frac{159.7\cdot 255.2}{159.7+255.2}\right)$	89.1	
		$\Delta E_r=\frac{1}{2}\left(1078.2+138+159.7+255.2-97.6-1076.4-39.9-497.1+\frac{159.7\cdot 255.2}{159.7+255.2}\right)$		9.2
179 R53	$CO^{*} + OH^{***} + * \rightarrow O^{*}=C=O^{*} + H^{***}$	$\Delta E_f=\frac{1}{2}\left(97.6+161.1+1076.4+429.9-2\cdot 804.3-15.2-255.2+\frac{15.2\cdot 255.2}{15.2+255.2}\right)$	0	
		$\Delta E_r=\frac{1}{2}\left(2\cdot 804.3+15.2+255.2-97.6-161.1-1076.4-429.9+\frac{15.2\cdot 255.2}{15.2+255.2}\right)$		64.2
	Desorption			

№	Reaction	Calculation	ΔE, [kJ/mol] frwrd	rev.
180	$CH_2=\underset{*}{C}H_2 \rightarrow CH_2=CH_2 + *$	$\Delta E_f = Q_{CH_2=\underset{*}{C}H_2}$	75.9	
		$\Delta E_r = 0$		0
181	$CH_3\underset{*}{C}H_3 \rightarrow CH_3CH_3 + *$	$\Delta E_f = Q_{CH_3\underset{*}{C}H_3}$	71.7	
		$\Delta E_r = 0$		0
R25	$\underset{*}{C}H_3\underset{*}{C}H_3 \rightarrow CH_3CH_3 + 2*$	$\Delta E_f = Q_{\underset{*}{C}H_3\underset{*}{C}H_3}$	10.8	
		$\Delta E_r = 0$		0
182 R27	$\underset{*}{C}H_2=\underset{*}{C}H_2 \rightarrow CH_2=CH_2 + 2*$	$\Delta E_f = Q_{\underset{*}{C}H_2=\underset{*}{C}H_2}$	11.3	
		$\Delta E_r = 0$		0
183	$\underset{*}{C}H\equiv\underset{*}{C}H \rightarrow CH\equiv CH + 2*$	$\Delta E_f = Q_{\underset{*}{C}H\equiv\underset{*}{C}H}$	21.3	
		$\Delta E_r = 0$		0
184 R26	$\underset{*}{C}H_4 \rightarrow CH_4 + *$	$\Delta E_f = Q_{\underset{*}{C}H_4}$	69.5	
		$\Delta E_r = 0$		0
185 R42	$H_2\underset{*}{O} \rightarrow H_2O + *$	$\Delta E_f = Q_{H_2\underset{*}{O}}$	39.9	
		$\Delta E_r = 0$		0
186 R57	$\underset{*}{C}O \rightarrow CO + *$	$\Delta E_f = Q_{\underset{*}{C}O}$	97.6	
		$\Delta E_r = 0$		0
187 R58	$\underset{*}{O}=C=\underset{*}{O} \rightarrow CO_2 + 2*$	$\Delta E_f = Q_{\underset{*}{O}=C=\underset{*}{O}}$	15.2	
		$\Delta E_r = 0$		0
188	$CH_3\underset{*}{C}H=CH_2 \rightarrow CH_3CH=CH_2 + *$	$\Delta E_f = Q_{CH_3\underset{*}{C}H=CH_2}$	77.6	

№	Reaction	Calculation	ΔE, [kJ/mol] frwrd	rev.
		$\Delta E_r = 0$		0
189	$CH_3CH=\underset{*}{C}H_2 \rightarrow CH_3CH=CH_2 + *$	$\Delta E_f = Q_{CH_3CH=\underset{*}{C}H_2}$	75.6	
		$\Delta E_r = 0$		0
190 R18	$CH_3\underset{*}{C}H=\underset{*}{C}H_2 \rightarrow CH_3CH=CH_2 + 2*$	$\Delta E_f = Q_{CH_3\underset{*}{C}H=\underset{*}{C}H_2}$	11.8	
		$\Delta E_r = 0$		0
	Desorption of radicals			
191 R85	$CH_3CH_2\underset{***}{C}H_2 \rightarrow CH_3CH_2\dot{C}H_2 + 3*$	$\Delta E_f = Q_{CH_3CH_2\underset{***}{C}H_2}$	164.2	
		$\Delta E_r = 0$		0
192	$CH_3\underset{***}{C}HCH_3 \rightarrow CH_3\dot{C}HCH_3 + 3*$	$\Delta E_f = Q_{CH_3\underset{***}{C}HCH_3}$	168.0	
		$\Delta E_r = 0$		0
193	$CH_3CH=\underset{***}{C}H \rightarrow CH_3CH=\dot{C}H + 3*$	$\Delta E_f = Q_{CH_3CH=\underset{***}{C}H}$	179.7	
		$\Delta E_r = 0$		0
194 R86	$CH_3\underset{***}{C}H_2 \rightarrow CH_3\dot{C}H_2 + 3*$	$\Delta E_f = Q_{CH_3\underset{***}{C}H_2}$	163.2	
		$\Delta E_r = 0$		0
195 R87	$CH_3\underset{***}{C}H \rightarrow CH_3\ddot{C}H + 3*$	$\Delta E_f = Q_{CH_3\underset{***}{C}H}$	293.3	
		$\Delta E_r = 0$		0
196	$CH_2=\underset{***}{C} \rightarrow CH_2=\ddot{C} + 3*$	$\Delta E_f = Q_{CH_2=\underset{***}{C}}$	298.1	
		$\Delta E_r = 0$		0
197	$CH\equiv\underset{***}{C} \rightarrow CH\equiv\dot{C} + 3*$	$\Delta E_f = Q_{CH\equiv\underset{***}{C}}$	224.4	
		$\Delta E_r = 0$		0

№	Reaction	Calculation	ΔE, [kJ/mol] frwrd	rev.
198	$CH_2{=}\underset{***}{C}H \rightarrow CH_2{=}\dot{C}H + 3*$	$\Delta E_f = Q_{CH_2=\underset{***}{C}H}$	180.7	
		$\Delta E_r = 0$		0
R88	$\underset{*}{C}H_2{=}\underset{***}{C}H \rightarrow CH_2{=}\dot{C}H + 4*$	$\Delta E_f = Q_{\underset{*}{C}H_2=\underset{***}{C}H}$	210.1	
		$\Delta E_r = 0$		0
199 R89	$\underset{***}{C}H_3 \rightarrow \dot{C}H_3 + 3*$	$\Delta E_f = Q_{\underset{***}{C}H_3}$	158.9	
		$\Delta E_r = 0$		0
200 R90	$\underset{***}{C}H_2 \rightarrow \ddot{C}H_2 + 3*$	$\Delta E_f = Q_{\underset{***}{C}H_2}$	283.4	
		$\Delta E_r = 0$		0
201	$\underset{***}{C}H \rightarrow \dddot{C}H + 3*$	$\Delta E_f = Q_{\underset{***}{C}H}$	408.2	
		$\Delta E_r = 0$		0
202 R91	$\underset{***}{H} \rightarrow \dot{H} + 3*$	$\Delta E_f = Q_{\underset{***}{H}}$	255.2	
		$\Delta E_r = 0$		0
203 R92	$\underset{***}{O} \rightarrow \ddot{O} + 3*$	$\Delta E_f = Q_{\underset{***}{O}}$	355.7	
		$\Delta E_r = 0$		0
204 R93	$\underset{***}{OH} \rightarrow \dot{O}H + 3*$	$\Delta E_f = Q_{\underset{***}{OH}}$	161.1	
		$\Delta E_r = 0$		0
205 R94	$CH_3\underset{***}{O} \rightarrow CH_3\dot{O} + 3*$	$\Delta E_f = Q_{CH_3\underset{***}{O}}$	171.3	
		$\Delta E_r = 0$		0
206	$\underset{***}{CH_2}\underset{***}{O} \rightarrow CH_2{=}O + 6*$	$\Delta E_f = 128 + 450.9 - 747.6$	0	
		$\Delta E_r = -128 - 450.9 + 747.6$		168.7

№	Reaction	Calculation	ΔE, [kJ/mol] frwrd	rev.
207	$H\underset{***}{C}=O \rightarrow H\dot{C}=O + 3*$	$\Delta E_f = Q_{H\underset{***}{C}=O}$	167.3	
		$\Delta E_r = 0$		0
208	$\underset{***}{C}H_2OH \rightarrow \dot{C}H_2OH + 3*$	$\Delta E_f = Q_{\underset{***}{C}H_2OH}$	160.6	
		$\Delta E_r = 0$		0
209 R95	$HC(O)\underset{***}{O} \rightarrow HC(O)\dot{O} + 3*$	$\Delta E_f = Q_{HC(O)\underset{***}{O}}$	162.8	
		$\Delta E_r = 0$		0
210	$\underset{***}{C}(O)OH \rightarrow \dot{C}(O)OH + 3*$	$\Delta E_f = Q_{\underset{***}{C}(O)OH}$	159.7	
		$\Delta E_r = 0$		0

Table 8.2.4.2: Activation barriers for gas-phase reactions, calculations using (3.1.2.5), with D_{AB} from Table 3.1.2.

№	Reaction	Calculation	ΔE, [kJ/mol] fwrd	rev.
		Dissociation C-H		
1 R59	$CH_3CH_2CH_3 \rightarrow CH_3CH_2\dot{C}H_2 + \dot{H}$	$\Delta E_f = 423.2 + \frac{8.31 \cdot 298.15}{1000}$	425.7	
		$\Delta E_r = -423.2 + \frac{8.31 \cdot 298.15}{1000}$		0
2 R61	$CH_3CH_2\dot{C}H_2 \rightarrow CH_3CH{=}CH_2 + \dot{H}$	$\Delta E_f = 407.9 + 408.6 - 736.5 + \frac{8.31 \cdot 298.15}{1000}$	82.5	
		$\Delta E_r = 736.5 - 407.9 - 408.6 + \frac{8.31 \cdot 298.15}{1000}$		0
3	$CH_3CH_2CH_3 \rightarrow CH_3\dot{C}HCH_3 + \dot{H}$	$\Delta E_f = 416 + 2.48$	418.5	
		$\Delta E_r = -416 + 2.48$		0
4		$\Delta E_f = 465 + 2.48$	467.5	

№	Reaction	Calculation	ΔE, [kJ/mol]	
			fwrd	rev.
	$CH_3CH=CH_2 \rightarrow CH_3CH=\dot{C}H + \dot{H}$	$\Delta E_r = -465 + 2.48$		0
5	$CH_3\dot{C}HCH_3 \rightarrow CH_3CH=CH_2 + \dot{H}$	$\Delta E_f = 415.1 + 419.5 - 736.5 + 2.48$	100.6	
		$\Delta E_f = -415.1 - 419.5 + 736.5 + 2.48$		0
6	$CH_2=\ddot{C} \rightarrow CH\equiv\dot{C} + \dot{H}$	$\Delta E_f = 415.1 + 419.5 - 736.5 + 2.48$	385.9	
		$\Delta E_r = -415.1 - 419.5 + 736.5 + 2.48$		0
7 R78	$CH_3\ddot{C}H \rightarrow CH_2=\dot{C}H + \dot{H}$	$\Delta E_f = 384.2 + 378 - 688.1 + 2.48$	76.6	
		$\Delta E_r = -384.2 - 378 + 688.1 + 2.48$		0
8 R65	$CH_3\dot{C}H_2 \rightarrow CH_2=CH_2 + \dot{H}$	$\Delta E_f = 420.7 + 418.4 - 728.3 + 2.48$	113.3	
		$\Delta E_r = -420.7 - 418.4 + 728.3 + 2.48$		0
9 R79	$CH_2=CH_2 \rightarrow CH_2=\dot{C}H + \dot{H}$	$\Delta E_f = 465.2 + 2.48$	467.7	
		$\Delta E_r = -465.2 + 2.48$		0
10	$CH_2=\dot{C}H \rightarrow CH\equiv CH + \dot{H}$	$\Delta E_f = 464.7 + 688.1 - 966.6 + 2.48$	188.7	
		$\Delta E_r = -464.7 - 688.1 + 966.6 + 2.48$		0
11	$CH\equiv CH \rightarrow CH\equiv\dot{C} + \dot{H}$	$\Delta E_f = 556 + 2.48$	558.5	
		$\Delta E_r = -556 + 2.48$		0
12 R67	$CH_3CH_3 \rightarrow CH_3\dot{C}H_2 + \dot{H}$	$\Delta E_f = 420.6 + 2.48$	423.1	
		$\Delta E_r = -420.6 + 2.48$		0
13 R63	$\dot{C}H_3 \rightarrow \dot{C}H_2 + \dot{H}$	$\Delta E_f = 461.7 + 2.48$	464.2	
		$\Delta E_r = -461.7 + 2.48$		0
14 R64	$\dot{C}H_3 + \dot{H} \rightarrow CH_4$	$\Delta E_f = -439.3 + 2.48$	0	
		$\Delta E_r = 439.3 + 2.48$		441.8
15 R60	$CH_3CH_2CH_3 \rightarrow CH_3\dot{C}H_2 + \dot{C}H_3$	$\Delta E_f = 370.1 + 2.48$	372.6	
		$\Delta E_r = -370.1 + 2.48$		0

№	Reaction	Calculation	ΔE, [kJ/mol]	
			fwrd	rev.
16 R62	$CH_3CH_2\dot{C}H_2 \rightarrow CH_3\dot{C}H_2 + \dot{C}H_2$	$\Delta E_f = 408.6 + 2.48$	411.1	
		$\Delta E_f = -408.6 + 2.48$		0
17	$CH_3CH=CH_2 \rightarrow CH_3\dot{C}H + \dot{C}H_2$	$\Delta E_f = 736.5 + 2.48$	739.0	
		$\Delta E_r = -736.5 + 2.48$		0
18	$CH_3CH=CH_2 \rightarrow \dot{C}H_3 + \dot{C}H=CH_2$	$\Delta E_f = 426.4 + 2.48$	428.9	
		$\Delta E_r = -426.4 + 2.48$		0
19	$CH_3\dot{C}HCH_3 \rightarrow CH_3\ddot{C}H + \dot{C}H_3$	$\Delta E_f = 419.5 + 2.48$	423.0	
		$\Delta E_r = -419.5 + 2.48$		0
20 R66	$CH_3CH_3 \rightarrow \dot{C}H_3 + \dot{C}H_3$	$\Delta E_f = 377.3 + 2.48$	379.8	
		$\Delta E_r = -377.3 + 2.48$		0
21	$CH_2=CH_2 \rightarrow \ddot{C}H_2 + \ddot{C}H_2$	$\Delta E_f = 728.3 + 2.48$	730.8	
		$\Delta E_r = -728.3 + 2.48$		0
22	$CH_3\dot{C}H_2 \rightarrow \dot{C}H_3 + \ddot{C}H_2$	$\Delta E_f = 418.4 + 2.48$	420.9	
		$\Delta E_r = -418.4 + 2.48$		0
23	$CH_3\dot{C}HCH_3 \rightarrow CH_3CH_2\dot{C}H_2$	$\Delta E_f = 415.1 - 407.9 + 2.48$	9.7	
		$\Delta E_r = -415.1 + 407.9 + 2.48$		0
24	$CH_3\ddot{C}H \rightarrow CH_2=CH_2$	$\Delta E_f = 384.2 + 378 - 728.3 - 465.2 + 2.48$	0	
		$\Delta E_r = -384.2 - 378 + 728.3 + 465.2 + 2.48$		433.8
25 R73	$\dot{H} + \ddot{O} \rightarrow \dot{O}H$	$\Delta E_f = -429.9 + 2.48$	0	
		$\Delta E_r = 429.9 + 2.48$		432.4
26 R76	$\dot{H} + \dot{O}H \rightarrow H_2O$	$\Delta E_f = -497.1 + 2.48$	0	
		$\Delta E_r = 497.1 + 2.48$		499.6
27		$\Delta E_f = 497.1 - 429.9 + 2.48$	69.7	

№	Reaction	Calculation	ΔE, [kJ/mol]	
			fwrd	rev.
R75	$H_2O + \ddot{O} \rightarrow \dot{O}H + \dot{O}H$	$\Delta E_r = -497.1 + 429.9 + 2.48$		0
28 R70	$\dot{C}H_3 + \ddot{O} \rightarrow CH_3\dot{O}$	$\Delta E_f = -382.9 + 2.48$	0	
		$\Delta E_r = 382.9 + 2.48$		385.4
29 R69	$CH_3\dot{O} \rightarrow CH_2{=}O + \dot{H}$	$\Delta E_f = 393.7 + 382.9 - 747.6 + 2.48$	31.5	
		$\Delta E_r = -393.7 - 382.9 + 747.6 + 2.48$		0
30	$\ddot{C}H_2 + \ddot{O} \rightarrow CH_2{=}O$	$\Delta E_f = -747.6 + 2.48$	0	
		$\Delta E_r = 747.6 + 2.48$		750.1
31	$\ddot{\ddot{C}}H + \ddot{O} \rightarrow H\dot{C}{=}O$	$\Delta E_f = -804.2 + 2.48$	0	
		$\Delta E_r = 804.2 + 2.48$		806.7
32	$CH_2{=}O \rightarrow H\dot{C}{=}O + \dot{H}$	$\Delta E_f = 369 + 2.48$	371.5	
		$\Delta E_r = -369 + 2.48$		0
33	$H\dot{C}{=}O \rightarrow CO + \dot{H}$	$\Delta E_f = 63.2 + 804.2 - 1076.4 + 2.48$	0	
		$\Delta E_r = -63.2 - 804.2 + 1076.4 + 2.48$		211.5
34	$CH_2{=}O + \dot{H} \rightarrow \dot{C}H_2OH$	$\Delta E_f = 747.6 - 444.7 - 423.7 + 2.48$	0	
		$\Delta E_r = -747.6 + 444.7 + 423.7 + 2.48$		123.3
35 R81	$CH_2{=}O + \ddot{O} \rightarrow \dot{H} + HC(O)\dot{O}$	$\Delta E_f = 369 - 421.3 + 2.48$	0	
		$\Delta E_r = -369 + 421.3 + 2.48$		54.8
36	$\dot{C}H_2OH \rightarrow \dot{C}H_2 + \dot{O}H$	$\Delta E_f = 444.7 + 2.48$	447.2	
		$\Delta E_r = -444.7 + 2.48$		0
37	$H\dot{C}{=}O + \ddot{O} \rightarrow HC(O)\dot{O}$	$\Delta E_f = -421.3 + 2.48$	0	
		$\Delta E_r = 421.3 + 2.48$		423.8
38 R84	$CO + \ddot{O} \rightarrow O{=}C{=}O$	$\Delta E_f = 1076.4 - 2 \cdot 804.3 + 2.48$	0	
		$\Delta E_r = -1076.4 + 2 \cdot 804.3 + 2.48$		534.7

№	Reaction	Calculation	ΔE, [kJ/mol] fwrd	ΔE, [kJ/mol] rev.
39 R77	$CH_3CH{=}CH_2 + \ddot{O} \rightarrow CH_3\ddot{C}H + CH_2{=}O$	$\Delta E_f = 736.5 - 747.6 + 2.48$	0	
		$\Delta E_r = -736.5 + 747.6 + 2.48$		13.6
40	$CH_3\ddot{C}H + H\dot{C}{=}O \rightarrow CH_3CH{=}\dot{C}H + \ddot{O}$	$\Delta E_f = 804.2 - 696.5 + 2.48$	110.1	
		$\Delta E_r = -804.2 + 696.5 + 2.48$		0
R80	$CH_3\ddot{C}H + \dot{H} \rightarrow CH_3\dot{C}H_2$	$\Delta E_f = -465.4 + 2.48$	0	
		$\Delta E_r = 465.4 + 2.48$		467.9
41	$H_2 \rightarrow \dot{H} + \dot{H}$	$\Delta E_f = 436 + 2.48$	438.5	
		$\Delta E_r = -436 + 2.48$		0
42	$O_2 \rightarrow \ddot{O} + \ddot{O}$	$\Delta E_f = 498.4 + 2.48$	500.9	
		$\Delta E_r = -498.4 + 2.48$		0
43 R74	$H_2 + \ddot{O} \rightarrow \dot{O}H + \dot{H}$	$\Delta E_f = 436 - 429.9 + 2.48$	8.6	
		$\Delta E_r = -436 + 429.9 + 2.48$		0
44 R71	$H_2 + O_2 \rightarrow 2{\cdot}\dot{O}H$	$\Delta E_f = 436 + 498.4 - 2{\cdot}429.9 + 2.48$	77.1	
		$\Delta E_r = -436 - 498.4 + 2{\cdot}429.9 + 2.48$		0
45 R72	$H_2O + \dot{H} \rightarrow H_2 + \dot{O}H$	$\Delta E_f = 497.1 - 436 + 2.48$	63.6	
		$\Delta E_r = -497.1 + 436 + 2.48$		0
46	$H_2 + O_2 \rightarrow \dot{O}OH + \dot{H}$	$\Delta E_f = 436 + 498.4 - 429.9 - 274.2 + 2.48$	232.8	
		$\Delta E_r = -436 - 498.4 + 429.9 + 274.2 + 2.48$		0
47	$\dot{O}OH \rightarrow \dot{O}H + \dot{O}$	$\Delta E_f = 274.2 + 2.48$	276.7	
		$\Delta E_r = -274.2 + 2.48$		0
48	$\dot{O}OH + \dot{H} \rightarrow 2{\cdot}\dot{O}H$	$\Delta E_f = 274.2 - 429.9 + 2.48$	0	
		$\Delta E_r = -274.2 + 429.9 + 2.48$		158.2

№	Reaction	Calculation	ΔE, [kJ/mol]	
			fwrd	rev.
49	$H_2 + \dot{O}OH \rightarrow \dot{O}H + H_2O$	$\Delta E_f = 436 + 274.2 - 497.1 + 2.48$	215.6	
		$\Delta E_r = -436 - 274.2 + 497.1 + 2.48$		0
50	$\dot{H} + O_2 \rightarrow \dot{O}OH$	$\Delta E_f = 498.4 - 429.9 - 274.2 + 2.48$	0	
		$\Delta E_r = -498.4 + 429.9 + 274.2 + 2.48$		208.2
51	$H_2 + O_2 \rightarrow H_2O + \dot{O}$	$\Delta E_f = 436 + 498.4 - 497.1 + 2.48$	439.8	
		$\Delta E_r = -436 - 498.4 + 497.1 + 2.48$		0
52	$\dot{C}H_3 + \dot{O}H \rightarrow CH_3\dot{O} + \dot{H}$	$\Delta E_f = 429.9 - 382.9 + 2.48$	49.5	
		$\Delta E_r = -429.9 + 382.9 + 2.48$		0
53 R82	$HC(O)\dot{O} \rightarrow O{=}C{=}O + \dot{H}$	$\Delta E_f = -46 + 421.3 - 530.4 + 2.48$	0	
		$\Delta E_r = 46 - 421.3 + 530.4 + 2.48$		157.6
54	$\dot{C}(O)OH \rightarrow O{=}C{=}O + \dot{H}$	$\Delta E_f = 138 + 37.3 - 530.4 + 2.48$	0	
		$\Delta E_r = -138 - 37.3 + 530.4 + 2.48$		357.6
55 R83	$HC(O)\dot{O} \rightarrow CO + \dot{O}H$	$\Delta E_f = 1562.8 - 1076.4 - 429.9 + 2.48$	59.0	
		$\Delta E_r = -1562.8 + 1076.4 + 429.9 + 2.48$		0
56	$CO + H_2O \rightarrow \dot{C}(O)OH + \dot{H}$	$\Delta E_f = 1076.4 + 497.1 - 1216.2 + 2.48$	359.8	
		$\Delta E_r = -1076.4 - 497.1 + 1216.2 + 2.48$		0
57	$CO + \dot{O}H \rightarrow O{=}C{=}O + \dot{H}$	$\Delta E_f = 1076.4 + 429.9 - 2 \cdot 804.3 + 2.48$	0	
		$\Delta E_r = -1076.4 - 429.9 + 2 \cdot 804.3 + 2.48$		104.8
58	$CH{\equiv}CH + \ddot{O} \rightarrow \ddot{C}H + H\dot{C}{=}O$	$\Delta E_f = 966.6 - 804.2 + 2.48$	164.9	
		$\Delta E_r = -966.6 + 804.2 + 2.48$		0
59 R68	$CH_2{=}CH_2 + \ddot{O} \rightarrow \ddot{C}H_2 + CH_2{=}O$	$\Delta E_f = 728.3 - 747.6 + 2.48$	0	
		$\Delta E_r = -728.3 + 747.6 + 2.48$		21.8

For reaction № 53 $D(R_1\text{-}R_2) = D(HC(O)\dot{O}) = 2\Delta H_f^0(O) + \Delta H_f^0(C) + \Delta H_f^0(H) - \Delta H_f^0(HC(O)\dot{O}) = 1562.8$, as we do not have ΔH_f^0 (HC:Ȯ) and D(HC(=O)Ȯ); for reaction № 54 $D(R_1\text{-}R_2) = D(\dot{C}(O)OH) = \Delta H_f^0(O) + \Delta H_f^0(C) + \Delta H_f^0(\dot{O}H) - \Delta H_f^0(\dot{C}(O)OH) = 1216.2$, as we do not have ΔH_f^0 (Ċ:OH) and D(Ċ (=O)OH).

8.3 GRAPH OF REACTION

Every reaction mechanism can be described as system of connected objects - a graph [65]. We depict the chemical substance as the edge and reaction as the vertex (node). Then we need to introduce additional nodes - sources/outflows of a substance (an act or reaction of income or outcome).

On Fig. 8.3.1 we can see the graphs of the mechanism of hydrogen combustion taken from [84]. The chosen approach force us to know which molecule will exactly participate in which reaction. Thus we have three graphs for the same mechanism of reaction.

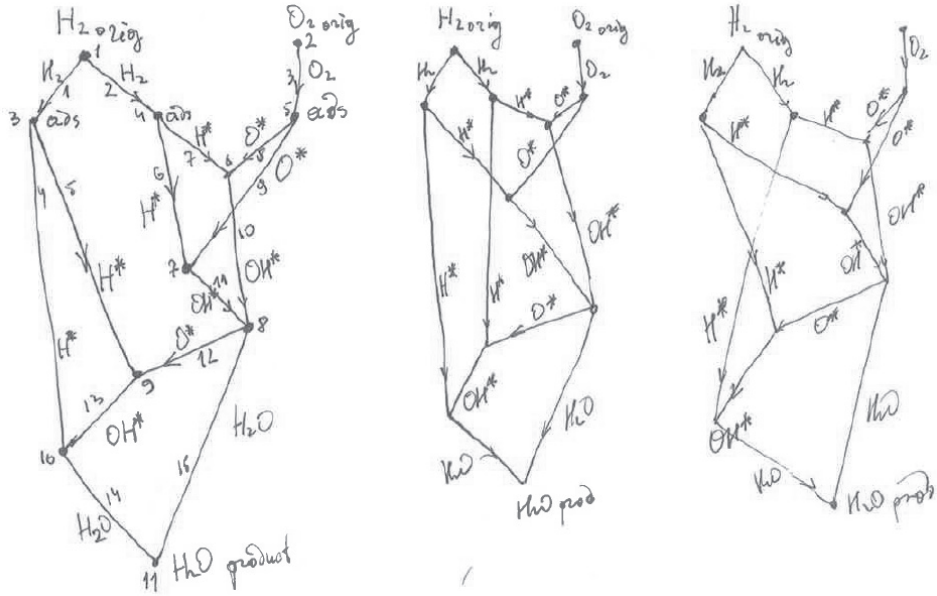

Fig. 8.3.1: Graphs of the mechanism of hydrogen combustion.

A graph can be represented by an adjacency matrix (the matrix where numbers of rows and columns represent the vertexes and the number placed on the cross of the row and column shows the amount of edges connecting appropriate vertexes; the row represents an origin vertex, the column represents an ending vertex for the edge).

Adjacency matrix for the first graph on Fig. 8.3.1:

vx	1	2	3	4	5	6	7	8	9	10	11
1	0	0	1	1	0	0	0	0	0	0	0
2	0	0	0	0	1	0	0	0	0	0	0
3	0	0	0	0	0	0	0	0	1	1	0
4	0	0	0	0	0	1	1	0	0	0	0
5	0	0	0	0	0	1	1	0	0	0	0
6	0	0	0	0	0	0	0	1	0	0	0
7	0	0	0	0	0	0	0	1	0	0	0
8	0	0	0	0	0	0	0	0	1	0	1
9	0	0	0	0	0	0	0	0	0	1	0
10	0	0	0	0	0	0	0	0	0	0	1
11	0	0	0	0	0	0	0	0	0	0	0

The adjacency matrix allows some analysis to be performed. Vertex with empty column (no incoming edges) - source of reagent; vertex with empty row (no outcoming edges) - outflow of product. So the number of empty columns is the number of reagents; the number of empty rows is the number of the products. The sum of the column elements for the vertex is the amount of moles in the left side of reaction; the sum of the row elements for the vertex is the amount of moles in the right side of reaction. For outflow the sum of the column elements is the amount of moles produced in the overall reaction; for source the sum of row elements is the amount of moles of initial reagents.

A graph can be represented by incidence matrix (the matrix where rows represent edges and columns represent vertexes; the number placed on the cross of the row and column shows the connection and direction of the connection between edge and vertex: –1 means that appropriate edge outcomes of the appropriate vertex, 1 means that appropriate edges incomes to the vertex).

Incidence matrix for the first graph on Fig. 8.3.1:

edg	vtx->	1	2	3	4	5	6	7	8	9	10	11
H2	**1**	–1	0	1	0	0	0	0	0	0	0	0
H2	**2**	–1	0	0	1	0	0	0	0	0	0	0
O2	**3**	0	–1	0	0	1	0	0	0	0	0	0

H*	**4**	0	0	−1	0	0	0	0	0	1	0
H*	**5**	0	0	−1	0	0	0	0	1	0	0
H*	**6**	0	0	0	−1	0	0	1	0	0	0	0
H*	**7**	0	0	0	−1	0	1	0	0	0	0	0
O*	**8**	0	0	0	0	−1	1	0	0	0	0	0
O*	**9**	0	0	0	0	−1	0	1	0	0	0	0
OH*	**10**	0	0	0	0	0	−1	0	1	0	0	0
OH*	**11**	0	0	0	0	0	0	−1	1	0	0	0
O*	**12**	0	0	0	0	0	0	0	−1	1	0	0
OH*	**13**	0	0	0	0	0	0	0	0	−1	1	0
H2O	**14**	0	0	0	0	0	0	0	0	0	−1	1
H2O	**15**	0	0	0	0	0	0	0	−1	0	0	1

If a vertex has only negative numbers in a column - it is a source of appropriate compound; if it has only positive numbers - it is outflow. The incidence matrix has similar properties as has the adjacency matrix.

Making summation of rows of similar substances we get the following incidence matrix (we entitle it D):

sbst	**vtx->**	**1**	**2**	**3**	**4**	**5**	**6**	**7**	**8**	**9**	**10**	**11**
H2	**1**	−2	0	1	1	0	0	0	0	0	0	0
O2	**2**	0	−1	0	0	1	0	0	0	0	0	0
H*	**3**	0	0	−2	−2	0	1	1	0	1	1	0
O*	**4**	0	0	0	0	−2	1	1	−1	1	0	0
OH*	**5**	0	0	0	0	0	−1	−1	2	−1	1	0
H2O	**6**	0	0	0	0	0	0	0	−1	0	−1	2

The matrix D is the matrix of reaction mechanism (here 2 moles of H_2 are produced in the first reaction (source) and 1 mole of it is consumed in the 3rd reaction and 1 mole in the 4th reaction (1st row in the matrix), etc.). Here the amount of identical columns - identical reactions - is the Horiuti stoichiometric number of this reaction in overall mechanism.

Combining similar reactions (columns) or discarding repeated reactions we get the following incidence matrix (entitled C):

sbst	**vtx->**	**1**	**2**	**3**	**4**	**5**	**6**	**7**	**8**

H2	**1**	−2	0	2	0	0	0	0	0
O2	**2**	0	−1	0	1	0	0	0	0
H*	**3**	0	0	−4	0	3	0	1	0
O*	**4**	0	0	0	−2	3	−1	0	0
OH*	**5**	0	0	0	0	−3	2	1	0
H2O	**6**	0	0	0	0	0	−1	−1	2

or:

sbst	**vtx->**	**1**	**2**	**3**	**4**	**5**	**6**	**7**	**8**
H2	**1**	−2	0	1	0	0	0	0	0
O2	**2**	0	−1	0	1	0	0	0	0
H*	**3**	0	0	−2	0	1	0	1	0
O*	**4**	0	0	0	−2	1	−1	0	0
OH*	**5**	0	0	0	0	−1	2	1	0
H2O	**6**	0	0	0	0	0	−1	−1	2

Then we can discard sources and outflows of substances which are supportive vertexes (vtx 1, 2 and 8) and we get incidence matrix (B):

sbst	**vtx->**	**1**	**2**	**3**	**4**	**5**
H2	**1**	1	0	0	0	0
O2	**2**	0	1	0	0	0
H*	**3**	−2	0	1	0	1
O*	**4**	0	−2	1	−1	0
OH*	**5**	0	0	−1	2	1
H2O	**6**	0	0	0	−1	−1

The matrix B is a matrix set of reactions constituting the overall mechanism (A):

1. H_2 -> 2*H*

2. O_2 -> 2*O*

3. H* + O* -> OH*

4. 2*OH* -> O* + H_2O

5. H* + OH* -> H_2O

Going in the opposite direction, starting with the set of supposed simple reactions and making transformations of matrices we can get all possible variants of the overall mechanism.

Algorithm:

1. Starting with supposed reactions (A) we make matrix of mechanism (B)

2. We multiply some of the columns by positive integers such that sum of every row become equal to 0 (except rows having only positive or only negative sign), in matrix B such rows are 3rd, 4th and 5th:

sbst	vtx->	1	2	3	4	5
H2	1	1	0	0	0	0
O2	2	0	1	0	0	0
H*	3	−2	0	1	0	1
O*	4	0	−2	1	−1	0
OH*	5	0	0	−1	2	1
H2O	6	0	0	0	−1	−1

We see that multiplying the 3rd column by 3 we reach the condition in 4th and 5th rows:

sbst	vtx->	1	2	3	4	5
H2	1	1	0	0	0	0
O2	2	0	1	0	0	0
H*	3	−2	0	3	0	1
O*	4	0	−2	3	−1	0
OH*	5	0	0	−3	2	1
H2O	6	0	0	0	−1	−1

But we still have a problem with 3rd row and multiplying 1st column by 2 we solve it:

sbst	vtx->	1	2	3	4	5
H2	1	2	0	0	0	0
O2	2	0	1	0	0	0
H*	3	−4	0	3	0	1

O*	**4**	0	−2	3	−1	0
OH*	**5**	0	0	−3	2	1
H2O	**6**	0	0	0	−1	−1

Multipliers that we used are the Horiuti numbers. There can exist different sets of multipliers.

3. We add columns (sources and outflows) such that every row has 0 in sum. Columns should have non-zero number only in one row:

sbst	**vtx->**			**1**	**2**	**3**	**4**	**5**	
H2	**1**	−2		2	0	0	0	0	
O2	**2**		1	0	1	0	0	0	
H*	**3**			−4	0	3	0	1	
O*	**4**			0	−2	3	−1	0	
OH*	**5**			0	0	−3	2	1	
H2O	**6**			0	0	0	−1	−1	2

Thus we get matrix C.

4. If some of the columns have numbers that can be divided by same integer, we divide it by this number and change initial column with this amount of new columns (for example, 3rd column is divided by 3, so we divide and replace initial one with 3 new columns):

sbst	**vtx->**				**1**	**2**	**3**			**4**	**5**	
H2	**1**	−2	0	2	0	0	0	0	0	0	0	0
O2	**2**	0	1	0	1	0	0	0	0	0	0	0
H*	**3**	0	0	−4	0	1	1	1	0	0	1	0
O*	**4**	0	0	0	−2	1	1	1	0	−1	0	0
OH*	**5**	0	0	0	0	−1	−1	−1	0	2	1	0
H2O	**6**	0	0	0	0	0	0	0	0	−1	−1	2

We do the same with column titled "1st" and get the matrix D.

5. We divide every row in a such way that new rows produced from initial have only two non-zero numbers, one "-1" and one "1". Many variants are possible. And these will be all possible mechanisms of the reaction.

Dividing H_2 row (from matrix D) gives 1 variant (two molecules of H_2 going from reaction 1 are identical and it does not matter which of them goes to reaction 3 and which to reaction 4):

sbst	vtx->	1	2	3	4	5	6	7	8	9	10	11
H2	1	−1	0	1	0	0	0	0	0	0	0	0
	2	−1	0	0	1	0	0	0	0	0	0	0

Dividing H* row gives 4 variants:

(1)

sbst	vtx->	1	2	3	4	5	6	7	8	9	10	11
H*	4	0	0	−1	0	0	1	0	0	0	0	0
	5	0	0	−1	0	0	0	1	0	0	0	0
	6	0	0	0	−1	0	0	0	0	1	0	0
	7	0	0	0	−1	0	0	0	0	0	1	0

(2)

sbst	vtx->	1	2	3	4	5	6	7	8	9	10	11
H*	4	0	0	−1	0	0	0	0	0	1	0	0
	5	0	0	−1	0	0	0	0	0	0	1	0
	6	0	0	0	−1	0	1	0	0	0	0	0
	7	0	0	0	−1	0	0	1	0	0	0	0

(3)

sbst	vtx->	1	2	3	4	5	6	7	8	9	10	11
H*	4	0	0	−1	0	0	1	0	0	0	0	0
	5	0	0	−1	0	0	0	0	0	1	0	0
	6	0	0	0	−1	0	0	1	0	0	0	0
	7	0	0	0	−1	0	0	0	0	0	1	0

(4)

sbst	vtx->	1	2	3	4	5	6	7	8	9	10	11
H*	4	0	0	−1	0	0	1	0	0	0	0	0
	5	0	0	−1	0	0	0	0	0	0	1	0
	6	0	0	0	−1	0	0	1	0	0	0	0
	7	0	0	0	−1	0	0	0	0	1	0	0

Dividing O* row gives 3 variants:

(1)

sbst	vtx->	1	2	3	4	5	6	7	8	9	10	11
O*	8	0	0	0	0	−1	1	0	0	0	0	0
	9	0	0	0	0	−1	0	1	0	0	0	0
	10	0	0	0	0	0	0	0	−1	1	0	0

(2)

sbst	vtx->	1	2	3	4	5	6	7	8	9	10	11
O*	8	0	0	0	0	−1	1	0	0	0	0	0
	9	0	0	0	0	−1	0	0	0	1	0	0
	10	0	0	0	0	0	0	1	−1	0	0	0

(3)

sbst	vtx->	1	2	3	4	5	6	7	8	9	10	11
O*	8	0	0	0	0	−1	0	0	0	1	0	0
	9	0	0	0	0	−1	0	1	0	0	0	0
	10	0	0	0	0	0	1	0	−1	0	0	0

Dividing OH* row gives 3 variants

(1)

sbst	vtx->	1	2	3	4	5	6	7	8	9	10	11

OH*	**11**	0	0	0	0	0	−1	0	1	0	0	0
	12	0	0	0	0	0	0	−1	1	0	0	0
	13	0	0	0	0	0	0	0	0	−1	1	0

(2)

sbst	**vtx->**	**1**	**2**	**3**	**4**	**5**	**6**	**7**	**8**	**9**	**10**	**11**
OH*	**11**	0	0	0	0	0	−1	0	1	0	0	0
	12	0	0	0	0	0	0	0	1	−1	0	0
	13	0	0	0	0	0	0	−1	0	0	1	0

(3)

sbst	**vtx->**	**1**	**2**	**3**	**4**	**5**	**6**	**7**	**8**	**9**	**10**	**11**
OH*	**11**	0	0	0	0	0	0	0	1	−1	0	0
	12	0	0	0	0	0	0	−1	1	0	0	0
	13	0	0	0	0	0	−1	0	0	0	1	0

Dividing H_2O row gives 1 variant:

sbst	**vtx->**	**1**	**2**	**3**	**4**	**5**	**6**	**7**	**8**	**9**	**10**	**11**
H2O	**14**	0	0	0	0	0	0	0	−1	0	0	1
	15	0	0	0	0	0	0	0	0	0	−1	1

Here we can discard some of the variants because in our case substances are identical (f.e. we have 2 molecules of H_2 participating and they both are identical) and some of different variants are actually the same. This is the case for variant (2) of H* which is identical to variant (1) and can be discarded.

If we suppose that a substance which is product in some reaction can not be the reagent in the same reaction or in the reaction before (for example: H + [O] -> OH; OH + OH -> H2O + {O}, {O} can not be [O]) we discard such variants. They are seen clearly when we have the matrix of the mechanism and have pairs of rows with opposite numbers in it:

(0 1 0 −1 0

0 −1 0 1 0)

Thus we can discard variants 2, 3 of O* and 2, 3 of OH*.

Thus we have only 3 different variants in H* flows and only 3 different reaction mechanisms.

This algorithm can be easily implemented in a computer program to operate with big complicated mechanisms.

This approach gives the possibility to automate the search of possible variants of reaction mechanisms; using the methods of graph theory it is possible to make topological characterization of the reaction mechanisms, searching for cycles or shortest pathways in complicated mechanisms.

The graphical representation is convenient for illustration of mechanisms, especially in isotopic research. This graph method can be useful for description of the mechanisms determined by spatial factors or for surface reactions mechanisms where free movement of species over surface is limited and relative disposition of reacting species is important.

This graph can be transformed to bipartite graph (graph where all vertexes are of two types) by shrinking together edges of one type and forming one common vertex out of them (this will be vertexes of type - substance, and we already have vertexes of type - reaction). The theory on using bipartite graphs for description of nonlinear mechanisms was widely developed [65].

8.4 LAYERS OF CATALYST PARTICLES IN REACTOR TUBE

Here we describe the geometry of ideal round particles of the catalyst placed in a tubular reactor.

Symbols used in calculations:

d - diameter of the particle

D - inner diameter of the reactor

N_{sph} - the amount of spherical catalyst particles in a probe

n_{sph} - the amount of spheres in one layer perpendicular to reactor axis and mixture feed

$n_{sph.hex}$ - the amount of spheres in one layer laying in hexagonal inscribed into circle(reactor tube)

$n_{sph.ad}$ - the amount of spheres in one layer laying between hexagonal and circle (reactor tube)

$n_{ad.l}$ - the amount of layers of spheres laying between hexagonal and circle

h_{cat} - the length of the catalyst bed in reactor (height of catalyst layer)

Schemes used in calculations are given on Figs. 8.4.1-8.4.4.

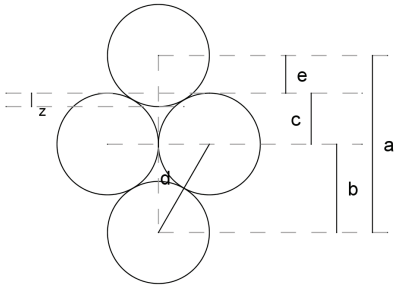

Fig. 8.4.1: Dimensions between close particles in layer.

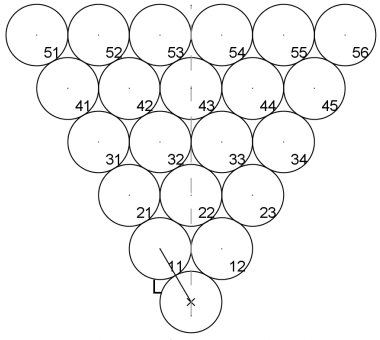

Fig. 8.4.2: Indexes of rows and spheres in the 1/6 part of hexagonal.

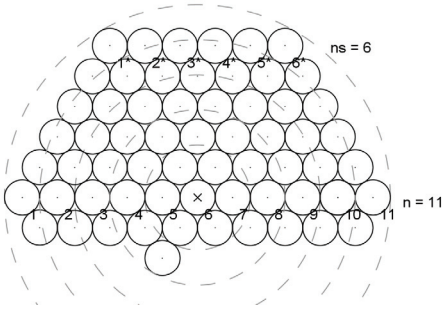

Fig. 8.4.3: Hexagonals formed by spheres placed in circles (reactor walls)

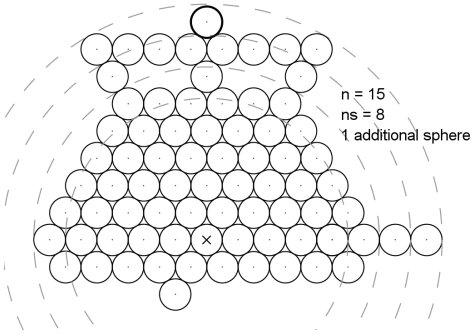

Fig. 8.4.4: Appearance of one additional sphere over side of hexagonal inscribed into circle

$$n_{sph}=n_{sph.hex}+6\cdot n_{sph.ad};$$

$$n=\frac{D}{d},\quad \textit{round til lesser odd integer};\qquad (8.4.1)$$

$$n_{sph.hex}=\frac{1}{4}\cdot\left(3\cdot n^2+1\right);$$

$$n_s=\frac{n+1}{2};$$

$$n_{ad.l}=\frac{(D-d)\cdot(2-\sqrt{3})}{2\cdot\sqrt{3}\cdot d},\quad \textit{round til lesser integer};$$

$$x=n_s+i,\ i\in[1,2\ldots n_{ad.l}];\qquad (8.4.2)$$

$$y=\frac{x+1}{2}-\frac{1}{2}\cdot\sqrt{\left(\frac{D}{d}-1\right)^2-3\cdot(x-1)^2}=\frac{x+1}{2}-\frac{1}{2}\cdot\sqrt{(n-1)^2-3\cdot(x-1)^2},\ \textit{round til greater integer};$$

$$n_{sph.ad}=n_{ad.l}\cdot(n_s+2)+\frac{1}{2}\cdot n_{ad.l}\cdot(n_{ad.l}+1)-2\cdot\sum_{i=1}^{n_{ad.l}} y;$$

$$n_{lr}=\frac{N_{sph}}{n_{sph}};\qquad (8.4.3)$$

$$h_{cat}=d\cdot\left(1+\frac{\sqrt{3}}{2}\cdot(n_{lr}-1)\right);$$

$$S(x)=\sum_{x=0}^{h_{cat}}\sum_{n_l=1}^{n_{lr}}\pi\cdot\left(r^2-\left(x+\sqrt{3}\cdot r\cdot(1-n_l)-r\right)^2\right)\cdot n_{sph}\qquad (8.4.4)$$

S_{max}, S_{min} - cross sectional area of the catalyst.

$$S_{max}=\pi\cdot r^2\cdot n_{sph};$$
$$S_{min}=\pi\cdot\left(r^2-r^2\cdot\left(\sqrt{3}-1\right)^2\right)\cdot n_{sph};\qquad (8.4.5)$$

The number of channels parallel to the gas feed residing between the particles of the layer perpendicular to the feed:

$$n_{chnl}=6\cdot\left(n_s-1+n_{ad.l}\right)+6\cdot\left(2\cdot n_{sph.ad}-n_{ad.l}\right)+\frac{3}{2}\cdot n^2-3\cdot n+\frac{3}{2}$$
$$=6\cdot\left(n_s-1+2\cdot n_{sph.ad}\right)+\frac{3}{2}\cdot n^2-3\cdot n+\frac{3}{2};\qquad (8.4.6)$$

Volume occupied by particles in the catalyst layer with cross section S_r and length l [85] and free volume:

$$S_r=\frac{\pi\cdot D^2}{4};$$
$$V_r=S_r\cdot l;$$
$$V_{sph}=\frac{\pi\cdot d^3}{6};\qquad (8.4.7)$$
$$V_{cat}=V_{sph}\cdot N_{sph};$$
$$V_{free}=V_r-V_{cat};$$

8.5 PFR MODEL EQUATION

We have a tubular reactor and a way of simulating it is to represent the reactor volume as a series of n stirred tanks (CSTR). As a practical matter, the conversion for a series of stirred tanks approaches a PFR for $n > 6$ ([78], p.19-9).

Every stirred tank is a part of tubular reactor with appropriate characteristics. But as soon as reaction goes with change in volume and at constant pressure the volumetric velocity changes. Stirred tanks are continuously connected and we keep the length of tank constant and residence time in tanks is different.

Taking 10 CSTR and V_{free} from (8.4.7) or from (8.5.4):

$$
\begin{aligned}
&l=\frac{L}{10};\\
&V_{free.CSTR}=V_{free.CSTR}(l)=\frac{\pi\cdot D^2}{4}\cdot l-\frac{\pi\cdot d^3}{6}\cdot N_{sph}(l);\\
&V_{free}=V_{cat}\cdot\frac{\epsilon}{1-\epsilon}=\frac{m_{cat}}{\rho_{cat}}\cdot\frac{\epsilon}{1-\epsilon};\qquad V_{free.CSTR}=\frac{m_{cat}}{10\cdot\rho_{cat}}\cdot\frac{1}{}\\
&\tau_1=\frac{V_{free.CSTR}}{V_0^{'}};\qquad \tau_2=\frac{V_{free.CSTR}}{V_1^{'}};
\end{aligned}
\qquad (8.5.1)
$$

Designating δ_a as the increase in the total mol per mol decrease of substance A according to the stoichiometric equation ([86], p.7-5):

$$\delta_a=\frac{\nu_c+\nu_d+\ldots-\nu_a-\nu_b-\ldots}{\nu_a};$$

$$V_0^{'}=\frac{n_{t_0}^{'}\cdot R\cdot T}{P};\qquad n_{t_0}^{'}=\frac{V_0^{'}\cdot P}{R\cdot T};\qquad n_{a_0}^{'}=n_{t_0}^{'}\cdot Y_{a_0};\qquad n_{t_1}^{'}=n_{t_0}^{'}+\delta_a\cdot\left(n_{a_0}^{'}-n_a^{'}\right.$$

$$
\begin{aligned}
&\frac{V_1^{'}\cdot P}{R\cdot T}=\frac{V_0^{'}\cdot P}{R\cdot T}+\delta_a\cdot\left(\frac{V_0^{'}\cdot P}{R\cdot T}\cdot Y_{a_0}-\frac{V_1^{'}\cdot P}{R\cdot T}\cdot Y_{a_1}\right);\\
&V_1^{'}=V_0^{'}+\delta_a\cdot\left(V_0^{'}\cdot Y_{a_0}-V_1^{'}\cdot Y_{a_1}\right)=V_0^{'}+\delta_a\cdot V_0^{'}\cdot Y_{a_0}-\delta_a\cdot V_1^{'}\cdot Y_{a_1};\\
&V_1^{'}\cdot\left(1+\delta_a\cdot Y_{a_1}\right)=V_0^{'}+\delta_a\cdot V_0^{'}\cdot Y_{a_0};\\
&V_1^{'}=\frac{\left(V_0^{'}+\delta_a\cdot V_0^{'}\cdot Y_{a_0}\right)}{\left(1+\delta_a\cdot Y_{a_1}\right)}=V_0^{'}\cdot\frac{\left(1+\delta_a\cdot Y_{a_0}\right)}{\left(1+\delta_a\cdot Y_{a_1}\right)};
\end{aligned}
\qquad (8.5.2)
$$

where V' - volumetric rate

If we keep *l* constant, we find time which elementary volume will spend in next tank with length l by (8.5.1).

The mass conservation equation for CSTR is ([78], p.19-8, p.7-12) and using (8.5.2):

$$V_0^{'}\cdot C_{a_0}=V_1^{'}\cdot C_{a_1}+V_r\cdot r(C,T)+V_r\cdot\frac{dC}{dt};$$

$$n_a^{'}=V^{'}\cdot C_a;\qquad n_a^{'}=\frac{V^{'}\cdot P}{R\cdot T}\cdot Y_a;\qquad C_a=\frac{P}{R\cdot T}\cdot Y_a;$$

$$V_0^{'}\cdot\frac{P}{R\cdot T}\cdot Y_{a_0}=V_1^{'}\cdot\frac{P}{R\cdot T}\cdot Y_{a_1}+V_r\cdot r(C,T)+V_r\cdot\frac{P}{R\cdot T}\cdot$$

$$\frac{dY_a}{dt}=\frac{V_0^{'}\cdot Y_{a_0}-V_1^{'}\cdot Y_{a_1}}{V_r}-\frac{R\cdot T}{P}\cdot r(C,T); \qquad (8.5.3)$$

$$t=\frac{V_r}{V^{'}};$$

$$\frac{dY_a}{dt}=\frac{1}{t}\cdot\left(Y_{a_0}-\frac{\left(1+\delta_a\cdot Y_{a_0}\right)}{\left(1+\delta_a\cdot Y_{a_1}\right)}\cdot Y_{a_1}\right)-\frac{R\cdot T}{P}\cdot r(C,T);$$

where r(C,T) - rate of reaction of component A per unite volume. We need transform the reaction rate from rate moles per second per volume to rate molecules per second per active site (starting with (8.5.3)):

$$\frac{dY_a}{dt}=\frac{1}{t}\cdot\left(Y_{a_0}-\frac{\left(1+\delta_a\cdot Y_{a_0}\right)}{\left(1+\delta_a\cdot Y_{a_1}\right)}\cdot Y_{a_1}\right)-\frac{R\cdot T}{P}\cdot r(C,T);$$

$$r(C,T)=\frac{n_{mol}}{t\cdot V_{free}};\qquad V_{free}=V_r-V_{cat};\qquad V_{cat}=(1-\epsilon)\cdot V_r;$$

$$\epsilon=\frac{V_{free}}{V_r},\quad thus:\qquad V_{free}=\frac{V_{cat}}{1-\epsilon}-V_{cat}=V_{cat}\cdot\frac{\epsilon}{1-\epsilon};$$

$$r(C,T)=\frac{n_{mol}}{t\cdot V_{cat}}\cdot\frac{1-\epsilon}{\epsilon};\qquad V_{cat}=\frac{m_{cat}}{\rho_{cat}};\qquad m_{cat}=\frac{S_{cat}}{S_t};$$

$$S_{cat}=\frac{n_{sites}}{C_t};\quad thus:\qquad V_{cat}=\frac{S_{cat}}{\rho_{cat}\cdot S_t}=\frac{n_{sites}}{\rho_{cat}\cdot S_t\cdot C_t};\qquad (8.5.4)$$

$$r(C,T)=\frac{n_{mol}\cdot\rho_{cat}\cdot S_t\cdot C_t}{t\cdot n_{sites}}\cdot\frac{1-\epsilon}{\epsilon};\qquad n_{mol}=\frac{n_{molec}}{N_A};$$

$$r_{per.site}(C,T)=\frac{n_{molec}}{t\cdot n_{sites}};\qquad r(C,T)=r_{per.site}(C,T)\cdot\frac{\rho_{cat}\cdot S_t\cdot C_t}{N_A}\cdot\frac{1-\epsilon}{\epsilon};$$

$$\frac{dY_a}{dt}=\frac{1}{t}\cdot\left(Y_{a_0}-\frac{\left(1+\delta_a\cdot Y_{a_0}\right)}{\left(1+\delta_a\cdot Y_{a_1}\right)}\cdot Y_{a_1}\right)-\frac{R\cdot T}{P}\cdot r_{per.site}(C,T)\cdot\frac{\rho_{cat}\cdot S_t\cdot C_t}{N_A}\cdot\frac{1-\epsilon}{\epsilon},$$

Here S_t - specific surface area of catalyst (metal plus support, [m^2/kg]), it can be measured by N_2-sorption experiments. ρ_{cat} - density of catalyst (metal plus support), it can be calculated:

$$\rho_{me}=\frac{m_{me}}{V_{me}};\qquad \rho_{sup}=\frac{m_{sup}}{V_{sup}};\qquad \rho_{cat}=\frac{m_{me}+m_{sup}}{V_{me}+V_{sup}};$$

$$\rho_{cat}=\frac{m_{me}+m_{sup}}{V_{me}+V_{sup}}=\frac{m_{me}+m_{sup}}{\frac{m_{me}}{\rho_{me}}+\frac{m_{sup}}{\rho_{sup}}}=\frac{\rho_{me}\cdot\rho_{sup}\cdot(m_{me}+m_{sup})}{m_{me}\cdot\rho_{sup}+m_{sup}\cdot\rho_{me}};\qquad (8.5.5)$$

$$m_{me}=y_{wt}\cdot m;\qquad m=m_{me}+m_{sup};$$

$$\rho_{cat}=\frac{\rho_{me}\cdot\rho_{sup}\cdot m}{y_{wt}\cdot m\cdot\rho_{sup}+(1-y_{wt})\cdot m\cdot\rho_{me}}=\frac{\rho_{me}\cdot\rho_{sup}}{y_{wt}\cdot\rho_{sup}+(1-y_{wt})\cdot\rho_{me}};$$

where y_{wt} - weight fraction of the metal.

Porosity ε can be calculated through ρ_{cat} (8.5.5) and measured pore volume V_{por}([cm^3/g]):

$$\epsilon = \frac{V_{free}}{V_{free}+V_{cat}}; \quad V_{por}\left[\frac{m^3}{kg}\right] = \frac{V_{free}}{m_{cat}} = \frac{V_{free}}{\rho_{cat}\cdot V_{cat}};$$
$$\epsilon = \frac{V_{free}}{V_{free}+\frac{V_{free}}{\rho_{cat}\cdot V_{por}}} = \frac{1}{\frac{\rho_{cat}\cdot V_{por}+1}{\rho_{cat}\cdot V_{por}}} = \frac{\rho_{cat}\cdot V_{por}}{\rho_{cat}\cdot V_{por}+1}; \qquad (8.5.6)$$

C_t - active site density on the catalyst surface (cm^{-2}) (overall - metal plus support) can be described as:

$$C_t = \frac{n_{sites}}{S_{cat}}; \quad C_{t.me} = \frac{n_{sites}}{S_{me}}; \quad S_t = \frac{S_{cat}}{m_{cat}};$$
$$C_t = \frac{n_{sites}/m_{cat}}{S_{cat}/m_{cat}} = \frac{n_{sites}/m_{cat}}{S_t}; \quad C_{t.me} = \frac{n_{sites}/m_{me}}{S_{t.me}};$$
$$m_{me} = y_{wt}\cdot m_{cat}; \quad C_{t.me} = \frac{n_{sites}/(y_{wt}\cdot m_{cat})}{S_{t.me}}; \quad \frac{n_{sites}}{m_{cat}} = C_{t.me}\cdot S_{t.me}\cdot y_{wt}; \qquad (8.5.7)$$
$$C_t = \frac{C_{t.me}\cdot S_{t.me}\cdot y_{wt}}{S_t};$$

$C_{t.me}$ - active site density on the metal surface (cm^{-2}) (table data), $S_{t.me}$ - specific surface area of the metal (cm^2/g metal) (measured [8]). Active site density on the metal surface can be calculated from crystal lattice parameters.

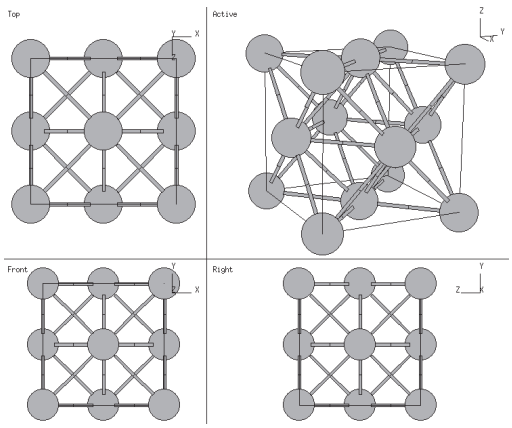

Fig. 8.5.1: The Face-Centered Cubic (A1) Lattice ([87])

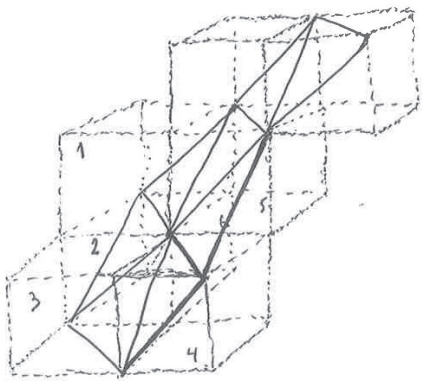

Fig. 8.5.2: Combined units forming (111) plane

Complete atom in the corner is formed by six units, complete atom on the cube face is formed by two units (Fig. 8.5.2). Thus for (111) plane in one crystal unit we have ([85], p. 183):

$$n_{atom}=3\cdot\frac{1}{6}+3\cdot\frac{1}{2}=2\,;$$

$$S_{(111)}=\sqrt{p\cdot(p-a)\cdot(p-b)\cdot(p-c)}\,;\qquad p=\frac{a+b+c}{2}\,;\qquad a=b=c=a_{cub}\cdot\sqrt{2}\,; \tag{8.5.8}$$

$$S_{(111)}=\sqrt{\frac{3\cdot\sqrt{2}}{2}\cdot a_{cub}\cdot\left(\frac{3\cdot\sqrt{2}}{2}\cdot a_{cub}-a_{cub}\cdot\sqrt{2}\right)\cdot\left(\frac{3\cdot\sqrt{2}}{2}\cdot a_{cub}-a_{cub}\cdot\sqrt{2}\right)\cdot\left(\frac{3\cdot\sqrt{2}}{2}\cdot a_{cub}-a_{cub}\cdot\sqrt{2}\right)}=\frac{\sqrt{3}}{2}\cdot a_{cub}^2\,;$$

Active site density on the metal surface:

$$C_{t.me}=\frac{n_{atom}}{S_{(111)}}=\frac{4}{\sqrt{3}\cdot a_{cub}^2}\left[\frac{1}{\mathring{A}^2}\right]=\frac{4\cdot10^{20}}{\sqrt{3}\cdot a_{cub}^2}\left[\frac{1}{m^2}\right]; \tag{8.5.9}$$

where a_{cub} is a lattice constant [Å] from Table 8.1.2.2. The active site here is one atom of an element. Given a_{cub} = 3.924 Å for Pt, $C_{t.me}$ = $1.5\cdot10^{19}$ 1/m^2. This is in agreement with data from [88] (p. 318), where surface area occupied by each surface atom in metallic Pt for plane {111} is given as 0.0666 nm^2 (rescaling to atoms per area gives $1.5\cdot10^{19}$ 1/m^2 as well).

The final formula is:

$$\frac{dY_a}{dt}=\frac{1}{t}\cdot\left(Y_{a_0}-\frac{\left(1+\delta_a\cdot Y_{a_0}\right)}{\left(1+\delta_a\cdot Y_{a_1}\right)}\cdot Y_{a_1}\right)-\frac{R\cdot T}{P}\cdot\frac{\rho_{cat}\cdot C_{t.me}\cdot S_{t.me}\cdot y_{wt}}{N_A}\cdot\frac{1-\epsilon}{\epsilon}\cdot r_{per.site}(C,T); \quad (8.5.10)$$

where ρ_{cat} calculated by (8.5.5), $C_{t.me}$ by (8.5.9), $S_{t.me}$ - measured, y_{wt} - measured, ε calculated by (8.5.6). The formula similar to (8.5.10) is used in [50].

This formula is useful when the reaction is known. If we have system with many reactions and final rout is unknown, we can use such derivation:

$$\frac{dn_a}{dt}=\frac{1}{t}\cdot\left(n_{a_{out}}-n_{a_{in}}\right)-\frac{n_{tot}^{in}\cdot R\cdot T}{P}\cdot r(C,T)\quad a);$$
$$\frac{dn_a}{dt}=\frac{n_{tot}^{in}\cdot R\cdot T}{P}\cdot r(C,T)\quad b); \quad (8.5.11)$$

where b) is for steady state conditions.

As we have gas-phase and surface reactions, we can use formula:

$$\frac{dY_a}{dt}=\frac{1}{t}\cdot\left(Y_{a_0}-\frac{\left(1+\delta_a\cdot Y_{a_0}\right)}{\left(1+\delta_a\cdot Y_{a_1}\right)}\cdot Y_{a_1}\right)-\frac{R\cdot T}{P}\cdot r(C,T)-\frac{R\cdot T}{P}\cdot\frac{\rho_{cat}\cdot C_{t.me}\cdot S_{t.me}\cdot y_{wt}}{N_A}\cdot\frac{1-\epsilon}{\epsilon}\cdot r_{per.site}(C,T); \quad (8.5.12)$$

or

$$\frac{dn_a}{dt}=\frac{n_{tot}^{in}\cdot R\cdot T}{P}\cdot r(C,T)+\frac{n_{tot}^{in}\cdot R\cdot T}{P}\cdot\frac{\rho_{cat}\cdot C_{t.me}\cdot S_{t.me}\cdot y_{wt}}{N_A}\cdot\frac{1-\epsilon}{\epsilon}\cdot r_{per.site}(C,T); \quad (8.5.13)$$

As we describe the reactor as a row of ten CSTRs the amount of active sites for every separate CSTR is ten times less appropriately:

$$\frac{dn_a}{dt}=\frac{n_{tot}^{in}\cdot R\cdot T}{P}\cdot r(C,T)+\frac{n_{tot}^{in}\cdot R\cdot T}{P}\cdot\frac{\rho_{cat}\cdot C_{t.me}\cdot S_{t.me}\cdot y_{wt}}{N_{CSTRs}\cdot N_A}\cdot\frac{1-\epsilon}{\epsilon}\cdot r_{per.site}(C,T); \quad (8.5.14)$$

8.6 MATLAB CODE

8.6.1 EQUILIBRIUM CONVERSION OF PROPANE

For the calculation of propane conversion versus temperature the Matlab code divided into three files was used (*commmon.m*, *propequat.m*, *propanequil.m*). *commmon.m* contains basic parameters such as thermodynamic properties, physical constants, reaction conditions; *propanequil.m* contains control code with calculation of equilibrium constant, plotting results; *propequat.m* contains equation which is to be solved in order to find equilibrium conversion.

PROPANEQUIL.M:

```
clear all
global KpT1 P
commmon;
P = 1; % pressure [atm]

for i=1:1:size(T,2)
    S_tott = S(i,:);
    S_tot = struct('H_', S_tott(1), 'H2', S_tott(2), 'CH3CH2CH3', S_tott(3),
'CH3CH2C_H2', S_tott(4), 'CH3CHdCH2', S_tott(5), 'O_', S_tott(6), 'O2',
S_tott(7), 'O_H', S_tott(8), 'H2O', S_tott(9),       'C_H', S_tott(10),  'CH4',
S_tott(11),  'CO', S_tott(12),   'CO2', S_tott(13),  'CH2dC_', S_tott(14),
'CH3CH3', S_tott(15), 'C_H2CHdCH2', S_tott(16), 'CH3O_', S_tott(17),
'CH3C_HCH3', S_tott(18), 'C_H3', S_tott(19), 'CH3C_H2', S_tott(20), 'C_H2',
S_tott(21), 'C_', S_tott(22), 'CH2dCH2', S_tott(23), 'CH2dC_H', S_tott(24),
'CHtCH', S_tott(25),  'HC_dO', S_tott(26), 'CH2dO', S_tott(27), 'CH3CH2C_H',
S_tott(28), 'CH3CHdC_H', S_tott(29), 'CHtC_', S_tott(30), 'CH3C_H',
S_tott(31), 'HCOO_', S_tott(32));
    clear  S_tott

    DGr = 1000*(dHf.CH3CHdCH2(i) + dHf.H2(i) - dHf.CH3CH2CH3(i)) -
T(i)*(S_tot.CH3CHdCH2 + S_tot.H2 - S_tot.CH3CH2CH3); % Gibb's energy
    KpT1 = exp(-(DGr)/(R*T(i))); % equilibrium constant
    x0 = 0.1;
    [x1,fval1] = fsolve(@propequat,x0); % solve the equation in propequat.m
and find equilibrium conversion
    eqConv1(i) = x1;
end

plot((T-273), eqConv1);
```

PROPEQUAT.M:

```
function F = propequat(x0)
global KpT1 P
```

```
F = (x0^2) * (KpT1 + P) - KpT1;
```

COMMMON.M:

```
%CONSTANTS
    R = 8.3146;         %[J/(K*mol)]    Gas constant
    kB = 1.380658e-23; %[J/K]           Boltzmann constant
    Na = 6.0221367e23; %[1/mol]         Avogadro constant
    h = 6.6262755e-34; %[Js]            Planck constant

    Mr = MolarMass({'H' 'H2' 'C3H8' 'C3H7' 'C3H6' 'O' 'O2' 'OH' 'H2O' 'CH'
'CH4' 'CO' 'CO2' 'C2H2' 'C2H6' 'C3H5' 'CH3O' 'C3H7' 'CH3' 'C2H5' 'CH2' 'C'
'C2H4' 'C2H3' 'C2H2' 'HCO' 'CH2O' 'C3H6' 'C3H5' 'C2H' 'C2H4' 'HCO2'});  %
function  MolarMass is used for calculation of masses of compaunds

    Po = 10^5;              %Pa    stand pressure
    To = 298.15;            %K   stand temperature
    Ptot=101325;            %[Pa] Total pressure
    Dhdrtlc = 2122;         %hydrotalcite density kg/m3
    ywt = 0.01;             %weight fraction of metall
    Vpor = 0.17*10^(-3);    % m3/kg volume of pores  from [8]
    StMe = 1.36*10^3;       % m2/kg metallic surface
    mcat = 0.15*10^(-3);    % kg  mass of cat
    V0 = 50*10^(-6)/60;     %m3/s = 50 ml/min

    nTot = Ptot*V0/(R*To);

% Gas-phase fractions in initial mixture
      Y0_CH3CH2C_H2   = 0;  %   32   'CH3CH2C.H2'
      Y0_CH3C_H2      = 0;  %   33   'CH3C.H2'
      Y0_CH3C_H       = 0;  %   34   'CH3C:H'
      Y0_CH2dC_H      = 0;  %   35   'CH2=C.H'
      Y0_C_H2         = 0;  %   36   'C:H2'
      Y0_C_H3         = 0;  %   37   'C.H3'
      Y0_H_           = 0;  %   38   'H.'
      Y0_O_           = 0;  %   39   'O:'
      Y0_O_H          = 0;  %   40   'O.H'
      Y0_CH3O_        = 0;  %   41   'CH3O.'
      Y0_HCOO_        = 0;  %   42   'HC(O)O.'
      Y0_CH2dO_       = 0;  %   43   'CH2=O'
      Y0_CH4          = 0;  %   44   'CH4'
      Y0_CH3CH3       = 0;  %   45   'CH3CH3'
      Y0_CH2dCH2      = 0;  %   46   'CH2=CH2'
      Y0_H2           = 0;%   47   'H2'
      Y0_O2           = 0;%   48   'O2'
      Y0_H2O          = 0;  %   49   'H2O'
      Y0_CO           = 0;  %   50   'CO'
      Y0_CO2          = 0;  %   51   'CO2'
      Y0_CH3CH2CH3    = 1/5;%   52   'CH3CH2CH3'
      Y0_CH3CHdCH2    = 0;  %   53   'CH3CH=CH2'
      Y0_N2           = 4/5;  %      'N2'

 %ThermoBuild is used for producing data
%http://www.grc.nasa.gov/WWW/CEAWeb/ceaThermoBuild.htm

%temperature interval
T=[273 278   283   288   293  298  298.15  303  308  313  318  323  328  333
   378 383   388   393   398  403  408  413  418  423  428  433  438  443
```

```
   493 498    503    508    513  518  523  528  533  538  543  548  553  558
   608 613    618    623    628  633  638  643  648  653  658  663  668  673
   723 728    733    738    743  748  753  758  763  768  773  778  783  788
                                        ....
   903 908    913    918    923  928  933  938  943  948  953  958  963 ....];

%thermodynamic properties (each row corresponds to appropriate temperature in
vector T):

%S     , J/mol-K
   %H_        H2           CH3CH2CH3  CH3CH2C_H2  CH3CHdCH2  O_   O2
   %1         2            3             4        5          6      7
S=[112.886   128.149      264.050      283.515  261.164  159.123  202.565
   113.263   128.669      265.306      284.733  262.270  159.523  203.097
   113.634   129.180      266.556      285.945  263.370  159.915  203.619
   113.998   129.684      267.801      287.152  264.463  160.300  204.133
   114.356   130.179      269.042      288.353  265.552  160.678  204.638
   114.707   130.667      270.278      289.550  266.635  161.049  205.135
                                       .....
   139.197   165.236      411.707      422.120  385.861  186.112  242.455
   139.304   165.391      412.594      422.930  386.595  186.220  ....... ];

% transformation of the matrix to struct (for more convenient usage)

SS = struct('H_', S(:,1), 'H2', S(:,2), 'CH3CH2CH3', S(:,3), 'CH3CH2C_H2',
S(:,4), 'CH3CHdCH2', S(:,5), 'O_', S(:,6), 'O2', S(:,7), 'O_H', S(:,8), 'H2O',
S(:,9), 'C_H', S(:,10), 'CH4', S(:,11),'CO', S(:,12), 'CO2', S(:,13),
      'CH2dC_', S(:,14), 'CH3CH3', S(:,15), 'C_H2CHdCH2', S(:,16), 'CH3O_',
S(:,17), 'CH3C_HCH3', S(:,18), 'C_H3', S(:,19), 'CH3C_H2', S(:,20), 'C_H2',
S(:,21), 'C_', S(:,22), 'CH2dCH2', S(:,23), 'CH2dC_H', S(:,24),  'CHtCH',
S(:,25),  'HC_dO', S(:,26), 'CH2dO', S(:,27), 'CH3CH2C_H', S(:,28),
'CH3CHdC_H', S(:,29), 'CHtC_', S(:,30), 'CH3C_H',  S(:,31), 'HCOO_', S(:,32));

%delta Hf
%kJ/mol
      %C_    H_           C_H2         C_H3   CH2dC_H      CH2dCH2
      CH3C_H2
      %1    2            3            4           5            6
       7
dHcom =[716.359     217.837      390.415  146.990  300.143  53.303  119.634
      716.425      217.870      390.407  146.925  300.053  53.144  119.440
      716.489      217.902      390.397  146.859  299.963  52.984  119.246
      716.553      217.934      390.387  146.793  299.872  52.824  119.051
      716.616      217.966      390.376  146.727  299.781  52.664  118.858
      716.678      217.998      390.365  146.660  299.690  52.505  118.664
                                       ......
      719.507      222.065      386.277  138.675  289.737  38.546  101.857
      719.504      222.094      386.244  138.634  289.685  38.494  .....];

dHf = struct('C_', dHcom(:,1), 'H_', dHcom(:,2), 'C_H2', dHcom(:,3), 'C_H3',
dHcom(:,4), 'CH2dC_H', dHcom(:,5), 'CH2dCH2', dHcom(:,6), 'CH3C_H2',
dHcom(:,7), 'CH3CHdCH2', dHcom(:,8), 'CH3CH2C_H2', dHcom(:,9),    'CH3C_HCH3',
dHcom(:,10), 'CH3CH2CH3', dHcom(:,11), 'H2', dHcom(:,12), 'O_', dHcom(:,13),
'O2', dHcom(:,14), 'O_H', dHcom(:,15), 'H2O', dHcom(:,16), 'C_H', dHcom(:,17),
'CH4', dHcom(:,18), 'CO', dHcom(:,19), 'CO2', dHcom(:,20), 'CH2dC_',
dHcom(:,21), 'CH3CH3', dHcom(:,22), 'C_H2CHdCH2', dHcom(:,23), 'CH3O_',
dHcom(:,24), 'CH3CH2C_H', dHcom(:,25), 'CH3CHdC_H', dHcom(:,26), 'CH3C_HC_H2',
dHcom(:,27), 'CH3C_HC_H', dHcom(:,28), 'CH3C_H', dHcom(:,29),  'C_H2C_H2',
dHcom(:,30), 'C_H2C_H', dHcom(:,31), 'C_HdC_H', dHcom(:,32), 'CHtCH',
dHcom(:,33), 'CHtC_', dHcom(:,34), 'C_H2O_', dHcom(:,35), 'CH2dO',
```

```
dHcom(:,36), 'HC_dO', dHcom(:,37), 'HCOO_', dHcom(:,38), 'C_dOO_',
dHcom(:,39), 'C_dO', dHcom(:,40));
clear dHcom;

% density kg/m3
        % Al    Be      Cr      Cu      Au      Ir      Fe      Pb      Mo
        % 1     2       3       4       5       6       7       8       9
Dens = [2710 3610   7140   8951   19340  22520  7870   11380  10250
       2710   3610   7140   8951   19340  22520  7870   11380  10250
       2710   3610   7140   8951   19340  22520  7870   11380  10250
       2710   3610   7140   8951   19340  22520  7870   11380  10250
       2710   3610   7140   8951   19340  22520  7870   11380  10250
       2710   3610   7140   8951   19340  22520  7870   11380  10250
                                    .....
       2591   0             7040   8686   18860  22250  7690   10430  10160
       2591   0             7040   8686   18860  22250  7690   10430  10160 ...];
```

MOLARMASS.M:

```
function [Mr]= MolarMass(name)
format short;

%%%%%%%%%%%%%%%%%%%%%%%%%%%%%%%%%%%%%%%%%%%%%%%%%%%%%%%%%%%%%%%%%%%%%%%
% http://www.chem.qmul.ac.uk/iupac/AtWt/
% ATOMIC WEIGHTS OF THE ELEMENTS 2007
% The table is based on the 2005 table at Pure Appl. Chem., 78, 2051-2066
(2006)
% with 2007 changes to the values for lutetium, molybdenum, nickel, ytterbium
and zinc.
% Mass number of the longest-lived isotope of hassium from Phys. Rev. Lett.,
97 242501 (2006)
% %%%%%%%%%%%%%%%%%%%%%%%%%%%%%%%%%%%%%%%%%%%%%%%%%%%%%%%%%%%%%%%%%%%%%%%

     % 1     2       3     4      5     6    7        8     9     10
Name={'H'    'He'   'Li'   'Be'   'B'    'C'    'N'    'O'    'F'    'Ne'... %1
      'Na'   'Mg'   'Al'   'Si'   'P'    'S'    'Cl'   'Ar'   'K'    'Ca'... %2
      'Sc'   'Ti'   'V'    'Cr'   'Mn'   'Fe'   'Co'   'Ni'   'Cu'   'Zn'... %3
      'Ga'   'Ge'   'As'   'Se'   'Br'   'Kr'   'Rb'   'Sr'   'Y'    'Zr'... %4
      'Nb'   'Mo'   'Tc'   'Ru'   'Rh'   'Pd'   'Ag'   'Cd'   'In'   'Sn'... %5
      'Sb'   'Te'   'I'    'Xe'   'Cs'   'Ba'   'La'   'Ce'   'Pr'   'Nd'... %6
      'Pm'   'Sm'   'Eu'   'Gd'   'Tb'   'Dy'   'Ho'   'Er'   'Tm'   'Yb'... %7
      'Lu'   'Hf'   'Ta'   'W'    'Re'   'Os'   'Ir'   'Pt'   'Au'   'Hg'... %8
      'Tl'   'Pb'   'Bi'   'Po'   'At'   'Rn'   'Fr'   'Ra'   'Ac'   'Th'... %9
      'Pa'   'U'    'Np'   'Pu'   'Am'   'Cm'   'Bk'   'Cf'   'Es'   'Fm'... %10
      'Md'   'No'   'Lr'   'Rf'   'Db'   'Sg'   'Bh'   'Hs'   'Mt'   'Ds'... %11
      'Rg'   'Uub'  'Uut'  'Uuq'  'Uup'  'Uuh'  'Uuo'};                     %12

% ATOMIC WEIGHTS OF THE ELEMENTS

AWOTE=[1.00794              %H     Hydrogen
       4.002602             %He Helium
       6.941                %Li Lithium
       9.012182             %Be Beryllium
       10.811               %B     Boron
       12.0107              %C     Carbon
       14.0067              %N      Nitrogen
       15.9994               %O      Oxygen
       18.9984032           %F      Fluorine
       20.1797             %Ne     Neon
```

```
                    ......
        204.3833            %Tl   Thallium
        207.2               %Pb   Lead
        208.98040           %Bi   Bismuth
        209                 %Po   Polonium
        210                 %At   Astatine
                    .......
        281                 %Ds   Darmstadtium
        280                 %Rg   Roentgenium
        285                 %Uub  Ununbium            !!! doesn't work
        284                 %Uut  Ununtrium            !!! doesn't work
        289                 %Uuq  Ununquadium           !!! doesn't work
        288                 %Uup  Ununpentium           !!! doesn't work
        293                 %Uuh  Ununhexium           !!! doesn't work
        294];          %Uuo      Ununoctium           !!! doesn't work

 sz = size(name);
 Mr=zeros(1, sz(2));

 for i=1:1:sz(2)
     subst = char(name(1,i));
     UPPER = isstrprop(subst, 'upper');
     LOWER = isstrprop(subst, 'lower');
     NUMBE = isstrprop(subst, 'digit');

     sf=size(subst);
     for j=1:1:sf(2)
         if UPPER(1,j) == 1
             if j == sf(2)                   %nothing after
                 Mr(1,i) = Mr(1,i) + AWOTE(strmatch(subst(1,j), Name,
'exact'), 1);
             elseif UPPER(1,j+1) == 1        %big after
                 Mr(1,i) = Mr(1,i) + AWOTE(strmatch(subst(1,j), Name,
'exact'), 1);
             end
         elseif LOWER(1,j) == 1              %small
             if j == sf(2)                   %nothing after
                 Mr(1,i) = Mr(1,i) + AWOTE(strmatch(strcat(subst(1,j-1),
subst(1,j)), Name, 'exact'), 1);
             elseif UPPER(1,j+1) == 1        %big after
                 Mr(1,i) = Mr(1,i) + AWOTE(strmatch(strcat(subst(1,j-1),
subst(1,j)), Name, 'exact'), 1);
             end
         elseif NUMBE(1,j) == 1              %number
             if UPPER(1,j-1) == 1            %big previous
                 Mr(1,i) = Mr(1,i) +
str2num(subst(1,j))*AWOTE(strmatch(subst(1,j-1), Name, 'exact'), 1);
             elseif LOWER(1,j-1) == 1         %small previous
                 Mr(1,i) = Mr(1,i) +
str2num(subst(1,j))*AWOTE(strmatch(strcat(subst(1,j-2), subst(1,j-1)), Name,
'exact'), 1);
             end
         end
     end
 end
```

8.6.2 GRAPH SCHEME

For the plotting of a reaction graph scheme (Fig. 3.1.3.1) the following Matlab code (file *reactPath.m*) was used.

REACTPATH.M:

```
clear all

%% initial data
% number of the node; nodes which are reactions (number of reaction and
activation
% energies forward/reverse) and compounds
% number   1           2            3            4            5            6

% nodes:   'R1 125/0', 'R2 125/0', 'R3 125/0', 'R4 125/0', 'R5 125/0', 'R6
125/0',
% number   ...
% nodes:   ...
% number   96           97                  98              99 ...
% nodes:   'R96 125/0', 'R97 125/0', 'CH3CH2CH3', 'CH3CH2C*H3', ...
% number     144          145    146    147  148     149        150
% nodes:     'HC(O)O.', 'H2O*', 'H2O', 'C*O', 'CO', 'O*=C=O*', 'CO2'

% construction of the graph matrix
% syntax :  GraphMatrix(NodeOut,NodeIn)
GraphMatrix = zeros(147);

GraphMatrix(96, 1) = 1; GraphMatrix(1, 97) = 1; GraphMatrix(96,  2) = 1;
GraphMatrix(2, 98) = 1; GraphMatrix(97, 3) = 1; GraphMatrix(3, 98) = 1;
GraphMatrix(97,  4) = 1; GraphMatrix(4, 99) = 1; GraphMatrix(98,  5) = 1;
GraphMatrix(5, 100) = 1; GraphMatrix(99,  6) = 1; GraphMatrix(6, 100) = 1;
GraphMatrix(97, 7) = 1; GraphMatrix(7, 106) = 1; GraphMatrix(7, 122) = 1;
GraphMatrix(98, 8) = 1; GraphMatrix(8, 106) = 1; GraphMatrix(8, 122) = 1;
GraphMatrix(99, 9) = 1; GraphMatrix(9, 106) = 1; GraphMatrix(9, 120) = 1;
GraphMatrix(100, 10) = 1; GraphMatrix(10, 106) = 1; GraphMatrix(10, 120) = 1;
GraphMatrix(100, 11) = 1; GraphMatrix(11, 101) = 1; GraphMatrix(100, 12) = 1;
GraphMatrix(12, 102) = 1; GraphMatrix(99, 13) = 1; GraphMatrix(13, 102) = 1;
GraphMatrix(101, 14) = 1; GraphMatrix(14, 102) = 1; GraphMatrix(102, 15) = 1;
GraphMatrix(15, 104) = 1; GraphMatrix(101, 16) = 1; GraphMatrix(16, 104) = 1;
GraphMatrix(102, 17) = 1; GraphMatrix(17, 114) = 1; GraphMatrix(17, 122) = 1;
GraphMatrix(102, 18) = 1; GraphMatrix(18, 103) = 1; GraphMatrix(106, 19) = 1;
GraphMatrix(19, 112) = 1; GraphMatrix(120, 20) = 1; GraphMatrix(20, 112) = 1;
GraphMatrix(120, 21) = 1; GraphMatrix(21, 122) = 1; GraphMatrix(106, 22) = 1;
GraphMatrix(22, 110) = 1; GraphMatrix(122, 23) = 1; GraphMatrix(23, 110) = 1;
GraphMatrix(122, 24) = 1; GraphMatrix(24, 124) = 1; GraphMatrix(110, 25) = 1;
GraphMatrix(25, 111) = 1; GraphMatrix(124, 26) = 1; GraphMatrix(26, 125) = 1;
GraphMatrix(112, 27) = 1; GraphMatrix(27, 113) = 1; GraphMatrix(112, 28) = 1;
GraphMatrix(28, 114) = 1; GraphMatrix(114, 29) = 1; GraphMatrix(29, 116) = 1;
GraphMatrix(116, 30) = 1; GraphMatrix(30, 117) = 1; GraphMatrix(117, 31) = 1;
GraphMatrix(31, 119) = 1; GraphMatrix(31, 118) = 1; GraphMatrix(119, 32) = 1;
GraphMatrix(32, 118) = 1; GraphMatrix(32, 128) = 1; GraphMatrix(126, 33) = 1;
GraphMatrix(33, 127) = 1; GraphMatrix(127, 34) = 1; GraphMatrix(34, 128) = 1;
GraphMatrix(130, 35) = 1; GraphMatrix(35, 131) = 1; GraphMatrix(131, 36) = 1;
GraphMatrix(36, 132) = 1; GraphMatrix(132, 37) = 1; GraphMatrix(127, 37) = 1;
GraphMatrix(37, 128) = 1; GraphMatrix(37, 134) = 1; GraphMatrix(134, 38) = 1;
GraphMatrix(38, 132) = 1; GraphMatrix(38, 142) = 1; GraphMatrix(128, 39) = 1;
GraphMatrix(132, 39) = 1; GraphMatrix(39, 134) = 1; GraphMatrix(128, 40) = 1;
```

```
GraphMatrix(134, 40) = 1; GraphMatrix(40, 142) = 1; GraphMatrix(127, 41) = 1;
GraphMatrix(134, 41) = 1; GraphMatrix(41, 128) = 1; GraphMatrix(41, 142) = 1;
GraphMatrix(142, 42) = 1; GraphMatrix(42, 143) = 1; GraphMatrix(132, 43) = 1;
GraphMatrix(122, 43) = 1; GraphMatrix(43, 136) = 1; GraphMatrix(122, 44) = 1;
GraphMatrix(134, 44) = 1; GraphMatrix(44, 136) = 1; GraphMatrix(136, 45) = 1;
GraphMatrix(118, 45) = 1; GraphMatrix(45, 122) = 1; GraphMatrix(45, 144) = 1;
GraphMatrix(132, 46) = 1; GraphMatrix(104, 46) = 1; GraphMatrix(46, 108) = 1;
GraphMatrix(46, 139) = 1; GraphMatrix(119, 47) = 1; GraphMatrix(132, 47) = 1;
GraphMatrix(47, 139) = 1; GraphMatrix(108, 48) = 1; GraphMatrix(120, 48) = 1;
GraphMatrix(48, 102) = 1; GraphMatrix(108, 49) = 1; GraphMatrix(49, 106) = 1;
GraphMatrix(139, 50) = 1; GraphMatrix(50, 144) = 1; GraphMatrix(144, 51) = 1;
GraphMatrix(132, 51) = 1; GraphMatrix(51, 146) = 1; GraphMatrix(118, 52) = 1;
GraphMatrix(132, 52) = 1; GraphMatrix(52, 144) = 1; GraphMatrix(144, 53) = 1;
GraphMatrix(134, 53) = 1; GraphMatrix(53, 146) = 1; GraphMatrix(139, 54) = 1;
GraphMatrix(132, 54) = 1; GraphMatrix(54, 140) = 1; GraphMatrix(140, 55) = 1;
GraphMatrix(55, 144) = 1; GraphMatrix(55, 134) = 1; GraphMatrix(140, 56) = 1;
GraphMatrix(56, 146) = 1; GraphMatrix(144, 57) = 1; GraphMatrix(57, 145) = 1;
GraphMatrix(146, 58) = 1; GraphMatrix(58, 147) = 1; GraphMatrix(96, 59) = 1;
GraphMatrix(59, 105) = 1; GraphMatrix(96, 60) = 1; GraphMatrix(60, 107) = 1;
GraphMatrix(60, 123) = 1; GraphMatrix(105, 61) = 1; GraphMatrix(61, 103) = 1;
GraphMatrix(105, 62) = 1; GraphMatrix(62, 107) = 1; GraphMatrix(62, 121) = 1;
GraphMatrix(121, 63) = 1; GraphMatrix(129, 63) = 1; GraphMatrix(63, 123) = 1;
GraphMatrix(123, 64) = 1; GraphMatrix(129, 64) = 1; GraphMatrix(64, 125) = 1;
GraphMatrix(107, 65) = 1; GraphMatrix(65, 113) = 1; GraphMatrix(123, 66) = 1;
GraphMatrix(66, 111) = 1; GraphMatrix(107, 67) = 1; GraphMatrix(67, 111) = 1;
GraphMatrix(113, 68) = 1; GraphMatrix(133, 68) = 1; GraphMatrix(68, 121) = 1;
GraphMatrix(68, 138) = 1; GraphMatrix(138, 69) = 1; GraphMatrix(129, 69) = 1;
GraphMatrix(69, 137) = 1; GraphMatrix(123, 70) = 1; GraphMatrix(133, 70) = 1;
GraphMatrix(70, 137) = 1; GraphMatrix(126, 71) = 1; GraphMatrix(130, 71) = 1;
GraphMatrix(71, 135) = 1; GraphMatrix(135, 72) = 1; GraphMatrix(126, 72) = 1;
GraphMatrix(72, 143) = 1; GraphMatrix(72, 129) = 1; GraphMatrix(129, 73) = 1;
GraphMatrix(133, 73) = 1; GraphMatrix(73, 135) = 1; GraphMatrix(135, 74) = 1;
GraphMatrix(129, 74) = 1; GraphMatrix(74, 126) = 1; GraphMatrix(74, 133) = 1;
GraphMatrix(135, 75) = 1; GraphMatrix(75, 143) = 1; GraphMatrix(75, 133) = 1;
GraphMatrix(129, 76) = 1; GraphMatrix(135, 76) = 1; GraphMatrix(76, 143) = 1;
GraphMatrix(103, 77) = 1; GraphMatrix(133, 77) = 1; GraphMatrix(77, 109) = 1;
GraphMatrix(77, 138) = 1; GraphMatrix(11, 78) = 1; GraphMatrix(78, 115) = 1;
GraphMatrix(115, 79) = 1; GraphMatrix(79, 113) = 1; GraphMatrix(109, 80) = 1;
GraphMatrix(80, 107) = 1; GraphMatrix(138, 81) = 1; GraphMatrix(133, 81) = 1;
GraphMatrix(81, 141) = 1; GraphMatrix(141, 82) = 1; GraphMatrix(82, 147) = 1;
GraphMatrix(141, 83) = 1; GraphMatrix(83, 135) = 1; GraphMatrix(83, 145) = 1;
GraphMatrix(145, 84) = 1; GraphMatrix(133, 84) = 1; GraphMatrix(84, 147) = 1;
GraphMatrix(99, 85) = 1; GraphMatrix(85, 105) = 1; GraphMatrix(106, 86) = 1;
GraphMatrix(86, 107) = 1; GraphMatrix(108, 87) = 1; GraphMatrix(87, 109) = 1;
GraphMatrix(114, 88) = 1; GraphMatrix(88, 115) = 1; GraphMatrix(122, 89) = 1;
GraphMatrix(89, 123) = 1; GraphMatrix(120, 90) = 1; GraphMatrix(90, 121) = 1;
GraphMatrix(128, 91) = 1; GraphMatrix(91, 129) = 1; GraphMatrix(132, 92) = 1;
GraphMatrix(92, 133) = 1; GraphMatrix(134, 93) = 1; GraphMatrix(93, 135) = 1;
GraphMatrix(136, 94) = 1; GraphMatrix(94, 137) = 1; GraphMatrix(140, 95) = 1;
GraphMatrix(95, 141) = 1;

NodeID = {'R1 0/72', 'R2 0/11', 'R3 61/0', 'R4 88/12', 'R5 73/6', 'R6 52/0',
'R7 100/0', 'R8 70/11', 'R9 115/0', 'R10 89/15', 'R11 59/83', 'R12 0/43', 'R13
0/17', 'R14 0/104', 'R15 66/47', 'R16 34/79', 'R17 80/11', 'R18 12/0', 'R19
9/2', 'R20 0/157', 'R21 26/108', 'R22 56/43', 'R23 5/75', 'R24 2/96', 'R25
11/0', 'R26 70/0', 'R27 11/0', 'R28 63/52', 'R29 70/0', 'R30 109/11', 'R31
92/155', 'R32 22/159', 'R33 0/27', 'R34 40/88', 'R35 0/44', 'R36 5/173', 'R37
36/63', 'R38 0/111', 'R39 84/64', 'R40 0/110',  'R41 0/96', 'R42 40/0', 'R43
35/75', 'R44 22/81', 'R45 0/143', 'R46 60/70', 'R47 0/199', 'R48 0/158', 'R49
28/108', 'R50 0/233', 'R51 0/85', 'R52 18/209', 'R53 0/64', 'R54 26/87', 'R55
0/106', 'R56 0/139', 'R57 98/0', 'R58 15/0', 'R59 426/0', 'R60 373/0', 'R61
```

```
83/0', 'R62 411/0', 'R63 0/464', 'R64 0/442', 'R65 113', 'R66 0/380', 'R67
0/423', 'R68 0/22', 'R69 0/32', 'R70 0/385', 'R71 77/0', 'R72 0/64', 'R73
0/432', 'R74 0/9', 'R75 0/70', 'R76 0/500', 'R77 0/14', 'R78 77/0', 'R79
0/468', 'R80 0/468', 'R81 0/55', 'R82 0/158', 'R83 59/0', 'R84 0/535', 'R85
164/0', 'R86 163/0', 'R87 293/0', 'R88 210/0', 'R89 159/0', 'R90 283/0', 'R91
255/0', 'R92 356/0', 'R93 161/0', 'R94 171/0', 'R95 163/0', 'CH3CH2CH3',
'CH3CH2C*H3', 'CH3C*H2C*H3', 'CH3CH2C***H2', 'CH3C*H2C***H2', 'CH3C*H2C***H',
'CH3C*H=C*H2', 'CH3CH=CH2', 'CH3C*H=C***H', 'CH3CH2C.H2', 'CH3C***H2',
'CH3C.H2',  'CH3C***H', 'CH3C:H', 'C*H3C*H3', 'CH3CH3', 'C*H2=C*H2',
'CH2=CH2', 'C*H2=C***H', 'CH2=C.H', 'C*H/=/C*H', 'CH/=/C***', 'C***', 'C***H',
'C***H2', 'C:H2', 'C***H3', 'C.H3', 'C*H4', 'CH4', 'H2', 'H*H*', 'H***', 'H.',
'O2', 'O*O*', 'O***', 'O:', 'O***H', 'O.H',
 'CH3O***', 'CH3O.', 'CH2=O', 'HC***=O', 'HC(O)O***', 'HC(O)O.', 'H2O*',
'H2O', 'C*O', 'CO', 'O*=C=O*', 'CO2'};

%construction of a graph
GRaPH = biograph(GraphMatrix, NodeID, 'LayoutType', 'hierarchical');

%% formatting the view
NodeReact = {'R1 0/72', 'R2 0/11', 'R3 61/0', 'R4 88/12', 'R5 73/6', 'R6
52/0', 'R7 100/0', 'R8 70/11', 'R9 115/0', 'R10 89/15', 'R11 59/83', 'R12
0/43', 'R13 0/17', 'R14 0/104', 'R15 66/47', 'R16 34/79', 'R17 80/11', 'R18
12/0', 'R19 9/2', 'R20 0/157',  'R21 26/108', 'R22 56/43', 'R23 5/75', 'R24
2/96', 'R25 11/0', 'R26 70/0', 'R27 11/0', 'R28 63/52', 'R29 70/0', 'R30
109/11',  'R31 92/155', 'R32 22/159', 'R33 0/27', 'R34 40/88', 'R35 0/44',
'R36 5/173', 'R37 36/63', 'R38 0/111', 'R39 84/64', 'R40 0/110',  'R41 0/96',
'R42 40/0', 'R43 35/75', 'R44 22/81', 'R45 0/143', 'R46 60/70', 'R47 0/199',
'R48 0/158', 'R49 28/108', 'R50 0/233',  'R51 0/85', 'R52 18/209', 'R53 0/64',
'R54 26/87', 'R55 0/106', 'R56 0/139', 'R57 98/0', 'R58 15/0', 'R59 426/0',
'R60 373/0',  'R61 83/0', 'R62 411/0', 'R63 0/464', 'R64 0/442', 'R65 113',
'R66 0/380', 'R67 0/423', 'R68 0/22', 'R69 0/32', 'R70 0/385',  'R71 77/0',
'R72 0/64', 'R73 0/432', 'R74 0/9', 'R75 0/70', 'R76 0/500', 'R77 0/14', 'R78
77/0', 'R79 0/468', 'R80 0/468',  'R81 0/55', 'R82 0/158', 'R83 59/0', 'R84
0/535', 'R85 164/0', 'R86 163/0', 'R87 293/0', 'R88 210/0', 'R89 159/0', 'R90
283/0',  'R91 255/0', 'R92 356/0', 'R93 161/0', 'R94 171/0', 'R95 163/0'};
NodeCompounds = {'CH3CH2CH3', 'CH3CH2C*H3', 'CH3C*H2C*H3',  'CH3CH2C***H2',
'CH3C*H2C***H2', 'CH3C*H2C***H', 'CH3C*H=C*H2', 'CH3CH=CH2', 'CH3C*H=C***H',
'CH3CH2C.H2', 'CH3C***H2', 'CH3C.H2',  'CH3C***H', 'CH3C:H', 'C*H3C*H3',
'CH3CH3', 'C*H2=C*H2', 'CH2=CH2', 'C*H2=C***H', 'CH2=C.H', 'C*H/=/C*H',
'CH/=/C***', 'C***', 'C***H', 'C***H2', 'C:H2', 'C***H3', 'C.H3', 'C*H4',
'CH4', 'H2', 'H*H*', 'H***', 'H.', 'O2', 'O*O*', 'O***', 'O:', 'O***H', 'O.H',
'CH3O***', 'CH3O.', 'CH2=O', 'HC***=O', 'HC(O)O***', 'HC(O)O.', 'H2O*', 'H2O',
'C*O', 'CO', 'O*=C=O*', 'CO2'};

for i=1:1:size(NodeReact,2)
    NodeRhandles = getnodesbyid(GRaPH, NodeReact(i));
    set(NodeRhandles, 'Shape', 'ellipse', 'Size', [5, 5], 'Color', [0.9, 0.9,
0.9], 'LineColor', [1, 1, 1], 'FontSize', 8);
end
for i=1:1:size(NodeCompounds,2)
    NodeChandles = getnodesbyid(GRaPH, NodeCompounds(i));
    set(NodeChandles, 'Shape', 'ellipse', 'Size', [5, 5], 'Color', [1, 1, 1],
'LineColor', [1, 1, 1], 'FontSize', 8);
end

%% display a graph
view(GRaPH);
```

8.6.3 REACTION MODEL

The code used for the model description and simulation is based on a sample code, which was obtained at the course "Modelling of Catalytic Reactions" of prof. De Chen. The code is divided into three files (*comb_v5.m*, *comb_Ecalc_v5.m*, *comb_difer_v5.m*), where *comb_v5.m* contains main code, *comb_Ecalc_v5.m* contains the adsorption heats as well as activation energies calculation, *comb_difer_v5.m* contains the system of differential equations. Here the files *commmon.m* and *molarmass.m* (see Ch. 8.6.1) are used as well.

COMB_V5.M:

```
clear all
global n0 tau T Ptot Po ntot R  i Na kf kr Ct St pCat ywt eps n0N2 KpT1 Nstp

t1=now; % counter for time of code execution

%%---------------------
commmon; % input parameters
%%---------------------

for i=1:1:size(T,2) % temperature

    %-------------------------------------------------------------------
 % ACTIVATION ENERGIES AND PREEXPONENTIAL FACTORS OF ELEMENTARY STEPS
    [Ef,Er] = comb_Ecalc_v5(i, dHf); % activation energies

    S_3D = R*(1.5*log(Mr)+2.5*log(T(i))-log(Ptot/101325)-1.1650); %   Sakur-
Tetrode
    S_tott = S(i,:);
    S_locc = S_tott - S_3D;

    % entropy S_tot - gas phase ; S_loc - on surface
       S_tot = struct('H_', S_tott(1), 'H2', S_tott(2), 'CH3CH2CH3', S_tott(3),
'CH3CH2C_H2', S_tott(4), 'CH3CHdCH2', S_tott(5), 'O_', S_tott(6), 'O2',
S_tott(7), 'O_H', S_tott(8), 'H2O', S_tott(9),       'C_H', S_tott(10),  'CH4',
S_tott(11),  'CO', S_tott(12),   'CO2', S_tott(13),  'CH2dC_', S_tott(14),
'CH3CH3', S_tott(15), 'C_H2CHdCH2', S_tott(16), 'CH3O_', S_tott(17),
'CH3C_HCH3', S_tott(18), 'C_H3', S_tott(19), 'CH3C_H2', S_tott(20), 'C_H2',
S_tott(21), 'C_', S_tott(22), 'CH2dCH2', S_tott(23), 'CH2dC_H', S_tott(24),
'CHtCH', S_tott(25),  'HC_dO', S_tott(26), 'CH2dO', S_tott(27), 'CH3CH2C_H',
S_tott(28), 'CH3CHdC_H', S_tott(29), 'CHtC_', S_tott(30), 'CH3C_H',
S_tott(31), 'HCOO_', S_tott(32));

       S_loc = struct('H_', S_locc(1), 'H2', S_locc(2), 'CH3CH2CH3', S_locc(3),
'CH3CH2C_H2', S_locc(4), 'CH3CHdCH2', S_locc(5), 'O_', S_locc(6), 'O2',
S_locc(7), 'O_H', S_locc(8), 'H2O', S_locc(9),       'C_H', S_locc(10),  'CH4',
S_locc(11),  'CO', S_locc(12),   'CO2', S_locc(13),  'CH2dC_', S_locc(14),
'CH3CH3', S_locc(15), 'C_H2CHdCH2', S_locc(16), 'CH3O_', S_locc(17),
'CH3C_HCH3', S_locc(18), 'C_H3', S_locc(19), 'CH3C_H2', S_locc(20), 'C_H2',
S_locc(21), 'C_', S_locc(22), 'CH2dCH2', S_locc(23), 'CH2dC_H', S_locc(24),
'CHtCH', S_locc(25),  'HC_dO', S_locc(26), 'CH2dO', S_locc(27), 'CH3CH2C_H',
```

```
S_locc(28), 'CH3CHdC_H', S_locc(29), 'CHtC_', S_locc(30), 'CH3C_H',
S_locc(31), 'HCOO_', S_locc(32));

    clear S_3D S_tott S_locc

   kr = 0; %reaction rate constant (reverse)
   kf = 0; %reaction rate constant (forward)

%  R1    CH3CH2CH3 + *  <=>  CH3CH2C*H3
dS_pl(1) = S_loc.CH3CH2CH3 - S_tot.CH3CH2CH3;
dS_mi(1) = S_loc.CH3CH2CH3 - S_loc.CH3CH2CH3;

%  R2    CH3CH2CH3 + *^2  <=>  CH3C*H2C*H3
dS_pl(2) = S_loc.CH3CH2CH3 - S_tot.CH3CH2CH3;
dS_mi(2) = S_loc.CH3CH2CH3 - S_loc.CH3CH2CH3;

%  R3   CH3CH2C*H3 + *  <=>  CH3C*H2C*H3
dS_pl(3) = S_loc.CH3CH2CH3 - S_loc.CH3CH2CH3;
dS_mi(3) = S_loc.CH3CH2CH3 - S_loc.CH3CH2CH3;

%  R4   CH3CH2C*H3 + *^5  <=>  CH3CH2C***H2 + H***
dS_pl(4) = S_loc.CH3CH2CH3 - S_loc.CH3CH2CH3;
dS_mi(4) = S_loc.CH3CH2CH3 - S_loc.CH3CH2C_H2 - S_loc.H_;

%  R5   CH3C*H2C*H3 + *^5  <=>  CH3C*H2C***H2 + H***
dS_pl(5) = S_loc.CH3CH2CH3 - S_loc.CH3CH2CH3;
dS_mi(5) = S_loc.CH3CH2CH3 - S_loc.CH3CH2C_H2 - S_loc.H_;

%  R6   CH3CH2C***H2 + *  <=>  CH3C*H2C***H2
dS_pl(6) = S_loc.CH3CH2C_H2 - S_loc.CH3CH2C_H2;
dS_mi(6) = S_loc.CH3CH2C_H2 - S_loc.CH3CH2C_H2;

%  R7   CH3CH2C*H3 + *^5  <=>  CH3C***H2 + C***H3
dS_pl(7) = S_loc.CH3CH2CH3 - S_loc.CH3CH2CH3;
dS_mi(7) = S_loc.CH3CH2CH3 - S_loc.CH3C_H2 - S_loc.C_H3;

%  R8   CH3C*H2C*H3 + *^4  <=>  CH3C***H2 + C***H3
dS_pl(8) = S_loc.CH3CH2CH3 - S_loc.CH3CH2CH3;
dS_mi(8) = S_loc.CH3CH2CH3 - S_loc.CH3C_H2 - S_loc.C_H3;

%  R9   CH3CH2C***H2 + *^3  <=>  CH3C***H2 + C***H2
dS_pl(9) = S_loc.CH3CH2C_H2 - S_loc.CH3CH2C_H2;
dS_mi(9) = S_loc.CH3CH2C_H2 - S_loc.CH3C_H2 - S_loc.C_H2;

%  R10  CH3C*H2C***H2 + *^2  <=>  CH3C***H2 + C***H2
dS_pl(10) = S_loc.CH3CH2C_H2 - S_loc.CH3CH2C_H2;
dS_mi(10) = S_loc.CH3CH2C_H2 - S_loc.CH3C_H2 - S_loc.C_H2;

%  R11  CH3C*H2C***H2 + *^3  <=>  CH3C*H2C***H + H***
dS_pl(11) = S_loc.CH3CH2C_H2 - S_loc.CH3CH2C_H2;
dS_mi(11) = S_loc.CH3CH2C_H2 - S_loc.CH3CH2C_H - S_loc.H_;

%  R12  CH3C*H2C***H2 + *  <=>  CH3C*H=C*H2 + H***
dS_pl(12) = S_loc.CH3CH2C_H2 - S_loc.CH3CH2C_H2;
dS_mi(12) = S_loc.CH3CH2C_H2 - S_loc.CH3CHdCH2 - S_loc.H_;

%  R13  CH3CH2C***H2 + *^2  <=>  CH3C*H=C*H2 + H***
dS_pl(13) = S_loc.CH3CH2C_H2 - S_loc.CH3CH2C_H2;
dS_mi(13) = S_loc.CH3CH2C_H2 - S_loc.CH3CHdCH2 - S_loc.H_;

%  R14  CH3C*H2C***H  <=>  CH3C*H=C*H2 + *^2
```

```
dS_pl(14) = S_loc.CH3CH2C_H - S_loc.CH3CH2C_H;
dS_mi(14) = S_loc.CH3CH2C_H - S_loc.CH3CHdCH2;

%  R15  CH3C*H=C*H2 + *^5  <=>  CH3C*H=C***H + H***
dS_pl(15) = S_loc.CH3CHdCH2 - S_loc.CH3CHdCH2;
dS_mi(15) = S_loc.CH3CHdCH2 - S_loc.CH3CHdC_H - S_loc.H_;

%  R16  CH3C*H2C***H + *^3  <=>  CH3C*H=C***H + H***
dS_pl(16) = S_loc.CH3CH2C_H - S_loc.CH3CH2C_H;
dS_mi(16) = S_loc.CH3CH2C_H - S_loc.CH3CHdC_H - S_loc.H_;

%  R17  CH3C*H=C*H2 + *^5  <=>  C***H3 + C*H2=C***H
dS_pl(17) = S_loc.CH3CHdCH2 - S_loc.CH3CHdCH2;
dS_mi(17) = S_loc.CH3CHdCH2 - S_loc.C_H3 - S_loc.CH2dC_H;

%  R18  CH3C*H=C*H2  <=>  CH3CHdCH2 + *^2
dS_pl(18) = S_loc.CH3CHdCH2 - S_loc.CH3CHdCH2;
dS_mi(18) = S_loc.CH3CHdCH2 - S_tot.CH3CHdCH2;

%  R19  CH3C***H2 + *^2  <=>  C*H2=C*H2 + H***
dS_pl(19) = S_loc.CH3C_H2 - S_loc.CH3C_H2;
dS_mi(19) = S_loc.CH3C_H2 - S_loc.CH2dCH2 - S_loc.H_;

%  R20  C*H2=C*H2 + *^4  <=>  C***H2^2
dS_pl(20) = S_loc.CH2dCH2 - S_loc.CH2dCH2;
dS_mi(20) = S_loc.CH2dCH2 - S_loc.C_H2 - S_loc.C_H2;

%  R21  C***H3 + *^3  <=>  C***H2 + H***
dS_pl(21) = S_loc.C_H3 - S_loc.C_H3;
dS_mi(21) = S_loc.C_H3 - S_loc.C_H2 - S_loc.H_;

%  R22  C*H3C*H3 + *^4  <=>  CH3C***H2 + H***
dS_pl(22) = S_loc.CH3CH3 - S_loc.CH3CH3;
dS_mi(22) = S_loc.CH3CH3 - S_loc.CH3C_H2 - S_loc.H_;

%  R23  C*H3C*H3 + *^4  <=>  C***H3^2
dS_pl(23) = S_loc.CH3CH3 - S_loc.CH3CH3;
dS_mi(23) = S_loc.CH3CH3 - S_loc.C_H3 - S_loc.C_H3;

%  R24  C***H3 + H***  <=>  C*H4 + *^5
dS_pl(24) = S_loc.CH4 - S_loc.C_H3 - S_loc.H_;
dS_mi(24) = S_loc.CH4 - S_loc.CH4;

%  R25  C*H3C*H3  <=>  CH3CH3 + *^2
dS_pl(25) = S_loc.CH3CH3 - S_loc.CH3CH3;
dS_mi(25) = S_loc.CH3CH3 - S_tot.CH3CH3;

%  R26  C*H4  <=>  CH4 + *
dS_pl(26) = S_loc.CH4 - S_loc.CH4;
dS_mi(26) = S_loc.CH4 - S_tot.CH4;

%  R27  C*H2=C*H2  <=>  CH2dCH2 + *^2
dS_pl(27) = S_loc.CH2dCH2 - S_loc.CH2dCH2;
dS_mi(27) = S_loc.CH2dCH2 - S_tot.CH2dCH2;

%  R28  C*H2=C*H2 + *^5  <=>  C*H2=C***H + H***
dS_pl(28) = S_loc.CH2dCH2 - S_loc.CH2dCH2;
dS_mi(28) = S_loc.CH2dCH2 - S_loc.CH2dC_H - S_loc.H_;

%  R29  C*H2=C***H + *  <=>  C*H/=/C*H + H***
dS_pl(29) = S_loc.CH2dC_H - S_loc.CH2dC_H;
```

```
dS_mi(29) = S_loc.CH2dC_H - S_loc.CHtCH - S_loc.H_;

%  R30  C*H/=/C*H + *^4  <=>  CH/=/C*** + H***
dS_pl(30) = S_loc.CHtCH - S_loc.CHtCH;
dS_mi(30) = S_loc.CHtCH - S_loc.CHtC_ - S_loc.H_;

%  R31  CH/=/C*** + *^3  <=>  C***H + C***
dS_pl(31) = S_loc.CHtC_ - S_loc.CHtC_;
dS_mi(31) = S_loc.CHtC_ - S_loc.C_H - S_loc.C_;

%  R32  C***H + *^3  <=>  C*** + H***
dS_pl(32) = S_loc.C_H - S_loc.C_H;
dS_mi(32) = S_loc.C_H - S_loc.C_ - S_loc.H_;

%  R33   H2 + *^2  <=>  H*H*
dS_pl(33) = S_loc.H2 - S_tot.H2;
dS_mi(33) = S_loc.H2 - S_loc.H2;

%  R34  H*H* + *^4  <=>  H***^2
dS_pl(34) = S_loc.H2 - S_loc.H2;
dS_mi(34) = S_loc.H2 - S_loc.H_ - S_loc.H_;

%  R35   O2 + *^2  <=>  O*O*
dS_pl(35) = S_loc.O2 - S_tot.O2;
dS_mi(35) = S_loc.O2 - S_loc.O2;

%  R36  O*O* + *^4  <=>  O***^2
dS_pl(36) = S_loc.O2 - S_loc.O2;
dS_mi(36) = S_loc.O2 - S_loc.O_ - S_loc.O_;

%  R37  H*H* + O*** + *  <=>  O***H + H***
dS_pl(37) = S_loc.H2 - S_loc.H2 - S_loc.O_;
dS_mi(37) = S_loc.O_H - S_loc.O_H - S_loc.H_;

%  R38  H2O* + O*** + *^2  <=>  O***H^2
dS_pl(38) = S_loc.H2O - S_loc.H2O - S_loc.O_;
dS_mi(38) = S_loc.O_H - S_loc.O_H - S_loc.O_H;

%  R39  H*** + O***  <=>  O***H + *^3
dS_pl(39) = S_loc.O_H - S_loc.O_ - S_loc.H_;
dS_mi(39) = S_loc.O_H - S_loc.O_H;

%  R40  H*** + O***H  <=>  H2O* + *^5
dS_pl(40) = S_loc.H2O - S_loc.O_H - S_loc.H_;
dS_mi(40) = S_loc.H2O - S_loc.H2O;

%  R41  H2O* + H*** + *  <=>  H*H* + O***H
dS_pl(41) = S_loc.H2O - S_loc.H2O - S_loc.H_;
dS_mi(41) = S_loc.H2 - S_loc.H2 - S_loc.O_H;

%  R42  H2O*  <=>  H2O + *
dS_pl(42) = S_loc.H2O - S_loc.H2O;
dS_mi(42) = S_loc.H2O - S_tot.H2O;

%  R43  C***H3 + O***  <=>  CH3O*** + *^3
dS_pl(43) = S_loc.CH3O_ - S_loc.C_H3 - S_loc.O_;
dS_mi(43) = S_loc.CH3O_ - S_loc.CH3O_;

%  R44  C***H3 + O***H  <=>  CH3O*** + H***
dS_pl(44) = S_loc.O_H - S_loc.C_H3 - S_loc.O_H;
dS_mi(44) = S_loc.CH3O_ - S_loc.CH3O_ - S_loc.H_;
```

```
%  R45  C*O + C***H3 + *^2  <=>  CH3O*** + C***
dS_pl(45) = S_loc.CO + S_loc.CH3O_ - S_loc.C_H3 - S_loc.CO;
dS_mi(45) = S_loc.CO + S_loc.CH3O_ - S_loc.CH3O_ - S_loc.C_;

%  R46   CH3C***H + HC***=O + *  <=>  CH3C*H=C***H + O***
dS_pl(46) = S_loc.HC_dO - S_loc.CH3C_H - S_loc.HC_dO;
dS_mi(46) = S_loc.CH3CHdC_H - S_loc.CH3CHdC_H - S_loc.O_;

%  R47  C***H + O***  <=>  HC***=O + *^3
dS_pl(47) = S_loc.HC_dO - S_loc.C_H - S_loc.O_;
dS_mi(47) = S_loc.HC_dO - S_loc.HC_dO;

%  R48  CH3C*H=C*H2 + *^4  <=>   CH3C***H + C***H2
dS_pl(48) = S_loc.CH3CHdCH2 - S_loc.CH3CHdCH2;
dS_mi(48) = S_loc.CH3CHdCH2 - S_loc.CH3C_H - S_loc.C_H2;

%  R49  CH3C***H2 + *^3  <=>   CH3C***H + H***
dS_pl(49) = S_loc.CH3C_H2 - S_loc.CH3C_H2;
dS_mi(49) = S_loc.CH3C_H2 - S_loc.CH3C_H - S_loc.H_;

%  R50  HC***=O + *  <=>  C*O + H***
dS_pl(50) = S_loc.HC_dO - S_loc.HC_dO;
dS_mi(50) = S_loc.HC_dO - S_loc.CO - S_loc.H_;

%  R51  C*O + O***  <=>  O*=C=O* + *^2
dS_pl(51) = S_loc.CO2 - S_loc.CO - S_loc.O_;
dS_mi(51) = S_loc.CO2 - S_loc.CO2;

%  R52  C*** + O***  <=>  C*O + *^5
dS_pl(52) = S_loc.CO - S_loc.C_ - S_loc.O_;
dS_mi(52) = S_loc.CO - S_loc.CO;

%  R53  C*O + O***H + *  <=>  O*=C=O* + H***
dS_pl(53) = S_loc.O_H - S_loc.O_H - S_loc.CO;
dS_mi(53) = S_loc.CO2 - S_loc.CO2 - S_loc.H_;

%  R54  HC***=O + O***  <=>   HC(O)O*** + *^3
dS_pl(54) = S_loc.HCOO_ - S_loc.HC_dO - S_loc.O_;
dS_mi(54) = S_loc.HCOO_ - S_loc.HCOO_;

%  R55   HC(O)O*** + *  <=>  C*O + O***H
dS_pl(55) = S_loc.HCOO_ - S_loc.HCOO_;
dS_mi(55) = S_loc.HCOO_ - S_loc.CO - S_loc.O_H;

%  R56   HC(O)O*** + *^2  <=>  O*=C=O* + H***
dS_pl(56) = S_loc.HCOO_ - S_loc.HCOO_;
dS_mi(56) = S_loc.HCOO_ - S_loc.CO2 - S_loc.H_;

%  R57  C*O  <=>  CO + *
dS_pl(57) = S_loc.CO - S_loc.CO;
dS_mi(57) = S_loc.CO - S_tot.CO;

%  R58  O*=C=O*  <=>  CO2 + *^2
dS_pl(58) = S_loc.CO2 - S_loc.CO2;
dS_mi(58) = S_loc.CO2 - S_tot.CO2;

%  R59   CH3CH2CH3  <=>  CH3CH2C_H2 + H_
dS_pl(59) = S_tot.CH3CH2CH3 - S_tot.CH3CH2CH3;
dS_mi(59) = S_tot.CH3CH2CH3 - S_tot.CH3CH2C_H2 - S_tot.H_;
```

```
%  R60   CH3CH2CH3  <=>  CH3C_H2 + C_H3
dS_pl(60) = S_tot.CH3CH2CH3 - S_tot.CH3CH2CH3;
dS_mi(60) = S_tot.CH3CH2CH3 - S_tot.CH3C_H2 - S_tot.C_H3;

%  R61   CH3CH2C_H2  <=>  CH3CHdCH2 + H_
dS_pl(61) = S_tot.CH3CH2C_H2 - S_tot.CH3CH2C_H2;
dS_mi(61) = S_tot.CH3CH2C_H2 - S_tot.CH3CHdCH2 - S_tot.H_;

%  R62   CH3CH2C_H2  <=>  CH3C_H2 + C_H2
dS_pl(62) = S_tot.CH3CH2C_H2 - S_tot.CH3CH2C_H2;
dS_mi(62) = S_tot.CH3CH2C_H2 - S_tot.CH3C_H2 - S_tot.C_H2;

%  R63   C_H3  <=>  C_H2 + H_
dS_pl(63) = S_tot.C_H3 - S_tot.C_H3;
dS_mi(63) = S_tot.C_H3 - S_tot.C_H2 - S_tot.H_;

%  R64   C_H3 + H_  <=>  CH4
dS_pl(64) = S_tot.CH4 - S_tot.C_H3 - S_tot.H_;
dS_mi(64) = S_tot.CH4 - S_tot.CH4;

%  R65   CH3C_H2  <=>  CH2dCH2 + H_
dS_pl(65) = S_tot.CH3C_H2 - S_tot.CH3C_H2;
dS_mi(65) = S_tot.CH3C_H2 - S_tot.CH2dCH2 - S_tot.H_;

%  R66   CH3CH3  <=>  C_H3^2
dS_pl(66) = S_tot.CH3CH3 - S_tot.CH3CH3;
dS_mi(66) = S_tot.CH3CH3 - S_tot.C_H3 - S_tot.C_H3;

%  R67   CH3CH3  <=>  CH3C_H2 + H_
dS_pl(67) = S_tot.CH3CH3 - S_tot.CH3CH3;
dS_mi(67) = S_tot.CH3CH3 - S_tot.CH3C_H2 - S_tot.H_;

%  R68   CH2dCH2 + O_  <=>  C_H2 + CH2dO
dS_pl(68) = S_tot.CH2dCH2 + S_tot.CH2dO - S_tot.CH2dCH2 - S_tot.O_;
dS_mi(68) = S_tot.CH2dCH2 + S_tot.CH2dO - S_tot.C_H2 - S_tot.CH2dO;

%  R69   CH3O_  <=>  CH2dO + H_
dS_pl(69) = S_tot.CH3O_ - S_tot.CH3O_;
dS_mi(69) = S_tot.CH3O_ - S_tot.CH2dO - S_tot.H_;

%  R70   C_H3 + O_  <=>  CH3O_
dS_pl(70) = S_tot.CH3O_ - S_tot.C_H3 - S_tot.O_;
dS_mi(70) = S_tot.CH3O_ - S_tot.CH3O_;

%  R71   H2 + O2  <=>  O_H^2
dS_pl(71) = S_tot.H2 + S_tot.O2 + 2*S_tot.O_H  - S_tot.H2 - S_tot.O2;
dS_mi(71) = S_tot.H2 + S_tot.O2 + 2*S_tot.O_H  - S_tot.O_H - S_tot.O_H;

%  R72   H2O + H_  <=>  H2 + O_H
dS_pl(72) = S_tot.H2O + S_tot.H2 - S_tot.H2O - S_tot.H_;
dS_mi(72) = S_tot.H2O + S_tot.H2 - S_tot.H2 - S_tot.O_H;

%  R73   H_ + O_  <=>  O_H
dS_pl(73) = S_tot.O_H - S_tot.O_ - S_tot.H_;
dS_mi(73) = S_tot.O_H - S_tot.O_H;

%  R74   H2 + O_  <=>  O_H + H_
dS_pl(74) = S_tot.H2 + S_tot.O_H - S_tot.H2 - S_tot.O_;
dS_mi(74) = S_tot.H2 + S_tot.O_H - S_tot.O_H - S_tot.H_;

%  R75   H2O + O_  <=>  O_H^2
```

```
dS_pl(75) = S_tot.H2O + S_tot.O_H - S_tot.H2O - S_tot.O_;
dS_mi(75) = S_tot.H2O + S_tot.O_H - S_tot.O_H - S_tot.O_H;

%  R76   H_ + O_H  <=>  H2O
dS_pl(76) = S_tot.H2O - S_tot.O_H - S_tot.H_;
dS_mi(76) = S_tot.H2O - S_tot.H2O;

%  R77   CH3CHdCH2 + O_  <=>  CH3C_H + CH2dO
dS_pl(77) = S_tot.CH3CHdCH2 + S_tot.CH2dO - S_tot.CH3CHdCH2 - S_tot.O_;
dS_mi(77) = S_tot.CH3CHdCH2 + S_tot.CH2dO - S_tot.CH3C_H - S_tot.CH2dO;

%  R78   CH3C_H  <=>  CH2dC_H + H_
dS_pl(78) = S_tot.CH3C_H + S_tot.CH2dC_H - S_tot.CH3C_H;
dS_mi(78) = S_tot.CH3C_H + S_tot.CH2dC_H - S_tot.CH2dC_H - S_tot.H_;

%  R79   CH2dCH2  <=>  CH2dC_H + H_
dS_pl(79) = S_tot.CH2dCH2 - S_tot.CH2dCH2;
dS_mi(79) = S_tot.CH2dCH2 - S_tot.CH2dC_H - S_tot.H_;

%  R80   CH3C_H + H_  <=>  CH3C_H2
dS_pl(80) = S_tot.CH3C_H2 - S_tot.CH3C_H - S_tot.H_;
dS_mi(80) = S_tot.CH3C_H2 - S_tot.CH3C_H2;

%  R81   CH2dO + O_  <=>  H_ + HCOO_
dS_pl(81) = S_tot.CH2dO + S_tot.HCOO_ - S_tot.CH2dO - S_tot.O_;
dS_mi(81) = S_tot.CH2dO + S_tot.HCOO_ - S_tot.HCOO_ - S_tot.H_;

%  R82   HCOO_  <=>  CO2 + H_
dS_pl(82) = S_tot.HCOO_ - S_tot.HCOO_;
dS_mi(82) = S_tot.HCOO_ - S_tot.CO2 - S_tot.H_;

%  R83   HCOO_  <=>  CO + O_H
dS_pl(83) = S_tot.HCOO_ - S_tot.HCOO_;
dS_mi(83) = S_tot.HCOO_ - S_tot.CO - S_tot.O_H;

%  R84   CO + O_  <=>  CO2
dS_pl(84) = S_tot.CO2 - S_tot.CO - S_tot.O_;
dS_mi(84) = S_tot.CO2 - S_tot.CO2;

%  R85  CH3CH2C***H2  <=>  CH3CH2C_H2 + *^3
dS_pl(85) = S_loc.CH3CH2C_H2 - S_loc.CH3CH2C_H2;
dS_mi(85) = S_loc.CH3CH2C_H2 - S_tot.CH3CH2C_H2;

%  R86  CH3C***H2  <=>  CH3C_H2 + *^3
dS_pl(86) = S_loc.CH3C_H2 - S_loc.CH3C_H2;
dS_mi(86) = S_loc.CH3C_H2 - S_tot.CH3C_H2;

%  R87   CH3C***H  <=>  CH3C_H + *^3
dS_pl(87) = S_loc.CH3C_H - S_loc.CH3C_H;
dS_mi(87) = S_loc.CH3C_H - S_tot.CH3C_H;

%  R88  C*H2=C***H  <=>  CH2dC_H + *^4
dS_pl(88) = S_loc.CH2dC_H - S_loc.CH2dC_H;
dS_mi(88) = S_loc.CH2dC_H - S_tot.CH2dC_H;

%  R89  C***H3  <=>  C_H3 + *^3
dS_pl(89) = S_loc.C_H3 - S_loc.C_H3;
dS_mi(89) = S_loc.C_H3 - S_tot.C_H3;

%  R90  C***H2  <=>  C_H2 + *^3
dS_pl(90) = S_loc.C_H2 - S_loc.C_H2;
```

```
dS_mi(90) = S_loc.C_H2 - S_tot.C_H2;

%  R91  H***  <=>  H_ + *^3
dS_pl(91) = S_loc.H_ - S_loc.H_;
dS_mi(91) = S_loc.H_ - S_tot.H_;

%  R92  O***  <=>  O_ + *^3
dS_pl(92) = S_loc.O_ - S_loc.O_;
dS_mi(92) = S_loc.O_ - S_tot.O_;

%  R93  O***H  <=>  O_H + *^3
dS_pl(93) = S_loc.O_H - S_loc.O_H;
dS_mi(93) = S_loc.O_H - S_tot.O_H;

%  R94  CH3O***  <=>  CH3O_ + *^3
dS_pl(94) = S_loc.CH3O_ - S_loc.CH3O_;
dS_mi(94) = S_loc.CH3O_ - S_tot.CH3O_;

%  R95   HC(O)O***  <=>  HCOO_ + *^3
dS_pl(95) = S_loc.HCOO_ - S_loc.HCOO_;
dS_mi(95) = S_loc.HCOO_ - S_tot.HCOO_;

    Aplus  = (exp(1)*kB*T(i)/h)*exp(dS_pl/R);
    Aminus = (exp(1)*kB*T(i)/h)*exp(dS_mi/R);

%% fine tuning of some of the preexponentials
    Aplus(42) = Aplus(42)*10;
    Aplus(33) = Aplus(33)*10;
    Aminus(35) = Aminus(35)*10;

     Aplus(1) = Aplus(1)*10;
     Aminus(26) = Aminus(26)*10^2;
     Aplus(18) = Aplus(18)*10;

    kf = Aplus.*exp(-Ef/(R*T(i)));
    kr = Aminus.*exp(-Er/(R*T(i)));

    clear dS_pl dS_mi Aplus Aminus Ef Er
  %%
    %Calculating the conversion at a spesific temperature
    %--------------------------------------------------------------------
     % density kg/m3
        % Al Be Cr Cu Au Ir Fe Pb Mo Ni Pt      Pd      Ag      Zn
        % 1  2  3  4  5  6  7  8  9  10 11      12      13      14

    % aCub = Ag         Au      Cu      Ir      Ni      Pd      Pt
    %        4.08626    4.07833 3.6147  3.8389  3.5238  3.8908  3.9240

    RoMe = Dens(i,11);
    RoSup = Dhdrtlc;
    RoCat = RoMe*RoSup/(ywt*RoSup+(1-ywt)*RoMe);% density
    Poros = RoCat*Vpor/(RoCat*Vpor+1); % porosity

    aCub = 3.9240;
    CtMe = 4*10^20/(sqrt(3)*aCub^2);    %active site density on metal surface

    % for reactor
    Ct = CtMe;
    St = StMe;
    pCat = RoCat;
    eps = Poros;
```

```
%% moles of components in initial mixture

    n0CH3CH2C_H2    =  Y0_CH3CH2C_H2*nTot ;
    n0CH3C_H2       =  Y0_CH3C_H2   *nTot ;
    n0CH3C_H        =  Y0_CH3C_H    *nTot ;
    n0CH2dC_H       =  Y0_CH2dC_H   *nTot ;
    n0C_H2          =  Y0_C_H2      *nTot ;
    n0C_H3          =  Y0_C_H3      *nTot ;
    n0H_             =  Y0_H_            *nTot ;
    n0O_            =  Y0_O_        *nTot ;
    n0O_H            =  Y0_O_H       *nTot ;
    n0CH3O_          =  Y0_CH3O_     *nTot ;
    n0HCOO_         =  Y0_HCOO_     *nTot ;
    n0CH2dO_     =  Y0_CH2dO_        *nTot ;
    n0CH4           =  Y0_CH4       *nTot ;
    n0CH3CH3        =  Y0_CH3CH3    *nTot ;
    n0CH2dCH2       =  Y0_CH2dCH2   *nTot ;
    n0H2             =  Y0_H2        *nTot ;
    n0O2             =  Y0_O2            *nTot ;
    n0H2O            =  Y0_H2O       *nTot ;
    n0CO             =  Y0_CO            *nTot ;
    n0CO2           =  Y0_CO2       *nTot ;
    n0CH3CH2CH3     =  Y0_CH3CH2CH3 *nTot ;
    n0CH3CHdCH2     =  Y0_CH3CHdCH2 *nTot ;
    n0N2             =  Y0_N2        *nTot ;

    ntot = nTot; % mols total
%%
    V = (V0/To)*T(i);       % space velocity at current temperature

    Nstp = 10; % the number of steps (CSTRs) in reactor
    VfreeCSTR = mcat*Poros/(Nstp*RoCat*(1-Poros));

    Nrun = 3; % the number of runs of smallest gas portions through reactor

  %% initial surface fractions of components (for first run in all CSTRs)

phi1(1,1:Nstp)  = 0;
phi2(1,1:Nstp)  = 0;
phi3(1,1:Nstp)  = 0;
phi4(1,1:Nstp)  = 0;
phi5(1,1:Nstp)  = 0;
phi6(1,1:Nstp)  = 0;
phi7(1,1:Nstp)  = 0;
phi8(1,1:Nstp)  = 0;
phi9(1,1:Nstp)  = 0;
phi10(1,1:Nstp) = 0;
phi11(1,1:Nstp) = 0;
phi12(1,1:Nstp) = 0;
phi13(1,1:Nstp) = 0;
phi14(1,1:Nstp) = 0;
phi15(1,1:Nstp) = 0;
phi16(1,1:Nstp) = 0;
phi17(1,1:Nstp) = 0;
phi18(1,1:Nstp) = 0;
phi19(1,1:Nstp) = 0;
phi20(1,1:Nstp) = 0;
phi21(1,1:Nstp) = 0;
phi22(1,1:Nstp) = 0;
phi23(1,1:Nstp) = 0;
```

```
phi24(1,1:Nstp) = 0;
phi25(1,1:Nstp) = 0;
phi26(1,1:Nstp) = 0;
phi27(1,1:Nstp) = 0;
phi28(1,1:Nstp) = 0;
phi29(1,1:Nstp) = 0;
phi30(1,1:Nstp) = 0;
phi31(1,1:Nstp) = 1;

    %%
for irun = 1:1:Nrun
     for isi=1:1:Nstp
         tau = VfreeCSTR/V;
         tspan=linspace(0,tau);%Spacetime linspace(0,tau,102);
       %phi and n
       %1  2  3  4  5  6  7  8  9  10 11 12 13 14 15 16 17 18 19 20 21 22 23
24 25 26 27 28 29 30 31 32 33 34 35 36  37 38 39 40 41 42 43 44 45 46 47 48 49
50 51 52 53
       yin=[phi1(irun,isi); phi2(irun,isi); phi3(irun,isi); phi4(irun,isi);
phi5(irun,isi); phi6(irun,isi); phi7(irun,isi); phi8(irun,isi);
phi9(irun,isi); phi10(irun,isi); phi11(irun,isi); phi12(irun,isi);
phi13(irun,isi); phi14(irun,isi); phi15(irun,isi); phi16(irun,isi);
phi17(irun,isi); phi18(irun,isi); phi19(irun,isi); phi20(irun,isi);
phi21(irun,isi); phi22(irun,isi); phi23(irun,isi); phi24(irun,isi);
phi25(irun,isi); phi26(irun,isi); phi27(irun,isi); phi28(irun,isi);
phi29(irun,isi); phi30(irun,isi); phi31(irun,isi); n0CH3CH2C_H2; n0CH3C_H2;
n0CH3C_H; n0CH2dC_H; n0C_H2; n0C_H3; n0H_; n0O_; n0O_H; n0CH3O_; n0HCOO_;
n0CH2dO_; n0CH4; n0CH3CH3; n0CH2dCH2; n0H2; n0O2; n0H2O; n0CO; n0CO2;
n0CH3CH2CH3 ; n0CH3CHdCH2];
       Options = odeset('RelTol',1e-3,'AbsTol',1e-6', 'NonNegative', [1 2 3 4
5 6 7 8 9 10 11 12 13 14 15 16 17 18  19 20 21 22 23 24 25 26 27 28 29 30 31
32 33 34 35 36 37 38 39 40 41 42 43 44 45 46 47 48 49 50 51 52 53]);

  %% transform surf fraction from sitesA/sitesTot to molecA/sitesTot
yin(1 ) =   (1/1)*yin(1);  % 'CH3CH2C*H3'
yin(2 ) =   (1/2)*yin(2);   % 'CH3C*H2C*H3'
yin(3 ) =   (1/3)*yin(3);   % 'CH3CH2C***H2'
yin(4 ) =   (1/4)*yin(4);   % 'CH3C*H2C***H2'
yin(5 ) =   (1/4)*yin(5);   % 'CH3C*H2C***H'
yin(6 ) =   (1/2)*yin(6);   % 'CH3C*H=C*H2'
yin(7 ) =   (1/3)*yin(7);   % 'CH3C***H2'
yin(8 ) =   (1/4)*yin(8);   % 'CH3C*H=C***H'
yin(9 ) =   (1/3)*yin(9);   % 'CH3C***H'
yin(10) =   (1/2)*yin(10);   %  'C*H3C*H3'
yin(11) =   (1/4)*yin(11);   %  'C*H2=C***H'
yin(12) =   (1/2)*yin(12);   %  'C*H2=C*H2'
yin(13) =   (1/2)*yin(13);   %  'C*H/=/C*H'
yin(14) =   (1/3)*yin(14);   %  'CH/=/C***'
yin(15) =   (1/3)*yin(15);   %  'C***'
yin(16) =   (1/3)*yin(16);   %  'C***H'
yin(17) =   (1/3)*yin(17);   %  'C***H2'
yin(18) =   (1/3)*yin(18);   %  'C***H3'
yin(19) =   (1/1)*yin(19);   %  'C*H4'
yin(20) =   (1/2)*yin(20);   %  'H*H*'
yin(21) =   (1/3)*yin(21);   %  'H***'
yin(22) =   (1/2)*yin(22);   %  'O*O*'
yin(23) =   (1/3)*yin(23);   %  'O***'
yin(24) =   (1/3)*yin(24);   %  'O***H'
yin(25) =   (1/3)*yin(25);   %  'CH3O***'
yin(26) =   (1/3)*yin(26);   %  'HC***=O'
yin(27) =   (1/3)*yin(27);   %  'HC(O)O***'
```

```
yin(28) =   (1/1)*yin(28);   %  'H2O*'
yin(29) =   (1/1)*yin(29);   %  'C*O'
yin(30) =   (1/2)*yin(30);   %  'O*=C=O*'
yin(31) =   (1/1)*yin(31);   %  '*'

 %%
       [t,yout]=ode15s(@comb_difer_v6,tspan,yin,Options);

%% reverse transform of surf fraction from molecA/sitesTot to sitesA/sitesTot
yout(size(yout,1),1 ) =   yout(size(yout,1),1 )*1;
yout(size(yout,1),2 ) =   yout(size(yout,1),2 )*2;
yout(size(yout,1),3 ) =   yout(size(yout,1),3 )*3;
yout(size(yout,1),4 ) =   yout(size(yout,1),4 )*4;
yout(size(yout,1),5 ) =   yout(size(yout,1),5 )*4;
yout(size(yout,1),6 ) =   yout(size(yout,1),6 )*2;
yout(size(yout,1),7 ) =   yout(size(yout,1),7 )*3;
yout(size(yout,1),8 ) =   yout(size(yout,1),8 )*4;
yout(size(yout,1),9 ) =   yout(size(yout,1),9 )*3;
yout(size(yout,1),10) =   yout(size(yout,1),10)*2;
yout(size(yout,1),11) =   yout(size(yout,1),11)*4;
yout(size(yout,1),12) =   yout(size(yout,1),12)*2;
yout(size(yout,1),13) =   yout(size(yout,1),13)*2;
yout(size(yout,1),14) =   yout(size(yout,1),14)*3;
yout(size(yout,1),15) =   yout(size(yout,1),15)*3;
yout(size(yout,1),16) =   yout(size(yout,1),16)*3;
yout(size(yout,1),17) =   yout(size(yout,1),17)*3;
yout(size(yout,1),18) =   yout(size(yout,1),18)*3;
yout(size(yout,1),19) =   yout(size(yout,1),19)*1;
yout(size(yout,1),20) =   yout(size(yout,1),20)*2;
yout(size(yout,1),21) =   yout(size(yout,1),21)*3;
yout(size(yout,1),22) =   yout(size(yout,1),22)*2;
yout(size(yout,1),23) =   yout(size(yout,1),23)*3;
yout(size(yout,1),24) =   yout(size(yout,1),24)*3;
yout(size(yout,1),25) =   yout(size(yout,1),25)*3;
yout(size(yout,1),26) =   yout(size(yout,1),26)*3;
yout(size(yout,1),27) =   yout(size(yout,1),27)*3;
yout(size(yout,1),28) =   yout(size(yout,1),28)*1;
yout(size(yout,1),29) =   yout(size(yout,1),29)*1;
yout(size(yout,1),30) =   yout(size(yout,1),30)*2;
yout(size(yout,1),31) =   yout(size(yout,1),31)*1;
%%
       reactSector(i,irun,isi,:) = yout(size(yout,1),:);

    n0CH3CH2C_H2   =  yout(size(yout,1),32) ;
    n0CH3C_H2      =  yout(size(yout,1),33) ;
    n0CH3C_H       =  yout(size(yout,1),34) ;
    n0CH2dC_H      =  yout(size(yout,1),35) ;
    n0C_H2         =  yout(size(yout,1),36) ;
    n0C_H3         =  yout(size(yout,1),37) ;
    n0H_            =  yout(size(yout,1),38) ;
    n0O_           =  yout(size(yout,1),39) ;
    n0O_H           =  yout(size(yout,1),40) ;
    n0CH3O_         =  yout(size(yout,1),41) ;
    n0HCOO_        =  yout(size(yout,1),42) ;
    n0CH2dO_    =  yout(size(yout,1),43) ;
    n0CH4          =  yout(size(yout,1),44) ;
    n0CH3CH3       =  yout(size(yout,1),45) ;
    n0CH2dCH2      =  yout(size(yout,1),46) ;
    n0H2            =  yout(size(yout,1),47) ;
    n0O2            =  yout(size(yout,1),48) ;
    n0H2O           =  yout(size(yout,1),49) ;
```

```
    n0CO            =  yout(size(yout,1),50) ;
    n0CO2           =  yout(size(yout,1),51) ;
    n0CH3CH2CH3     =  yout(size(yout,1),52) ;
    n0CH3CHdCH2     =  yout(size(yout,1),53) ;

    ntot = sum(yout(size(yout,1),32:53)) + n0N2;

       V = ntot*R*T(i)/Ptot;

       end

    n0CH3CH2C_H2    =  Y0_CH3CH2C_H2*nTot ;
    n0CH3C_H2       =  Y0_CH3C_H2   *nTot ;
    n0CH3C_H        =  Y0_CH3C_H    *nTot ;
    n0CH2dC_H       =  Y0_CH2dC_H   *nTot ;
    n0C_H2          =  Y0_C_H2      *nTot ;
    n0C_H3          =  Y0_C_H3      *nTot ;
    n0H_             =  Y0_H_            *nTot ;
    n0O_            =  Y0_O_        *nTot ;
    n0O_H            =  Y0_O_H       *nTot ;
    n0CH3O_          =  Y0_CH3O_     *nTot ;
    n0HCOO_         =  Y0_HCOO_     *nTot ;
    n0CH2dO_     =  Y0_CH2dO_        *nTot ;
    n0CH4           =  Y0_CH4       *nTot ;
    n0CH3CH3        =  Y0_CH3CH3    *nTot ;
    n0CH2dCH2       =  Y0_CH2dCH2   *nTot ;
    n0H2             =  Y0_H2        *nTot ;
    n0O2             =  Y0_O2            *nTot ;
    n0H2O            =  Y0_H2O       *nTot ;
    n0CO             =  Y0_CO            *nTot ;
    n0CO2           =  Y0_CO2       *nTot ;
    n0CH3CH2CH3     =  Y0_CH3CH2CH3 *nTot ;
    n0CH3CHdCH2     =  Y0_CH3CHdCH2 *nTot ;

    ntot = nTot;
    V = (V0/To)*T(i);

%% surface fractions of components (after irun run in all CSTRs) as initial
surf fract for irun+1

phi1(irun+1,1:Nstp)  = reactSector(i,irun,1:Nstp,1);
phi2(irun+1,1:Nstp)  = reactSector(i,irun,1:Nstp,2);
phi3(irun+1,1:Nstp)  = reactSector(i,irun,1:Nstp,3);
phi4(irun+1,1:Nstp)  = reactSector(i,irun,1:Nstp,4);
phi5(irun+1,1:Nstp)  = reactSector(i,irun,1:Nstp,5);
phi6(irun+1,1:Nstp)  = reactSector(i,irun,1:Nstp,6);
phi7(irun+1,1:Nstp)  = reactSector(i,irun,1:Nstp,7);
phi8(irun+1,1:Nstp)  = reactSector(i,irun,1:Nstp,8);
phi9(irun+1,1:Nstp)  = reactSector(i,irun,1:Nstp,9);
phi10(irun+1,1:Nstp) = reactSector(i,irun,1:Nstp,10);
phi11(irun+1,1:Nstp) = reactSector(i,irun,1:Nstp,11);
phi12(irun+1,1:Nstp) = reactSector(i,irun,1:Nstp,12);
phi13(irun+1,1:Nstp) = reactSector(i,irun,1:Nstp,13);
phi14(irun+1,1:Nstp) = reactSector(i,irun,1:Nstp,14);
phi15(irun+1,1:Nstp) = reactSector(i,irun,1:Nstp,15);
phi16(irun+1,1:Nstp) = reactSector(i,irun,1:Nstp,16);
phi17(irun+1,1:Nstp) = reactSector(i,irun,1:Nstp,17);
phi18(irun+1,1:Nstp) = reactSector(i,irun,1:Nstp,18);
phi19(irun+1,1:Nstp) = reactSector(i,irun,1:Nstp,19);
phi20(irun+1,1:Nstp) = reactSector(i,irun,1:Nstp,20);
phi21(irun+1,1:Nstp) = reactSector(i,irun,1:Nstp,21);
```

```
phi22(irun+1,1:Nstp) = reactSector(i,irun,1:Nstp,22);
phi23(irun+1,1:Nstp) = reactSector(i,irun,1:Nstp,23);
phi24(irun+1,1:Nstp) = reactSector(i,irun,1:Nstp,24);
phi25(irun+1,1:Nstp) = reactSector(i,irun,1:Nstp,25);
phi26(irun+1,1:Nstp) = reactSector(i,irun,1:Nstp,26);
phi27(irun+1,1:Nstp) = reactSector(i,irun,1:Nstp,27);
phi28(irun+1,1:Nstp) = reactSector(i,irun,1:Nstp,28);
phi29(irun+1,1:Nstp) = reactSector(i,irun,1:Nstp,29);
phi30(irun+1,1:Nstp) = reactSector(i,irun,1:Nstp,30);
phi31(irun+1,1:Nstp) = reactSector(i,irun,1:Nstp,31);

%%
end

%%
testit(i,:)=[yout(size(yout,1),:)];%102

    disp(i);

%% Finding the equilibrium conversiom of C3H8 and equilibrium yield of C3H6
%     %--------------------------------------------------------------------
    DGr1 = 1000*(dHf.CH3CHdCH2(i) + dHf.H2(i) - dHf.CH3CH2CH3(i)) -
T(i)*(S_tot.CH3CHdCH2 + S_tot.H2 - S_tot.CH3CH2CH3);
    KpT1 = exp(-(DGr1)/(R*T(i)));
    x0z = 0.1;
    [x1z,fval1] = fsolve(@propequil_v5,x0z);

    eqConv1(i) = x1z;
    eqYield1(i) = x1z;

    %% --------------------------------------------------------------------
    %% Finding the equilibrium conversiom of CO in WGS
%    %--------------------------------------------------------------------
    DGr2 = 1000*(dHf.CO2(i) + dHf.H2(i) - dHf.CO(i) - dHf.H2O(i)) -
T(i)*(S_tot.CO2 + S_tot.H2 - S_tot.CO - S_tot.H2O);
    KpT2 = exp(-(DGr2)/(R*T(i)));
    x00z = 0.9;
    [x2z,fval2] = fsolve(@COequil_v5,x00z);

    eqConv2(i) = x2z;
    %% --------------------------------------------------------------------



end

%% Ploting the results
%---------------------------------------------------------------------
%Cycling Through Line Colors and Styles, default ColorOrder is black
set(0,'DefaultAxesColorOrder',[0 0 0],...
      'DefaultAxesLineStyleOrder','-|-.|--|:|s|d|+|x|o|*|^|v|>|<|p|h|-s|-d|-
+|-x|-o|-*|-^|-v|->|-<|-p|-h|--s|--d|--+|--x|--o|--*|--^|--v|-->|--<|--p|--
h|:s|:d|:+|:x|:o|:*|:^|:v|:>|:<|:p|:h|-.s|-.d|-.
+|-.x|-.o|-.*|-.^|-.v|-.>|-.<|-.p|-.h');
xlimMin = 200;
xlimMax = 700;
totF = sum(testit(:,32:53)') + n0N2;
figure();

% Propane conversion
subplot(3,1,1)
```

```
hold on
plot((T-273),((n0CH3CH2CH3-testit(:,52)')./n0CH3CH2CH3), (T-273), eqConv1);
title('\bf{Conversion }','FontSize',14)
legend('Conv C3H8', 'Eq conv');
xlabel('\bf{Temperature [^oC]}')
ylabel('\bf{Conversion C3H8}')
xlim([xlimMin xlimMax]);
% ------------------

% CO conversion
% subplot(3,1,1)
% hold on
% plot((T-273),((n0CO-testit(:,50)')./n0CO), (T-273), eqConv2);
% title('\bf{CO conversion }','FontSize',14)
% legend('Conv CO', 'Eq conv');
% xlabel('\bf{Temperature [^oC]}')
% ylabel('\bf{Conversion CO}')
% xlim([xlimMin xlimMax]);
%--------------------

subplot(3,1,2)
plot((T-273),testit(:,1)',(T-273), testit(:,2)',(T-273), testit(:,3)',(T-273),
testit(:,4)',(T-273), testit(:,5)',(T-273), testit(:,6)',(T-273),
testit(:,7)',(T-273), testit(:,8)',(T-273), testit(:,9)',(T-273),
testit(:,10)',(T-273), testit(:,11)',(T-273), testit(:,12)',(T-273),
testit(:,13)',(T-273), testit(:,14)',(T-273), testit(:,15)',(T-273),
testit(:,16)',(T-273), testit(:,17)',(T-273), testit(:,18)',(T-273),
testit(:,19)',(T-273), testit(:,20)',(T-273), testit(:,21)',(T-273),
testit(:,22)',(T-273), testit(:,23)', (T-273), testit(:,24)',(T-273),
testit(:,25)',(T-273), testit(:,26)',(T-273), testit(:,27)',(T-273),
testit(:,28)', (T-273), testit(:,29)',(T-273), testit(:,30)', (T-273),
testit(:,31)');
title('\bf{Surface fraction}','FontSize',14)
xlabel('\bf{Temperature [^oC]}')
ylabel('\bf{Fraction}')
legend('CH3CH2C*H3', 'CH3C*H2C*H3', 'CH3CH2C***H2', 'CH3C*H2C***H2',
'CH3C*H2C***H', 'CH3C*H=C*H2', 'CH3C***H2', 'CH3C*H=C***H', 'CH3C***H',
'C*H3C*H3', 'C*H2=C***H', 'C*H2=C*H2', 'C*H/=/C*H', 'CH/=/C***', 'C***',
'C***H', 'C***H2', 'C***H3', 'C*H4', 'H*H*', 'H***', 'O*O*', 'O***', 'O***H',
'CH3O***', 'HC***=O', 'HC(O)O***', 'H2O*', 'C*O', 'O*=C=O*', '*');
xlim([xlimMin xlimMax]);

subplot(3,1,3)
plot((T-273),(testit(:,44)'./totF(:)'),(T-273), (testit(:,45)'./totF(:)' ),(T-
273), (testit(:,46)'./totF(:)' ), (T-273), (testit(:,47)'./totF(:)'), (T-273),
(testit(:,48)'./totF(:)'), (T-273), (testit(:,49)'./totF(:)'), (T-273),
(testit(:,50)'./totF(:)'), (T-273), (testit(:,51)'./totF(:)'), (T-273),
(testit(:,52)'./totF(:)'), (T-273), (testit(:,53)'./totF(:)'));
title('\bf{Gas phase fraction}','FontSize',14)
xlabel('\bf{Temperature [^oC]}')
ylabel('\bf{Fraction}')
legend('CH4',  'C2H6' , 'C2H4', 'H2', 'O2', 'H2O', 'CO', 'CO2', 'C3H8',
'C3H6', 2);
xlim([xlimMin xlimMax]);
%%

figure();
subplot(3,1,1)
plot((T-273),((n0O2-testit(:,48)')./n0O2));
title('\bf{Conversion O2}','FontSize',14)
legend('Conv O2');
```

```
xlabel('\bf{Temperature [^oC]}')
ylabel('\bf{Conversion O2}')
xlim([xlimMin xlimMax]);

subplot(3,1,2)
plot((T-273),((testit(:,53)')./n0CH3CH2CH3), (T-273), eqYield1);
title('\bf{Yield C3H6}','FontSize',14)
legend('Yield C3H6', 'Eq yield');
xlabel('\bf{Temperature [^oC]}')
ylabel('\bf{Yield C3H6}')
xlim([xlimMin xlimMax]);

subplot(3,1,3)
plot((T-273),(((1/2)*testit(:,49)')./n0O2));
title('\bf{Yield H2O (O2)}','FontSize',14)
legend('Yield H2O (O2)');
xlabel('\bf{Temperature [^oC]}')
ylabel('\bf{Yield H2O (O2)}')
xlim([xlimMin xlimMax]);


%% Propane conversion, surface and gas-phase fractions for 1st, 5th and 10th
stage of reactor
figure();
subplot(3,3,1)
plot((T-273),((n0CH3CH2CH3-reactSector(:,irun,1,52)')./n0CH3CH2CH3));
title('\bf{Conversion, stage 1}','FontSize',14);
legend('Conv C3H8');
xlim([xlimMin xlimMax]);
ylim([0 1]);
grid on

subplot(3,3,2)
plot((T-273),((n0CH3CH2CH3-reactSector(:,irun,5,52)')./n0CH3CH2CH3));
title('\bf{Conversion, stage 5}','FontSize',14);
xlim([xlimMin xlimMax]);
ylim([0 1]);
grid on

subplot(3,3,3)
plot((T-273),((n0CH3CH2CH3-reactSector(:,irun,10,52)')./n0CH3CH2CH3));
title('\bf{Conversion, stage 10}','FontSize',14);
xlim([xlimMin xlimMax]);
ylim([0 1]);
grid on

subplot(3,3,4)
plot((T-273),reactSector(:,irun,1,1)',(T-273), reactSector(:,irun,1,2)',(T-
273), reactSector(:,irun,1,3)',(T-273), reactSector(:,irun,1,4)',(T-273),
reactSector(:,irun,1,5)',(T-273), reactSector(:,irun,1,6)',(T-273),
reactSector(:,irun,1,7)',(T-273), reactSector(:,irun,1,8)',(T-273),
reactSector(:,irun,1,9)',(T-273), reactSector(:,irun,1,10)',(T-273),
reactSector(:,irun,1,11)',(T-273), reactSector(:,irun,1,12)',(T-273),
reactSector(:,irun,1,13)',(T-273), reactSector(:,irun,1,14)',(T-273),
reactSector(:,irun,1,15)',(T-273), reactSector(:,irun,1,16)',(T-273),
reactSector(:,irun,1,17)',(T-273), reactSector(:,irun,1,18)',(T-273),
reactSector(:,irun,1,19)',(T-273), reactSector(:,irun,1,20)',(T-273),
reactSector(:,irun,1,21)',(T-273), reactSector(:,irun,1,22)',(T-273),
reactSector(:,irun,1,23)', (T-273), reactSector(:,irun,1,24)',(T-273),
reactSector(:,irun,1,25)',(T-273), reactSector(:,irun,1,26)',(T-273),
reactSector(:,irun,1,27)',(T-273), reactSector(:,irun,1,28)', (T-273),
```

```
reactSector(:,irun,1,29)',(T-273), reactSector(:,irun,1,30)', (T-273),
reactSector(:,irun,1,31)');
title('\bf{Surface fraction, stage 1}','FontSize',14)
xlabel('\bf{Temperature [^oC]}')
ylabel('\bf{Fraction}')
legend('CH3CH2C*H3', 'CH3C*H2C*H3', 'CH3CH2C***H2', 'CH3C*H2C***H2',
'CH3C*H2C***H', 'CH3C*H=C*H2', 'CH3C***H2', 'CH3C*H=C***H', 'CH3C***H',
'C*H3C*H3', 'C*H2=C***H', 'C*H2=C*H2', 'C*H/=/C*H', 'CH/=/C***', 'C***',
'C***H', 'C***H2', 'C***H3', 'C*H4', 'H*H*', 'H***', 'O*O*', 'O***', 'O***H',
'CH3O***', 'HC***=O', 'HC(O)O***', 'H2O*', 'C*O', 'O*=C=O*', '*');
xlim([xlimMin xlimMax]);
ylim([0 1]);
grid on

subplot(3,3,5)
plot((T-273),reactSector(:,irun,5,1)',(T-273), reactSector(:,irun,5,2)',(T-
273), reactSector(:,irun,5,3)',(T-273), reactSector(:,irun,5,4)',(T-273),
reactSector(:,irun,5,5)',(T-273), reactSector(:,irun,5,6)',(T-273),
reactSector(:,irun,5,7)',(T-273), reactSector(:,irun,5,8)',(T-273),
reactSector(:,irun,5,9)',(T-273), reactSector(:,irun,5,10)',(T-273),
reactSector(:,irun,5,11)',(T-273), reactSector(:,irun,5,12)',(T-273),
reactSector(:,irun,5,13)',(T-273), reactSector(:,irun,5,14)',(T-273),
reactSector(:,irun,5,15)',(T-273), reactSector(:,irun,5,16)',(T-273),
reactSector(:,irun,5,17)',(T-273), reactSector(:,irun,5,18)',(T-273),
reactSector(:,irun,5,19)',(T-273), reactSector(:,irun,5,20)',(T-273),
reactSector(:,irun,5,21)',(T-273), reactSector(:,irun,5,22)',(T-273),
reactSector(:,irun,5,23)', (T-273), reactSector(:,irun,5,24)',(T-273),
reactSector(:,irun,5,25)',(T-273), reactSector(:,irun,5,26)',(T-273),
reactSector(:,irun,5,27)',(T-273), reactSector(:,irun,5,28)', (T-273),
reactSector(:,irun,5,29)',(T-273), reactSector(:,irun,5,30)', (T-273),
reactSector(:,irun,5,31)');
title('\bf{Surface fraction, stage 5}','FontSize',14)
xlabel('\bf{Temperature [^oC]}')
ylabel('\bf{Fraction}')
xlim([xlimMin xlimMax]);
ylim([0 1]);
grid on

subplot(3,3,6)
plot((T-273),reactSector(:,irun,10,1)',(T-273), reactSector(:,irun,10,2)',(T-
273), reactSector(:,irun,10,3)',(T-273), reactSector(:,irun,10,4)',(T-273),
reactSector(:,irun,10,5)',(T-273), reactSector(:,irun,10,6)',(T-273),
reactSector(:,irun,10,7)',(T-273), reactSector(:,irun,10,8)',(T-273),
reactSector(:,irun,10,9)',(T-273), reactSector(:,irun,10,10)',(T-273),
reactSector(:,irun,10,11)',(T-273), reactSector(:,irun,10,12)',(T-273),
reactSector(:,irun,10,13)',(T-273), reactSector(:,irun,10,14)',(T-273),
reactSector(:,irun,10,15)',(T-273), reactSector(:,irun,10,16)',(T-273),
reactSector(:,irun,10,17)',(T-273), reactSector(:,irun,10,18)',(T-273),
reactSector(:,irun,10,19)',(T-273), reactSector(:,irun,10,20)',(T-273),
reactSector(:,irun,10,21)',(T-273), reactSector(:,irun,10,22)',(T-273),
reactSector(:,irun,10,23)', (T-273), reactSector(:,irun,10,24)',(T-273),
reactSector(:,irun,10,25)',(T-273), reactSector(:,irun,10,26)',(T-273),
reactSector(:,irun,10,27)',(T-273), reactSector(:,irun,10,28)', (T-273),
reactSector(:,irun,10,29)',(T-273), reactSector(:,irun,10,30)', (T-273),
reactSector(:,irun,10,31)');
title('\bf{Surface fraction, stage 10}','FontSize',14)
xlabel('\bf{Temperature [^oC]}')
ylabel('\bf{Fraction}')
xlim([xlimMin xlimMax]);
ylim([0 1]);
grid on
```

```
tF1(:,:) = reactSector(:,irun,1,32:53);
tF5(:,:) = reactSector(:,irun,5,32:53);
tF10(:,:) = reactSector(:,irun,10,32:53);
totF1 = sum(tF1')+ n0N2;
totF5 = sum(tF5')+ n0N2;
totF10 = sum(tF10')+ n0N2;

subplot(3,3,7)
plot((T-273),(reactSector(:,irun,1,44)'./totF1(:)'),(T-273),
(reactSector(:,irun,1,45)'./totF1(:)' ),(T-273),
(reactSector(:,irun,1,46)'./totF1(:)' ), (T-273),
(reactSector(:,irun,1,47)'./totF1(:)'), (T-273),
(reactSector(:,irun,1,48)'./totF1(:)'), (T-273),
(reactSector(:,irun,1,49)'./totF1(:)'), (T-273),
(reactSector(:,irun,1,50)'./totF1(:)'), (T-273),
(reactSector(:,irun,1,51)'./totF1(:)'), (T-273),
(reactSector(:,irun,1,52)'./totF1(:)'), (T-273),
(reactSector(:,irun,1,53)'./totF1(:)'));
title('\bf{Gas phase fraction, stage 1}','FontSize',14)
legend('CH4',  'C2H6' , 'C2H4', 'H2', 'O2', 'H2O', 'CO', 'CO2', 'C3H8',
'C3H6', 2);%'*', )
xlim([xlimMin xlimMax]);
ylim([0 1]);
grid on

subplot(3,3,8)
plot((T-273),(reactSector(:,irun,5,44)'./totF5(:)'),(T-273),
(reactSector(:,irun,5,45)'./totF5(:)' ),(T-273),
(reactSector(:,irun,5,46)'./totF5(:)' ), (T-273),
(reactSector(:,irun,5,47)'./totF5(:)'), (T-273),
(reactSector(:,irun,5,48)'./totF5(:)'), (T-273),
(reactSector(:,irun,5,49)'./totF5(:)'), (T-273),
(reactSector(:,irun,5,50)'./totF5(:)'), (T-273),
(reactSector(:,irun,5,51)'./totF5(:)'), (T-273),
(reactSector(:,irun,5,52)'./totF5(:)'), (T-273),
(reactSector(:,irun,5,53)'./totF5(:)'));
title('\bf{Gas phase fraction, stage 5}','FontSize',14)
xlim([xlimMin xlimMax]);
ylim([0 1]);
grid on

subplot(3,3,9)
plot((T-273),(reactSector(:,irun,10,44)'./totF10(:)'),(T-273),
(reactSector(:,irun,10,45)'./totF10(:)' ),(T-273),
(reactSector(:,irun,10,46)'./totF10(:)' ), (T-273),
(reactSector(:,irun,10,47)'./totF10(:)'), (T-273),
(reactSector(:,irun,10,48)'./totF10(:)'), (T-273),
(reactSector(:,irun,10,49)'./totF10(:)'), (T-273),
(reactSector(:,irun,10,50)'./totF10(:)'), (T-273),
(reactSector(:,irun,10,51)'./totF10(:)'), (T-273),
(reactSector(:,irun,10,52)'./totF10(:)'), (T-273),
(reactSector(:,irun,10,53)'./totF10(:)'));
title('\bf{Gas phase fraction, stage 10}','FontSize',14)
xlim([xlimMin xlimMax]);
ylim([0 1]);
grid on

%% surface plot for conversion
% figure();
% [X,Y] = meshgrid((T-273),1:10);
```

```
% for iq = 1:1:size((T-273),2)
%     for jq = 1:1:10
%         Z(iq,jq) = ((n0CH3CH2CH3-reactSector(iq,jq,52)')./n0CH3CH2CH3);
%     end
% end
% surf(X,Y,Z');
% title('\bf{Conversion}','FontSize',14);
% xlim([xlimMin xlimMax]);
% xlabel('\bf{Temperature [^oC]}');
% ylabel('\bf{Reactor sector}');
%%

t2=now; % counter for time of code execution
t=datevec(t2-t1)
```

COMB_ECALC_V5.M:

```
function [Ef,Er] = comb_Ecalc_v5(I, dHf)
global R T

% atomic binding energy, kcal/mol to kJ/mol
%                      Pd      Pt     Ni       Au    Ag    Cu
QoC = 90*4.184;   %96     %90    %102.6     %65     %66.2  %72
QoH = 36.6*4.184; %37.2   %36.6    %37.8     %27.6   %31.2  %33.6
QoO = 51.0*4.184; %52.3   %51.0    %69.0     %45.0   %48.0  %61.8

n = 3;
QC = QoC*(2-1/n);
QH = QoH*(2-1/n);
QO = QoO*(2-1/n);

%% heats of chemisorption

Dc3h8n = 3*dHf.H_(I) + dHf.CH3C_H2(I) + dHf.C_(I) - dHf.CH3CH2CH3(I);
Qc3h8n = QoC^2/(QoC+Dc3h8n);

Dc2h5_ch3 = dHf.CH3C_H2(I) + dHf.C_H3(I) - dHf.CH3CH2CH3(I);
Dc2h5nnn = 2*dHf.H_(I) + dHf.C_H3(I) + dHf.C_(I) - dHf.CH3C_H2(I);
Dch3nnn = 3*dHf.H_(I) + dHf.C_(I) - dHf.C_H3(I);
DA_B = Dc2h5_ch3;
DiA  = Dc2h5nnn;
Q0A  = QoC^2/(QoC+DiA);
DiB  = Dch3nnn;
Q0B  = QoC^2/(QoC+DiB);
a = Q0A^2*(Q0A+2*Q0B)/(Q0A+Q0B)^2;
b = Q0B^2*(Q0B+2*Q0A)/(Q0B+Q0A)^2;
Qc3h8in = (a*b*(a + b) + DA_B*(a - b)^2)/(a*b + DA_B*(a + b));

Dc3h7nnn = 2*dHf.H_(I) + dHf.CH3C_H2(I) + dHf.C_(I) - dHf.CH3CH2C_H2(I);
Qc3h7nnn = (1/2)*(QoC^2/(QoC/n + Dc3h7nnn) + QC^2/(QC + Dc3h7nnn));

Dc2h5_ch2 = dHf.CH3C_H2(I) + dHf.C_H2(I) - dHf.CH3CH2C_H2(I);
Dch2nnn = 2*dHf.H_(I) + dHf.C_(I) - dHf.C_H2(I);
DA_B = Dc2h5_ch2;
DiA  = Dc2h5nnn;
Q0A  = QoC^2/(QoC+DiA);
DiB  = Dch2nnn;
Q0B  = (1/2)*(QoC^2/(QoC/n + DiB) + QC^2/(QC + DiB));
a = Q0A^2*(Q0A+2*Q0B)/(Q0A+Q0B)^2;
```

```
b = Q0B^2*(Q0B+2*Q0A)/(Q0B+Q0A)^2;
Qc3h7innn = (a*b*(a + b) + DA_B*(a - b)^2)/(a*b + DA_B*(a + b));

Dc2h5_ch = dHf.CH3C_H2(I) + dHf.C_H(I) - dHf.CH3CH2C_H(I);
Dchnnn = dHf.H_(I) + dHf.C_(I) - dHf.C_H(I);
DA_B = Dc2h5_ch;
DiA  = Dc2h5nnn;
Q0A  = QoC^2/(QoC+DiA);
DiB  = Dchnnn;
Q0B  = QC^2/(QC + DiB);
a = Q0A^2*(Q0A+2*Q0B)/(Q0A+Q0B)^2;
b = Q0B^2*(Q0B+2*Q0A)/(Q0B+Q0A)^2;
Qc3h6innn = (a*b*(a + b) + DA_B*(a - b)^2)/(a*b + DA_B*(a + b));

Dc2h4_ch2 = dHf.CH3C_H(I) + dHf.C_H2(I) - dHf.CH3CHdCH2(I);
Dc2h4nnn = dHf.H_(I) + dHf.C_(I) - dHf.C_H3(I);
DA_B = Dc2h4_ch2;
DiA  = Dc2h4nnn;
Q0A  = QoC^2/(QoC+DiA);
DiB  = Dch2nnn;
Q0B  = QoC^2/(QoC+DiB);
a = Q0A^2*(Q0A+2*Q0B)/(Q0A+Q0B)^2;
b = Q0B^2*(Q0B+2*Q0A)/(Q0B+Q0A)^2;
Qc3h6in = (a*b*(a + b) + DA_B*(a - b)^2)/(a*b + DA_B*(a + b));

Qc2h5nnn = (1/2)*(QoC^2/(QoC/n + Dc2h5nnn) + QC^2/(QC + Dc2h5nnn));

Dc2h4_ch = dHf.CH3C_H(I) + dHf.C_H(I) - dHf.CH3CHdC_H(I);
DA_B = Dc2h4_ch;
DiA  = Dc2h4nnn;
Q0A  = QoC^2/(QoC+DiA);
DiB  = Dchnnn;
Q0B  = (1/2)*(QoC^2/(QoC/n + DiB) + QC^2/(QC + DiB));
a = Q0A^2*(Q0A+2*Q0B)/(Q0A+Q0B)^2;
b = Q0B^2*(Q0B+2*Q0A)/(Q0B+Q0A)^2;
Qc3h5innn = (a*b*(a + b) + DA_B*(a - b)^2)/(a*b + DA_B*(a + b));

Qc2h4nnn = QC^2/(QC + Dc2h4nnn);

Dch3_ch3 = dHf.C_H3(I) + dHf.C_H3(I) - dHf.CH3CH3(I);
DA_B = Dch3_ch3;
DiA  = Dch3nnn;
Q0A  = QoC^2/(QoC+DiA);
Qc2h6in = 9*Q0A^2/(6*Q0A + 16*DA_B);

Dch2_ch = dHf.C_H2(I) + dHf.C_H(I) - dHf.CH2dC_H(I);
DA_B = Dch2_ch;
DiA  = Dch2nnn;
Q0A  = QoC^2/(QoC+DiA);
DiB  = Dchnnn;
Q0B  = (1/2)*(QoC^2/(QoC/n + DiB) + QC^2/(QC + DiB));
a = Q0A^2*(Q0A+2*Q0B)/(Q0A+Q0B)^2;
b = Q0B^2*(Q0B+2*Q0A)/(Q0B+Q0A)^2;
Qc2h3innn = (a*b*(a + b) + DA_B*(a - b)^2)/(a*b + DA_B*(a + b));

Dch2_ch2 = dHf.C_H2(I) + dHf.C_H2(I) - dHf.CH2dCH2(I);
DA_B = Dch2_ch2;
DiA  = Dch2nnn;
Q0A  = QoC^2/(QoC+DiA);
Qc2h4in = 9*Q0A^2/(6*Q0A + 16*DA_B);
```

```
Dch_ch = dHf.C_H(I) + dHf.C_H(I) - dHf.CHtCH(I);
DA_B = Dch_ch;
DiA  = Dchnnn;
Q0A  = QoC^2/(QoC+DiA);
Qc2h2in = 9*Q0A^2/(6*Q0A + 16*DA_B);

Dc2hnnn = dHf.C_H(I) + dHf.C_(I) - dHf.CHtC_(I);
Qc2hnnn = (1/2)*(QoC^2/(QoC/n + Dc2hnnn) + QC^2/(QC + Dc2hnnn));

Qchnnn = QC^2/(QC + Dchnnn);

Qch2nnn = QC^2/(QC + Dch2nnn);

Qch3nnn = (1/2)*(QoC^2/(QoC/n + Dch3nnn) + QC^2/(QC + Dch3nnn));

Dch4n = 4*dHf.H_(I) + dHf.C_(I) - dHf.CH4(I);
Qch4n = QoC^2/(QoC+Dch4n);

Dh_h = dHf.H_(I) + dHf.H_(I) - dHf.H2(I);
DA_B = Dh_h;
Q0A  = QoH;
Qh2in = 9*Q0A^2/(6*Q0A + 16*DA_B);

Do_o = dHf.O_(I) + dHf.O_(I) - dHf.O2(I);
DA_B = Do_o;
Q0A  = QoO;
Qo2in = 9*Q0A^2/(6*Q0A + 16*DA_B);

Dohnnn = dHf.O_(I) + dHf.H_(I) - dHf.O_H(I);
Qohnnn = QO^2/(QO+Dohnnn);

Dch3onnn = dHf.C_H3(I) + dHf.O_(I) - dHf.CH3O_(I);
Qch3onnn = QO^2/(QO+Dch3onnn);

Dhconnn = dHf.H_(I) + dHf.C_(I) + dHf.O_(I) - dHf.HC_dO(I);
Qhconnn = (1/2)*(QoC^2/(QoC/n + Dhconnn) + QC^2/(QC + Dhconnn));

Dhcoonnn = dHf.HC_dO(I)  + dHf.O_(I) - dHf.HCOO_(I);
Qhcoonnn = QO^2/(QO+Dhcoonnn);

Dh2on = 2*dHf.H_(I)  + dHf.O_(I) - dHf.H2O(I);
Qh2on = QoO^2/(QoO+Dh2on);

Dcon = dHf.C_(I)  + dHf.O_(I) - dHf.CO(I);
Qcon = QoC^2/(QoC+Dcon);

Do_c_o = dHf.C_(I)  + 2*dHf.O_(I) - dHf.CO2(I);
Qco2in = 9*QoO^2/(6*QoO + 16*Do_c_o);

%% reactions
%  R1    CH3CH2CH3 + *  <=>  CH3CH2C*H3
Ef(1) = 0;
Er(1) = Qc3h8n;

%  R2    CH3CH2CH3 + *^2  <=>  CH3C*H2C*H3
Ef(2) = 0;
Er(2) = Qc3h8in;

%  R3   CH3CH2C*H3 + *  <=>  CH3C*H2C*H3
Ef(3) = Qc3h8n - Qc3h8in;
Er(3) = -Ef(3);
```

```
%  R4   CH3CH2C*H3 + *^5  <=>  CH3CH2C***H2 + H***
Dch3ch2ch2_h = dHf.CH3CH2C_H2(I) + dHf.H_(I) - dHf.CH3CH2CH3(I);
Ef(4) = (1/2)*(Qc3h8n + Dch3ch2ch2_h - Qc3h7nnn - QH + Qc3h7nnn*QH/(Qc3h7nnn +
QH));
Er(4) = (1/2)*(-Qc3h8n - Dch3ch2ch2_h + Qc3h7nnn + QH + Qc3h7nnn*QH/(Qc3h7nnn
+ QH));

%  R5   CH3C*H2C*H3 + *^5  <=>  CH3C*H2C***H2 + H***
Ef(5) = (1/2)*(Qc3h8in + Dch3ch2ch2_h - Qc3h7innn - QH + Qc3h7innn*QH/
(Qc3h7innn + QH));
Er(5) = (1/2)*(-Qc3h8in - Dch3ch2ch2_h + Qc3h7innn + QH + Qc3h7innn*QH/
(Qc3h7innn + QH));

%  R6   CH3CH2C***H2 + *  <=>  CH3C*H2C***H2
Ef(6) = Qc3h7nnn - Qc3h7innn;
Er(6) = -Ef(6);

%  R7   CH3CH2C*H3 + *^5  <=>  CH3C***H2 + C***H3
Ef(7) = (1/2)*(Qc3h8n + Dc2h5_ch3 - Qc2h5nnn - Qch3nnn + Qc2h5nnn*Qch3nnn/
(Qc2h5nnn + Qch3nnn));
Er(7) = (1/2)*(-Qc3h8n - Dc2h5_ch3 + Qc2h5nnn + Qch3nnn + Qc2h5nnn*Qch3nnn/
(Qc2h5nnn + Qch3nnn));

%  R8   CH3C*H2C*H3 + *^4  <=>  CH3C***H2 + C***H3
Ef(8) = (1/2)*(Qc3h8in + Dc2h5_ch3 - Qc2h5nnn - Qch3nnn + Qc2h5nnn*Qch3nnn/
(Qc2h5nnn + Qch3nnn));
Er(8) = (1/2)*(-Qc3h8in - Dc2h5_ch3 + Qc2h5nnn + Qch3nnn + Qc2h5nnn*Qch3nnn/
(Qc2h5nnn + Qch3nnn));

%  R9   CH3CH2C***H2 + *^3  <=>  CH3C***H2 + C***H2
Ef(9) = (1/2)*(Qc3h7nnn + Dc2h5_ch2 - Qc2h5nnn - Qch2nnn + Qc2h5nnn*Qch2nnn/
(Qc2h5nnn + Qch2nnn));
Er(9) = (1/2)*(-Qc3h7nnn - Dc2h5_ch2 + Qc2h5nnn + Qch2nnn + Qc2h5nnn*Qch2nnn/
(Qc2h5nnn + Qch2nnn));

%  R10  CH3C*H2C***H2 + *^2  <=>  CH3C***H2 + C***H2
Ef(10) = (1/2)*(Qc3h7innn + Dc2h5_ch2 - Qc2h5nnn - Qch2nnn + Qc2h5nnn*Qch2nnn/
(Qc2h5nnn + Qch2nnn));
Er(10) = (1/2)*(-Qc3h7innn - Dc2h5_ch2 + Qc2h5nnn + Qch2nnn +
Qc2h5nnn*Qch2nnn/(Qc2h5nnn + Qch2nnn));

%  R11  CH3C*H2C***H2 + *^3  <=>  CH3C*H2C***H + H***
Dch3ch2ch_h = dHf.CH3CH2C_H(I) + dHf.H_(I) - dHf.CH3CH2C_H2(I);
Ef(11) = (1/2)*(Qc3h7innn + Dch3ch2ch_h - Qc3h6innn - QH + Qc3h6innn*QH/
(Qc3h6innn + QH));
Er(11) = (1/2)*(-Qc3h7innn - Dch3ch2ch_h + Qc3h6innn + QH + Qc3h6innn*QH/
(Qc3h6innn + QH));

%  R12  CH3C*H2C***H2 + *  <=>  CH3C*H=C*H2 + H***
Dch3ch_hch2 = dHf.CH3C_HC_H2(I) + dHf.H_(I) - dHf.CH3CH2C_H2(I);
Ef(12) = (1/2)*(Qc3h7innn + Dch3ch_hch2 + Dc2h5_ch2 - Dc2h4_ch2 - Qc3h6in - QH
+ Qc3h6in*QH/(Qc3h6in + QH));
Er(12) = (1/2)*(-Qc3h7innn - Dch3ch_hch2 - Dc2h5_ch2 + Dc2h4_ch2 + Qc3h6in +
QH + Qc3h6in*QH/(Qc3h6in + QH));

%  R13  CH3CH2C***H2 + *^2  <=>  CH3C*H=C*H2 + H***
Ef(13) = (1/2)*(Qc3h7nnn + Dch3ch_hch2 + Dc2h5_ch2 - Dc2h4_ch2 - Qc3h6in - QH
+ Qc3h6in*QH/(Qc3h6in + QH));
Er(13) = (1/2)*(-Qc3h7nnn - Dch3ch_hch2 - Dc2h5_ch2 + Dc2h4_ch2 + Qc3h6in + QH
+ Qc3h6in*QH/(Qc3h6in + QH));
```

```
%  R14  CH3C*H2C***H  <=>  CH3C*H=C*H2 + *^2
Dch3ch_hch = dHf.CH3C_HC_H(I) + dHf.H_(I) - dHf.CH3CH2C_H(I);
Dch3chdch_h = dHf.CH3CHdC_H(I) + dHf.H_(I) - dHf.CH3CHdCH2(I);
Ef(14) = Qc3h6innn + Dch3ch_hch + Dc2h5_ch - Dc2h4_ch2 - Dch3chdch_h -
Qc3h6in;
Er(14) = -Ef(14);

%  R15  CH3C*H=C*H2 + *^5  <=>  CH3C*H=C***H + H***
Ef(15) = (1/2)*(Qc3h6in + Dch3chdch_h - Qc3h5innn - QH + Qc3h5innn*QH/
(Qc3h5innn + QH));
Er(15) = (1/2)*(-Qc3h6in - Dch3chdch_h + Qc3h5innn + QH + Qc3h5innn*QH/
(Qc3h5innn + QH));

%  R16  CH3C*H2C***H + *^3  <=>  CH3C*H=C***H + H***
Ef(16) = (1/2)*(Qc3h6innn + Dc2h5_ch + Dch3ch_hch - Dc2h4_ch - Qc3h5innn - QH
+ Qc3h5innn*QH/(Qc3h5innn + QH));
Er(16) = (1/2)*(-Qc3h6innn - Dc2h5_ch - Dch3ch_hch + Dc2h4_ch + Qc3h5innn + QH
+ Qc3h5innn*QH/(Qc3h5innn + QH));

%  R17  CH3C*H=C*H2 + *^5  <=>  C***H3 + C*H2=C***H
Dch3_c2h3 = dHf.C_H3(I) + dHf.CH2dC_H(I) - dHf.CH3CHdCH2(I);
Ef(17) = (1/2)*(Qc3h6in + Dch3_c2h3 - Qch3nnn - Qc2h3innn + Qch3nnn*Qc2h3innn/
(Qch3nnn + Qc2h3innn));
Er(17) = (1/2)*(-Qc3h6in - Dch3_c2h3 + Qch3nnn + Qc2h3innn +
Qch3nnn*Qc2h3innn/(Qch3nnn + Qc2h3innn));

%  R18  CH3C*H=C*H2  <=>  CH3CHdCH2 + *^2
Ef(18) = Qc3h6in;
Er(18) = 0;

%  R19  CH3C***H2 + *^2  <=>  C*H2=C*H2 + H***
Dch3_ch2 = dHf.C_H3(I) + dHf.C_H2(I) - dHf.CH3C_H2(I);
Dch2_hch2 = dHf.C_H2C_H2(I) + dHf.H_(I) - dHf.CH3C_H2(I);
Ef(19) = (1/2)*(Qc2h5nnn + Dch3_ch2 + Dch2_hch2 - Dch2_ch2 - Qc2h4in - QH +
Qc2h4in*QH/(Qc2h4in + QH));
Er(19) = (1/2)*(-Qc2h5nnn - Dch3_ch2 - Dch2_hch2 + Dch2_ch2 + Qc2h4in + QH +
Qc2h4in*QH/(Qc2h4in + QH));

%  R20  C*H2=C*H2 + *^4  <=>  C***H2^2
Ef(20) = (1/2)*(Qc2h4in + Dch2_ch2 - Qch2nnn - Qch2nnn + Qch2nnn*Qch2nnn/
(Qch2nnn + Qch2nnn));
Er(20) = (1/2)*(-Qc2h4in - Dch2_ch2 + Qch2nnn + Qch2nnn + Qch2nnn*Qch2nnn/
(Qch2nnn + Qch2nnn));

%  R21  C***H3 + *^3  <=>  C***H2 + H***
Dch2_h = dHf.C_H2(I) + dHf.H_(I) - dHf.C_H3(I);
Ef(21) = (1/2)*(Qch3nnn + Dch2_h - Qch2nnn - QH + Qch2nnn*QH/(Qch2nnn + QH));
Er(21) = (1/2)*(-Qch3nnn - Dch2_h + Qch2nnn + QH + Qch2nnn*QH/(Qch2nnn + QH));

%  R22  C*H3C*H3 + *^4  <=>  CH3C***H2 + H***
Dch3ch2_h = dHf.CH3C_H2(I) + dHf.H_(I) - dHf.CH3CH3(I);
Ef(22) = (1/2)*(Qc2h6in + Dch3ch2_h - Qc2h5nnn - QH + Qc2h5nnn*QH/(Qc2h5nnn +
QH));
Er(22) = (1/2)*(-Qc2h6in - Dch3ch2_h + Qc2h5nnn + QH + Qc2h5nnn*QH/(Qc2h5nnn +
QH));

%  R23  C*H3C*H3 + *^4  <=>  C***H3^2
Ef(23) = (1/2)*(Qc2h6in + Dch3_ch3 - Qch3nnn - Qch3nnn + Qch3nnn*Qch3nnn/
(Qch3nnn + Qch3nnn));
```

```
Er(23) = (1/2)*(-Qc2h6in - Dch3_ch3 + Qch3nnn + Qch3nnn + Qch3nnn*Qch3nnn/
(Qch3nnn + Qch3nnn));

%  R24  C***H3 + H***  <=>  C*H4 + *^5
Dch3_h = dHf.C_H3(I) + dHf.H_(I) - dHf.CH4(I);
Ef(24) = (1/2)*(-Qch4n - Dch3_h + Qch3nnn + QH + Qch3nnn*QH/(Qch3nnn + QH));
Er(24) = (1/2)*(Qch4n + Dch3_h - Qch3nnn - QH + Qch3nnn*QH/(Qch3nnn + QH));

%  R25  C*H3C*H3  <=>  CH3CH3 + *^2
Ef(25) = Qc2h6in;
Er(25) = 0;

%  R26  C*H4  <=>  CH4 + *
Ef(26) = Qch4n;
Er(26) = 0;

%  R27  C*H2=C*H2  <=>  CH2dCH2 + *^2
Ef(27) = Qc2h4in;
Er(27) = 0;

%  R28  C*H2=C*H2 + *^5  <=>  C*H2=C***H + H***
Dch2dch_h = dHf.CH2dC_H(I) + dHf.H_(I) - dHf.CH2dCH2(I);
Ef(28) = (1/2)*(Qc2h4in + Dch2dch_h - Qc2h3innn - QH + Qc2h3innn*QH/(Qc2h3innn
+ QH));
Er(28) = (1/2)*(-Qc2h4in - Dch2dch_h + Qc2h3innn + QH + Qc2h3innn*QH/
(Qc2h3innn + QH));

%  R29  C*H2=C***H + *  <=>  C*H/=/C*H + H***
Dch_hdch = dHf.C_HdC_H(I) + dHf.H_(I) - dHf.CH2dC_H(I);
Ef(29) = (1/2)*(Qc2h3innn + Dch2_ch + Dch_hdch - Dch_ch - Qc2h2in - QH +
Qc2h2in*QH/(Qc2h2in + QH));
Er(29) = (1/2)*(-Qc2h3innn - Dch2_ch - Dch_hdch + Dch_ch + Qc2h2in + QH +
Qc2h2in*QH/(Qc2h2in + QH));

%  R30  C*H/=/C*H + *^4  <=>  CH/=/C*** + H***
Dchtc_h = dHf.CHtC_(I) + dHf.H_(I) - dHf.CHtCH(I);
Ef(30) = (1/2)*(Qc2h2in + Dchtc_h - Qc2hnnn - QH + Qc2hnnn*QH/(Qc2hnnn + QH));
Er(30) = (1/2)*(-Qc2h2in - Dchtc_h + Qc2hnnn + QH + Qc2hnnn*QH/(Qc2hnnn +
QH));

%  R31  CH/=/C*** + *^3  <=>  C***H + C***
Dch_c = dHf.C_H(I) + dHf.C_(I) - dHf.CHtC_(I);
Ef(31) = (1/2)*(Qc2hnnn + Dch_c - Qchnnn - QC + Qchnnn*QC/(Qchnnn + QC));
Er(31) = (1/2)*(-Qc2hnnn - Dch_c + Qchnnn + QC + Qchnnn*QC/(Qchnnn + QC));

%  R32  C***H + *^3  <=>  C*** + H***
Dc_h = dHf.C_(I) + dHf.H_(I) - dHf.C_H(I);
Ef(32) = (1/2)*(Qchnnn + Dc_h - QC - QH + QC*QH/(QC + QH));
Er(32) = (1/2)*(-Qchnnn - Dc_h + QC + QH + QC*QH/(QC + QH));

%  R33   H2 + *^2  <=>  H*H*
Ef(33) = 0;
Er(33) = Qh2in;

%  R34  H*H* + *^4  <=>  H***^2
Ef(34) = (1/2)*(Qh2in + Dh_h - QH - QH + QH*QH/(QH + QH));
Er(34) = (1/2)*(-Qh2in - Dh_h + QH + QH + QH*QH/(QH + QH));

%  R35   O2 + *^2  <=>  O*O*
Ef(35) = 0;
Er(35) = Qo2in;
```

```
%  R36  O*O* + *^4  <=>  O***^2
Ef(36) = (1/2)*(Qo2in + Do_o - QO - QO + QO*QO/(QO + QO));
Er(36) = (1/2)*(-Qo2in - Do_o + QO + QO + QO*QO/(QO + QO));

%  R37  H*H* + O*** + *  <=>  O***H + H***
Do_h = dHf.O_(I) + dHf.H_(I) - dHf.O_H(I);
Ef(37) = (1/2)*(Qh2in + QO + Dh_h - Do_h - Qohnnn - QH + Qohnnn*QH/(Qohnnn +
QH));
Er(37) = (1/2)*(-Qh2in - QO - Dh_h + Do_h + Qohnnn + QH + Qohnnn*QH/(Qohnnn +
QH));

%  R38  H2O* + O*** + *^2  <=>  O***H^2
Dho_h = dHf.O_H(I) + dHf.H_(I) - dHf.H2O(I);
Ef(38) = (1/2)*(Qh2on + QO + Dho_h - Do_h - Qohnnn - Qohnnn + Qohnnn*Qohnnn/
(Qohnnn + Qohnnn));
Er(38) = (1/2)*(-Qh2on - QO - Dho_h + Do_h + Qohnnn + Qohnnn + Qohnnn*Qohnnn/
(Qohnnn + Qohnnn));

%  R39  H*** + O***  <=>  O***H + *^3
Ef(39) = (1/2)*(-Qohnnn - Do_h + QH + QO + QH*QO/(QH + QO));
Er(39) = (1/2)*(Qohnnn + Do_h - QH - QO + QH*QO/(QH + QO));

%  R40  H*** + O***H  <=>  H2O* + *^5
Ef(40) = (1/2)*(-Qh2on - Dho_h + QH + Qohnnn + QH*Qohnnn/(QH + Qohnnn));
Er(40) = (1/2)*(Qh2on + Dho_h - QH - Qohnnn + QH*Qohnnn/(QH + Qohnnn));

%  R41  H2O* + H*** + *  <=>  H*H* + O***H
Ef(41) = (1/2)*(Qh2on + QH + Dho_h - Dh_h - Qh2in - Qohnnn + Qh2in*Qohnnn/
(Qh2in + Qohnnn));
Er(41) = (1/2)*(-Qh2on - QH - Dho_h + Dh_h + Qh2in + Qohnnn + Qh2in*Qohnnn/
(Qh2in + Qohnnn));

%  R42  H2O*  <=>  H2O + *
Ef(42) = Qh2on;
Er(42) = 0;

%  R43  C***H3 + O***  <=>  CH3O*** + *^3
Dch3_o = dHf.O_(I) + dHf.C_H3(I) - dHf.CH3O_(I);
Ef(43) = (1/2)*(-Qch3onnn - Dch3_o + QO + Qch3nnn + QO*Qch3nnn/(QO +
Qch3nnn));
Er(43) = (1/2)*(Qch3onnn + Dch3_o - QO - Qch3nnn + QO*Qch3nnn/(QO + Qch3nnn));

%  R44  C***H3 + O***H  <=>  CH3O*** + H***
Ef(44) = (1/2)*(Qch3nnn + Qohnnn + Do_h - Dch3_o - Qch3onnn - QH +
Qch3onnn*QH/(Qch3onnn + QH));
Er(44) = (1/2)*(-Qch3nnn - Qohnnn - Do_h + Dch3_o + Qch3onnn + QH +
Qch3onnn*QH/(Qch3onnn + QH));

%  R45  C*O + C***H3 + *^2  <=>  CH3O*** + C***
Dc_o = dHf.O_(I) + dHf.C_(I) - dHf.CO(I);
Ef(45) = (1/2)*(Qcon + Qch3nnn + Dc_o - Dch3_o - Qch3onnn - QC + Qch3onnn*QC/
(Qch3onnn + QC));
Er(45) = (1/2)*(-Qcon - Qch3nnn - Dc_o + Dch3_o + Qch3onnn + QC + Qch3onnn*QC/
(Qch3onnn + QC));

%  R46   CH3C***H + HC***=O + *  <=>  CH3C*H=C***H + O***
Dhc_o = dHf.C_H(I) + dHf.O_(I) - dHf.HC_dO(I);
Ef(46) = (1/2)*(Qc2h4nnn + Qhconnn + Dhc_o - Dc2h4_ch - Qc3h5innn - QO +
Qc3h5innn*QO/(Qc3h5innn + QO));
```

```
Er(46) = (1/2)*(-Qc2h4nnn - Qhconnn - Dhc_o + Dc2h4_ch + Qc3h5innn + QO +
Qc3h5innn*QO/(Qc3h5innn + QO));

%  R47  C***H + O***  <=>  HC***=O + *^3
Ef(47) = (1/2)*(-Qhconnn - Dhc_o + Qchnnn + QO + Qchnnn*QO/(Qchnnn + QO));
Er(47) = (1/2)*(Qhconnn + Dhc_o - Qchnnn - QO + Qchnnn*QO/(Qchnnn + QO));

%  R48  CH3C*H=C*H2 + *^4  <=>   CH3C***H + C***H2
Ef(48) = (1/2)*(Qc3h6in + Dc2h4_ch2 - Qc2h4nnn - Qch2nnn + Qc2h4nnn*Qch2nnn/
(Qc2h4nnn + Qch2nnn));
Er(48) = (1/2)*(-Qc3h6in - Dc2h4_ch2 + Qc2h4nnn + Qch2nnn + Qc2h4nnn*Qch2nnn/
(Qc2h4nnn + Qch2nnn));

%  R49  CH3C***H2 + *^3  <=>   CH3C***H + H***
Dch3ch_h = dHf.CH3C_H(I) + dHf.H_(I) - dHf.CH3C_H2(I);
Ef(49) = (1/2)*(Qc2h5nnn + Dch3ch_h - Qc2h4nnn - Qch2nnn + Qc2h4nnn*Qch2nnn/
(Qc2h4nnn + Qch2nnn));
Er(49) = (1/2)*(-Qc2h5nnn - Dch3ch_h + Qc2h4nnn + Qch2nnn + Qc2h4nnn*Qch2nnn/
(Qc2h4nnn + Qch2nnn));

%  R50  HC***=O + *  <=>  C*O + H***
Dh_co = dHf.H_(I) + dHf.C_dO(I) - dHf.HC_dO(I);
Ef(50) = (1/2)*(Qhconnn + Dhc_o + Dh_co - Dc_o - Qcon - QH + Qcon*QH/(Qcon +
QH));
Er(50) = (1/2)*(Qhconnn + Dhc_o + Dh_co - Dc_o - Qcon - QH + Qcon*QH/(Qcon +
QH));

%  R51  C*O + O***  <=>  O*=C=O* + *^2
Ef(51) = (1/2)*(-Qco2in - Do_c_o + Dc_o + Qcon + QO + Qcon*QO/(Qcon + QO));
Er(51) = (1/2)*(Qco2in + Do_c_o - Dc_o - Qcon - QO + Qcon*QO/(Qcon + QO));

%  R52  C*** + O***  <=>  C*O + *^5
Ef(52) = (1/2)*(-Qcon - Dc_o + QC + QO + QC*QO/(QC + QO));
Er(52) = (1/2)*(Qcon + Dc_o - QC - QO + QC*QO/(QC + QO));

%  R53  C*O + O***H + *  <=>  O*=C=O* + H***
Ef(53) = (1/2)*(Qcon + Qohnnn + Do_h + Dc_o - Do_c_o - Qco2in - QH +
Qco2in*QH/(Qco2in + QH));
Er(53) = (1/2)*(-Qcon - Qohnnn - Do_h - Dc_o + Do_c_o + Qco2in + QH +
Qco2in*QH/(Qco2in + QH));

%  R54  HC***=O + O***  <=>   HC(O)O*** + *^3
Dhco_o = dHf.HC_dO(I) + dHf.O_(I) - dHf.HCOO_(I);
Ef(54) = (1/2)*(-Qhcoonnn - Dhco_o + Qhconnn + QO + Qhconnn*QO/(Qhconnn +
QO));
Er(54) = (1/2)*(Qhcoonnn + Dhco_o - Qhconnn - QO + Qhconnn*QO/(Qhconnn + QO));

%  R55   HC(O)O*** + *  <=>  C*O + O***H
DDhcoo = dHf.H_(I) + 2*dHf.O_(I) + dHf.C_(I)- dHf.HCOO_(I);
Ef(55) = (1/2)*(Qhcoonnn + DDhcoo - Dc_o - Do_h - Qcon - Qohnnn + Qcon*Qohnnn/
(Qcon + Qohnnn));
Er(55) = (1/2)*(-Qhcoonnn - DDhcoo + Dc_o + Do_h + Qcon + Qohnnn +
Qcon*Qohnnn/(Qcon + Qohnnn));

%  R56   HC(O)O*** + *^2  <=>  O*=C=O* + H***
Dh_coo = dHf.H_(I) + dHf.C_dOO_(I) - dHf.HCOO_(I);
Doc_o  = dHf.O_(I) + dHf.C_dO(I) - dHf.CO2(I);
Ef(56) = (1/2)*(Qhcoonnn + Dh_coo + Dhco_o - Doc_o - Qco2in - QH + Qco2in*QH/
(Qco2in + QH));
Er(56) = (1/2)*(-Qhcoonnn - Dh_coo - Dhco_o + Doc_o + Qco2in + QH + Qco2in*QH/
(Qco2in + QH));
```

```
%  R57  C*O  <=>  CO + *
Ef(57) = Qcon;
Er(57) = 0;

%  R58  O*=C=O*  <=>  CO2 + *^2
Ef(58) = Qco2in;
Er(58) = 0;

%  R59   CH3CH2CH3  <=>  CH3CH2C_H2 + H_
Ef(59) = Dch3ch2ch2_h + R*T(I)/1000;
Er(59) = -Dch3ch2ch2_h + R*T(I)/1000;

%  R60   CH3CH2CH3  <=>  CH3C_H2 + C_H3
Ef(60) = Dc2h5_ch3 + R*T(I)/1000;
Er(60) = -Dc2h5_ch3 + R*T(I)/1000;

%  R61   CH3CH2C_H2  <=>  CH3CHdCH2 + H_
Ef(61) = Dch3ch_hch2 + Dc2h5_ch2 - Dc2h4_ch2 + R*T(I)/1000;
Er(61) = -Dch3ch_hch2 - Dc2h5_ch2 + Dc2h4_ch2 + R*T(I)/1000;

%  R62   CH3CH2C_H2  <=>  CH3C_H2 + C_H2
Ef(62) = Dc2h5_ch2 + R*T(I)/1000;
Er(62) = -Dc2h5_ch2 + R*T(I)/1000;

%  R63   C_H3  <=>  C_H2 + H_
Ef(63) = Dch2_h + R*T(I)/1000;
Er(63) = -Dch2_h + R*T(I)/1000;

%  R64   C_H3 + H_  <=>  CH4
Ef(64) = -Dch3_h + R*T(I)/1000;
Er(64) = Dch3_h + R*T(I)/1000;

%  R65   CH3C_H2  <=>  CH2dCH2 + H_
Ef(65) = Dch2_hch2 + Dch3_ch2 - Dch2_ch2 + R*T(I)/1000;
Er(65) = -Dch2_hch2 - Dch3_ch2 + Dch2_ch2 + R*T(I)/1000;

%  R66   CH3CH3  <=>  C_H3^2
Ef(66) = Dch3_ch3 + R*T(I)/1000;
Er(66) = -Dch3_ch3 + R*T(I)/1000;

%  R67   CH3CH3  <=>  CH3C_H2 + H_
Ef(67) = Dch3ch2_h + R*T(I)/1000;
Er(67) = -Dch3ch2_h + R*T(I)/1000;

%  R68   CH2dCH2 + O_  <=>  C_H2 + CH2dO
Dch2_o = dHf.O_(I) + dHf.C_H2(I) - dHf.CH2dO(I);
Ef(68) = Dch2_ch2 - Dch2_o + R*T(I)/1000;
Er(68) = -Dch2_ch2 + Dch2_o + R*T(I)/1000;

%  R69   CH3O_  <=>  CH2dO + H_
Dch2_ho = dHf.H_(I) + dHf.C_H2O_(I) - dHf.CH3O_(I);
Ef(69) = Dch3_o + Dch2_ho - Dch2_o + R*T(I)/1000;
Er(69) = -Dch3_o - Dch2_ho + Dch2_o + R*T(I)/1000;

%  R70   C_H3 + O_  <=>  CH3O_
Ef(70) = -Dch3_o + R*T(I)/1000;
Er(70) = Dch3_o + R*T(I)/1000;

%  R71   H2 + O2  <=>  O_H^2
Ef(71) = Dh_h + Do_o - 2*Do_h + R*T(I)/1000;
```

```
Er(71) = -Dh_h - Do_o + 2*Do_h + R*T(I)/1000;

%  R72   H2O + H_  <=>  H2 + O_H
Ef(72) = Dho_h - Dh_h + R*T(I)/1000;
Er(72) = -Dho_h + Dh_h + R*T(I)/1000;

%  R73   H_ + O_  <=>  O_H
Ef(73) = -Do_h + R*T(I)/1000;
Er(73) = Do_h + R*T(I)/1000;

%  R74   H2 + O_  <=>  O_H + H_
Ef(74) = Dh_h - Do_h + R*T(I)/1000;
Er(74) = -Dh_h + Do_h + R*T(I)/1000;

%  R75   H2O + O_  <=>  O_H^2
Ef(75) = Dho_h - Do_h + R*T(I)/1000;
Er(75) = -Dho_h + Do_h + R*T(I)/1000;

%  R76   H_ + O_H  <=>  H2O
Ef(76) = Do_h - Dho_h + R*T(I)/1000;
Er(76) = -Do_h + Dho_h + R*T(I)/1000;

%  R77   CH3CHdCH2 + O_  <=>  CH3C_H + CH2dO
Ef(77) = Dc2h4_ch2 - Dch2_o + R*T(I)/1000;
Er(77) = -Dc2h4_ch2 + Dch2_o + R*T(I)/1000;

%  R78   CH3C_H  <=>  CH2dC_H + H_
Dch2_hch = dHf.H_(I) + dHf.C_H2C_H(I) - dHf.CH3C_H(I);
Dch3_ch = dHf.C_H3(I) + dHf.C_H(I) - dHf.CH3C_H(I);
Ef(78) = Dch2_hch + Dch3_ch - Dch2_ch + R*T(I)/1000;
Er(78) = -Dch2_hch - Dch3_ch + Dch2_ch + R*T(I)/1000;

%  R79   CH2dCH2  <=>  CH2dC_H + H_
Ef(79) = Dch2dch_h + R*T(I)/1000;
Er(79) = -Dch2dch_h + R*T(I)/1000;

%  R80   CH3C_H + H_  <=>  CH3C_H2
Ef(80) = -Dch3ch_h + R*T(I)/1000;
Er(80) = Dch3ch_h + R*T(I)/1000;

%  R81   CH2dO_ + O_  <=>  H_ + HCOO_
Dch_hdo = dHf.H_(I) + dHf.HC_dO(I) - dHf.CH2dO(I);
Ef(81) = Dch_hdo - Dhco_o + R*T(I)/1000;
Er(81) = -Dch_hdo + Dhco_o + R*T(I)/1000;

%  R82   HCOO_  <=>  CO2 + H_
Ef(82) = Dh_coo + Dhco_o - Doc_o + R*T(I)/1000;
Er(82) = -Dh_coo - Dhco_o + Doc_o + R*T(I)/1000;

%  R83   HCOO_  <=>  CO + O_H
Ef(83) = DDhcoo - Dc_o - Do_h + R*T(I)/1000;
Er(83) = -DDhcoo + Dc_o + Do_h + R*T(I)/1000;

%  R84   CO + O_  <=>  CO2
Ef(84) = Dc_o - Do_c_o + R*T(I)/1000;
Er(84) = -Dc_o + Do_c_o + R*T(I)/1000;

%  R85  CH3CH2C***H2  <=>  CH3CH2C_H2 + *^3
Ef(85) = Qc3h7nnn;
Er(85) = 0;
```

```
%  R86  CH3C***H2  <=>  CH3C_H2 + *^3
Ef(86) = Qc2h5nnn;
Er(86) = 0;

%  R87   CH3C***H  <=>  CH3C_H + *^3
Ef(87) = Qc2h4nnn;
Er(87) = 0;

%  R88  C*H2=C***H  <=>  CH2dC_H + *^4
Ef(88) = Qc2h3innn;
Er(88) = 0;

%  R89  C***H3  <=>  C_H3 + *^3
Ef(89) = Qch3nnn;
Er(89) = 0;

%  R90  C***H2  <=>  C_H2 + *^3
Ef(90) = Qch2nnn;
Er(90) = 0;

%  R91  H***  <=>  H_ + *^3
Ef(91) = QH;
Er(91) = 0;

%  R92  O***  <=>  O_n + *^3
Ef(92) = QO;
Er(92) = 0;

%  R93  O***H  <=>  O_H + *^3
Ef(93) = Qohnnn;
Er(93) = 0;

%  R94  CH3O***  <=>  CH3O_ + *^3
Ef(94) = Qch3onnn;
Er(94) = 0;

%  R95   HC(O)O***  <=>  HCOO_ + *^3
Ef(95) = Qhcoonnn;
Er(95) = 0;

for ir=1:1:95
    if Ef(ir) < 0
        Ef(ir)= 0;
    end
    if Er(ir) < 0
        Er(ir)= 0;
    end
end

Ef = Ef*1000;
Er = Er*1000;
end
```

COMB_DIFER_V5.M:

```
function dn=comb_difer_v5(t,n)%t

global T ntot Ptot  i Na  kf kr R Ct St pCat ywt eps n0N2 Nstp
```

```
% partial pressures
nTOT = sum(n(32:53))+ n0N2;

PCH3CH2C_H2   = (n(32)/nTOT)*Ptot;  %   32   'CH3CH2C.H2'
PCH3C_H2      = (n(33)/nTOT)*Ptot;  %   33   'CH3C.H2'
PCH3C_H       = (n(34)/nTOT)*Ptot;  %   34   'CH3C:H'
PCH2dC_H      = (n(35)/nTOT)*Ptot;  %   35   'CH2=C.H'
PC_H2         = (n(36)/nTOT)*Ptot;  %   36   'C:H2'
PC_H3         = (n(37)/nTOT)*Ptot;  %   37   'C.H3'
PH_             = (n(38)/nTOT)*Ptot;  %   38   'H.'
PO_           = (n(39)/nTOT)*Ptot;  %   39   'O:'
PO_H        = (n(40)/nTOT)*Ptot;  %   40   'O.H'
PCH3O_      = (n(41)/nTOT)*Ptot;  %   41   'CH3O.'
PHCOO_        = (n(42)/nTOT)*Ptot;  %   42   'HC(O)O.'
PCH2dO_           = (n(43)/nTOT)*Ptot;  %   43   'CH2=O'
PCH4          = (n(44)/nTOT)*Ptot;  %   44   'CH4'
PCH3CH3       = (n(45)/nTOT)*Ptot;  %   45   'CH3CH3'
PCH2dCH2      = (n(46)/nTOT)*Ptot;  %   46   'CH2=CH2'
PH2         = (n(47)/nTOT)*Ptot;  %   47   'H2'
PO2             = (n(48)/nTOT)*Ptot;  %   48   'O2'
PH2O        = (n(49)/nTOT)*Ptot;  %   49   'H2O'
PCO             = (n(50)/nTOT)*Ptot;  %   50   'CO'
PCO2          = (n(51)/nTOT)*Ptot;  %   51   'CO2'
PCH3CH2CH3    = (n(52)/nTOT)*Ptot;  %   52   'CH3CH2CH3'
PCH3CHdCH2    = (n(53)/nTOT)*Ptot;  %   53   'CH3CH=CH2'
%%

% reactions ( forward - reverse )
%%
R1 = ( kf(1)*PCH3CH2CH3*n(31) - kr(1)*n(1) ); R2 = ( kf(2)*PCH3CH2CH3*n(31)^2
- kr(2)*n(2) );
R3 = ( kf(3)*n(1)*n(31) - kr(3)*n(2) ); R4 = ( kf(4)*n(1)*n(31)^5 -
kr(4)*n(3)*n(21) );
R5 = ( kf(5)*n(2)*n(31)^5 - kr(5)*n(4)*n(21) ); R6 = ( kf(6)*n(3)*n(31) -
kr(6)*n(4) );
R7   = ( kf(7)*n(1)*n(31)^5 - kr(7)*n(7)*n(18) ); R8   = ( kf(8)*n(2)*n(31)^4
- kr(8)*n(7)*n(18) );
R9   = ( kf(9)*n(3)*n(31)^3 - kr(9)*n(7)*n(17) ); R10  = ( kf(10)*n(4)*n(31)^2
- kr(10)*n(7)*n(17) );
R11  = ( kf(11)*n(4)*n(31)^3 - kr(11)*n(5)*n(21) ); R12  = ( kf(12)*n(4)*n(31)
- kr(12)*n(6)*n(21) );
R13  = ( kf(13)*n(3)*n(31)^2 - kr(13)*n(6)*n(21) ); R14  = ( kf(14)*n(5) -
kr(14)*n(6)*n(31)^2 );
R15  = ( kf(15)*n(6)*n(31)^5 - kr(15)*n(8)*n(21) ); R16  =
( kf(16)*n(5)*n(31)^3 - kr(16)*n(8)*n(21) );
R17  = ( kf(17)*n(6)*n(31)^5 - kr(17)*n(18)*n(11) ); R18  = ( kf(18)*n(6) -
kr(18)*PCH3CHdCH2*n(31)^2 );
R19 = ( kf(19)*n(7)*n(31)^2 - kr(19)*n(12)*n(21) ); R20 =
( kf(20)*n(12)*n(31)^4 - kr(20)*n(17)^2 );
R21 = ( kf(21)*n(18)*n(31)^3 - kr(21)*n(17)*n(21) ); R22 =
( kf(22)*n(10)*n(31)^4 - kr(22)*n(7)*n(21) );
R23  = ( kf(23)*n(10)*n(31)^4 - kr(23)*n(18)^2 ); R24  = ( kf(24)*n(18)*n(21)
- kr(24)*n(19)*n(31)^5 );
R25  = ( kf(25)*n(10) - kr(25)*PCH3CH3*n(31)^2 ); R26  = ( kf(26)*n(19) -
kr(26)*PCH4*n(31) );
R27  = ( kf(27)*n(12) - kr(27)*PCH2dCH2*n(31)^2 ); R28  =
( kf(28)*n(12)*n(31)^5 - kr(28)*n(11)*n(21) );
R29  = ( kf(29)*n(11)*n(31) - kr(29)*n(13)*n(21) ); R30  =
( kf(30)*n(13)*n(31)^4 - kr(30)*n(14)*n(21) );
R31  = ( kf(31)*n(14)*n(31)^3 - kr(31)*n(16)*n(15) ); R32  =
( kf(32)*n(16)*n(31)^3 - kr(32)*n(15)*n(21) );
```

```
R33  = ( kf(33)*PH2*n(31)^2 - kr(33)*n(20) ); R34  = ( kf(34)*n(20)*n(31)^4 -
kr(34)*n(21)^2 );
R35  = ( kf(35)*PO2*n(31)^2 - kr(35)*n(22) ); R36  = ( kf(36)*n(22)*n(31)^4 -
kr(36)*n(23)^2 );
R37  = ( kf(37)*n(20)*n(23)*n(31) - kr(37)*n(24)*n(21) ); R38  =
( kf(38)*n(28)*n(23)*n(31)^2 - kr(38)*n(24)^2 );
R39  = ( kf(39)*n(21)*n(23) - kr(39)*n(24)*n(31)^3 ); R40  =
( kf(40)*n(21)*n(24) - kr(40)*n(28)*n(31)^5 );
R41  = ( kf(41)*n(28)*n(21)*n(31) - kr(41)*n(20)*n(24) ); R42  =
( kf(42)*n(28) - kr(42)*PH2O*n(31) );
R43  = ( kf(43)*n(18)*n(23) - kr(43)*n(25)*n(31)^3 ); R44  =
( kf(44)*n(18)*n(24) - kr(44)*n(25)*n(21) );
R45  = ( kf(45)*n(29)*n(18)*n(31)^2 - kr(45)*n(25)*n(15) ); R46  =
( kf(46)*n(9)*n(26)*n(31) - kr(46)*n(8)*n(23) );
R47  = ( kf(47)*n(16)*n(23) - kr(47)*n(26)*n(31)^3 ); R48  =
( kf(48)*n(6)*n(31)^4 - kr(48)*n(9)*n(17) );
R49  = ( kf(49)*n(7)*n(31)^3 - kr(49)*n(9)*n(21) ); R50  =
( kf(50)*n(26)*n(31) - kr(50)*n(29)*n(21) );
R51  = ( kf(51)*n(29)*n(23) - kr(51)*n(30)*n(31)^2 ); R52  =
( kf(52)*n(15)*n(23) - kr(52)*n(29)*n(31)^5 );
R53  = ( kf(53)*n(29)*n(24)*n(31) - kr(53)*n(30)*n(21) ); R54  =
( kf(54)*n(26)*n(23) - kr(54)*n(27)*n(31)^3 );
R55  = ( kf(55)*n(27)*n(31) - kr(55)*n(29)*n(24) ); R56  =
( kf(56)*n(27)*n(31)^2 - kr(56)*n(30)*n(21) );
R57  = ( kf(57)*n(29) - kr(57)*PCO*n(31) ); R58  = ( kf(58)*n(30) -
kr(58)*PCO2*n(31)^2 );
R59  = ( kf(59)*PCH3CH2CH3 - kr(59)*PCH3CH2C_H2*PH_ ); R60  =
( kf(60)*PCH3CH2CH3 - kr(60)*PCH3C_H2*PC_H3 );
R61  = ( kf(61)*PCH3CH2C_H2 - kr(61)*PCH3CHdCH2*PH_ ); R62  =
( kf(62)*PCH3CH2C_H2 - kr(62)*PCH3C_H2*PC_H2 );
R63  = ( kf(63)*PC_H3 - kr(63)*PC_H2*PH_ ); R64  = ( kf(64)*PC_H3*PH_ -
kr(64)*PCH4 );
R65  = ( kf(65)*PCH3C_H2 - kr(65)*PCH2dCH2*PH_ ); R66  = ( kf(66)*PCH3CH3 -
kr(66)*PC_H3^2 );
R67  = ( kf(67)*PCH3CH3 - kr(67)*PCH3C_H2*PH_ ); R68  = ( kf(68)*PCH2dCH2*PO_
- kr(68)*PC_H2*PCH2dO_ );
R69  = ( kf(69)*PCH3O_ - kr(69)*PCH2dO_*PH_ ); R70  = ( kf(70)*PC_H3*PO_ -
kr(70)*PCH3O_ );
R71  = ( kf(71)*PH2*PO2 - kr(71)*PO_H^2 ); R72  = ( kf(72)*PH2O*PH_ -
kr(72)*PH2*PO_H );
R73  = ( kf(73)*PH_*PO_ - kr(73)*PO_H ); R74  = ( kf(74)*PH2*PO_ -
kr(74)*PO_H*PH_ );
R75  = ( kf(75)*PH2O*PO_ - kr(75)*PO_H^2 ); R76  = ( kf(76)*PH_*PO_H -
kr(76)*PH2O );
R77  = ( kf(77)*PCH3CHdCH2*PO_ - kr(77)*PCH3C_H*PCH2dO_ ); R78  =
( kf(78)*PCH3C_H - kr(78)*PCH2dC_H*PH_ );
R79  = ( kf(79)*PCH2dCH2 - kr(79)*PCH2dC_H*PH_ ); R80  = ( kf(80)*PCH3C_H*PH_
- kr(80)*PCH3C_H2 );
R81  = ( kf(81)*PCH2dO_*PO_ - kr(81)*PH_*PHCOO_ ); R82  = ( kf(82)*PHCOO_ -
kr(82)*PCO2*PH_ );
R83  = ( kf(83)*PHCOO_ - kr(83)*PCO*PO_H ); R84  = ( kf(84)*PCO*PO_ -
kr(84)*PCO2 );
R85  = ( kf(85)*n(3) - kr(85)*PCH3CH2C_H2*n(31)^3 ); R86  = ( kf(86)*n(7) -
kr(86)*PCH3C_H2*n(31)^3 );
R87  = ( kf(87)*n(9) - kr(87)*PCH3C_H*n(31)^3 ); R88  = ( kf(88)*n(11) -
kr(88)*PCH2dC_H*n(31)^4 );
R89  = ( kf(89)*n(18) - kr(89)*PC_H3*n(31)^3 ); R90  = ( kf(90)*n(17) -
kr(90)*PC_H2*n(31)^3 );
R91  = ( kf(91)*n(21) - kr(91)*PH_*n(31)^3 ); R92  = ( kf(92)*n(23) -
kr(92)*PO_*n(31)^3 );
```

```
R93  = ( kf(93)*n(24) - kr(93)*PO_H*n(31)^3 ); R94  = ( kf(94)*n(25) -
kr(94)*PCH3O_*n(31)^3 );
R95  = ( kf(95)*n(27) - kr(95)*PHCOO_*n(31)^3 );

dn = zeros(53,1);

dn(1 ) = ( +R1 -R3 -R4 -R7 );  % 'CH3CH2C*H3'
dn(2 ) = ( +R2 +R3 -R5 -R8 );  % 'CH3C*H2C*H3'
dn(3 ) = ( -R6 +R4 -R13 -R9 -R85 );  % 'CH3CH2C***H2'
dn(4 ) = ( +R6 +R5 -R11 -R12 -R10 );  % 'CH3C*H2C***H2'
dn(5 ) = ( +R11 -R16 -R14 );  % 'CH3C*H2C***H'
dn(6 ) = ( +R13 +R12 -R15 -R48 -R17 +R14 -R18 );  % 'CH3C*H=C*H2'
dn(7 ) = ( -R49 -R19 +R22 +R8 +R10 +R7 +R9 -R86 );  % 'CH3C***H2'
dn(8 ) = ( +R15 +R16 +R46 );  % 'CH3C*H=C***H'
dn(9 ) = ( +R49 +R48 -R46 -R87 );  % 'CH3C***H'
dn(10) = ( -R22 -R23 -R25 );  %  'C*H3C*H3'
dn(11) = ( +R28 -R29 +R17 -R88 );  %  'C*H2=C***H'
dn(12) = ( +R19 -R28 -R20 -R27 );  %  'C*H2=C*H2'
dn(13) = ( +R29 -R30 );  %  'C*H/=/C*H'
dn(14) = ( +R30 -R31 );  %  'CH/=/C***'
dn(15) = ( +R32 +R31 -R52 +R45 );  %  'C***'
dn(16) = ( -R32 +R31 -R47 );  %  'C***H'
dn(17) = ( +R21 +R10 +R9 +R48 +2*R20 -R90 );  %  'C***H2'
dn(18) = ( -R21 -R24 +R8 +R7 +R17 +2*R23 -R45 -R43 -R44 -R89 );  %  'C***H3'
dn(19) = ( +R24 -R26 );  %  'C*H4'
dn(20) = ( +R33 -R37 +R41 -R34 );  %  'H*H*'
dn(21) = ( +R4 +R13 +R5 +R11 +R12 +R15 +R16 +R49 +R19 +R28 +R29 +R30 +R22 +R21
+R32 -R24 -R39 -R40 +R37 -R41 +R50 +2*R34 +R44 +R56 +R53 -R91 );  %  'H***'
dn(22) = ( +R35 -R36 );  %  'O*O*'
dn(23) = ( -R39 -R38 -R37 -R52 -R43 -R47 -R54 -R51 +R46 +2*R36 -R92 );  %
'O***'
dn(24) = ( +R39 -R40 +2*R38 +R37 +R41 -R44 +R55 -R53 -R93 );  %  'O***H'
dn(25) = ( +R45 +R43 +R44 -R94 );  %  'CH3O***'
dn(26) = ( +R47 -R50 -R54 -R46 );  %  'HC***=O'
dn(27) = ( +R54 -R56 -R55 -R95 );  %  'HC(O)O***'
dn(28) = ( +R40 -R38 -R41 -R42 );  %  'H2O*'
dn(29) = ( +R52 -R45 +R50 -R51 +R55 -R53 -R57 );  %  'C*O'
dn(30) = ( +R51 +R56 +R53 -R58 );  %  'O*=C=O*'
dn(31) = ( -R1 -2*R2 -2*R33 -2*R35 -R3 -R6 -5*R4 -2*R13 -5*R5 -3*R11 -R12
-5*R15 -3*R16-3*R49 -2*R19 -5*R28 -R29 -4*R30 -4*R22 -3*R21 -3*R32 +5*R24
-4*R8 -2*R10 -5*R7 -3*R9 -4*R48 -5*R17 -3*R31 -4*R23 -4*R20 +2*R14 +3*R39
+5*R40 -2*R38 -R37 -R41 +5*R52 -2*R45 +3*R43 +3*R47 -R50 +3*R54 +2*R51 -R46
-4*R34 -4*R36 -2*R56 -R55 -R53 +2*R25 +2*R27 +R26 +R42 +R57 +2*R58 +2*R18
+3*R85 +3*R86 +3*R87 +4*R88 +3*R89 +3*R90 +3*R91 +3*R92 +3*R93 +3*R94
+3*R95 );  %  '*'
% only surface
dn(32) =   (ntot*R*T(i)/Ptot)*(Ct*St*pCat*ywt/(Nstp*Na))*((1-eps)/eps)*(+R85);
%  'CH3CH2C.H2'
dn(33) =   (ntot*R*T(i)/Ptot)*(Ct*St*pCat*ywt/(Nstp*Na))*((1-eps)/eps)*(+R86);
%  'CH3C.H2'
dn(34) =   (ntot*R*T(i)/Ptot)*(Ct*St*pCat*ywt/(Nstp*Na))*((1-eps)/eps)*(+R87);
%  'CH3C:H'
dn(35) =   (ntot*R*T(i)/Ptot)*(Ct*St*pCat*ywt/(Nstp*Na))*((1-eps)/eps)*(+R88);
%  'CH2=C.H'
dn(36) =   (ntot*R*T(i)/Ptot)*(Ct*St*pCat*ywt/(Nstp*Na))*((1-eps)/eps)*(+R90);
%  'C:H2'
dn(37) =   (ntot*R*T(i)/Ptot)*(Ct*St*pCat*ywt/(Nstp*Na))*((1-eps)/eps)*(+R89);
% 'C.H3'
dn(38) =   (ntot*R*T(i)/Ptot)*(Ct*St*pCat*ywt/(Nstp*Na))*((1-eps)/eps)*(+R91);
%  'H.'
```

```
dn(39) =   (ntot*R*T(i)/Ptot)*(Ct*St*pCat*ywt/(Nstp*Na))*((1-eps)/eps)*(+R92);
%  'O:'
dn(40) =   (ntot*R*T(i)/Ptot)*(Ct*St*pCat*ywt/(Nstp*Na))*((1-eps)/eps)*(+R93);
%  'O.H'
dn(41) =   (ntot*R*T(i)/Ptot)*(Ct*St*pCat*ywt/(Nstp*Na))*((1-eps)/eps)*(+R94);
%  'CH3O.'
dn(42) =   (ntot*R*T(i)/Ptot)*(Ct*St*pCat*ywt/(Nstp*Na))*((1-eps)/eps)*(+R95);
%  'HC(O)O.'
dn(43) =   (ntot*R*T(i)/Ptot)*(Ct*St*pCat*ywt/(Nstp*Na))*((1-eps)/eps)*(0);  %
'CH2=O'
dn(44) =   (ntot*R*T(i)/Ptot)*(Ct*St*pCat*ywt/(Nstp*Na))*((1-eps)/eps)*(+R26);
%  'CH4'
dn(45) =   (ntot*R*T(i)/Ptot)*(Ct*St*pCat*ywt/(Nstp*Na))*((1-eps)/eps)*(+R25);
%  'CH3CH3'
dn(46) =   (ntot*R*T(i)/Ptot)*(Ct*St*pCat*ywt/(Nstp*Na))*((1-eps)/eps)*(+R27);
%  'CH2=CH2'
dn(47) =   (ntot*R*T(i)/Ptot)*(Ct*St*pCat*ywt/(Nstp*Na))*((1-eps)/eps)*(-R33);
%  'H2'
dn(48) =   (ntot*R*T(i)/Ptot)*(Ct*St*pCat*ywt/(Nstp*Na))*((1-eps)/eps)*(-R35);
%  'O2'
dn(49) =   (ntot*R*T(i)/Ptot)*(Ct*St*pCat*ywt/(Nstp*Na))*((1-eps)/eps)*(+R42);
%  'H2O'
dn(50) =   (ntot*R*T(i)/Ptot)*(Ct*St*pCat*ywt/(Nstp*Na))*((1-eps)/eps)*(+R57);
%  'CO'
dn(51) =   (ntot*R*T(i)/Ptot)*(Ct*St*pCat*ywt/(Nstp*Na))*((1-eps)/eps)*(+R58);
%  'CO2'
dn(52) =   (ntot*R*T(i)/Ptot)*(Ct*St*pCat*ywt/(Nstp*Na))*((1-eps)/eps)*(-R1
-R2);  %  'CH3CH2CH3'
dn(53) =   (ntot*R*T(i)/Ptot)*(Ct*St*pCat*ywt/(Nstp*Na))*((1-eps)/eps)*(+R18);
%  'CH3CH=CH2'

% gas phase + surface
% % dn(32) =   (ntot*R*T(i)/(Ptot))*(+R59 -R61 -R62) +
(ntot*R*T(i)/Ptot)*(Ct*St*pCat*ywt/(Na))*((1-eps)/eps)*(+R85);  %
'CH3CH2C.H2'
% % dn(33) =   (ntot*R*T(i)/(Ptot))*(-R65 +R67 +R60 +R62 +R80) +
(ntot*R*T(i)/Ptot)*(Ct*St*pCat*ywt/(Na))*((1-eps)/eps)*(+R86);  %  'CH3C.H2'
% % dn(34) =   (ntot*R*T(i)/(Ptot))*(-R78 +R77 -R80) +
(ntot*R*T(i)/Ptot)*(Ct*St*pCat*ywt/(Na))*((1-eps)/eps)*(+R87);  %  'CH3C:H'
% % dn(35) =   (ntot*R*T(i)/(Ptot))*(+R78 +R79) +
(ntot*R*T(i)/Ptot)*(Ct*St*pCat*ywt/(Na))*((1-eps)/eps)*(+R88);  %  'CH2=C.H'
% % dn(36) =   (ntot*R*T(i)/(Ptot))*(+R63 +R62 +R68) +
(ntot*R*T(i)/Ptot)*(Ct*St*pCat*ywt/(Na))*((1-eps)/eps)*(+R90);  %  'C:H2'
% % dn(37) =   (ntot*R*T(i)/(Ptot))*(-R63 -R64 +R60 +2*R66 -R70) +
(ntot*R*T(i)/Ptot)*(Ct*St*pCat*ywt/(Na))*((1-eps)/eps)*(+R89);  % 'C.H3'
% % dn(38) =   (ntot*R*T(i)/(Ptot))*(+R59 +R61 +R78 +R65 +R79 +R67 +R63 -R64
-R73 -R76 +R69 +R81 -R80 +R74 -R72 +R82) + (ntot*R*T(i)/Ptot)*(Ct*St*pCat*ywt/
(Na))*((1-eps)/eps)*(+R91);  %  'H.'
% % dn(39) =   (ntot*R*T(i)/(Ptot))*(-R73 -R75 -R70 -R81 -R84 -R77 -R74 -R68)
+     (ntot*R*T(i)/Ptot)*(Ct*St*pCat*ywt/(Na))*((1-eps)/eps)*(+R92);  %  'O:'
% % dn(40) =   (ntot*R*T(i)/(Ptot))*(+R73 -R76 +2*R75 +R74 +2*R71 +R72 +R83) +
(ntot*R*T(i)/Ptot)*(Ct*St*pCat*ywt/(Na))*((1-eps)/eps)*(+R93);  %  'O.H'
% % dn(41) =   (ntot*R*T(i)/(Ptot))*(+R70 -R69) +
(ntot*R*T(i)/Ptot)*(Ct*St*pCat*ywt/(Na))*((1-eps)/eps)*(+R94);  %  'CH3O.'

% % dn(42) =   (ntot*R*T(i)/(Ptot))*(+R81 -R82 -R83) +
(ntot*R*T(i)/Ptot)*(Ct*St*pCat*ywt/(Na))*((1-eps)/eps)*(+R95);  %  'HC(O)O.'
% % dn(43) =   (ntot*R*T(i)/(Ptot))*(+R69 -R81 +R77 +R68) +
(ntot*R*T(i)/Ptot)*(Ct*St*pCat*ywt/(Na))*((1-eps)/eps)*(0);  %  'CH2=O'
% % dn(44) =   (ntot*R*T(i)/(Ptot))*(+R64) +
(ntot*R*T(i)/Ptot)*(Ct*St*pCat*ywt/(Na))*((1-eps)/eps)*(+R26);  %  'CH4'
```

```
% % dn(45) =   (ntot*R*T(i)/(Ptot))*(-R67 -R66) +
(ntot*R*T(i)/Ptot)*(Ct*St*pCat*ywt/(Na))*((1-eps)/eps)*(+R25);  %  'CH3CH3'
% % dn(46) =   (ntot*R*T(i)/(Ptot))*(+R65 -R79 -R68) +
(ntot*R*T(i)/Ptot)*(Ct*St*pCat*ywt/(Na))*((1-eps)/eps)*(+R27);  %  'CH2=CH2'
% % dn(47) =   (ntot*R*T(i)/(Ptot))*(-R74 -R71 +R72) +
(ntot*R*T(i)/Ptot)*(Ct*St*pCat*ywt/(Na))*((1-eps)/eps)*(-R33);  %  'H2'
% % dn(48) =   (ntot*R*T(i)/(Ptot))*(-R71) +
(ntot*R*T(i)/Ptot)*(Ct*St*pCat*ywt/(Na))*((1-eps)/eps)*(-R35);  %  'O2'
% % dn(49) =   (ntot*R*T(i)/(Ptot))*(+R76 -R75 -R72) +
(ntot*R*T(i)/Ptot)*(Ct*St*pCat*ywt/(Na))*((1-eps)/eps)*(+R42);  %  'H2O'
% % dn(50) =   (ntot*R*T(i)/(Ptot))*(-R84 +R83) +
(ntot*R*T(i)/Ptot)*(Ct*St*pCat*ywt/(Na))*((1-eps)/eps)*(+R57);  %  'CO'
% % dn(51) =   (ntot*R*T(i)/(Ptot))*(+R84 +R82) +
(ntot*R*T(i)/Ptot)*(Ct*St*pCat*ywt/(Na))*((1-eps)/eps)*(+R58);  %  'CO2'
% % dn(52) =   (ntot*R*T(i)/(Ptot))*(-R59 -R60) +
(ntot*R*T(i)/Ptot)*(Ct*St*pCat*ywt/(Na))*((1-eps)/eps)*(-R1 -R2);  %
'CH3CH2CH3'
% % dn(53) =   (ntot*R*T(i)/(Ptot))*(+R61 -R77) +
(ntot*R*T(i)/Ptot)*(Ct*St*pCat*ywt/(Na))*((1-eps)/eps)*(+R18);  %  'CH3CH=CH2'
```

COEQUAT.M:

```
function F = propequat(x0)
global KpT2

F = KpT2*(1 - x0)^2 -  x0^2 ;
```

8.6.4 COMPOSITION-PROPERTY DIAGRAMS

The code used for plotting simplex diagrams is based on a sample code from [89], [74], [90]. A set of files - *myterconPt.m, myterplot.m, mytercontourPt.m, myterlabelPt.m* - is used for construction of full triangle with experimental points (gas compositions) on it. *myterconPt.m* - main file, *myterplot.m* prepares a ternary axis system, *mytercontourPt.m* plots the values in the input vector as a contour plot in a ternary diagram, *myterlabelPt.m* adds labels to a ternary plot. File *regrOptimPt.m* contains code for rescaling simplex to pseudovariables, fitting the polynomial to experimental results and plotting the fitted polynomial as contour plot on a rescaled simplex diagram.

MYTERCONPT.M:

```
% Main file for ternary plot
close all;clear all
% Load the data from data_trianglePt.dat
%   File format: 1. column: O2 fraction
%                2. column: Propane fraction
%                3. column: H2 fraction
%                4. column: function value (conversion, yield ...)
```

```
%   The data matrix is called A
load data_trianglePt.dat;
A = data_trianglePt;
%%%%%%%%%%%%%%%%%%%%%%%%%%%%%%%%%%%%%%%%%%%%%%%%%%%%%%%%%%%%%%%%%%%%%%%%%%%%%%%
%%   CODE FOR THE CONTOUR PLOT
%%%%%%%%%%%%%%%%%%%%%%%%%%%%%%%%%%%%%%%%%%%%%%%%%%%%%%%%%%%%%%%%%%%%%%%%%%%%%%%
figure
% Plot the ternary axis system
[h,hg,htick]=myterplot;
% Plot the data
%                        O2   C3H8    H2
[hcb]=mytercontourPt(A(:,1),A(:,2),A(:,3),A(:,4),linspace(min(A(:,4)),max(A(:,
4)),15));
% Add the labels
hlabels=myterlabelPt('H2','C3H8','O2');
%--  Change the color of the grid lines
set(hg(:,3),'color','k')
set(hg(:,2),'color','k')
set(hg(:,1),'color','k')
%--  Modify the labels
set(hlabels,'fontsize',12)
set(hlabels(3),'color','k')
set(hlabels(2),'color','k')
set(hlabels(1),'color','k')
%--  Modify the tick labels
set(htick(:,1),'color','k','linewidth',3)
set(htick(:,2),'color','k','linewidth',3)
set(htick(:,3),'color','k','linewidth',3)
%-- Change some defaults
set(gcf,'paperpositionmode','auto','inverthardcopy','off')
```

MYTERPLOT.M:

```
function [h,hg,htick]=myterplot
% perpares a ternary axis system
% It returns three handels:
% - h:      plot handel;
% - hg:     to change each grid line separately
% - htick:  to edit the tick labels
outline = [0 0; 0.5 sin(pi/3); 1 0; 0 0];
h = plot(outline(:,1),outline(:,2),'-k');
d1=cos(pi/3);
d2=sin(pi/3);
l=linspace(0,1,11);
hold on
for i=2:length(l)-1
   hg(i-1,3)=plot([l(i)*d1 1-l(i)*d1],[l(i)*d2
l(i)*d2],':k','linewidth',0.25);
   hg(i-1,1)=plot([l(i) l(i)+(1-l(i))*d1],[0 (1-
l(i))*d2],':k','linewidth',0.25);
   hg(i-1,2)=plot([(1-l(i))*d1 1-l(i)],[(1-l(i))*d2 0],':k','linewidth',0.25);
end
hold off
axis image
axis off
% Make x-tick labels
for i=1:11
    htick(i,1)=text(l(i),-0.025,num2str(l(i)));
```

```
    htick(i,3)=text(1-
l(i)*cos(pi/3)+0.025,l(i)*sin(pi/3)+0.025,num2str(l(i)));
    htick(i,2)=text(0.5-l(i)*cos(pi/3)-0.06,sin(pi/3)*(1-l(i)),num2str(l(i)));
end
```

MYTERCONTOURPT.M:

```
function [hcb]=mytercontourPt(c1,c2,c3,d,values)
% plots the values in the
% vector d as a contour plot in a ternary diagram.
% The three vectors c1,c2,c3 define the position of a data value within the
% ternary diagram.
% The values to be contoured can be specified in the optional vector VALUES
% (as in Matlab's own contour function).
% The ternary axis system is created within the function.
% Axis label can be added using the terlabel function.
% The function returns three handels: hg can be used to modify the grid lines,
% htick must be used to access the tick label properties, and hcb is the
handle
% for the colorbar.

hold on
% points on plot
%O2:C3H8:H2
redy = [44 56 0; 0 100 0; 0 19 81; 30 70 0; 15 85 0; 0 71 29; 0 41 59; 30 45
25; 15 30 55; 15 58 27; 33 60 07; 08 82 10; 07 34 59; 21 71 08; 08 59 33; 18
45 37; 23 58 19];
divisor = 100;
x = (redy(:,2) + (0.5 .* redy(:,1))) / divisor;
y = (redy(:,1) .* sin(pi/3)) / divisor;
plot(x,y,'ok', 'MarkerFaceColor', 'k');

% left side of a small triangle
newt = [44 56 0; 0 16 84];
x = (newt(:,2) + (0.5 .* newt(:,1))) / divisor;
y = (newt(:,1) .* sin(pi/3)) / divisor;
plot(x,y,'-k');

hold off
axis image
caxis([min(d) max(d)])
hcb = 1;
```

MYTERLABELPT.M:

```
function handels=myterlabelPt(label1,label2,label3)
% adds labels to a ternary plot.
% The labels can be modified through the handel vector HANDELS.

if nargout >= 1
    handels=ones(3,1);
    handels(1)=text(0.5,-0.05,label2,'horizontalalignment','center');
    handels(2)=text(0.15,sqrt(3)/4+0.05,label1,'horizontalalignment','center',
'rotation',60);
    handels(3)=text(0.85,sqrt(3)/4+0.05,label3,'horizontalalignment','center',
'rotation',-60);
else
```

```
    text(0.5,-0.05,label2,'horizontalalignment','center');
    text(0.15,sqrt(3)/4+0.05,label1,'horizontalalignment','center','rotation',
60);
    text(0.85,sqrt(3)/4+0.05,label3,'horizontalalignment','center','rotation',
-60);
end
```

REGROPTIMPT.M:

```
clear all

load H2O_650.dat;    % X1 (C(O2))       X2 (C(C3H8)) X3 (C(H2))   Y (Yield )
A = H2O_650;
clear H2O_650

Y = A(:,4); %— A n-by-1 vector of observed response

X(:,:) = A(:,1:3);

%%%%%%%%%%%%%%%%%%%%%%%%%%%%%
%convertion to pseudovariables
x_1_1 = 0.44; x_2_1 = 0.56; x_3_1 = 0; %x_comp_vertex
x_1_2 = 0;    x_2_2 = 1;    x_3_2 = 0;
x_1_3 = 0;    x_2_3 = 0.16; x_3_3 = 0.84;

% solving systems of equations A*X = B
B1= [1; ...
     0; ...
     0];

B2= [0; ...
     1; ...
     0];

A0 = [x_1_1 x_2_1 x_3_1; ...
     x_1_2 x_2_2 x_3_2; ...
     x_1_3 x_2_3 x_3_3];

X1  = A0\B1;%X1
X2  = A0\B2;%X2

z_1_1 = X1(1); z_1_2= X1(2); z_1_3= X1(3);
z_2_1 = X2(1); z_2_2= X2(2); z_2_3= X2(3);

%disp([z_1_1 z_1_2 z_1_3 z_2_1 z_2_2 z_2_3]);

Z(:,1) = z_1_1 + X(:,2).*( z_1_2 - z_1_1 ) + X(:,3).*( z_1_3 - z_1_1 );
Z(:,2) = z_2_1 + X(:,2).*( z_2_2 - z_2_1 ) + X(:,3).*( z_2_3 - z_2_1 );
Z(:,3) = 1 - Z(:,1) - Z(:,2);

Z = round(Z*100)/100;
%%disp(Z); %disp(X2);

%%%%%%%%%%%%%%%%%%%%%%%%%%%%%%%%%%
% regression analysis
reactants = [Z(:,1) Z(:,2) Z(:,3)];%— A n-by-3 matrix of reactant
concentrations
```

```
beta = [1 1 1 1 1 1 1 1 1 1]';%— A 5-by-1 vector of initial parameter
estimates
% xn — The names of the reactants
% yn — The name of the response

b = nlinfit(reactants,Y,@regropt,beta);

disp(b'); % parameters of the polynomial

%%%%%%%%%%%%%%%%%%%%%%%%%%%%%%%%%%%%
% adequacy check (with 1 check point)
%s^2y reproducibility variance
%s^2_y the variance of the predicted values of the response
% x(i)- fraction (e.g. x1 = 0.5, x2= 0.3, x3 = 0.2)

%pp 279-280, 133
%check point    x =   18   68     14     0.33  ; z = 0.4000    0.4200    0.1800
x = [0.4000    0.4200    0.1800];
y = 0.33;

%the number of points
N=max(size(X));

%the number of measurements in a center of plan
nn = 2;

%second Y2=: 13     58     30     0.36
Y2 = 0.37;
Ymean = (Y(7) + Y2)/2;

%reproducibility variance in a center of plan
S2E = ((Y(7) - Ymean)^2 + (Y2  - Ymean)^2)/(nn-1)

% for 3rd polynomial dzeta
Sci = 0;
Sciij = 0;
Scijj = 0;
Scijk = 0;
for i=1:1:3
    Sci = Sci + (x(i)*(3*x(i)-1)*(3*x(i)-2)/2)^2;
    for j=1:1:3
        if i<j
            Sciij = Sciij + (9*x(i)*x(j)*(3*x(i)-1)/2)^2;
            Scijj = Scijj + (9*x(i)*x(j)*(3*x(j)-1)/2)^2;
        end
        for k=1:1:3
            if i<j  && j<k
                Scijk = Scijk + (27*x(i)*x(j)*x(k))^2;
            end
        end
    end
end

dz = Sci + Sciij + Scijj + Scijk
Yrasch = b(1)*x(1) + b(2)*x(2) + b(3)*x(3) + b(4)*x(1).*x(2) + b(5)*x(1).*x(3)
+ b(6)*x(2).*x(3) + ...
       b(7)*x(1).*x(2).*(x(1)-x(2)) + b(8)*x(1).*x(3).*(x(1)-x(3)) +
b(9)*x(2).*x(3).*(x(2)-x(3)) +  ...
       b(10)*x(1).*x(2).*x(3)
dY = abs(y - Yrasch)
t = dY*sqrt(1)/(sqrt(S2E*(1+dz)))
```

```
delt = 12.7*sqrt(S2E*dz/2);

YYY = b(1)*Z(:,1) + b(2)*Z(:,2) + b(3)*Z(:,3) + b(4)*Z(:,1).*Z(:,2) +
b(5)*Z(:,1).*Z(:,3) + b(6)*Z(:,2).*Z(:,3) + ...
       b(7)*Z(:,1).*Z(:,2).*(Z(:,1)-Z(:,2)) + b(8)*Z(:,1).*Z(:,3).*(Z(:,1)-
Z(:,3)) + b(9)*Z(:,2).*Z(:,3).*(Z(:,2)-Z(:,3)) +  ...
       b(10)*Z(:,1).*Z(:,2).*Z(:,3);

S2AD = sum((Y-YYY).^2)/(N-10)
fad = N-10;
F = S2AD/S2E

%%%%%%%%%%%%%%%%%%%%%%%%%%%%%%%%
% plots
% figure
% %from regression analysis
N = 100;
CC1 = linspace(0,100,N); % O2
CC2 = linspace(0,100,N); % C3H8
%%%%%%%%%%%%%%%%%%%%%%%%%%%%%%%%
%Data for plotting 3d plus contour
for j = 1:N
    for i = 1:N
        if i <= N - j + 1
            XX(i,j) = (CC2(i) + CC1(j)/2)/100;
            YY(i,j) = (CC1(j)*sin(pi/3))/100;
            z1 = CC1(j)/100;
            z2 = CC2(i)/100;
            z3 = 1-z1-z2;
            ZZ(i,j) = b(1)*z1 + b(2)*z2 + b(3)*z3 + b(4)*z1.*z2 + b(5)*z1.*z3
+ b(6)*z2.*z3  + ...
                      b(7)*z1.*z2.*(z1-z2) + b(8)*z1.*z3.*(z1-z3) +
b(9)*z2.*z3.*(z2-z3) + b(10)*z1.*z2.*z3;
             %%%%%%%%%%%%%%%%%%%%
             % error, doveriteln interval
             x=[z1 z2 z3];
                Sci = 0;
                Sciij = 0;
                Scijj = 0;
                Scijk = 0;
                for iz=1:1:3
                    Sci = Sci + (x(iz)*(3*x(iz)-1)*(3*x(iz)-2)/2)^2;
                    for jz=1:1:3
                        if iz<jz
                            Sciij = Sciij + (9*x(iz)*x(jz)*(3*x(iz)-1)/2)^2;
                            Scijj = Scijj + (9*x(iz)*x(jz)*(3*x(jz)-1)/2)^2;
                        end
                        for kz=1:1:3
                            if iz<jz && jz<kz
                                Scijk = Scijk + (27*x(iz)*x(jz)*x(kz))^2;
                            end
                        end
                    end
                end
                dzz(i,j) = Sci + Sciij + Scijj + Scijk  ;
                delt(i,j) = 12.7*sqrt(S2E*dzz(i,j)/2);
             %%%%%%%%%%%%%%%%%%%%
        else
            XX(i,j) = XX(i-1,j);
            YY(i,j) = YY(i-1,j);
            ZZ(i,j) = ZZ(i-1,j);
```

```
            delt(i,j) = delt(i-1,j);
            dzz(i,j) = dzz(i-1,j);
        end
    end
end
%%%%%%%%%%%%%%%%%%%%%%%%%%%%%%%

% find max of function
[C,I] = max(ZZ);
[MAX, IND] = max(C);
Xx = XX(I(IND),IND);
Yy = YY(I(IND),IND);
Zz = MAX;
%     pseudovariable z
Co2 = Yy/(sin(pi/3));
Cc3h8 = Xx-Yy/(2*sin(pi/3));
Ch2 = 1-Co2-Cc3h8;
% real x
Co2x = Co2*0.44 %x1
Ch2x = Ch2*0.84 %x3
Cc3h8x = 1 - Co2x - Ch2x %x2

%%%%%%%%%%%%%%%%%%%%%%%%%%%%%%%
%plot 3d with contour
figure
 hold on

 % plot experim points
 scatter3((Z(:,2) + Z(:,1)/2), (Z(:,1)*sin(pi/3)), Y, 'filled', 'Marker', 'o',
'MarkerFaceColor', 'k');

 %plot max point
 scatter3(Xx, Yy, Zz, 'filled',  'Marker', 'd','MarkerEdgeColor', 'k',
'MarkerFaceColor', 'k' );

 outline = [0 0 0; 0.5 sin(pi/3) 0; 1 0 0; 0 0 0];
 plot3(outline(:,1),outline(:,2),outline(:,3),'-k','linewidth',2);

% line of maximum, autoregime  x 0.2 0.8 0 ; 0.2 0.6 0.2; 0.2 0.4 0.4
% z      0.4500 0.3100 0.2400; 0.4500 0.0700 0.4800;  0.4500    0.5500
0
 maximum = [0.4500 0.5500 0; 0.4500 0.0700 0.4800];
 x = (maximum(:,2) + (0.5 .* maximum(:,1))) ;
 y = (maximum(:,1) .* sin(pi/3)) ;
 plot3(x,y,[0 0],'-k');

% line of stoechiometric ratio 2H2+O2->2H2O, x 0.01 0.97 0.02 ; 0.2 0.6 0.2;
0.2 0.4 0.4
% z  0.0200 0.9500 0.0300; 0.4500 0.0700 0.4800
 maximum = [0 1 0; 0.4500 0.0700 0.4800];
 x = (maximum(:,2) + (0.5 .* maximum(:,1))) ;
 y = (maximum(:,1) .* sin(pi/3)) ;
 plot3(x,y,[0 0],'--k');

d1=cos(pi/3);
d2=sin(pi/3);
l=linspace(0,1,6);
hold on

% line of C3H8 axis  x 0  56        44;     44  56 0
%                                z 0    0.4800 0.5200; 1.0000 0  0
```

```
maximum = [0    0.4800    0.5200;    1.0000         0         0];
x = (maximum(:,2) + (0.5 .* maximum(:,1))) ;
y = (maximum(:,1) .* sin(pi/3)) ;
% plot3(x,y,[0 0],'-r');
tg =(y(1)-y(2))/(x(1)-x(2));
w1=tan(pi/3);
w2=tan(-pi/3);

for i=2:length(l)-1
   hg(i-1,3)=plot3([l(i)*d1 1-l(i)*d1],[l(i)*d2 l(i)*d2], [0 0],
':k','linewidth',0.25);
   if i<=3
       hg(i-1,1)=plot3([l(i) -tg*l(i)/(w1-tg)],[0 -w1*tg*l(i)/(w1-tg)], [0 0],
':k','linewidth',0.25); % %plot3([l(i) l(i)+(1-l(i))*d1],[0 (1-l(i))*d2], [0
0], ':k','linewidth',0.25)
   elseif i>3
       hg(i-1,1)=plot3([l(i) (-tg*l(i)-w1)/(w2-tg)],[0 w2*(-tg*l(i)-w1)/(w2-
tg)+w1], [0 0], ':k','linewidth',0.25);
   end
   hg(i-1,2)=plot3([(1-l(i))*d1 1-l(i)],[(1-l(i))*d2 0], [0 0],
':k','linewidth',0.25); %;
end

%  %--  Change the color of the grid lines
%  set(hg(:,3),'color','b')
%  set(hg(:,2),'color',[0 0.5 0])
%  set(hg(:,1),'color','r')

%plot contour lines on the plane
   [c,h]=contour(XX,YY,ZZ,[0.1 0.2 0.3 0.4 ], 'k');
   clabel(c,h);
   set(h,'linewidth',1)

%errors (doveriteln interval)
% %   dzzz = [0.6:0.1:1];
% %   levels = 12.7*sqrt(S2E*dzzz/2);
% %   levels = round(levels*1000)/1000;
% %
% %   [c1,h1]=contour(XX,YY,delt,levels, 'k');
% %   clabel(c1,h1);
% %   set(h1,'linewidth',1)

hold off
axis image

% angle of view
az = 0;
el = 89.9;
view(az, el);

axis off
% Make x-tick labels
l1=linspace(0,0.44,6);% O2
l2=linspace(0.16,1,6);% C3H8
l3=linspace(0,0.84,6);% H2

for i=1:length(l1)
    htick(i,1)=text(l(i),-0.025, 0, num2str(l2(i)));
    htick(i,3)=text(1-l(i)*cos(pi/3)+0.025,l(i)*sin(pi/3)+0.025, 0,
num2str(l1(i)));
```

```
    htick(i,2)=text(0.5-l(i)*cos(pi/3)-0.06,sin(pi/3)*(1-l(i)),0,
num2str(l3(i)));
end
%--  Modify the tick labels
set(htick(:,1),'color','k','linewidth',3)
set(htick(:,2),'color','k','linewidth',3)

%axis labels
    hlabels=ones(3,1);
    hlabels(1)=text(0.5,-0.05, 0,'C3H8','horizontalalignment','center');
    hlabels(2)=text(0.15,sqrt(3)/4+0.05,
0,'H2','horizontalalignment','center','rotation',60);
    hlabels(3)=text(0.85,sqrt(3)/4+0.05,
0,'O2','horizontalalignment','center','rotation',-60);

%--  Modify the labels
set(hlabels,'fontsize',12)
set(hlabels(3),'color','k')
set(hlabels(2),'color','k')
set(hlabels(1),'color','k')
```

REGROPT.M:

```
function yhat = regropt(beta,x)
% a function of the vector of
%   parameters, BETA, and the matrix of data, X.

b1 = beta(1);
b2 = beta(2);
b3 = beta(3);
b12 = beta(4);
b13 = beta(5);
b23 = beta(6);
g12 = beta(7);
g13 = beta(8);
g23 = beta(9);
b123 = beta(10);

x1 = x(:,1);
x2 = x(:,2);
x3 = x(:,3);

yhat = b1*x1 + b2*x2 + b3*x3 + b12*x1.*x2 + b13*x1.*x3 + b23*x2.*x3 + ...
       g12*x1.*x2.*(x1-x2) + g13*x1.*x3.*(x1-x3) + g23*x2.*x3.*(x2-x3) +
b123*x1.*x2.*x3;
```

8.7 STATISTICAL ANALYSIS

Statistical analysis is made to check the adequacy of the fitted polynomial (see Ch. 4.2.2) as well as to find the confidence intervals for the values predicted by the polynomial.

When checking the adequacy of the model we suppose that x_i (composition of feed mixture) is determined without errors, error mean square (Table 8.7.1) is identical for all points and responses are mean values of that measured in m=2 parallel measurements.

Two measurements were made in point [13]:[58]:[30] for calculation of error mean square (s^2_{rep}) in the centre of the experimental plan ([90] p. 33):

$$s^2_{rep} = \sum_{u=1}^{m} \frac{(y_u - \bar{y})^2}{m-1} \quad , \qquad \bar{y} = \sum_{u=1}^{m} \frac{y_u}{m} \quad ; \tag{8.7.1}$$

where m is the number of measurements (m=2), y_u - measured value, $\bar{y}$ - mean value.

Table 8.7.1: Error mean square s^2_{rep}.

Experiment	y, C_3H_6 yield, [fraction]	y_{mean}	s^2_{rep}
12	0.36	0.365	0.00005
12 rep.	0.37		

The F-test ([73], pp. 132-133):

$$F = \frac{s^2_{ad}}{s^2_{rep}} \quad ; \tag{8.7.2}$$

where s_{ad} is a the adequacy of the variance (dispersion of adequacy).

As experiments are made without parallel measurements and for error mean square was made a series of measurements m=2 in one point the dispersion of variance is:

$$s^2_{ad} = \frac{\sum_{i=1}^{n} (y_i - \hat{y}_i)^2}{n-l} \quad ; \tag{8.7.3}$$

where y_i is a measured value in experiment i, $\hat{y}_i$ - value calculated by fitted polynomial for experimental conditions i, n - the number of experiments, l - the number of parameters in the equation.

$$f_{ad} = n - l \quad ; \qquad f_{rep} = \sum_{i=1}^{n} (m_i - 1) \quad ; \tag{8.7.4}$$

where is f_{ad} and f_{rep} are the numbers of degree of dispersion of variance and error mean square respectively. The result of F-test calculation is present in Table 8.7.2.

Table 8.7.2: F-test.

s^2_{rep}	s^2_{ad}	F	f_{ad}	f_{rep}	F (α = 0.1)
0.00005	0.0017	34	6	1	58

The polynomial (4.2.2.8) is adequate to experiment with a significance level α = 0.1 as $F_{calc} < F_{table}$ (34<58).

The validity check of the model is made for every control point. For this the value t is calculated (t-test) ([74], p. 47):

$$t = \frac{\Delta y \cdot \sqrt{m}}{\sqrt{s_y^2 \cdot (1 + \xi)}} \quad ; \qquad \Delta y = |\bar{y} - \hat{y}| \quad ; \tag{8.7.5}$$

where $s^2_y = s^2_{rep}$, m - the number of repeated measurements (identical for every control point (m=1)), ξ - constraint force between x and y.

t is a Student function and is compared with the table value $t_{\alpha/l}(f_{rep})$, where α - significance level (α=0.05); l - number of control points (l=1); f_{rep} - number of degrees of freedom of error mean square (8.7.4).

For the polynomial of 3rd order ξ is ([73], p. 280):

$$\xi = \sum_{1 \leqslant i \leqslant q} c_i^2 + \sum_{1 \leqslant i < j \leqslant q} c_{ij}^2 + \sum_{1 \leqslant i < j \leqslant q} c_{ijj}^2 + \sum_{1 \leqslant i < j < k \leqslant q} c_{ijk}^2 \ ;$$

$$c_i = \frac{1}{2} \cdot x_i \cdot (3 \cdot x_i - 1) \cdot (3 \cdot x_i - 2) \ ;$$
$$c_{ij} = \frac{9}{2} \cdot x_i \cdot x_j \cdot (3 \cdot x_i - 1) \ ;$$
$$c_{ijj} = \frac{9}{2} \cdot x_i \cdot x_j \cdot (3 \cdot x_j - 1) \ ;$$
$$c_{ijk} = 27 \cdot x_i \cdot x_j \cdot x_k \ ; \qquad (8.7.6)$$

The result of t-test calculation is present in Table 8.7.3.

Table 8.7.3: t-test in check point ($[O_2]$:$[C_3H_8]$:$[H_2]$ = 18:68:14).

$s^2_{y,}$	ξ, (8.7.6)	y_{exp}	y_{calc}, (4.2.2.8)	t, (8.7.5)	f_{rep}, (8.7.4)	$t_{\alpha = 0.05}(f_{rep})$
0.00005	0.7932	0.33	0.36	2.64	1	12.71

The equation is adequate to the experiment with significance level α = 0.05, as $t_{calc} < t_{table}$ (2.64<12.71).

8.8 CORRECTION OF RESULTS OF EXPERIMENTS WITH HIGH PRESSURE DROP

The difference for propane conversion (Fig. 8.8.1) and for yields of the products for high and low pressure at temperatures 350~575 ℃ is small (in the range of tolerance). But for temperatures 600~650 ℃ we see a sharp increase in the conversion and yields for experiments at high pressure.

The experiments made at both high and low pressures are 10, 16, 17. Experiments 1, 2, 3, 5, 6, 11, 12, 13, 15 were carried out at low pressure drop; 4, 7, 8, 9, 14 - only at high pressure drop.

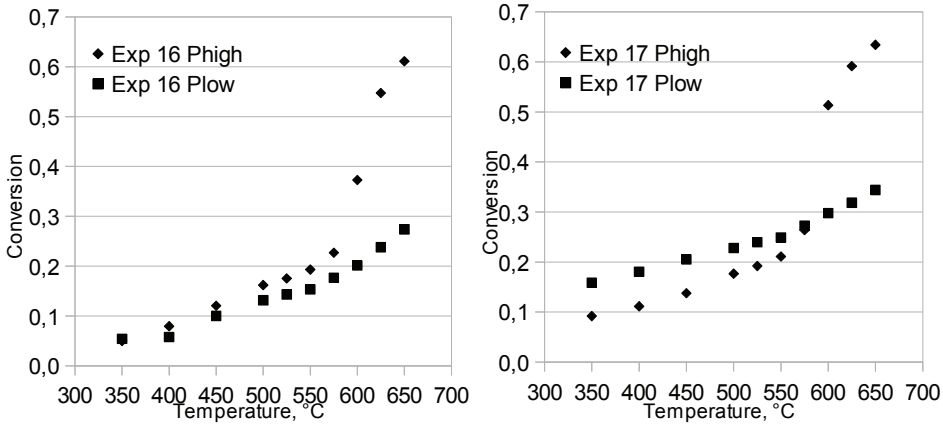

Fig. 8.8.1: Propane conversions for experiments 16 and 17 performed at pressures 1.4 (Plow) and 2.8 atm (Phigh).

High pressure drop was not controllable but a result of an imperfect catalyst bed placement, thus changes in the experimental results compared to low pressure results are not only caused by the thermodynamic or kinetic issues connected to the pressure change, but also by a difference in catalyst bed packing (i.e. diffusion issues).

Experiment 4 can be compared with experiment 1 as both does not include hydrogen. We see (Fig. 8.8.2*a*, *b*) the trend in change of lines of conversion and yields plotted for 1st experiment and see the same trend on plots for 4 experiment until temperature 600 °C where we have a drastic change connected to the operation at high pressure. At the same time the trend for conversion after 600 °C for 4th is approximately the same as for experiment 1 and for experiment 4 till 575 °C but some step higher. Thus we need to find the increase step and reduce a measured result by this step.

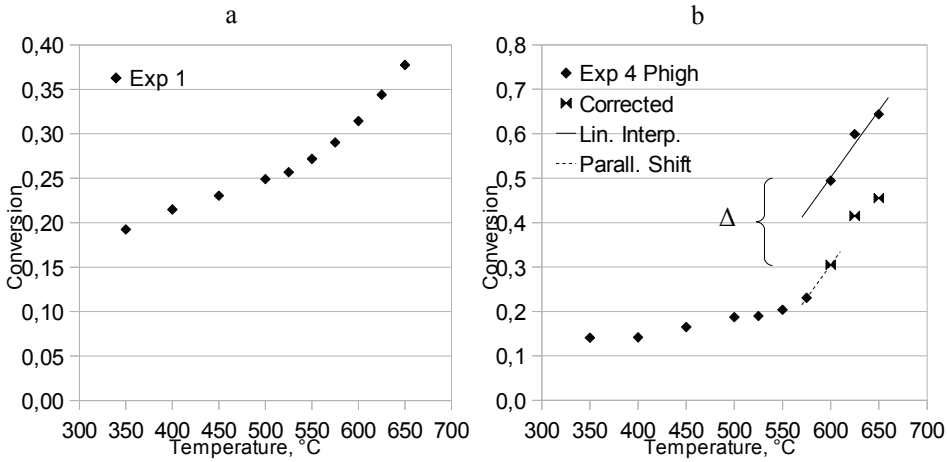

Fig. 8.8.2: Propane conversions for experiments 1 and 4. Linear interpolation and parallel shift of it determines Δ - step used to correct conversion values.

We determine the trend by linear interpolation of the conversion in points at 600, 625, 650 °C for experiment 4 (Fig. 8.8.2*b*). Using the angle from the linear equation we plot a line on the plot of conversion for experiment 4 starting from 575 and till 600 °C. Thus we find an expected value for 600 °C. At 600 °C we find delta between expected and measured values and use this delta to find expected results from the measured results at 625 and 650 °C.

As we can see on Figs. 8.8.1 and 8.8.2, three last points for high pressure experiment are placed more steep than appropriate points for low pressure. Making simple shift we do not decrease this feature, but still get reasonable results laying in the range of tolerance.

We can compare results for experiment 7 with experiment 3 and 6 as they all does not include oxygen. We see that although 7 was performed at higher pressure, this did not obviously influenced the results.

For experiment 8 we perform the same procedure as for 4. We can compare it with experiment 17 as they both include similar oxygen/hydrogen ratio. We make linear interpolation of results in points at 600~650 °C for experiment 8, plot appropriate line starting from 575 till 600 °C, get an expected value for 600 °C, find delta between

expected and measured values and use this delta to find expected results from measured results at points 625 and 650 °C.

For experiment 9 we perform the same procedure. We can compare it with experiment 13 as they both include most similar oxygen/hydrogen ratio.

For experiment 14 we perform the same procedure. We can compare it with experiment 11 as they both include most similar oxygen/hydrogen ratio.

8.9 CALCULATION PROCEDURES FOR CONVERSIONS, SELECTIVITIES AND YIELDS

8.9.1 CALCULATION OF THE MASS BALANCES FROM THE GC CHROMATOGRAMS

The measured data are flow velocities of compounds (calculated via internal standard):

$$\upsilon^{\text{in}}_{H_2},\quad \upsilon^{\text{in}}_{C_3H_8},\quad \upsilon^{\text{in}}_{O_2};$$

$$\upsilon^{\text{out}}_{H_2},\quad \upsilon^{\text{out}}_{C_3H_8},\quad \upsilon^{\text{out}}_{O_2},\quad \upsilon^{\text{out}}_{C_3H_6},\quad \upsilon^{\text{out}}_{CO_2},\quad \upsilon^{\text{out}}_{CO},\quad \upsilon^{\text{out}}_{H_2O},\quad \upsilon^{\text{out}}_{C_2H_4},\quad \upsilon^{\text{out}}_{C_2H_6},\quad \upsilon^{\text{out}}_{CH_4};$$

Mass balances - flows of atoms O, H, C in measured components:

$$\upsilon^{\text{in}}_{C}:\quad 3\cdot\upsilon^{\text{in}}_{C_3H_8};$$

$$\upsilon^{\text{out}}_{C}:\quad 3\cdot\upsilon^{\text{out}}_{C_3H_8},\quad 3\cdot\upsilon^{\text{out}}_{C_3H_6},\quad \upsilon^{\text{out}}_{CO_2},\quad \upsilon^{\text{out}}_{CO},\quad 2\cdot\upsilon^{\text{out}}_{C_2H_4},\quad 2\cdot\upsilon^{\text{out}}_{C_2H_6},\quad \upsilon^{\text{out}}_{CH_4};$$

$$\upsilon^{\text{in}}_{H}:\quad 2\cdot\upsilon^{\text{in}}_{H_2},\quad 8\cdot\upsilon^{\text{in}}_{C_3H_8};$$

$$\upsilon^{\text{out}}_{H}:\quad 2\cdot\upsilon^{\text{out}}_{H_2},\quad 8\cdot\upsilon^{\text{out}}_{C_3H_8},\quad 6\cdot\upsilon^{\text{out}}_{C_3H_6},\quad 2\cdot\upsilon^{\text{out}}_{H_2O},\quad 4\cdot\upsilon^{\text{out}}_{C_2H_4},\quad 6\cdot\upsilon^{\text{out}}_{C_2H_6},\quad 4\cdot\upsilon^{\text{out}}_{CH_4};$$

$$\upsilon^{\text{in}}_{O}:\quad 2\cdot\upsilon^{\text{in}}_{O_2};$$

$$\upsilon^{\text{out}}_{O}:\quad 2\cdot\upsilon^{\text{out}}_{CO_2},\quad \upsilon^{\text{out}}_{CO},\quad 2\cdot\upsilon^{\text{out}}_{O_2},\quad \upsilon^{\text{out}}_{H_2O};$$

Carbon formation and formation of other hydrocarbons are not measured. We suppose that other oxygen compounds are not produced.

Based on oxygen atoms balance we can calculate the amount of water formed, and then the deficiency of in/out flows of C and H:

$$\upsilon_{H_2O}^{out}=2\cdot\upsilon_{O_2}^{in}-2\cdot\upsilon_{CO_2}^{out}-\upsilon_{CO}^{out}-2\cdot\upsilon_{O_2}^{out};$$

$$D_H^{\%}=\frac{\upsilon_H^{in}-\upsilon_H^{out}}{\upsilon_H^{in}}\cdot 100\%=\frac{2\cdot\upsilon_{H_2}^{in}+8\cdot\upsilon_{C_3H_8}^{in}-2\cdot\upsilon_{H_2}^{out}-8\cdot\upsilon_{C_3H_8}^{out}-6\cdot\upsilon_{C_3H_6}^{out}-2\cdot\upsilon_{H_2O}^{out}-4\cdot\upsilon_{C_2H_4}^{out}-6\cdot\upsilon_{C_2H_6}^{out}-4\cdot\upsilon_{CH_4}^{out}}{2\cdot\upsilon_{H_2}^{in}+8\cdot\upsilon_{C_3H_8}^{in}}\cdot 100\%; \quad (8.9.1.1)$$

$$D_C^{\%}=\frac{\upsilon_C^{in}-\upsilon_C^{out}}{\upsilon_C^{in}}\cdot 100\%=\frac{3\cdot\upsilon_{C_3H_8}^{in}-3\cdot\upsilon_{C_3H_8}^{out}-3\cdot\upsilon_{C_3H_6}^{out}-\upsilon_{CO_2}^{out}-\upsilon_{CO}^{out}-2\cdot\upsilon_{C_2H_4}^{out}-2\cdot\upsilon_{C_2H_6}^{out}-\upsilon_{CH_4}^{out}}{3\cdot\upsilon_{C_3H_8}^{in}}\cdot 100\%;$$

8.9.2 CALCULATION OF CONVERSIONS, SELECTIVITIES AND YIELDS

From the gas flow a probe is automatically taken by MicroGC for analysis. We use two methods for calculation of components amounts - method of absolute calibration and method of internal standard ([91] p.396).

Y_i^{in}, Y_i^{out} - molar fractions of component in input flow and output flow,

$$Y_i=\frac{n_i}{n_{tot}}=\frac{\upsilon_i}{\upsilon_{tot}} \quad (8.9.2.1)$$

where $\upsilon_i, \upsilon_{tot}$ - flow rates [ml/min] of components and total.

A chromatograph signal for a component is proportional to the concentration of this component in a gas mixture. Relation between concentration and molar fraction in gas mixture:

$$C_i=\frac{m_i}{V_{tot}}=\frac{n_i\cdot M_i}{V_{tot}}=\frac{V_i\cdot M_i}{V_M\cdot V_{tot}}=Y_i\cdot\frac{M_i}{V_M}; \quad (8.9.2.2)$$

In the method of absolute calibration the set of mixtures with uniformly distributed concentrations of components is analysed by GC and calibration curves are plotted:

$$Y_i = a_i + b_i \cdot P_i; \qquad (8.9.2.3)$$

where Y_i - molar fraction, P_i - parameter of the signal (height or area of the peak).

This method was used for determination of the concentrations of components that we have in initial mixture: helium, hydrogen, propane, oxygen, nitrogen. Peaks of helium and hydrogen stay too close and have some overlapping, so heights of the peaks were used for analysis as least influenced by overlapping [91]. For all other components areas of the peaks where used in analysis.

The method of internal standard is based on comparison of measured peak parameter (P_i) of the substance to be detected with analogous parameter (P_{st}) of substance added in known amount.

Weight fraction of substance *i* (in %) can be found ([91], p.399):

$$X_i = \frac{m_i}{m_{pr}} \cdot 100 = \frac{P_i \cdot K_i \cdot m_{st}}{P_{st}} \cdot \frac{100}{m_{pr}}; \qquad (8.9.2.4)$$

where m_i, m_{pr}, m_{st} are masses of the component of interest, of the probe and of internal standard; K_i is a calibration factor for substance *i* by internal standard, P_i, P_{st} - parameter of the signal (area of the peak) of unknown component and internal standard.

$$K_i = \frac{P_{st} \cdot m_i}{P_i \cdot m_{st}}; \qquad (8.9.2.5)$$

Molar fractions can be found by the same approach:

$$K_i^{mol} = K_i \cdot \frac{M_{st}}{M_i} = \frac{S_{st} \cdot n_i}{S_i \cdot n_{st}} = \frac{S_{st} \cdot \upsilon_i}{S_i \cdot \upsilon_{st}} = \frac{S_{st} \cdot Y_i}{S_i \cdot Y_{st}};$$

$$Y_i = \frac{\upsilon_i}{\upsilon_{tot}} \cdot 100\,\% = \frac{S_i \cdot K_i^{mol} \cdot \upsilon_{st}}{S_{st} \cdot \upsilon_{tot}} \cdot 100\,\% = \frac{S_i \cdot K_i^{mol} \cdot Y_{st}}{S_{st}}; \qquad (8.9.2.6)$$

where S_i, S_{st} are areas of the peaks.

This method was used for determination of the concentrations of such components as C_3H_6, CO, CO_2, CH_4, C_2H_4, C_2H_6. The nitrogen was used as internal standard. Two calibration gas mixtures were used to determine K values for pairs component-nitrogen. Five analyses of every gas mixture where performed, the average area for every peak was found. K factors were found based on these average areas.

Using molar fractions and known flow rate of inert component (nitrogen) the flow rates of components in the outflow were found.

$$\upsilon_{st}^{\text{in}} = Y_{st}^{\text{in}} \cdot \upsilon_{tot}^{\text{in}}; \qquad \upsilon_{tot}^{\text{out}} = \frac{\upsilon_{st}^{\text{in}}}{Y_{st}^{\text{out}}} = \frac{Y_{st}^{\text{in}} \cdot \upsilon_{tot}^{\text{in}}}{Y_{st}^{\text{out}}}; \tag{8.9.2.7}$$

$$\upsilon_i^{\text{out}} = Y_i^{\text{out}} \cdot \upsilon_{tot}^{\text{out}} = Y_i^{\text{out}} \cdot \frac{Y_{st}^{\text{in}} \cdot \upsilon_{tot}^{\text{in}}}{Y_{st}^{\text{out}}};$$

Conversions are calculated as follows:

$$\chi_i = \frac{n_i^{\text{in}} - n_i^{\text{out}}}{n_i^{\text{in}}} = \frac{\upsilon_i^{\text{in}} - \upsilon_i^{\text{out}}}{\upsilon_i^{\text{in}}} \quad , \tag{8.9.2.8}$$

taking into account the gas law and that P and T are equal in inflow and outflow.

Selectivites are calculated as follows ([92], p.119):

$$\sigma_B = \frac{\nu_A}{\nu_B} \cdot \frac{\upsilon_B^{\text{out}}}{\upsilon_A^{\text{in}} - \upsilon_A^{\text{out}}}; \tag{8.9.2.9}$$

where ν_A, ν_B are the stoichiometric coefficients.

Selectivities for compounds are:

$$\sigma_{C_3H_6}=\frac{\upsilon^{out}_{C_3H_6}}{\upsilon^{in}_{C_3H_8}-\upsilon^{out}_{C_3H_8}};\qquad \sigma^{(1)}_{CO_2}=\frac{\upsilon^{out}_{CO_2}}{\upsilon^{in}_{O_2}-\upsilon^{out}_{O_2}};\qquad \sigma^{(2)}_{CO_2}=\frac{1}{3}\cdot\frac{\upsilon^{out}_{CO_2}}{\upsilon^{in}_{C_3H_8}-\upsilon^{out}_{C_3H_8}};$$

$$\sigma_{H_2O}=\frac{1}{2}\cdot\frac{\upsilon^{out}_{H_2O}}{\upsilon^{in}_{O_2}-\upsilon^{out}_{O_2}};\qquad \sigma^{(1)}_{CO}=\frac{1}{2}\cdot\frac{\upsilon^{out}_{CO}}{\upsilon^{in}_{O_2}-\upsilon^{out}_{O_2}};\qquad \sigma^{(2)}_{CO}=\frac{1}{3}\cdot\frac{\upsilon^{out}_{CO}}{\upsilon^{in}_{C_3H_8}-\upsilon^{out}_{C_3H_8}};\qquad (8.9.2.10)$$

$$\sigma_{C_2H_4}=\frac{2}{3}\cdot\frac{\upsilon^{out}_{C_2H_4}}{\upsilon^{in}_{C_3H_8}-\upsilon^{out}_{C_3H_8}};\qquad \sigma_{CH_4}=\frac{1}{3}\cdot\frac{\upsilon^{out}_{CH_4}}{\upsilon^{in}_{C_3H_8}-\upsilon^{out}_{C_3H_8}};$$

$$\sigma_{C_2H_6}=\frac{2}{3}\cdot\frac{\upsilon^{out}_{C_2H_6}}{\upsilon^{in}_{C_3H_8}-\upsilon^{out}_{C_3H_8}};$$

Here we can describe the amount of consumed propane (component A) through the amounts of produced and detected products:

$$\upsilon^{in}_A-\upsilon^{out}_A=\frac{\nu_A}{\nu_B}\cdot\upsilon^{out}_B+\frac{\nu'_A}{\nu_C}\cdot\upsilon^{out}_C+\frac{\nu''_A}{\nu_D}\cdot\upsilon^{out}_D+\ldots;$$

$$\sigma_B=\frac{\nu_A}{\nu_B}\cdot\frac{\upsilon^{out}_B}{\frac{\nu_A}{\nu_B}\cdot\upsilon^{out}_B+\frac{\nu'_A}{\nu_C}\cdot\upsilon^{out}_C+\frac{\nu''_A}{\nu_D}\cdot\upsilon^{out}_D+\ldots};\qquad (8.9.2.11)$$

Products yields are calculated as follows:

$$\eta_B=\frac{\nu_A}{\nu_B}\cdot\frac{\upsilon^{out}_B}{\upsilon^{in}_A};\qquad (8.9.2.12)$$

$$\eta_{C_3H_6}=\frac{\upsilon^{out}_{C_3H_6}}{\upsilon^{in}_{C_3H_8}};\qquad \eta_{H_2O}=\frac{1}{2}\cdot\frac{\upsilon^{out}_{H_2O}}{\upsilon^{in}_{O_2}};\qquad \eta^{(1)}_{CO_2}=\frac{\upsilon^{out}_{CO_2}}{\upsilon^{in}_{O_2}};\qquad \eta^{(2)}_{CO_2}=\frac{1}{3}\cdot\frac{\upsilon^{out}_{CO_2}}{\upsilon^{in}_{C_3H_8}};\qquad \eta_{CO}=\frac{1}{2}\cdot\frac{\upsilon^{out}_{CO}}{\upsilon^{in}_{O_2}};\qquad (8.9.2.13)$$

MISPRINTS

Some of the formulae have misendings

Formula №	Formula with complete ending
(2.6.2.5.)	$$\frac{d\theta_*}{dt}=-r_1-r_2+r_3+r_4=-k_1^f\cdot p_A\cdot\theta_*+k_1^r\cdot\theta_A-k_2^f\cdot p_B\cdot\theta_*+k_2^r\cdot\theta_B+ +k_3^f\cdot\theta_A\cdot\theta_B-k_3^r\cdot\theta_{AB}\cdot\theta_*+r_4+k_4^f\cdot\theta_{AB}-k_4^r\cdot p_{AB}\cdot\theta_*$$
(8.4.6.)	$$n_{chnl}=6\cdot(n_s-1+n_{ad.l})+6\cdot(2\cdot n_{sph.ad}-n_{ad.l})+\frac{3}{2}\cdot n^2-3\cdot n+\frac{3}{2}= =6\cdot(n_s-1+2\cdot n_{sph.ad})+\frac{3}{2}\cdot n^2-3\cdot n+\frac{3}{2};$$
(8.5.1.)	$$V_{free.CSTR}=\frac{m_{cat}}{10\cdot\rho_{cat}}\cdot\frac{\epsilon}{1-\epsilon};$$
(8.5.2.)	$$n'_{t_1}=n'_{t_0}+\delta_a\cdot(n'_{a_0}-n'_{a_1});$$
(8.5.3.)	$$V'_0\cdot\frac{P}{R\cdot T}\cdot Y_{a_0}=V'_1\cdot\frac{P}{R\cdot T}\cdot Y_{a_1}+V_r\cdot r(C,T)+V_r\cdot\frac{P}{R\cdot T}\cdot\frac{dY_a}{dt};$$